Kadanoff-Baym Theory for Thermalization of Quantum Fields

Akihiro Nishiyama
Institute of Physics, University of Tokyo, Komaba, Tokyo 153-8902, Japan

January 29, 2010

Abstract

We present a theoretical study of thermalization of quantum fields with Kadanoff-Baym (KB) equation. First we introduce a field theoretical technique known as 2 Particle Irreducible (2PI) effective action and review derivation of equation of motion for mean fields and fluctuations, then derive Kadanoff-Baym equation in scalar and gauge theories. In order to analyze thermalization processes we introduce relativistic entropy current based on the first order gradient expansion of Kadanoff-Baym equation. Then we show that in taking into account next-to-leading order (NLO) self-energy of the coupling expansion in ϕ^4 theory (in symmetric phase $\langle\hat{\phi}\rangle = 0$), it is possible to prove the H-theorem within the 1st order gradient expansion. We also show that it is possible to prove the H-theorem for KB equation with NLO self-energy of $1/N$ expansion in $O(N)$ theory (in symmetric phase). Furthermore we suggest a possibility for H-theorem to be satisfied in KB equation with leading-order (LO) self-energy of the coupling expansion in non-Abelian gauge theory. In $d+1$ dimensions ($d \geq 2$) LO particle number changing processes, such as 0-to-3, 1-to-2 and 2-to-1, which are prohibited in the normal Boltzmann approach with on-shell particles, may contribute to entropy production in KB approach although we must deal with gauge dependence and infrared divergence to complete the proof. Next we perform numerical simulations in spatially homogeneous configurations to investigate thermalization properties of the system in $1+1$ and $2+1$ dimensions for ϕ^4 theory with NLO self-energy of the coupling expansion and $1+1$ dimensions for $O(N)$ theory with NLO self-energy of $1/N$ expansion. We also estimate the time evolution of the kinetic entropy in the case of scalar ϕ^4 and $O(N)$ theory. Then we find that at later times $X^0 \gg 1/m$, where m represents mass of particles, the kinetic entropy increases monotonically and approaches the equilibrium value, although the limited time interval at the earlier times $X^0 \sim 1/m$ invalidates the use of it. No thermalization occurs in the simulations with the normal Boltzmann equation with 2-to-2 collision term in 1+1 dimensions, while it occurs in the simulations with KB equation in $1+1$ dimensions. It is due to two types of offshell effects: memory effects and spectral functions with the decay width.

Contents

1 Introduction

Quantum Chromodynamics (QCD) has by now been well established as the fundamental theory of strong interaction. QCD describes interaction of quarks, the constituents of hadrons, via the non-Abelian gauge interaction associated with the color charges carried by the quarks. Owing to the asymptotic freedom[1, 2, 3], the theory has been tested with perturbative methods of computations for the processes involving large momentum transfer such as deep inelastic scattering (DIS) of leptons off hadrons.

At the HERA collider, electrons are scattered off protons at the center-of-mass energy $\sqrt{s} \sim$ 300GeV and probe constituents of protons such as quarks and gluons of transverse size $r \sim 1/Q$ and longitudinal momentum fractions $x \sim Q^2/s$ where Q is a photon virtuality [4]. HERA is able to probe small x regime (down to 10^{-5}) where the physics is mainly dominated by gluons. It is well described by the Balitsky-Fadin-Kuraev-Lipatov (BFKL) equation [5, 6, 7] where the summation over the infrared logarithms $\sum_n \left(\alpha_s \ln \frac{1}{x}\right)^n$ with appropriate coefficients.

QCD predicts a phase transition at sufficiently high energy density from hadronic matter to the Quark-Gluon Plasma (QGP) consisting of deconfined quarks and gluons. The transition is one of the several transitions occurring in the early universe [8]. It is believed to have occurred during the first few microseconds after the big bang. It has been expected that the quark-gluon plasma may be reproduced againin ultra-relativistic heavy-ion collisions on the earth [9, 10]. High energy nucleus-nucleus collisions have been done from mid 80's using existing hadron accelerators (AGS at Brookhaven and SPS at CERN) with fixed nuclear targets. The experiments of heavy-ion collisions to create and study QGP have been under way since 2001 at RHIC and will be done soon in CERN. Experiments have been done at RHIC for pp and d+Au collisions at a nucleon-nucleon center-of-mass energy $\sqrt{s_{NN}}$ = 200 GeV and in Au+Au collisions at $\sqrt{s_{NN}}$ = 62.4 GeV, 130 GeV and 200 GeV. In pp, d+Au and Au+Au collisions, transverse momentum spectra, average transverse momenta, anti-baryon and strangeness production rates, particle yield ratios are measured as a function of the event multiplicity. The details of experiments can be found in Ref. [11]-[16].

There are various stages in heavy ion collisions [17, 18], starting with initial energy deposition in mid-rapidity region, followed by a thermalization of partons (formation of QGP), a hydrodynamic expansion and hadronization of Quark-Gluon Plasma and finally a kinetic freeze-out into free streaming particles which will be observed by a detector (Fig. 1). In ultrarelativistic heavy ion collisions, the relevant degrees of freedom of the incident nucleus are described by two sheet of classical transverse gluonic fields [20]. They are based on the QCD effective theory called Color Glass Condensate (CGC) that treats dense small-x degrees of freedom in terms of the color field. In the framework of CGC, it has been suggested that longitudinal color electric and magnetic fields may be created after two Lorentz contracted thin nuclei pass through each other [21], then nonequilibrium state composed of these strong fields and partons would follow. This intermediate gluonic state appearing between the first impact and the equilibrated QGP has been named Glasma [22].

The data in the heavy-ion experiments at RHIC suggest that the matter constituted by partons (quarks and gluons) are produced, it thermalizes very fast ($\tau_{\rm eq} = 0.6 \sim 1$ fm/c) and its behavior is quantitatively well described by the perfect-fluid hydrodynamics [23]-[28]. The topics around the problems of thermalization of the matter in relativistic Au+Au or Pb+Pb collisions are on interest in this field of physics. There are many dynamical models based on fast thermalization: hydrodynamic model[29, 30, 31] hybrid model with hadronic cascade[32] and hydro-kinetic approach[33] Then the discovery and theoretical treatment of elliptic flows at RHIC[34] provide strong support for fast thermalization of the produced matter. According to the hydrodynamic model, initial spatial anisotropy in the transverse plane left after fast thermalization in the peripheral heavy-ion collision is essential to the production of large pressure gradient and the pressure gradient produces the anisotropy of transverse momentum spectra expressed by v_2 coefficients. Hydrodynamics requires the system to be close to local thermal equilibrium. Unless the fast local equilibrium is achieved in the process, the flow is isotropic in the transverse plane and it contradicts the experimental data[35]. Then quantitative agreement requires that the hydrodynamics starts after the system

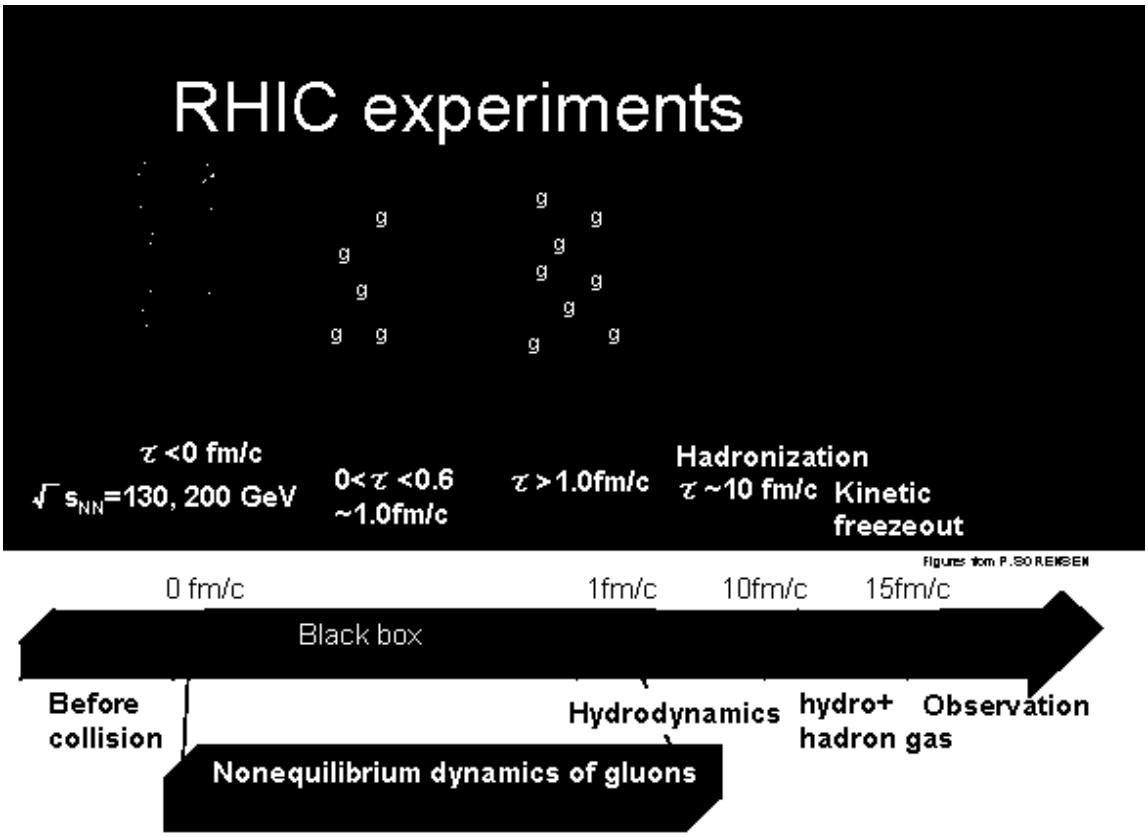

Figure 1: Sketch of relativistic heavy ion collisions at RHIC [19].

thermalizes at small $\tau_{\rm eq}$ of order of $0.6 \sim 1$ fm/c which is very fast compared with perturbative analysis [36].

Ideal fluid simulations for heavy-ion collisions at RHIC have been done in 2+1 dimensions [35], [37]-[42] and in 3+1 dimensions [25]-[28], [43]-[47]. Furthermore simulations of viscous hydrodynamics have been performed up to 2+1 dimensions [48]-[50]. In 2+1 dimensions longitudinal boost-invariance is assumed in the simulations, i.e. initial density profiles are independent of space-time rapidity $\eta_s = \frac{1}{2}\ln\left[(z+t)/(z-t)\right]$ where z is the beam direction. There initial transverse distributions of energy and baryon density must be determined to simulate in the above approaches. For setting initial conditions of hydrodynamics, two leading models are under study: The Glauber model[51, 52] and the Kharzeev-Levin-Nardi (KLN) model [53]-[59] based on the Color Glass Condensate (CGC) theory.

However since preequilibrium simulations are lacking, it is difficult to precisely determine the initial conditions of hydrodynamics phenomenologically. The microscopic processes that generate the initial conditions are still poorly understood. It has not been also well understood yet how the fast thermalization of produced gluonic system occurs before simulations of ideal hydrodynamics set in. One of the aims in the present research is to derive the initial conditions of hydrodynamics. So far plasma instabilities, for example Weibel type [60], are intensively investigated, where the coupled equations of motion for 'soft' classical gauge fields and 'hard' classical partons with anisotropic initial momentum distribution. Quantitative estimates of the dynamics rely on a separation of scales between 'soft' and 'hard' momenta for sufficiently small characteristic running gauge coupling [61]-[64]. Normally Yang-Mills equation is applied for the soft fields, while Boltzmann-Vlasov equation is used for the hard partons. The latter is based on kinetic theory with collisions for hard particles coupled to a soft classical field and it has been developed in plasma physics where the long range Coulomb force plays an essential role. However this approach has two drawbacks. First Boltzmann equation should not be applied for dense system, such as Glasma. Field theoretical analyses are necessary for the produced dense gluonic system. Secondly it lacks particle decay processes, such as $g \leftrightarrow gg$ and $g \leftrightarrow ggg$. They are possible when we treat the off-shellness of particles (Off-shell effects), but kinematically prohibited in the normal Boltzmann approach. They may contribute to thermalization processes of the system. Kadanoff-Baym theory that we try to apply to gluonic states is based on well-established field theoretical approach and can trace dynamics with offshell propagation of particles. Thermalization of gluons with this theory has not been investigated so far.

However QCD is known to be limited in a very narrow range of applicability. The existence of weakly coupled quark-gluon matter was anticipated on the basis of asymptotic freedom of QCD [1, 2, 3]. Thus let us consider the high temperature regions by adopting the fact that at sufficiently high temperature the gauge coupling constant becomes small enough to use weak coupling expansion [65, 66]. The description of QGP from the point of view of weakly coupled matter is not complicated. Many properties are similar to normal electromagnetic plasma in the relativistic regime [67, 68, 69].

The Kadanoff-Baym theory that we try to apply to QCD has the following history. As early as 1960s, based on a functional formulation of Luttinger and Ward [70], Baym and Kadanoff studied the Dyson-Schwinger equation for the two-point function $G(x,y)$ [71]. Then Baym reformulated it in terms of variational principle, introducing the so-called Φ-derivable approximation [72, 73]. The functional $\Phi[G]$ is given by a truncated set of closed two-particle irreducible (2PI) diagrams, and generates the driving terms of the equations of motion. The main virtue of this approximation is that the resulting KB equations conserve the energy and momentum of the system. This approach was extended to relativistic systems and formulated using the path integral by Cornwall, Jackiw and Tomboulis in [74]. It can be extended further to more general non-equilibrium many-body systems based on the Schwinger-Keldysh real-time path integral method [75, 76, 77].

Nonequilibrium quantum field theoretical approach plays a significant role in a variety of areas of physics, such as cosmology, ultrarelativistic heavy ion collisions, or condensed matter physics. For cosmology there is the issue of reheating of the early universe[78, 79]. In order to explain the hot universe observed from the cosmic microwave background after the inflation, there must appear enormous entropy growth due to particle production from the mean field (inflaton field).

During the early stage of inflation, all energy is contained in a slowly evolving inflaton field. Particle production from a coherently oscillating inflaton field occurs in nonperturbative regime of a parametric-resonance instability. Thus it is necessary to trace the time evolution of such quantum processes with nonperturbative field theoretical approach [80, 81, 82, 83]. Furthermore this approach can be applied to other nonequilibrium phenomena in condensed matter physics as well as cosmology. An example is the study of Bose-Einstein Condensate(BEC) [84, 85, 86, 87]. In the study we need both gapless excitation above the condensate and conservation laws of particle number and energy-momentum [88]. 2PI effective action approach is a candidate for the study of BEC since it yields a theory which is both gapless and conserving [89]. In practice, we take a truncation of the full effective action, but it may violate the property of gapless excitation [90]. It has been become expected to apply these approaches to nonequilibrium processes in the heavy ion collisions.

So far the real-time field dynamics has been investigated by several authors. A seminal work was carried out by Danielewicz[91], who for the first time studied the full KB equations in the context of the heavy ion collisions at non-relativistic energies. He used a spatially homogeneous initial condition with the non-spherical Fermi distribution for the nucleon momentum. Thermalization problem in the relativistic $\lambda\phi^4$ scalar field theory in 1+1 [92, 93], 2+1 [94] and 3+1 dimensions [95], has been numerically investigated with keeping the NLO skeleton diagrams of Φ in the symmetric phase. Similar analyses have been also done in the broken phase in 1+1 [96] and 3+1 [97] dimensions by solving the coupled equations of the mean field and fluctuations. Recently the numerical study has been extended to the system in an expanding (Friedmann-Robertson-Walker) background [82]. Similarly in the $O(N)$ theory the next-to-leading order in $1/N$ expansion of skeletons is derived in Ref. [98] and numerically investigated in the symmetric phase in Ref. [99]. In the broken phase in the $O(N)$ theory, numerical analyses have been done in Refs. [83, 81]. Next-to-Next-to-leading order is also derived in Ref. [100], and the rapid convergence property for moderate values of $1/N$ is estimated [101]. The study is not restricted into bosons. Extension to Yukawa model has been done in Ref. [102] with LO skeleton expansion in 3+1 dimensions, and comparison of Quantum dynamics with the Boltzmann dynamics has been done in Ref. [103]. Fermion-induced instability is also estimated by combining $1/N$ (N is the number of mesons) expansion and LO boson-fermion interacting diagram in Yukawa model [104]. Moreover the quark-meson model is investigated in Ref. [105] and characteristic nonequilibrium phenomena, such as an early prethermalization of the equation of state, have been quantitatively studied. Importantly, all these analyses indicate that thermalization is achieved in course of the time evolution of the system independently of the initial conditions. The number distribution functions of the quasi-particles are found to approach the Bose-Einstein or Fermi-Dirac distribution. Near equilibrium transport coefficients are estimated in the O(N) with NLO of $1/N$ expansion in Ref. [106]. Moreover in large N_f gauge theories, the shear viscosity and the electric conductivity are calculated with NLO of $1/N_f$ expansion in Ref. [107]. In the context of the analysis of thermalization, kinetic entropy based on the KB equation which satisfies H-theorem is introduced in both non-relativistic ϕ^4 theory in Refs. [108, 109] and relativistic case and is numerically estimated in Ref. [110]. The above thermalization properties is consistent to the H-theorem in ϕ^4 theory, and it can be in the other theories. The proof of H-theorem is one of the criteria to investigate without numerical simulation whether the thermalization occur in the system or not.

Our work is directed toward theoretical understanding of thermalization of quantum fields with off-shell effects and based on the kinetic entropy and proof of H-theorem in KB equation. Once system entropy is introduced appropriately in field theories, thermalization of quantum field will be quantitatively characterized. It remains an open question how to choose the gross variables and define the corresponding entropy in non-equilibrium situations. No entropy production occurs in fully microscopic approach [111]. In this paper we shall adopt the variable $G(x, y)$ and introduce kinetic entropy in relativistic quantum field theory in the first order of the gradient expansion of KB equation. It provides us a criterion of how each microscopic process contributes to thermalization of the system. The KB theory based on 2PI effective action deals with the evolution of the field $\langle\phi\rangle$ and the two-point Green's function $G(x, y)$, and effectively contain particle number changing

processes, such as $1 \leftrightarrow 3$ in the NLO of coupling and $1/N$ expansion in scalar theory (and $1 \leftrightarrow 2$ in LO of coupling expansion in gauge theory), if interpreted in the particle basis. In contrast, the Boltzmann equation includes only the $2 \leftrightarrow 2$ scattering processes in this order. This difference affects the evolution of quantum field, especially entropy production of the system. We prove that the evolution of Green's function with nonzero collision term ($C \neq 0$), which contain the above particle number changing processes, contributes to entropy production at the level of Green's functions in scalar theory due to H-theorem and also extend the analyses to gauge theory. We expect that this aspect of entropy production in KB equations is important to understand the possibility of the fast thermalization.

For demonstration, we numerically solve the non-equilibrium dynamics of $\lambda\phi^4$ theory and $O(N)$ theory on the basis of the KB equations. In order to reduce the numerical cost, we restrict our simulations to the spatially uniform case without the mean field $\langle\phi\rangle = 0$ and expansion of the system in $1+1$ and $2+1$ dimensions for ϕ^4 theory and in $1+1$ dimensions for $O(N)$ theory. We start the numerical analyses with the non-thermal initial conditions, and show the time evolution of the system through the particle number distribution functions, total energy, entropy density and so on.

This paper is organized as follows. In Sec. 2 we review the formation of 2 particle irreducible (2PI) effective action and the derivation of Kadanoff-Baym (KB) equation with non-secularity and universality at late times. In Sec. 3 we show the derivation of KB equation with next-to-leading order (NLO) self-energy of the coupling in ϕ^4 theory. Here we introduce the kinetic entropy for the relativistic KB equation in the first order in the gradient expansion and show the H-theorem for NLO self-energy of the coupling. The expression for the entropy is found to be a natural extension of the non-relativistic one in Refs. [108, 109]. We also present the numerical simulations with KB equation and estimate the particle number distribution and this entropy of the system in far-from equilibrium. In Sec. 4 we show the derivation of KB equation with NLO self-energy of $1/N$ expansion in $O(N)$ theory. Here we show that the kinetic entropy derived in the previous section satisfies H-theorem for the self-energy without changing its expression. Next we also show the numerical simulations of the KB equation and estimate the entropy in the time evolution. Next Sec. 5 is devoted to review some technical approaches to thermal gauge theory beyond the naive perturbation theory before getting into far-from equilibrium. Here we compare merits and demerits of each approach. In Sec. 6 we show the formation of 2PI effective action and the derivation of KB equation in non-Abelian gauge theory. We try to derive the kinetic entropy for KB equation in the first order gradient expansion and show its H-theorem for leading order (LO) self-energy of the coupling in temporal axial gauge (TAG). Finally Sec. 7 is devoted to summary of this study.

2 Preparation

In this section at first we introduce the 2 particle irreducible (2PI) effective action in non-equilibrium field theories [74]. N particle effective action is powerful theoretical approach to nonequilibrium quantum fields. In particular 2PI effective action gives a powerful tool to provide the controlled dynamics in nonequilibrium quantum field theory. This technique provides an efficient approximation schemes to analyze in and out of equilibrium system where resummations are needed [89].

Next we show the derivation of an equation of motion of mean field and Schwinger-Dyson equation for quantum fluctuations by taking the stationary point of the effective action. By truncating or classifying the series of diagrams it is possible to trace the time evolution of mean fields and fluctuations.

Finally we consider the problems of secularity and the realization of universality in late-time behavior. There we find that naive perturbation and 1PI technique suffer from secular terms which grow with time and prevent us from studying non-equilibrium processes. We study how 2PI approach achieves the controlled time evolution of mean field and fluctuations without secularity in far from equilibrium. Moreover 2PI technique achieves the universality at late time, that is the property of the system is independent of the details of initial conditions and determined only by its total energy and conserved charges. One of the reasons of the universality is the non-linearity of the equation of motion after infinite iteration procedures of fluctuations in 2PI technique.

2.1 N Particle Irreducible Effective Action

In this subsection we introduce 1 particle irreducible (1PI) and 2 particle irreducible (2PI) effective action. Let us begin with the following quantum field theory for a real scalar field $\hat{\phi}$ with the classical action $S[\hat{\phi}]$

$$S[\hat{\phi}] = \int d^{d+1}x \left(\frac{1}{2}\partial^\mu \hat{\phi}_a(x)\partial_\mu \hat{\phi}_a(x) - \frac{m^2}{2}\hat{\phi}_a(x)\hat{\phi}_a(x) - \frac{V^{(3)}_{abc}}{3!}\hat{\phi}_a(x)\hat{\phi}_b(x)\hat{\phi}_c(x) - \frac{V^{(4)}_{abcd}}{4!}\hat{\phi}_a(x)\hat{\phi}_b(x)\hat{\phi}_c(x)\hat{\phi}_d(x) \right) \tag{1}$$

where $V^{(n)}_{a\cdots}$ are symmetric in the indices.

To provide the (connected) Green's functions it is convenient to give the following generating functional $Z[J,K]$ ($W[J,K]$) with two external sources or components of the initial density matrix,

$$\begin{aligned} Z[J,K] &= \exp(iW[J,K]) = \mathrm{Tr}\,(\rho(t)) \\ &= \int \Pi_{\mathbf{x}} d\hat{\phi}_a(\mathbf{x},a)\langle\phi(x)|\rho(t)|\phi(x)\rangle \\ &= \int \mathcal{D}\hat{\phi} \exp\left(i\left[S[\hat{\phi}] + \int_x J_a(x)\hat{\phi}_a(x) + \frac{1}{2}\int_{x,y} K_{ab}(x,y)\hat{\phi}_a(x)\hat{\phi}_b(x) \right] \right) \end{aligned} \tag{2}$$

where the time integral is on closed time path used in Refs. [75, 76, 77, 114] as shown in Fig. 2. The sources J_a and K_{ab} come from both external source and Gaussian initial density matrix. We restrict ourselves into such a Gaussian type of density matrix. The expectation value can be derived by differentiating the $W[J,K]$ with respect to $J_a(x)$ and $K_{ab}(x,y)$ and taking the limit of zero source $J,\ K=0$ as

$$\left. \frac{\delta^n W[J,K]}{\delta J_{a_1}(x_1)\delta J_{a_2}(x_2)\cdots\delta J_{a_n}(x_n)} \right|_{J,K=0} = G_{a_1 a_2 \cdots a_n}(x_1, x_2, \cdots, x_n),$$

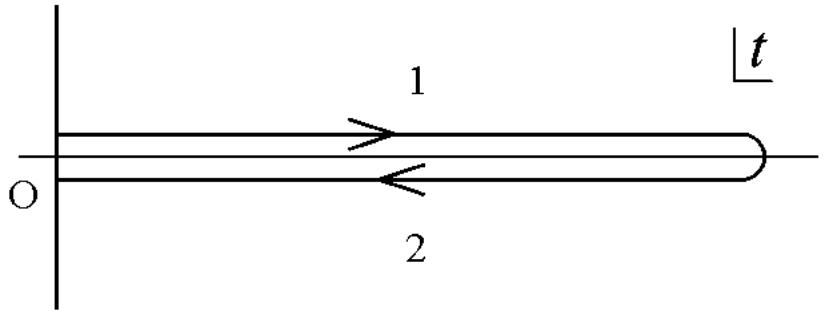

Figure 2: Time contour of Closed Time Path formalism. The contour 1 denotes the path from 0 to infinity and 2 represents the path from infinity to 0.

$$\left.\frac{\delta W[J,K]}{\delta J_a(x)}\right|_{J,K=0} = \phi_a(x), \quad \left.\frac{\delta^2 W[J,K]}{\delta J_a(x)\delta J_b(y)}\right|_{J,K=0} = G_{ab}(x,y),$$
$$\left.\frac{\delta W[J,K]}{\delta K_{ab}(x,y)}\right|_{J,K=0} = \frac{1}{2}\left(\phi_a(x)\phi_b(y) + G_{ab}(x,y)\right) \quad \text{etc.} \tag{3}$$

We shall construct 1PI effective action via a Legendre transform with respect to the source term linear in the field,

$$\Gamma^K[\phi] = W[J,K] - \int_x \frac{\delta W[J,K]}{\delta J_a(x)} J_a(x) = W[J,K] - \int_x \phi_a(x) J_a(x). \tag{4}$$

Then we obtain

$$\frac{\delta \Gamma^K[\phi]}{\delta \phi_a(x)} = \frac{\delta W[J,K]}{\delta J_b(y)}\frac{\delta J_b(y)}{\delta \phi_a(x)} - \frac{\delta J_b(y)}{\delta \phi_a(x)}\phi_b(y) - J_a(x) = -J_a(x) \tag{5}$$

where the first two terms in the R.H.S. cancel due to the relation $\delta W[J,K]/\delta J_b(y) = \phi_b(y)$. The explicit form of the 1PI effective action $\Gamma^{K=0}[\phi]$ for vanishing source $K = 0$ is written as

$$\Gamma^{K=0}[\phi] = S[\phi] + \frac{i}{2}\mathrm{Trln} G_0^{-1}(\phi) + \cdots \tag{6}$$

where $iG_0^{-1}[\phi] = \left.\frac{\delta^2 S[\phi]}{\delta\phi_a(x)\phi_b(y)}\right|_{\phi=0}$ due to the relation

$$\begin{aligned}
\Gamma^{K=0}[\phi] &= -i\ln Z[J,K=0] - J\cdot\phi \\
&= -i\ln \int D\hat{\phi} \exp\left[i\left(S[\phi] + (\hat{\phi}-\phi)\left(\frac{\delta S}{\delta\phi} + J\right) + \frac{1}{2}(\hat{\phi}-\phi)\frac{\delta^2 S}{\delta\phi\delta\phi}(\hat{\phi}-\phi) + \cdots\right)\right] \\
&= -i\ln\left(\exp\left[iS[\phi]+\cdots\right]\det\left(iG_0^{-1}\right)^{-\frac{1}{2}}\right) \\
&= S[\phi] + \frac{i}{2}\mathrm{trln}\left(G_0^{-1}\right) + \cdots.
\end{aligned} \tag{7}$$

In the presence of two-point source K, 1PI effective action can be derived by changing $S[\hat{\phi}] \to S^K[\hat{\phi}] \equiv S[\hat{\phi}] + \frac{1}{2}\int_{x,y} K_{ab}(x,y)\hat{\phi}_a(x)\hat{\phi}_b(y)$ and $G_0^{-1} \to G_0^{-1} - iK$ as

$$\Gamma^K[\phi] = S^K[\phi] + \frac{i}{2}\mathrm{trln}\left[iG_0^{-1}(\phi) - iK\right] + \cdots. \tag{8}$$

From the 1PI effective action (8) we find the exact inverse Green's functions by second differentiation of the field ϕ as

$$\begin{aligned}\frac{\delta^2\Gamma^K[\phi]}{\delta\phi_a(x)\delta\phi_b(y)} &= iG^{-1}_{ab}(x,y) \\ &= i\left[G^{-1}_{0ab}(x,y) - iK_{ab}(x,y) - \Sigma^K_{ab}(x,y)\right] \end{aligned} \tag{9}$$

where the inverse Green's function $iG^{ab}_{0ab}(x,y;\phi) = \frac{\delta^2 S[\phi]}{\delta\phi_a(x)\delta\phi_b(y)}$ can be derived as

$$iG^{-1}_{0ab}(x,y;\phi) = -\left[\left(\partial_x^2 + m^2\right)\delta_{ab} + V^{(3)}_{abc}\phi_c(x) + \frac{V^{(4)}_{abcd}}{2}\phi_c(x)\phi_d(x)\right]\delta^{d+1}(x-y), \tag{10}$$

and $\Sigma^K_{ab}(x,y)$ contains only one-particle irreducible diagrams, which cannot be separated by cutting one internal line.

We can derive the 2PI effective action by performing the Legendre transformation of $\Gamma^K[\phi]$ with respect to the two-point source K as

$$\begin{aligned}\Gamma[\phi,G] &= \Gamma^K[\phi] - \int_{xy}\frac{\delta W[J,K]}{\delta K_{ab}(x,y)}K_{ba}(y,x) \\ &= \Gamma^K[\phi] - \frac{1}{2}\int_{xy}K_{ab}(x,y)\phi_a(x)\phi_b(y) - \frac{1}{2}\mathrm{Tr}KG \\ &= S[\phi] + \frac{i}{2}\mathrm{Trln}\left[G_0^{-1}(\phi) - iK\right] - \frac{1}{2}\mathrm{Tr}KG \end{aligned} \tag{11}$$

where we have used (8).

Since $\Gamma[\phi,G]$ is the Legendre transformation of $W[J,K]$ written as

$$\begin{aligned}\Gamma[\phi,G] &= W[J,K] - \int_x\frac{\delta W[J,K]}{\delta J_a(x)}J_a(x) - \int_{xy}\frac{\delta W[J,K]}{\delta K_{ab}(x,y)}K_{ba}(y,x) \\ &= W[J,K] - \int_x\phi_a(x)J_a(x) - \frac{1}{2}\int_{xy}K_{ab}(x,y)\phi_a(x)\phi_b(y) - \frac{1}{2}\mathrm{Tr}GK, \end{aligned} \tag{12}$$

$\Gamma[\phi,G]$ satisfies the following stationary relations:

$$\begin{aligned}\frac{\delta\Gamma[\phi,G]}{\delta\phi_a(x)} &= -J_a(x) - \int_y K_{ab}(x,y)\phi_b(y), \\ \frac{\delta\Gamma[\phi,G]}{\delta G_{ab}(x,y)} &= -\frac{1}{2}K_{ab}(x,y). \end{aligned} \tag{13}$$

This stationary relations give the equations of motion for ϕ and G.

If we set $G^{-1} = G_0^{-1}(\phi) - iK$ by neglecting Σ term, we can rewrite down as

$$\Gamma[\phi,G] \simeq S[\phi] + \frac{i}{2}\mathrm{Trln}G^{-1} + \frac{i}{2}\mathrm{Tr}G_0^{-1}G + \mathrm{const} \tag{14}$$

with $\mathrm{Tr}G^{-1}G = \mathrm{Tr}\mathbf{1} = \mathrm{const}$.

The verification of the above trial in this order is to differentiating $\Gamma[\phi,G]$ by G and extract the equation

$$\begin{aligned}\frac{\delta\Gamma}{\delta G} &\simeq -\frac{i}{2}G^{-1} + \frac{i}{2}G_0^{-1}(\phi) = -\frac{1}{2}K \\ \longrightarrow G^{-1} &= G_0^{-1}(\phi) - iK. \end{aligned} \tag{15}$$

When we extract the information beyond this order, we add $\Gamma_2[\phi, G]$ term to give the exact $\Gamma[\phi, G]$ to the one-loop type expression (14):

$$\Gamma[\phi, G] = S[\phi] + \frac{i}{2}\mathrm{Tr}\ln G^{-1} + \frac{i}{2}\mathrm{Tr}G_0^{-1}(\phi)G + \Gamma_2[\phi, G] + \text{const.} \tag{16}$$

The meaning of the $\Gamma_2[\phi, G]$ can be found by differentiating this $\Gamma[\phi, G]$ with respect to G and deriving the expression

$$G^{-1}_{ab}(x, y) = G^{-1}_{0,ab}(x, y; \phi) - iK_{ab}(x, y) - \Sigma_{ab}(x, y; \phi, G), \tag{17}$$

where we have defined

$$\Sigma_{ab}(x, y; \phi, G) \equiv 2i\frac{\delta\Gamma_2[\phi, G]}{\delta G_{ab}(x, y)}. \tag{18}$$

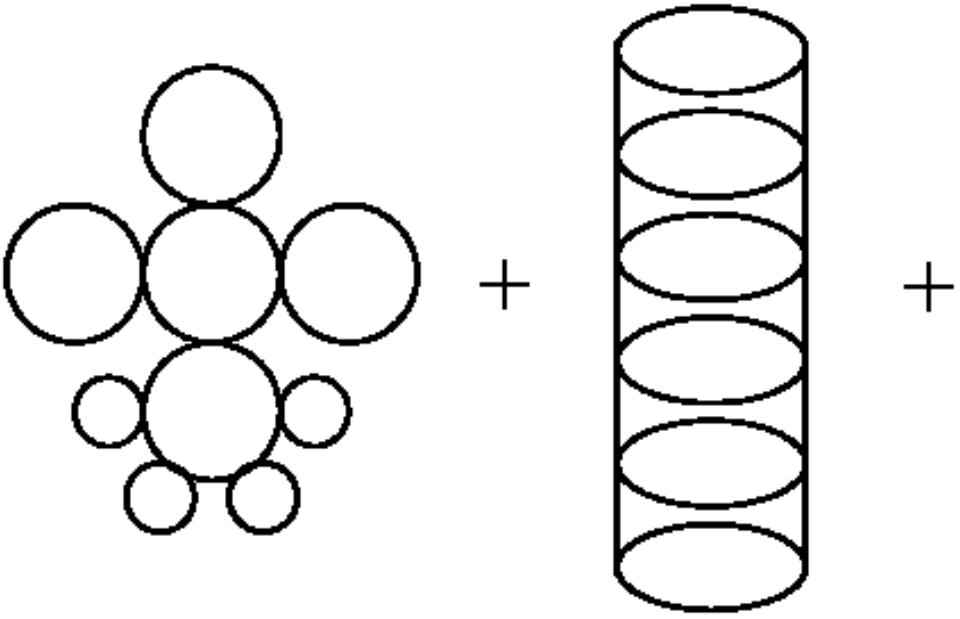

Figure 3: The daisy and the ladder diagrams.

Here let us compare the exact Schwinger Dyson equation (9) and the above relation (17), we can observe that

$$\Sigma_{ab}(x, y; \phi, G) = \Sigma^K_{ab}(x, y; \phi). \tag{19}$$

$\Sigma_{ab}(x, y; \phi, G)$ is the functional G-derivative of $\Gamma_2[\phi, G]$, and $\Sigma^K_{ab}(x, y; \phi)$ is the self energy only 1PI diagrams contribute with Green's function lines associated the effective Green's function $(G_0^{-1} - K)^{-1}$. Then the full Green's function G is given by an infinite series in terms of G_0,K and Σ:

$$\begin{aligned} G &= \frac{1}{G_0^{-1} - iK} + \frac{1}{G_0^{-1} - iK}\Sigma\frac{1}{G_0^{-1} - iK} \\ &\quad + \frac{1}{G_0^{-1} - iK}\Sigma\frac{1}{G_0^{-1} - iK}\Sigma\frac{1}{G_0^{-1} - iK} + \cdots. \end{aligned} \tag{20}$$

Since only 1PI diagrams contribute to $\Sigma(\phi, G)$, we can conclude that $\Gamma_2[\phi, G]$ contains only components from two-particle-irreducible (2PI) diagrams. The diagrams which are called two-particle-irreducible have the properties that they do not become disconnected by cutting two lines. This

means 2PI diagrams in $\Gamma_2[\phi, G]$ have the structure $\tilde{V}GG\tilde{V}'$ where $\tilde{V}, \tilde{V}'$ represents the parts of diagrams, so that $\Sigma(\phi, G) \sim \tilde{V}G\tilde{V}'$ and Σ becomes 1PI. If $\Gamma_2[\phi, G]$ has two-particle-reducible components, Σ has one-particle-reducible components. Such a structure cannot occur for the proper self-energy. Therefore the daisy and the ladder diagrams which are two particle reducible and depicted in Fig.3 are not contained in $\Gamma_2[\phi, G]$. Due to (20) 2PI are obtained from infinite series of 1PI diagrams (daisy and ladder and their combinations), and all the 2PI diagrams contain full series of daisy and ladder resummations. This properties can be also verified from another derivation of 2PI effective action. (See Appendix A.)

The examples of 2PI diagrams are shown in Fig.4. The diagrams contributing $\Sigma[\phi, G]$ are obtained by cutting one Green's function as depicted in Fig.4, and the series of self energy $\Sigma[\phi, G]$ are 1PI.

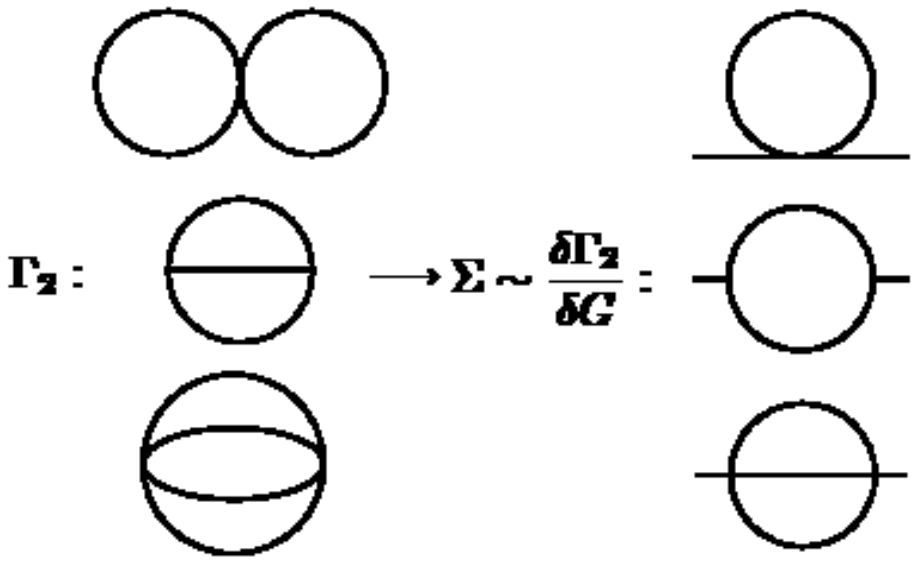

Figure 4: Two-Particle-Irreducible diagrams in Γ_2 and self energy Σ where each line represents Green's functions G.

Feynman rules of the loop or coupling expansion in 2PI effective action is the same as 1PI effective action except two points. First as a Green's function line we use the full Green's function G. Secondly we keep only 2PI diagrams. As a practice we express diagrams in Fig.4 by equations. We have a interaction term

$$iS_{int}[\hat{\phi}] = -\int_x \frac{i}{3!} V^{(3)}_{abc}(x)\hat{\phi}_a(x)\hat{\phi}_b(x)\hat{\phi}_c(x) - \int_x \frac{i}{4!} V^{(4)}_{abcd}(x)\hat{\phi}_a(x)\hat{\phi}_b(x)\hat{\phi}_c(x)\hat{\phi}_d(x) \tag{21}$$

where $V^{(3)}_{abc}(x)$ and $V^{(4)}_{abcd}(x)$ represent cubic and quartic vertices. When we assume $\phi \equiv \langle \hat{\phi}_a \rangle = 0$,

three diagrams of $\Gamma_2[\phi, G]$ can be written down as

$$
\begin{aligned}
i\Gamma_2^{(1)} &= \frac{-i}{4!}\int_x V^{(4)}_{abcd}(x)G_{ab}(x,x)G_{cd}(x,x)\times 3 = -\frac{i}{8}\int_x V^{(4)}_{abcd}(x)G_{ab}(x,x)G_{cd}(x,x),\\
i\Gamma_2^{(2)} &= \frac{1}{2}\cdot\frac{-i}{3!}\cdot\frac{-i}{3!}\int_{xy} V^{(3)}_{abc}(x)G_{ad}(x,y)G_{be}(x,y)G_{cf}(x,y)V^{(3)}_{def}(y)\times 3!\\
&= -\frac{1}{12}\int_{xy} V^{(3)}_{abc}(x)G_{ad}(x,y)G_{be}(x,y)G_{cf}(x,y)V^{(3)}_{def}(y),\\
i\Gamma_2^{(3)} &= \frac{1}{2}\cdot\frac{-i}{4!}\cdot\frac{-i}{4!}\int_{xy} V^{(4)}_{abcd}(x)G_{ae}(x,y)G_{bf}(x,y)G_{cg}(x,y)G_{dh}(x,y)V^{(4)}_{efgh}(y)\times 4!\\
&= -\frac{1}{48}\int_{xy} V^{(4)}_{abcd}(x)G_{ae}(x,y)G_{bf}(x,y)G_{cg}(x,y)G_{dh}(x,y)V^{4}_{efgh}(y),
\end{aligned}
\tag{22}
$$

where we have used the fact that Feynman rules are applied to $i\times\Gamma_2[\phi,G]$. The self energies can be derived by $\Sigma = 2i\delta\Gamma_2/\delta G$ as

$$
\begin{aligned}
\Sigma^{(1)}_{ab}(x,y) &= \frac{-i}{2}V^{(4)}_{abcd}(x)G_{cd}(x,y)\delta_C(x-y),\\
\Sigma^{(2)}_{ad}(x,y) &= -\frac{1}{2}V^{(3)}_{abc}(x)V^{(3)}_{def}(y)G_{bf}(x,y)G_{cg}(x,y),\\
\Sigma^{(3)}_{ae}(x,y) &= -\frac{1}{6}V^{(4)}_{abcd}(x)V^{(4)}_{efgh}(y)G_{bf}(x,y)G_{cg}(x,y)G_{dh}(x,y).
\end{aligned}
\tag{23}
$$

The above procedure can be generalized to construct NPI effective actions. For the NPI effective action the skeleton diagrams are calculated using dressed propagators as well as dressed N-point proper vertices; the $(N+1)$-point vertex is bare.

2.2 Realization of non-secularity and universality

There are various powerful approaches to study thermal equilibrium as well as the vacuum. However when we investigate the nonequilibrium situations, we encounter additional difficulties. The first aspect is the issue of secularity. In the perturbation theory we suffer from the presence of secular terms, which grow with time and invalidate the analysis of the nonequilibrium system even in a weak coupling case. They also appear in standard $1/N$ expansions where N represents the number of field components despite its nonperturbative analysis. In addition we require universality: the late-time behavior in the system is independent of the details of its initial conditions. In other words the property of the system must be determined only by its energy density and conserved charges at late time. In order to realize both non-secularity and universality it is necessary to employ nonlinear dynamics with resummation. In the nonequilibrium quantum field theories N-particle irreducible approach is the promising systematic approaches to cure the problem of secularity and to realize the universality[113]. 2PI formalism is the simplest example which has both non-secularity and universality.[1]

2.2.1 Secularity

Here we shall consider the secularity problem which occurs in naive perturbation theory of a relativistic real scalar theory with $\mathcal{L} = \frac{1}{2}(\partial\hat{\phi})^2 - \frac{m^2}{2}\hat{\phi}^2 - \frac{\lambda}{4!}\hat{\phi}^4$. We restrict ourselves the system without the condensate $\langle\hat{\phi}\rangle = 0$ and assume spatial homogeneity.

In the closed time path (CTP) formalism the time ordered Green's function in the matrix

[1] 1PI still has the problem of secularity.

notation is given by

$$
\begin{aligned}
G^{a\,b}(x,y) &= \begin{pmatrix} G^{11}(x,y) & G^{12}(x,y) \\ G^{21}(x,y) & G^{22}(x,y) \end{pmatrix} \\
&\equiv \begin{pmatrix} \mathrm{Tr}\left[\rho T\left(\hat{\phi}(x)\hat{\phi}(y)\right)\right] & \mathrm{Tr}\left[\rho\left(\hat{\phi}(y)\hat{\phi}(x)\right)\right] \\ \mathrm{Tr}\left[\rho\left(\hat{\phi}(x)\hat{\phi}(y)\right)\right] & \mathrm{Tr}\left[\rho\tilde{T}\left(\hat{\phi}(x)\hat{\phi}(y)\right)\right] \end{pmatrix}
\end{aligned} \tag{24}
$$

where T and $\tilde{T}$ are time ordering and anti-time ordering symbol, respectively, and $a, b = 1, 2$ denotes the branch of the time contour of Fig.2 in the previous section. For free field $\lambda = 0$ the bare Green's function $G_0^{ab}(x,y)$ is given by

$$
\begin{aligned}
G_0^{11}(x,y) &= \int \frac{d^{d+1}p}{(2\pi)^{d+1}} e^{-ip\cdot(x-y)} \left[\frac{i}{p^2-m^2+i\epsilon} + 2\pi\delta(p^2-m^2)n_{\mathbf{p}}^0\right] \\
G_0^{12}(x,y) &= \int \frac{d^{d+1}p}{(2\pi)^{d+1}} e^{-ip\cdot(x-y)} 2\pi\delta(p^2-m^2)\left[\theta(-p^0)+n_{\mathbf{p}}^0\right] \\
G_0^{21}(x,y) &= \int \frac{d^{d+1}p}{(2\pi)^{d+1}} e^{-ip\cdot(x-y)} 2\pi\delta(p^2-m^2)\left[\theta(p^0)+n_{\mathbf{p}}^0\right] \\
G_0^{22}(x,y) &= \int \frac{d^{d+1}p}{(2\pi)^{d+1}} e^{-ip\cdot(x-y)} \left[\frac{-i}{p^2-m^2-i\epsilon} + 2\pi\delta(p^2-m^2)n_{\mathbf{p}}^0\right]
\end{aligned} \tag{25}
$$

from $(\partial_x^2 + m^2)G_0(x,y) = -i\delta_C(x-y)$. Here the number density $n_{\mathbf{p}}^0$ is derived from

$$
\omega_{\mathbf{p}}(2n_{\mathbf{p}}^0+1) = \left[\partial_{x^0}\partial_{y^0}G_0^{12}(x^0,y^0,\mathbf{p}) + \omega_{\mathbf{p}}^2 G_0^{12}(x^0,y^0,\mathbf{p})\right]\big|_{x^0=y^0}, \quad \omega_{\mathbf{p}} = \sqrt{\mathbf{p}^2+m^2}, \tag{26}
$$

after the Fourier transformation with respect to the relative space $\mathbf{x}-\mathbf{y}$. In the analogy of the above $n_{\mathbf{p}}^0$ we can introduce an effective particle number density $n_{\mathbf{p}}(t)$:

$$
\omega_{\mathbf{p}}(2n_{\mathbf{p}}(t)+1) = \left[\partial_{x^0}\partial_{y^0}G^{12}(x^0,y^0,\mathbf{p}) + \omega_{\mathbf{p}}^2 G^{12}(x^0,y^0,\mathbf{p})\right]\big|_{x^0=y^0=t}, \quad \omega_{\mathbf{p}} = \sqrt{\mathbf{p}^2+m^2}, \tag{27}
$$

Next let us consider the Green's function with two-loop self energy $\Sigma_{2-\mathrm{loop}}(x-y) = -i\lambda G_0(x,x)\delta_C(x-y) - \lambda^2 G_0(x-y)^3/6$. Since the first term contributes to a simple mass shift and plays no role for the present discussion, we shall neglect it in the following analysis. Hence we write

$$
\Sigma_{2-\mathrm{loop}}(x-y) = -\frac{\lambda}{6}G_0^3(x-y). \tag{28}
$$

For $O(\lambda^2)$ the Green's function $G_{2-\mathrm{loop}}(x,y)$ is described as

$$
G_{2-\mathrm{loop}}(x,y) = G_0(x-y) + \int_C dudv G_0(x-u)\Sigma_{2-\mathrm{loop}}(u-v)G_0(v-y). \tag{29}
$$

By rewriting (29) with the number density $n_{\mathbf{p}}(t)$ (27) and $n_{\mathbf{p}}^0$ (26), $n_{\mathbf{p}}(t)$ is described by

$$
n_{\mathbf{p}}(t) - n_{\mathbf{p}}^0 = (1+n_{\mathbf{p}}^0)S_{\mathbf{p}}^{12}(t) - n_{\mathbf{p}}^0 S_{\mathbf{p}}^{21}(t), \tag{30}
$$

where S^{12} and S^{21} come from $G_0\cdot\Sigma_{2-\mathrm{loop}}\cdot G_0$ and are given with the Fourier transformed self-energy $\Sigma_{2-\mathrm{loop}}(\omega,\mathbf{p})$ as

$$
S^{12,\,21}(t) = -\frac{1}{\omega_{\mathbf{p}}}\int\frac{d\omega}{2\pi}\Sigma_{2-\mathrm{loop}}^{12,\,21}(\omega,\mathbf{p})\frac{2\sin^2(\omega-\omega_{\mathbf{p}})t}{(\omega-\omega_{\mathbf{p}})^2}. \tag{31}
$$

In the large time limit, we obtain

$$
S^{12,\,21}(t) \simeq -\frac{\Sigma_{2-\mathrm{loop}}^{12,\,21}(\omega_{\mathbf{p}},\mathbf{p})}{2\omega_{\mathbf{p}}} \times t. \tag{32}
$$

We find that the secularity occurs whenever the self-energy does not vanish ($\Sigma_{2-\mathrm{loop}}/2\omega_{\mathbf{p}} \neq 0$). Normally for the two-loop order the self-energy $\Sigma_{2-\mathrm{loop}}$ has non-zero value since

$$\Sigma^{12}_{2-\mathrm{loop}}(\omega_{\mathbf{p}}, \mathbf{p}) = -\frac{\lambda^2}{2}\int \frac{d^dq}{(2\pi)^d 2\omega_{\mathbf{q}}}\frac{d^dk}{(2\pi)^d 2\omega_{\mathbf{k}}}\frac{d^dr}{(2\pi)^d 2\omega_{\mathbf{r}}}\delta^{d+1}(q+k-r-p)\times n^0_{\mathbf{q}} n^0_{\mathbf{k}}(1+n^0_{\mathbf{r}}) \quad (33)$$

represents the contribution of 2-to-2 scattering processes $q + k \to r + p$ and does not vanish on-shell. Hence the problem of secularity remains. The problems of secularity also occur in higher order $G_0 \cdot (\Sigma_{2-\mathrm{loop}} \cdot G_0)^n$ for $n = 2, 3, \cdots$. The standard approach to improve these problems is to sum over infinite series of these secular terms:

$$\begin{aligned} G_2 &= G_0 + G_0 \cdot \Sigma_{2-\mathrm{loop}} \cdot G_0 + G_0 \cdot \Sigma_{2-\mathrm{loop}} \cdot G_0 \cdot \Sigma_{2-\mathrm{loop}} \cdot G_0 + \cdots \\ &= G_0 + G_0 \cdot \Sigma_{2-\mathrm{loop}} \cdot G_{2-\mathrm{loop}} \\ &= G_0 + G_0 \cdot \frac{(G_0 \cdot \Sigma_{2-\mathrm{loop}} \cdot G_0)}{G_0 - G_0 \cdot \Sigma_{2-\mathrm{loop}} \cdot G_0}. \end{aligned} \quad (34)$$

This is the usual resummation in terms of one-particle-irreducible (1PI) proper vertices. Then for the two-loop order 1PI Green's function becomes non-secular.

However the problem still remains in 1PI. As an example let us consider the following higher order $O(\lambda^4)$ self-energy:

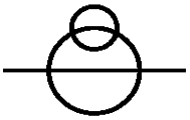

$$\sim \lambda^4 G_0^2(x-y) \times \left[\int_C du dv\; G_0(x-u) G_0^3(u-v) G_0(v-y)\right]. \quad (35)$$

This self-energy contains the same structure of secularity in the bracket and diverges at large times. Secularity appears in 4-loop order self-energy. Thus at higher order the problems of secularity occur one after another even if they are resolved in the lower order self-energy. Therefore we need to adopt resummation schemes beyond 1PI in order to resolve the problems of secularity which appears any higher-loop order self-energy.

Next we shall consider the resummation scheme beyond 1PI. The 4-loop self-energy is given by the sum of (29) and (35):

$$\Sigma_{4-\mathrm{loop}} = -\frac{\lambda^2}{6} G_0^2 \left(G_0 + G_0 \cdot \Sigma_{2-\mathrm{loop}} \cdot G_0\right). \quad (36)$$

By use of the analogy of 1PI resummation, we can remove the secularity in the bracket by summing over all 1PI insertion of $\Sigma_{2-\mathrm{loop}}$ as

$$-(\lambda^2/6)G_0^2(G_0 + G_0 \cdot \Sigma_{2-\mathrm{loop}} \cdot G_0 + G_0 \cdot \Sigma_{2-\mathrm{loop}} \cdot G_0 \cdot \Sigma_{2-\mathrm{loop}} \cdot G_0 + \cdots) = -(\lambda^2/6)G_0^2 G_2. \quad (37)$$

In the similar way we resum self-energy insertions on the other two Green's functions. As a result we obtain the following expression

$$\Sigma_{[2]} = -\frac{\lambda^2}{6} G_2^3 \quad (38)$$

where $G_2^{-1} = G_0^{-1} - \Sigma_{2-\mathrm{loop}}$ from (34) and $\Sigma_{2-\mathrm{loop}} = -(\lambda^2/6)G_0^3$. Hence the secularity in $\Sigma_{4-\mathrm{loop}}$ self-energy can be removed after the resummation. The secularity in 4-loop order self-energy appears on one internal line and is removed by resummation of infinite series of $\Sigma_{2-\mathrm{loop}}$ and replacement of the internal line by resumed G_2. In the similar way new secularity which appears in the 6-loop order self-energy described in the left diagram of Fig.5 is also removed by the following iteration. The left diagram has one secular part $G_0 \cdot \Sigma_{2-\mathrm{loop}} \cdot G_0$. First remove this secularity by resummation $G_0 \cdot \Sigma_{2-\mathrm{loop}} \cdot G_0 \to G_{[2]} = G_2 = G_0 + G_0 \cdot \Sigma_{2-\mathrm{loop}} \cdot G_0 + \cdots = 1/(G_0^{-1} - \Sigma_{2-\mathrm{loop}})$. Next we perform the same resummation for the other two internal line G_0 by $G_{[2]}$, then we obtain the middle

diagram in Fig.5. The middle diagram has the secular part $G_0 \cdot \Sigma_{[2]} \cdot G_0$ where $\Sigma_{[2]} = -\frac{\lambda^2}{6} G_{[2]}^3$. This secular part can be removed by the resummation $G_0 \cdot \Sigma_{[2]} \cdot G_0 \to G_{[4]} = G_0 + G_0 \cdot \Sigma_{[2]} \cdot G_0 + \cdots = 1/(G_0^{-1} - \Sigma_{[2]})$. Finally replace the other two internal line G_0 by $G_{[4]}$, then we obtain the non-secular $\Sigma_{[4]} = -\frac{\lambda^4}{6} G_{[4]}^3$ described in the right diagram of Fig.5. Similarly new secular terms which appear

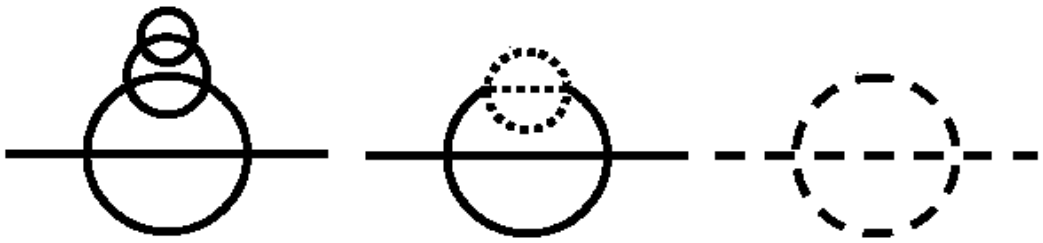

Figure 5: Procedure of removing the secularity of 6-loop order self-energy. In the left figure each line represents G_0, in the middle figure dotted line denotes $G_{[2]}$ and in the right figure broken line is $G_{[4]}$.

in 8-loop, 10-loop and higher loop order self-energy are removed in the process of constructing $\Sigma_{[6]}, \Sigma_{[8]}, \cdots$. Thus we can automatically remove secularity by repeating infinitely many iterations described in the following equation:

$$
\begin{aligned}
& & \Sigma_{[0]} &= -\frac{\lambda^2}{6} G_{[0]}^3, \quad G_{[0]} = G_0, \quad \Sigma_{[0]} = \Sigma_{2-\text{loop}} \\
G_{[2]}^{-1} = G_{[0]}^{-1} - \Sigma_{[0]}, \quad & \to & \Sigma_{[2]} &= -\frac{\lambda^2}{6} G_{[2]}^3, \quad G_{[2]} = G_2 \\
G_{[4]}^{-1} = G_{[0]}^{-1} - \Sigma_{[2]}, \quad & \to & \Sigma_{[4]} &= -\frac{\lambda^2}{6} G_{[4]}^3, \\
& & \cdots & \\
G_{[2(n+1)]}^{-1} = G_{[0]}^{-1} - \Sigma_{[2n]}, \quad & \to & \Sigma_{[2(n+1)]} &= -\frac{\lambda^2}{6} G_{[2(n+1)]}^3, \\
& & \cdots & \\
G_{[\infty]}^{-1} = G_{[0]}^{-1} - \Sigma_{[\infty]}. & & & \qquad (39)
\end{aligned}
$$

We can notice that after infinite series of iterations any 1PI $\Sigma_{2-\text{loop}}$ insertions are already included in $G_{[\infty]}$. As a result the non-linear equation with respect to full Green function $G = G_{[\infty]}$ is derived,

$$G^{-1} = G_0^{-1} - \Sigma[G] \qquad (40)$$

where

$$\Sigma[G] = -\frac{\lambda^2}{6} G^3. \qquad (41)$$

This Schwinger-Dyson equation is effectively described in 2PI effective action and secularity in this equation is already removed after the construction of the full Green's functions by infinite series of iterations.

2.2.2 Universality

In the previous subsection we see that it is possible to construct the Schwinger-Dyson equation with non-secularity by infinite series of iterations in constructing the full Green's functions. Here we can find that the procedure to construct the nonlinear SD equation in the previous subsection also guarantee the universality at late time in the on-shell limit.

First we start with 1PI equation $G_0^{-1}\cdot G_2 = 1 + \Sigma_{2-\mathrm{loop}}\cdot G_2$ in (34). From this equation the time evolution equation of the number density $n_{\mathbf{p}}(t)$ is given by

$$\begin{aligned}\omega_{\mathbf{p}}\partial_t n_{\mathbf{p}}(t) &= \mathrm{Re}\int_0^t dz^0\Big[\Sigma^{12}_{2-\mathrm{loop}}(t,z^0;\mathbf{p})(i\partial_t-\omega_{\mathbf{p}})G^{21}_{2-\mathrm{loop}}(z^0,t;\mathbf{p})\\ &\quad -\Sigma^{21}_{2-\mathrm{loop}}(t,z^0;\mathbf{p})(i\partial_t-\omega_{\mathbf{p}})G^{12}_{2-\mathrm{loop}}(z^0,t;\mathbf{p})\Big],\end{aligned} \tag{42}$$

by use of time derivative. Let us adopt the free-field like ansatz: $(i\partial_t-\omega_{\mathbf{p}})\,G^{12}_{2-\mathrm{loop}}(z^0,t;\mathbf{p}) = -n_{\mathbf{p}}e^{-i\omega_{\mathbf{p}}(z^0-t)}$ and $(i\partial_t-\omega_{\mathbf{p}})\,G^{21}_{2-\mathrm{loop}}(z^0,t;\mathbf{p}) = -(1+n_{\mathbf{p}})e^{-i\omega_{\mathbf{p}}(z^0-t)}$, by exchanging $n^0_{\mathbf{p}}$ to $n_{\mathbf{p}}(t)$ for G_0 in (25) where we have neglected the terms time derivative $\partial_t n_{\mathbf{p}}(t)$. Then we obtain the following evolution equation:

$$\partial_t n_{\mathbf{p}}(t) = (1+n_{\mathbf{p}}(t))\partial_t S^{12}_{\mathbf{p}}(t) - n_{\mathbf{p}}(t)\partial_t S^{21}_{\mathbf{p}}(t), \tag{43}$$

where $S^{12,\,21}_{\mathbf{p}}$ is given in (31). At the late time we find that because of (32) the $n_{\mathbf{p}}(t)$ has the following behavior

$$n_{\mathbf{p}}(t) \simeq n^0_{\mathbf{p}}e^{-\gamma_{\mathbf{p}}t} - \frac{\Sigma^{12}(\omega_{\mathbf{p}},\mathbf{p})}{2\omega_{\mathbf{p}}\gamma_{\mathbf{p}}}\left(1-e^{-\gamma_{\mathbf{p}}t}\right) \to \frac{\Sigma^{12}}{\Sigma^{21}-\Sigma^{12}}, \tag{44}$$

where $\gamma_{\mathbf{p}} \equiv \frac{\Sigma^{12}-\Sigma^{21}}{2\omega_{\mathbf{p}}}$. $\Sigma^{12,\,21}$ is determined by $n^0_{\mathbf{p}}$, so that this equation has no universal structure. The dependence of initial conditions stems from the linearity of the equation (402b). In order to achieve the late time universality we should introduce some non-linear equation.

Next let us consider the nonlinear SD equation (40) based on 2PI effective action. The nonlinearity comes from the iteration procedure to remove the secularity in any higher loop self-energy. We first restrict ourselves to discussions about its on-shell limit of the SD equation. From (40) time evolution equation of number density $n_{\mathbf{p}}(t)$ is given by

$$\begin{aligned}\omega_{\mathbf{p}}\partial n_{\mathbf{p}}(t) &= \frac{\lambda^2}{4}\int\frac{d^dq}{(2\pi)^d2\omega_{\mathbf{q}}}\frac{d^dk}{(2\pi)^d2\omega_{\mathbf{k}}}\frac{d^dr}{(2\pi)^d2\omega_{\mathbf{r}}}(2\pi)^{d+1}\delta^{(d+1)}(q+k-r-p)\\ &\quad\times\Big[n_{\mathbf{q}}(t)n_{\mathbf{k}}(t)(1+n_{\mathbf{r}}(t))(1+n_{\mathbf{p}}(t))\\ &\quad -n_{\mathbf{p}}(t)n_{\mathbf{r}}(t)(1+n_{\mathbf{k}}(t))(1+n_{\mathbf{q}}(t))\Big].\end{aligned} \tag{45}$$

The details of derivation are given in Ref. [114] or Appendix D with Sec. 3.1. The solution for $\partial_t n_{\mathbf{p}}(t) = 0$ is well known and given by the Bose distribution:

$$\frac{1+n^{\mathrm{eq}}_{\mathbf{p}}}{n^{\mathrm{eq}}_{\mathbf{p}}} = e^{(\omega_{\mathbf{p}}-\mu)/T}, \quad \text{or } n^{\mathrm{eq}}_{\mathbf{p}} = \frac{1}{e^{(\omega_{\mathbf{p}}-\mu)/T}-1}. \tag{46}$$

The number density $n^{\mathrm{eq}}_{\mathbf{p}}$ at equilibrium is determined only by its temperature T and chemical potential μ. The chemical potential is determined by the total energy and conserved charges. Thus the property of the system at late time is independent of initial conditions, and universality at late time is realized.

Finally we should comment on off-shell propagation which is peculiar in time evolution with SD equation. The SD equation contains quantum nonequilibrium processes beyond the Boltzmann equation (45) which stem from memory integral and the off-shellness which naturally appear in the nonequilibrium field theoretical approach. In this subsection we have considered the late time universality or thermalization only in the on-shell limit. Since the 2-to-2 scattering processes shown in (45) have a significant role even in the quantum dynamics based on SD equation, the thermalization might occur in the quantum dynamics based on SD equation. However, it remains difficult to confirm whether the thermalization occurs and the late time universality is realized in the offshell propagation with SD equation since the original SD equation has a time-reversible structure

although it has a nonlinear structure. In this paper we will discuss time-irreversibility, late-time universality and thermalization with entropy production. Then we will see that it is possible to confirm that time-irreversibility is realized in 1st order gradient expansion of SD equation and that within 1st order gradient expansion kinetic entropy increases monotonically at the level of Green's functions. There it is shown that any change of two independent Green's functions G^{12} and G^{21} which stems from nonzero collision term $C \neq 0$ contributes to entropy production within 1st order gradient expansion of SD equation. As a result late time universality, where the Green's functions are determined by the solution of the stationary relation $C = 0$ and dependent only on total energy and conserved charges, is realized[2].

[2]However why the thermalization occurs in the original time reversible SD equation without gradient expansion remains unclear (although in numerical simulations late time universality seems to be realized in the original equation).

3 Scalar ϕ^4 Theory

Non-equilibrium quantum field theories provide a suitable framework to investigate a large variety of topical problems in high energy particle physics, astrophysics, cosmology, as well as condensed matter physics[89, 112]. In the context of heavy ion collision physics, the early time evolution of the colliding system toward the quark-gluon plasma (QGP) state has attracted a lot of theoretical interests for recent years. Success of ideal hydrodynamic models for describing bulk properties of the matter created at Brookhaven's Relativistic Heavy Ion Collider (RHIC) seems suggesting that the produced system is strongly interacting and nearly thermalized within a short time[115] compared with perturbative analysis[36].

In the earliest stage of the high-energy nuclear collisions, the system will be so dense that it would be more suitable to describe the system in terms of the quantum field degrees of freedom than in the particle basis. As a first step of this approach toward the early time dynamics of the nuclear collisions, we study here the non-equilibrium $\lambda\phi^4$ scalar field theory on the basis of the Kadanoff-Baym (KB) equations. We introduce the kinetic entropy based on KB equation with first order gradient expansion and show the H-theorem for NLO self-energy of the coupling expansion. Then at the level of Green's functions $G(X,p)$ it is shown that entropy production occurs in the time evolution of KB equation with nonzero collision term ($C \neq 0$), which contain particle number changing processes $3 \leftrightarrow 1$ as well as $2 \leftrightarrow 2$ scattering processes. The introduced entropy gives us a criteria how fast the system approaches thermal equilibrium.

We shall numerically solve the non-equilibrium dynamics of $\lambda\phi^4$ theory in 1+1 and 2+1 dimensions on the basis of the KB equations. In order to reduce the numerical cost, Our simulations are restricted to the spatially uniform case without the mean field $\langle\phi\rangle = 0$ and expansion of the system. We begin the simulations with the non-thermal initial conditions, and show the time evolution of the system through the particle number distribution functions, the energy content, the entropy production and so on.

3.1 Kadanoff Baym equation at $O(\lambda^2)$ in ϕ^4 theory

We briefly review the derivation of Kadanoff-Baym equation and fix our notations[89]. For the scalar field theory $\mathcal{L} = \frac{1}{2}\partial_\mu\hat{\phi}\partial^\mu\hat{\phi} - \frac{1}{2}m^2\hat{\phi}^2 - \frac{1}{4!}\lambda\hat{\phi}^4$, the 2PI effective action with non-vanishing mean field $\phi \equiv \langle\hat{\phi}\rangle \neq 0$ (broken phase) is written as

$$\Gamma[\phi, G] \quad = \quad S[\phi] + \frac{i}{2}\mathrm{Trln}\,(G)^{-1} + \frac{i}{2}G_0^{-1}G + \frac{1}{2}\Phi[\phi, G]\,. \tag{47}$$

Here $iG_0^{-1}(x,y) = -\left(\partial_x^2 + m^2 + \frac{\lambda}{2}\phi(x)^2\right)\delta_{\mathcal{C}}(x-y)$ is the free Green's function and G is the full Green's function, both of which are defined on the2 closed time path $\mathcal{C}$. The functional $\frac{1}{2}\Phi[\phi, G]$ in (47) is generally a sum of all possible 2PI graphs written in terms of ϕ and G. A graph is called 2PI when it remains connected upon cutting two Green's function lines.

The stationary condition for the effective action (47)

$$\frac{\delta\Gamma}{\delta\phi} = 0, \quad \frac{\delta\Gamma}{\delta G} = 0 \tag{48}$$

gives rise to the equation for the mean field ϕ

$$\frac{\delta S[\phi]}{\delta\phi(x)} - \frac{1}{2}\lambda G(x,x)\phi = -\frac{1}{2}\frac{\delta\Phi[\phi, G]}{\delta\phi(x)}, \tag{49}$$

and the Schwinger-Dyson equation for the Green's function $G(x,y)$

$$G^{-1}(x,y) = G_0^{-1}(x,y) - \Sigma(x,y) \tag{50}$$

with the proper self-energy defined as $\Sigma = i\delta\Phi[G]/\delta G$. The self-energy is divided into the local and the non-local part $\Sigma = \Sigma_{\mathrm{loc}} + \Sigma_{\mathrm{nonl}}$. The Σ_{loc} contributes to the effective mass while the Σ_{nonl}

induces the mode-coupling between the different wavenumbers. The 2PI effective action should be invariant under the symmetry transformations of the system. Although we need to approximate the functional $\Phi[G]$ in practical applications, any truncation of $\frac{1}{2}\Phi[\phi, G]$ which preserves the symmetry property gives the equations of motion consistent with the corresponding conservation laws[71, 72].

It is very useful to decompose the two-point function $G(x, y)$ into two real functions, the statistical function $F(x, y)$ and the spectral function $\rho(x, y)$ defined, respectively, as

$$F(x,y) = \frac{1}{2}\left\langle \left\{ \hat{\phi}(x), \hat{\phi}(y) \right\} \right\rangle - \phi(x)\phi(y) = \frac{1}{2}\left[G^{21}(x,y) + G^{12}(x,y) \right] \tag{51}$$

and

$$\rho(x,y) = i\left\langle \left[\hat{\phi}(x), \hat{\phi}(y) \right] \right\rangle = i\left[G^{21}(x,y) - G^{12}(x,y) \right] \ , \tag{52}$$

where $\langle \cdots \rangle$ represents the expectation value taken over a certain density matrix. The indices 1 and 2 specify the branch of the contour $\mathcal{C}$ in the Schwinger-Keldysh formalism. The function F is called the statistical function because it turns out to be the Bose distribution function in the equilibrium state. The Schwinger-Dyson equation (50) can be equivalently rewritten in terms of $F(x, y)$ and $\rho(x, y)$ as coupled integro-differential equations

$$\left(\partial^2 + m^2 + \frac{\lambda}{2}\phi(x)^2 + \Sigma_{\rm loc}(x) \right) F(x,y) = \int_{t_0}^{y^0} dz \Sigma_F(x,z)\rho(z,y) - \int_{t_0}^{x^0} dz \Sigma_\rho(x,z)F(z,y) \tag{53}$$

$$\left(\partial^2 + m^2 + \frac{\lambda}{2}\phi(x)^2 + \Sigma_{\rm loc}(x) \right) \rho(x,y) = -\int_{y^0}^{x^0} dz \Sigma_\rho(x,z)\rho(z,y) \ , \tag{54}$$

where t_0 is the initial time. Note that the non-local self-energy has been re-expressed similarly as

$$\Sigma_F(x,y) = \frac{1}{2}\left[\Sigma^{21}_{\rm nonl}(x,y) + \Sigma^{12}_{\rm nonl}(x,y) \right] \ , \tag{55}$$

$$\Sigma_\rho(x,y) = i\left[\Sigma^{21}_{\rm nonl}(x,y) - \Sigma^{12}_{\rm nonl}(x,y) \right] \ . \tag{56}$$

The set of equations (53) and (54) is called the Kadanoff-Baym equation, which is the *two-time* formalism and describes the time evolution of the system from a certain initial configuration for F and ρ. Note that at each time step the spectral function ρ must satisfy the conditions following from the commutation relations:

$$\begin{aligned} \rho(x,y)|_{x^0\to y^0} &= 0 \ , \\ \partial_{x^0}\rho(x,y)|_{x^0\to y^0} &= \delta^d(\mathbf{x}-\mathbf{y}) \ , \\ \partial_{x^0}\partial_{y^0}\rho(x,y)|_{x^0\to y^0} &= 0 \ . \end{aligned} \tag{57}$$

Importantly, Eqs. (53) and (54) are non-local in time due to the so-called memory integrals appearing on the RHS. In other words, the evolution is non-Markovian depending on the evolution history in the past. This property is common for the equation of motion for the mean field. (See below.) In many stable systems, however, the integrand of the memory integral dies away exponentially and the macroscopic time scale is separated from the microscopic one.

It is instructive to consider the case of a uniform equilibrium state with a small value for the self-energy $\Sigma_\rho(p^0, p)$. Then we find that the spectral function ρ turns out to be the Breit-Wigner form (See Sec. 3.2),

$$\rho(p^0,p) = \frac{-\Sigma_\rho}{\left[(p^0)^2 - \Omega^2_{\mathbf{p}}\right]^2 - \Sigma_\rho^2/4} \to 2\pi i\epsilon(p^0)\delta((p^0)^2 - \Omega^2_{\mathbf{p}}) \ , \tag{58}$$

where $\Omega^2_{\mathbf{p}} = \mathbf{p}^2 + m^2 + {\rm Re}\Sigma_R$ is the single particle energy including the mean-field effect. The arrow denotes the quasi-particle limit $\Sigma_\rho \to 0$. In this limit the ρ becomes a delta-function and the statistical function F reduces to the Bose distribution

$$F(p^0,p) = 2\pi\delta((p^0)^2 - \Omega^2_{\mathbf{p}})\left(\frac{1}{2} + \frac{1}{e^{\beta p^0} - 1} \right) \ . \tag{59}$$

Figure 6: Local tadpole and nonlocal diagrams.

In this paper we restrict ourselves to the spatially homogeneous situation. From the translational invariance, the statistical function $F(x,y) = F(x^0, y^0, \mathbf{x}-\mathbf{y})$ and the spectral function $\rho(x,y) = \rho(x^0, y^0, \mathbf{x}-\mathbf{y})$ can be Fourier transformed to $F(x^0, y^0; \mathbf{p})$ and $\rho(x^0, y^0; \mathbf{p})$. Then KB equations are simplified in the momentum space as

$$\left(\partial_0^2 + \mathbf{p}^2 + m^2 + \frac{\lambda}{2}\phi(x^0)^2 + \Sigma_{\rm loc}(x^0)\right) F(x^0, y^0; \mathbf{p}) = \int_{t_0}^{y^0} dz^0 \Sigma_F(x^0, z^0; \mathbf{p}) \rho(z^0, y^0; \mathbf{p}) - \int_{t_0}^{x^0} dz^0 \Sigma_\rho(x^0, z^0; \mathbf{p}) F(z^0, y^0; \mathbf{p}) \ , \quad \text{(60a)}$$

$$\left(\partial_0^2 + \mathbf{p}^2 + m^2 + \frac{\lambda}{2}\phi(x^0)^2 + \Sigma_{\rm loc}(x^0)\right) \rho(x^0, y^0, \mathbf{p}) = -\int_{y^0}^{x^0} dz^0 \Sigma_\rho(x^0, z^0; \mathbf{p}) \rho(z^0, y^0; \mathbf{p}) \ . \quad \text{(60b)}$$

Regarding the functional $\Phi[G]$, we approximate it with the skeleton diagrams obtained at the next-leading order in λ. The self-energy Σ then becomes the sum of the local tadpole diagram, the nonlocal diagram with the mean fields and the nonlocal sunset diagram (Fig. 6):

$$\Sigma_{\rm loc}(x) = \Sigma_{\rm tad}(x) = \frac{\lambda}{2} F(x,x), \quad (61)$$

$$\Sigma^{ab}_{\rm sun}(x,y) = -\frac{\lambda^2}{6} G^{ab}(x,y)^3 - \frac{\lambda^2}{2}\phi^a(x) G^{ab}(x,y)^3 \phi^b(y) \quad (62)$$

where indices a, b denote the branch 1 and 2 of Schwinger-Keldysh contour $\mathcal{C}$. Furthermore the nonlocal part is divided into Σ_F and Σ_ρ and written explicitly in terms of F and ρ as

$$\begin{aligned}
\Sigma_F(x^0, z^0; \mathbf{p}) &= -\frac{\lambda^2}{2}\phi(x^0)\phi(z^0) \int \frac{d^dk}{(2\pi)^d} \\
&\quad \times \left[F(x^0, z^0; \mathbf{p}-\mathbf{k}) F(x^0, z^0; \mathbf{k}) - \frac{1}{4}\rho(x^0, z^0; \mathbf{p}-\mathbf{k})\rho(x^0, z^0; \mathbf{k}) \right] \\
&\quad -\frac{\lambda^2}{6} \int \frac{d^dk}{(2\pi)^d} \frac{d^dq}{(2\pi)^d} F(x^0, z^0; \mathbf{p}-\mathbf{k}-\mathbf{q}) \\
&\quad \times \left[F(x^0, z^0; \mathbf{k}) F(x^0, z^0; \mathbf{q}) - \frac{3}{4}\rho(x^0, z^0; \mathbf{k})\rho(x^0, z^0; \mathbf{q}) \right] , \quad (63) \\
\Sigma_\rho(x^0, z^0; \mathbf{p}) &= -\lambda^2 \phi(x^0)\phi(z^0) \int \frac{d^dk}{(2\pi)^d} F(x^0, z^0; \mathbf{p}-\mathbf{k}) \rho(x^0, z^0; \mathbf{k}) \\
&\quad -\frac{\lambda^2}{2} \int \frac{d^dk}{(2\pi)^d} \frac{d^dq}{(2\pi)^d} \rho(x^0, z^0; \mathbf{p}-\mathbf{k}-\mathbf{q}) \\
&\quad \times \left[F(x^0, z^0; \mathbf{k}) F(x^0, z^0; \mathbf{q}) - \frac{1}{12}\rho(x^0, z^0; \mathbf{k})\rho(x^0, z^0; \mathbf{q}) \right] . \quad (64)
\end{aligned}$$

We solve these KB equations (60) with the self-energy functions (61), (63) and (64) numerically by setting $\phi = 0$ in Sec. 3.4 and 3.5.

In the similar way we can derive the equation of motion of the mean field $\phi(x)$ from Eq. (49):

$$\left[\partial_x^2 + m^2 + \frac{\lambda}{6}\phi(x)^2 + \Sigma_{\rm loc}(x)\right]\phi(x) = \int_{t_0}^{x^0} dz^0 \int d^d z \tilde{\Sigma}_\rho(x,z)\phi(z), \tag{65}$$

where

$$\tilde{\Sigma}_\rho(x,z) = \frac{\lambda}{2}\rho(x,z)\left(F(x,z)^2 - \frac{1}{12}\rho(x,z)^2\right). \tag{66}$$

If we assume the spatially homogeneous case, we rewrite from (65) as,

$$\left[\partial_{x^0}^2 + m^2 + \frac{\lambda}{6}\phi(x^0)^2 + \Sigma_{\rm loc}(x^0)\right]\phi(x^0) = \int_{t_0}^{x^0} dz^0 \tilde{\Sigma}_\rho(x^0,z^0;\mathbf{p}=\mathbf{0})\phi(z^0), \tag{67}$$

where

$$\begin{aligned}\tilde{\Sigma}_\rho(x^0,z^0;\mathbf{p}=\mathbf{0}) &= \frac{\lambda}{2}\int\frac{d^dk}{(2\pi)^d}\int\frac{d^dq}{(2\pi)^d}\rho(x^0,z^0;\mathbf{k}+\mathbf{q}) \\ &\quad\left(F(x^0,z^0;\mathbf{k})F(x^0,z^0;\mathbf{q}) - \frac{1}{12}\rho(x^0,z^0;\mathbf{k})\rho(x^0,z^0;\mathbf{q})\right).\end{aligned} \tag{68}$$

The total set of the equations of motion in NLO of coupling expansion is Eq. (65) with (66) for the mean fields and the Kadanoff-Baym equation (53) and (54) with self energy functions (55), (56) , (61) and (62). In the spatially homogeneous case the set is reduced to be Eq.(67) with (68) for the mean fields and Eq. (60) with the self-energy functions (61), (63) and (64).

We need to specify the initial condition for ρ and F at $x^0 = y^0 = t_0$ in order to solve this evolution equations. For the spectral function ρ it is fixed by the commutation relation as given in Eqs. (57). For the statistical function F, we choose to set the initial conditions of the following functional form

$$F(x^0,y^0;\mathbf{p})\big|_{x^0=y^0=t_0} = \frac{1}{\omega(\mathbf{p})}\left(n_{\mathbf{p}} + \frac{1}{2}\right), \tag{69}$$

$$\partial_{x^0}F(x^0,y^0;\mathbf{p})\big|_{x^0=y^0=t_0} = 0, \tag{70}$$

$$\partial_{x^0}\partial_{y^0}F(x^0,y^0;\mathbf{p})\big|_{x^0=y^0=t_0} = \omega(\mathbf{p})\left(n_{\mathbf{p}} + \frac{1}{2}\right), \tag{71}$$

where $\omega(\mathbf{p})^2 = \mathbf{p}^2 + m^2$ and $n_{\mathbf{p}}$ is a function we can freely specify. This form is assumed in analogy with the equilibrium solution in the quasi-particle limit.

At later times in course of the evolution, we *define* the particle number distribution $n_{\mathbf{p}}(X^0)$ and the frequency $\tilde{\omega}_{\mathbf{p}}(X^0)$ in terms of $F(x^0,y^0;\mathbf{p})$ [92, 94, 97, 95, 89]

$$n_{\mathbf{p}}(X^0) + \frac{1}{2} = \left[\partial_{x^0}\partial_{y^0}F(x^0,y^0;\mathbf{p})\Big|_{x^0=y^0=X^0}F(X^0,X^0;\mathbf{p}) - \left(\partial_{x^0}F(x^0,y^0;\mathbf{p})\Big|_{x^0=y^0=X^0}\right)^2\right]^{1/2} \tag{72}$$

$$\tilde{\omega}_{\mathbf{p}}(X^0) = \left[\frac{\partial_{x^0}\partial_{y^0}F(x^0,y^0;\mathbf{p})\big|_{x^0=y^0=X^0}}{F(X^0,X^0;\mathbf{p})}\right]^{1/2}. \tag{73}$$

Strictly speaking, these definitions (72) and (73) are valid only when the quasi-particle picture works well. Nevertheless, we expect that these quantities are good estimators to characterize the behavior of the system evolution. The system is expected to have a quasi-particle spectrum for a sufficiently small coupling λ as shown in $1+1$ [92, 93], $2+1$ [94] and $3+1$[97, 95] dimensions.

Before proceeding to the next section let us compare the KB equations with the Boltzmann equation in 1+1 dimensions. In the homogeneous system the Boltzmann equation becomes

$$\begin{aligned}\Omega_{\mathbf{p}}\frac{\partial}{\partial t}n_{\mathbf{p}}(t) &= \frac{\lambda^2}{4}\int\frac{d^dp_1}{(2\pi)^d}\frac{d^dp_2}{(2\pi)^d}\frac{d^dp_3}{(2\pi)^d}\frac{1}{8\Omega_{\mathbf{p_1}}\Omega_{\mathbf{p_2}}\Omega_{\mathbf{p_3}}}\\ &\times[(1+n_{\mathbf{p_3}})(1+n_{\mathbf{p}})n_{\mathbf{p_1}}n_{\mathbf{p_2}}-n_{\mathbf{p_3}}n_{\mathbf{p}}(1+n_{\mathbf{p_1}})(1+n_{\mathbf{p_2}}))]\\ &\times(2\pi)^{d+1}\delta^d(\mathbf{p_1}+\mathbf{p_2}-\mathbf{p_3}-\mathbf{p})\delta(\Omega_{\mathbf{p_1}}+\Omega_{\mathbf{p_2}}-\Omega_{\mathbf{p_3}}-\Omega_{\mathbf{p}})\ , \end{aligned} \tag{74}$$

where $\Omega_p=\sqrt{\mathbf{p}^2+\mu^2(t)}$ and the mass $\mu^2(t)$ is the self-consistent solution of

$$\mu(t)^2=m^2+\frac{\lambda}{2}\int\frac{d^dk}{(2\pi)^d}\frac{n_{\mathbf{k}}(t)}{\sqrt{\mu(t)^2+\mathbf{k}^2}}\ . \tag{75}$$

In fact, this Boltzmann equation can be derived from the KB equations at the 1st order in the gradient expansion and with the Markov and quasi-particle approximations[114]. We remark here that in 1+1 dimensions the Boltzmann equation cannot lead to thermalization because the particle momenta must be unchanged in each 2-to-2 collision in order to satisfy the energy and momentum conservations.

3.2 Entropy of the relativistic Kadanoff-Baym equations in ϕ^4 theory

The approach to the equilibrium state will be quantitatively characterized if a system entropy can be introduced properly. In fact it is an open question how to choose the gross variables and define the corresponding entropy of the system in general non-equilibrium situations. There is no entropy production in fully microscopic calculations. We use the variable $G(x,y)$ in the KB approach. In the non-relativistic case, the kinetic entropy is introduced at the first order of the gradient expansion in Refs. [108] and [109] [3]. To our knowledge, the entropy production has not ever been estimated in the relativistic KB dynamics. Here we shall extend the entropy to the relativistic case in the first order of the gradient expansion. This will provide us, for example, of a criteria how much each microscopic process contributes to thermalization of the system.

In this subsection we derive the expression for the relativistic entropy in terms of the two-point functions $G(x,y)$ for the $\lambda\phi^4$ theory, as an extension from the non-relativistic entropy current given in [108] and [109].

We start with the Schwinger-Dyson equation (50) in the case of $\phi=0$. Multiplying G from the right and left hand sides of Eq. (50), respectively, we obtain

$$-\left[\partial_x^2+m^2+\frac{\lambda}{2}G^{aa}(x,x)\right]G^{ab}(x,y)-i\int dz\Sigma^{ac}_{\rm nonl}(x,z)c^{cd}G^{db}(z,y)=ic^{ab}\delta(x-y)\ , \tag{76}$$

$$-\left[\partial_y^2+m^2+\frac{\lambda}{2}G^{bb}(y,y)\right]G^{ab}(x,y)-i\int dzG(x,z)^{ac}c^{cd}\Sigma^{db}_{\rm nonl}(z,y)=ic^{ab}\delta(x-y)\ , \tag{77}$$

where a and b assign the branch 1 and 2 of the Schwinger-Keldysh contour $\mathcal{C}$ and $c^{ab}=\mathrm{diag}(1,-1)$. We introduce the "center-of-mass" coordinate $X=(x+y)/2$ and the relative coordinate $x-y$. Then making the difference of these equations (77) and (76) and performing the Fourier transform with respect to the relative coordinate $x-y$, we find

$$\begin{aligned}&\left[2ip\cdot\frac{\partial}{\partial X}-\frac{i}{2}\cdot\frac{\lambda}{2}\int\frac{d^{d+1}k}{(2\pi)^{d+1}}\left(\frac{\partial G^{aa}(X,k)}{\partial X}+\frac{\partial G^{bb}(X,k)}{\partial X}\right)\cdot\frac{\partial}{\partial p}\right]G^{ab}\\ &= i\int d(x-y)e^{ip\cdot(x-y)}\int dz(\Sigma^{ac}_{\rm nonl}(x,z)c^{cd}G^{db}(z,y)-G^{ac}(x,z)c^{cd}\Sigma^{db}_{\rm nonl}(z,y))\ , \end{aligned} \tag{78}$$

[3] However, their expressions are different from each other in the higher order terms of the skeleton expansion.

where p and k are the momentum conjugate to $x-y$. When we make the sum of them and perform the Fourier transform, we get the expression

$$\begin{aligned}
&\left[p^2 - m^2 - \frac{\lambda}{4}\left(\int \frac{d^{d+1}k}{(2\pi)^{d+1}}(G^{aa}(X,p) + G^{bb}(X,p))\right)\right] G^{ab}(X,p) \\
&= \quad ic^{ab} + \frac{i}{2}\int d(x-y)e^{-ip\cdot(x-y)} \int dz(\Sigma^{ac}_{\rm nonl}(x,z)c^{cd}G^{db}(z,y) + G^{ac}(x,z)c^{cd}\Sigma^{db}_{\rm nonl}(z,y)). \quad (79)
\end{aligned}$$

The interval of $x^0 - y^0$ is finite for a fixed X^0 when we start the evolution at $x^0 = y^0 = 0$. It is therefore important to note that for the Fourier transformation in $x^0 - y^0$ this interval needs to be sufficiently large as compared with the microscopic correlation time. One should be aware of this limitation.

The gradient expansion with respect to the center-of-mass coordinate X is adequate when the X-dependence of the system is smooth enough (See for example [116, 108]). We keep just the first order terms in the gradient expansion of Green's functions and the self energies here. For the expansion of the right hand side of Eqs. (78) and (79), we use the formula for two point functions $K(x,y)$ and $L(x,y)$:

$$\begin{aligned}
\int d(x-y)e^{ip\cdot(x-y)} \int dz K(x,z)L(z,y) \quad &= \quad \tilde{K}(X,p)\tilde{L}(X,p) \\
&+\frac{i}{2}\left(\frac{\partial \tilde{K}}{\partial p^\mu}\frac{\partial \tilde{L}}{\partial X_\mu} - \frac{\partial \tilde{K}}{\partial X^\mu}\frac{\partial \tilde{L}}{\partial p_\mu}\right) + O\left(\frac{\partial^2}{\partial X^2}\right) , \quad (80)
\end{aligned}$$

where $\tilde{K}(X,p)$ and $\tilde{L}(X,p)$ are the Fourier-transforms in $x-y$. We remark here the scale separation between X^0 and $x^0 - y^0$. We implicitly assume that the time dependence on the former is smooth and mild while the time correlation in the latter is much shorter. At the very early time of the evolution, this separation cannot be expected and the gradient expansion should be invalid.

The derivation of the entropy current is most simplified in terms of the retarded propagator $G_R = i(G^{11} - G^{12})$. To the first order in the gradient expansion, Eqs. (78) and (79) reduce to the equations for G_R:

$$\left[\frac{\partial\left(M - \frac{1}{2}\Sigma_\rho\right)}{\partial p^\mu}\frac{\partial}{\partial X_\mu} - \frac{\partial\left(M - \frac{1}{2}\Sigma_\rho\right)}{\partial X^\mu}\frac{\partial}{\partial p_\mu}\right] G_R(X,p) \quad = \quad 0 \, , \quad (81)$$

$$\left(M - \tfrac{1}{2}\Sigma_\rho\right) G_R(X,p) \quad = \quad -1 \, , \quad (82)$$

where M denotes[4]

$$M = p^2 - m^2 - {\rm Re}\Sigma_R, \quad \Sigma_R = \Sigma^{11} - \Sigma^{12} \, . \quad (83)$$

In deriving Eqs. (81) and (82) we have used the well-known relations $\Sigma^{11} + \Sigma^{22} = \Sigma^{12} + \Sigma^{21}$, $G^{11} + G^{22} = G^{12} + G^{21}$ and $2i{\rm Im}\Sigma_R = \Sigma_\rho$. The formal solution of the above simultaneous equations (81) and (82) is written as [116]

$$G_R(X,p) = \frac{-1}{M - \frac{1}{2}\Sigma_\rho} \, . \quad (84)$$

One should note here that M (Σ_ρ) is real (imaginary). Therefore, the real and imaginary parts of the retarded propagator G_R are given as

$${\rm Re}G_R(X,p) \quad = \quad -\frac{M}{M^2 - \frac{1}{4}\Sigma_\rho^2} \, , \quad (85)$$

$$\rho(X,p) = 2i{\rm Im}G_R(X,p) \quad = \quad -\frac{\Sigma_\rho}{M^2 - \frac{1}{4}\Sigma_\rho^2} \, . \quad (86)$$

[4]Please don't confuse this M with a mass function. Both M and Σ have mass-dimension 2.

We see that the spectral function $\rho(X,p)$ has the Breit-Wigner form (58) in the first order approximation of the gradient expansion.

Now we are ready for writing down the entropy current. The "derivation" goes somewhat in a heuristic way. We make the difference of Eq. (78) for $(a,b)=(1,2)$ multiplied by $\ln(iG^{12}/\rho)$ and Eq. (78) for $(a,b)=(2,1)$ multiplied by $\ln(iG^{21}/\rho)$. Then we integrate the resultant expression over $d^{d+1}p/(2\pi)^{d+1}$ to arrive at the following equation:

$$\partial_\mu s^\mu = \frac{1}{2}\int \frac{d^{d+1}p}{(2\pi)^{d+1}} \ln\frac{G^{12}}{G^{21}} C(X,p). \tag{87}$$

Here the term C,

$$C(X,p) = i\left(\Sigma_\rho(X,p)\ F(X,p) - \Sigma_F(X,p)\ \rho(X,p)\right), \tag{88}$$

may be identified as the collision term in the Boltzmann limit. In Eq. (87), we define the entropy current $s^\mu(X)$ as

$$\begin{aligned} s^\mu &= \int \frac{d^{d+1}p}{(2\pi)^{d+1}} \left[\left(p^\mu - \frac{1}{2}\frac{\partial \mathrm{Re}\Sigma_R}{\partial p_\mu}\right)\left(-G^{12}\ln\frac{iG^{12}}{\rho} + G^{21}\ln\frac{iG^{21}}{\rho}\right)\right. \\ &\left. -\frac{1}{2}\mathrm{Re}G_R\ \left(-\frac{\partial}{\partial p_\mu}\left(\frac{\Sigma_\rho}{i}\frac{iG^{12}}{\rho}\right)\ln\frac{iG^{12}}{\rho} + \frac{\partial}{\partial p_\mu}\left(\frac{\Sigma_\rho}{i}\frac{iG^{21}}{\rho}\right)\ln\frac{iG^{21}}{\rho}\right)\right], \end{aligned} \tag{89}$$

where we have used the relations $i(\Sigma^{11}-\Sigma^{22}) = 2\mathrm{Re}\Sigma_R$ and $i(G^{11}-G^{22}) = 2\mathrm{Re}G_R$. We have also applied the approximations $\Sigma^{12} \simeq \Sigma_\rho \frac{G^{12}}{\rho}$ and $\Sigma^{21} \simeq \Sigma_\rho \frac{G^{21}}{\rho}$ in the first order gradient expansion [108, 117].

When we write the two-point functions in the form of the Kadanoff-Baym Ansatz $G^{12} = -i\rho f$ and $G^{21} = -i\rho(1+f)$ with a real function f, the above expression for the entropy current becomes

$$\begin{aligned} s^\mu &= \int \frac{d^{d+1}p}{(2\pi)^{d+1}} \left\{ \frac{\rho}{i}\left(p^\mu - \frac{\partial \mathrm{Re}\Sigma_R}{\partial p_\mu}\right)\left(-f\ln f + (1+f)\ln(1+f)\right)\right. \\ &\left. -\frac{1}{2}\mathrm{Re}G_R\left[-\frac{\partial}{\partial p_\mu}\left(\frac{\Sigma_\rho}{i}f\right)\ln f\ + \frac{\partial}{\partial p_\mu}\left(\frac{\Sigma_\rho}{i}(1+f)\right)\ln(1+f)\ \right]\right\}. \end{aligned} \tag{90}$$

After integration by parts over p^μ in the second line, we obtain a simple expression:

$$s^\mu = \int \frac{d^{d+1}p}{(2\pi)^{d+1}} \left[\frac{\rho}{i}\left(p^\mu - \frac{1}{2}\frac{\partial \mathrm{Re}\Sigma_R}{\partial p_\mu}\right) + \frac{\Sigma_\rho}{i}\frac{1}{2}\frac{\partial \mathrm{Re}G_R}{\partial p_\mu}\right]\sigma\ , \tag{91}$$

where we introduced the notation

$$\sigma(X,p) = -f\ln f + (1+f)\ln(1+f)\ . \tag{92}$$

One must distinguish this "occupation number" function f in the Kadanoff-Baym Ansatz from the distribution function $n_{\mathbf{p}}$ defined in (72) [5]

Substituting the solution (85) for G_R, we can write the entropy current more explicitly as

$$s^\mu = \int \frac{d^{d+1}p}{(2\pi)^{d+1}} \left[\frac{\rho}{i}\left(1 + \frac{M^2 - \frac{\Sigma_\rho^2}{4} - 2M^2}{M^2 - \frac{\Sigma_\rho^2}{4}}\right)\left(p^\mu - \frac{1}{2}\frac{\partial \mathrm{Re}\Sigma_R}{\partial p_\mu}\right) + \frac{\rho}{4i}\frac{M\Sigma_\rho \frac{\partial \Sigma_\rho}{\partial p_\mu}}{M^2 - \frac{\Sigma_\rho^2}{4}}\right]\sigma\ . \tag{93}$$

This expression further simplifies with use of (86) to[6]

$$s^\mu = \int \frac{d^{d+1}p}{(2\pi)^{d+1}} \frac{\rho^2\Sigma_\rho}{2i}\left[\left(p^\mu - \frac{1}{2}\frac{\partial \mathrm{Re}\Sigma_R}{\partial p_\mu}\right) - \frac{1}{2}\frac{M}{\Sigma_\rho}\frac{\partial \Sigma_\rho}{\partial p_\mu}\right]\sigma\ . \tag{94}$$

[5] In computing σ, one may have a difficulty of the negative $p^0\rho(p^0)$ and $f(p^0)$ obtained by the Fourier transform over finite time interval $x^0 - y^0$, although they must be positive in equilibrium.

[6] The tadpole part should be the renormalized one in this expression in 1+1 dimensions.

This is one of the main results of this work. This expression of the entropy current is a natural extension to the relativistic case. The only difference between non-relativistic [108, 109] and our relativistic case is the factor $\frac{1}{2}$ in front of the momentum derivative of the self-energy. We remark here that there is a discussion about the memory correction terms to the kinetic entropy in the non-relativistic case in Refs. [108] and [109] when we deal with the skeleton diagrams $\Sigma_{\rm nonl}$ beyond the NLO in λ.

In the quasi-particle limit, $\Sigma_{\rm nonl} \to 0$, we know that $G^{12} = -i\rho f = 2\pi\delta((p^0)^2 - \Omega_{\mathbf{p}}^2)(\theta(-p^0) + n_{\mathbf{p}})$ and $G^{21} = -i\rho(1+f) = 2\pi\delta((p^0)^2 - \Omega_{\mathbf{p}}^2)(\theta(p^0) + n_{\mathbf{p}})$. In this limit the expression of the entropy current for $\mu = 0$ reduces to the well-known form of the entropy density for bosons

$$s^0 = \int \frac{d^d p}{(2\pi)^d} \left[-n_{\mathbf{p}} \ln n_{\mathbf{p}} + (1+n_{\mathbf{p}}) \ln(1+n_{\mathbf{p}}) \right] , \tag{95}$$

as it should be.

Finally we show the fact that this entropy current obtained in the NLO in λ satisfies the H-theorem. Namely, the RHS of Eq. (87) is positive semi-definite. This can be verified by substituting the expressions for Σ_F (63) and Σ_ρ (64) into the RHS of (87). As a result we obtain the relation

$$\begin{aligned}
\partial_\mu s^\mu(X) &= \int \frac{d^{d+1}p}{(2\pi)^{d+1}} \frac{1}{2} \ln \frac{G^{12}}{G^{21}} C \\
&= \frac{1}{8} \cdot \frac{\lambda^2}{3!} \int \frac{d^{d+1}p}{(2\pi)^{d+1}} \frac{d^{d+1}q}{(2\pi)^{d+1}} \frac{d^{d+1}k}{(2\pi)^{d+1}} \frac{d^{d+1}r}{(2\pi)^{d+1}} (2\pi)^{d+1} (p+q-k-r) \\
&\times \left[G^{12}(p,X) G^{12}(q,X) G^{21}(k,X) G^{21}(r,X) - G^{21}(p,X) G^{21}(q,X) G^{12}(k,X) G^{12}(r,X) \right] \\
&\times \ln \frac{G^{12}(p,X) G^{12}(q,X) G^{21}(k,X) G^{21}(r,X)}{G^{21}(p,X) G^{21}(q,X) G^{12}(k,X) G^{12}(r,X)} \geq 0 ,
\end{aligned} \tag{96}$$

where we have used $G^{12}(-k,X) = G^{21}(k,X)$. The last inequality holds since $(x-y)\ln\frac{x}{y} \geq 0$. Thus we proved that the H-theorem is fulfilled in the NLO in $\lambda\phi^4$ theory. However, at higher orders in the coupling constant λ, the definition of the entropy current and the proof of the H-theorem are open problems.

3.3 Energy Momentum Tensor

We derive the expression for the energy-momentum tensor, $\Theta^{\mu\nu}$, of the $\lambda\phi^4$ theory (in the symmetric phase, $\langle\hat{\phi}\rangle = 0$). The 2PI effective action $\Gamma[G]$ Eq. (47) is invariant under the translation $x^\mu \to x^\mu + \epsilon^\mu$. Following Noether's procedure, we apply the position dependent translation $x^\mu \to x^\mu + \epsilon^\mu(x)$ to compute the change of the action $\delta\Gamma = \int_x \partial_\nu \left[\epsilon_\mu(x)\Theta^{\mu\nu}(x)\right]$. For ϵ_ν independent of x, we can prove the current conservation $\partial_\nu \Theta^{\mu\nu} = 0$ as a result of the invariance of the action $\delta\Gamma = 0$. The energy-momentum tensor $\Theta^{\mu\nu}$ reads from $\delta\Gamma$ as the coefficient factor of $\partial_\nu \epsilon_\mu(x)$ [72, 118, 97].

Under the position dependent translation, Green's function changes as

$$G(x,y) \to G'(x,y) \equiv G(x+\epsilon(x), y+\epsilon(y)) = G(x,y) + \epsilon^\lambda(x)\partial_\lambda^x G(x,y) + \epsilon^\lambda(y)\partial_\lambda^y G(x,y). \tag{97}$$

Then the change of each term in the action (47) is calculated as follows: the first term in Eq. (47) leaves no ϵ term

$$\begin{aligned}
\delta\left[\frac{i}{2}\mathrm{Tr}\ln G^{-1}\right] &= -\frac{i}{2}\mathrm{Tr}\frac{1}{G}\delta G = -\frac{i}{2}\int_{x,y} G^{-1}(x,y)\left[\epsilon^\mu(y)\partial_\mu^y G(y,x) + \epsilon^\mu(x)\partial_\mu^x G(y,x)\right] \\
&= -i\int_x \epsilon^\mu(x)\partial_\mu^x \delta(x-x) = 0 .
\end{aligned} \tag{98}$$

The second term gives rise to

$$\begin{aligned}\delta\left[\frac{i}{2}G_0^{-1}G\right] &= -\frac{i}{2}\int_{x,y}\left[\left(\partial_x^2+m^2\right)\delta(x-y)\right]\delta G(x,y)\\ &= -\frac{1}{2}\int_x \epsilon^\mu(x)\partial_x^\nu\Big[\delta(x-y)\partial_\mu^x\partial_\nu^y\left(G(x,y)+G(y,x)\right)\\ &\quad -\delta(x-y)g_{\mu\nu}\partial_x^\lambda\partial_\lambda^y G(x,y)+m^2 g_{\mu\nu}\delta(x-y)G(x,y)\Big]\,, \end{aligned} \tag{99}$$

where we have used

$$\int_{x,y}\partial_x^\mu\left[\delta(x-y)G(x,y)\right]=\int_{x,y}\delta(x-y)\left[\partial_x^\mu G(y,x)+\partial_x^\mu G(x,y)\right]\,. \tag{100}$$

The third term yields

$$\delta\left[\frac{1}{2}\Phi[G]\right]=\frac{1}{2}\int_{x,y}\frac{\delta\Phi}{\delta G(x,y)}\left(\epsilon^\mu(x)\partial_\mu^x G(x,y)+\partial^\mu(y)\partial_\mu^y G(x,y)\right). \tag{101}$$

The third term $\delta\left[\frac{1}{2}\Phi[G]\right]$ can be rewritten more conveniently by use of the Jacobian. For example the tadpole part in $\Phi[G]$ changes under the translation as

$$\delta\left[\lambda\int_x G(x,x)^2\right]=2\lambda\int_x G(x,x)\left(\epsilon^\mu(x)\partial_\mu^x G(x,y)+\epsilon(y)^\mu\partial_\mu^y G(x,y)\right). \tag{102}$$

However we observe that the translation can be dealt with the change of variables in the integral as

$$\lambda\int_x G(x+\epsilon(x),\ x+\epsilon(x))^2 \;=\; \int_{x'}\det\left(1+\frac{\partial x^\mu}{\partial x'^\nu}\right)G(x',\ x')^2 \tag{103}$$

and therefore the change can be recast to

$$\delta\left[\lambda\int_x G(x,\ x)^2\right] \;=\; -\lambda\int_{x'}\frac{\partial^\mu\epsilon}{\partial x^\mu}\,G(x',x')^2=-\lambda\int_x\frac{\partial^\mu\epsilon}{\partial x^\mu}\,G(x,x)^2\,. \tag{104}$$

In this way, the total change of $\Phi[G]$ can be re-expressed by using the Jacobian. Furthermore, the number of integration coincides with the power of the coupling λ in general. This means that the Jacobians under the translation can be absorbed in the change of the coupling $\lambda\to\lambda\zeta(x)$ and that $\delta\Phi$ can be rewritten as [72, 118, 97]

$$\delta\left[\frac{1}{2}\Phi\right]=\int_x\partial_\mu\epsilon(x)^\mu\frac{\delta\Phi}{\delta\zeta(x)}\Big|_{\zeta=1}. \tag{105}$$

Since $\delta\Gamma=\int_x\partial_\nu\epsilon_\mu(x)\Theta^{\mu\nu}(x)$, the energy-momentum tensor is found as

$$\begin{aligned}\Theta^{\mu\nu}(x) &= \frac{1}{2}\int_y\Big[\delta(x-y)\partial_x^\mu\partial_y^\nu\left(G(x,y)+G(y,x)\right)-\delta(x-y)g^{\mu\nu}\partial_x^\lambda\partial_\lambda^y G(x,y)\\ &\quad +g^{\mu\nu}\delta(x-y)m^2G(x,y)\Big]-\frac{1}{2}g^{\mu\nu}\frac{\delta\Phi}{\delta\zeta(x)}\Big|_{\zeta=1}\end{aligned} \tag{106}$$

In the case of uniform space in 1+1 dimensions, by taking the Fourier transform with respect to the spatial relative coordinate, we obtain the explicit expressions for the energy Θ^{00} and the pressure Θ^{11} as[7]:

$$\Theta^{00}(X^0)=\frac{1}{2}\int\frac{d^dp}{(2\pi)^d}(\mathbf{p}^2+m^2+\partial_{x^0}\partial_{y^0})F(x^0,y^0;\mathbf{p})\Big|_{x^0=y^0=X^0}-\frac{1}{2}\frac{\delta\Phi}{\delta\zeta}-\text{counter term}\,, \tag{107}$$

$$\Theta^{11}(X^0)=\frac{1}{2}\int\frac{d^dp}{(2\pi)^d}\left(\mathbf{p}^2-m^2+\partial_{x^0}\partial_{y^0}\right)F(x^0,y^0;\mathbf{p})\Big|_{x^0=y^0=X^0}+\frac{1}{2}\frac{\delta\Phi}{\delta\zeta}+\text{counter term}\,. \tag{108}$$

[7]The counter term in energy and pressure is the same.

Here the counter term cancels out the divergence in $\frac{\delta\Phi}{\delta\zeta}$. In $1+1$ dimensions the divergence is only in the tadpole part which can be in the similar manner to that of [92].

In the NLO in λ of the skeleton expansion, the tadpole and sunset diagrams contribute to $\delta\Phi/\delta\zeta$. Then the total energy and pressure are decomposed as

$$E_{\rm tot}(X^0) = E_{\rm kin}(X^0) + E_{\rm tad}(X^0) + E_{\rm sun}(X^0)\,, \tag{109a}$$

$$P_{\rm tot}(X^0) = P_{\rm kin}(X^0) + P_{\rm tad}(X^0) + P_{\rm sun}(X^0)\,, \tag{109b}$$

where

$$E_{\rm kin}(X^0) = \frac{1}{2}\int\frac{d^dp}{(2\pi)^d}(\mathbf{p}^2 + m^2 + \partial_{x^0}\partial_{y^0})F(x^0,y^0;\mathbf{p})|_{x^0=y^0=X^0}\,, \tag{110a}$$

$$P_{\rm kin}(X^0) = \frac{1}{2}\int\frac{d^dp}{(2\pi)^d}(\mathbf{p}^2 - m^2 + \partial_{x^0}\partial_{y^0})F(x^0,y^0;\mathbf{p})|_{x^0=y^0=X^0}\,, \tag{110b}$$

$$E_{\rm tad}(X^0) = -P_{\rm tad}(X^0) = \frac{1}{4}\int\frac{d^dp}{(2\pi)^d}\Sigma_{\rm tad}(X^0)F(X^0,X^0;\mathbf{p}) + \frac{1}{2}\int\frac{d^dp}{(2\pi)^d}\delta m^2_{\rm tad}\ F(X^0,X^0;\mathbf{p})\,, \tag{110c}$$

$$E_{\rm sun}(X^0) = -P_{\rm sun}(X^0) = \frac{1}{4}\int\frac{d^dp}{(2\pi)^d}I(X^0,\mathbf{p})\,. \tag{110d}$$

Here $\delta m^2_{\rm tad}$ denotes the mass counter term:

$$\delta m^2_{\rm tad} = -\frac{\lambda}{2}\int\frac{d^dp}{(2\pi)^d}\frac{1}{2\omega_{\mathbf{p}}}\,, \tag{111}$$

and

$$I(X^0,\mathbf{p}) \quad = \int_0^{X^0}dt'\left[\Sigma_\rho(X^0,t';\mathbf{p})F(t',X^0;\mathbf{p}) - \Sigma_F(X^0,t';\mathbf{p})\rho(t',X^0;\mathbf{p})\right] \tag{112}$$

is finite in 1+1 dimensions.

In the case of 2+1 dimensions the differences from 1+1 dimensions are only the form of Θ^{ij} and the renormalization of sunset diagrams. First the spatial parts of energy-momentum tensor are given by

$$\begin{aligned}\Theta^{11} &= \frac{1}{2}\int\frac{d^dp}{(2\pi)^d}\left({p_1}^2 - {p_2}^2 - m^2 + \partial_{x^0}\partial_{y^0}\right)F(x^0,y^0;\mathbf{p})\Big|_{x^0=y^0=X^0} + \frac{1}{2}\frac{\delta\Phi}{\delta\zeta} + \text{counter term}\\ \Theta^{22} &= \frac{1}{2}\int\frac{d^dp}{(2\pi)^d}\left({p_2}^2 - {p_1}^2 - m^2 + \partial_{x^0}\partial_{y^0}\right)F(x^0,y^0;\mathbf{p})\Big|_{x^0=y^0=X^0} + \frac{1}{2}\frac{\delta\Phi}{\delta\zeta} + \text{counter term}\end{aligned} \tag{113}$$

Next in 2+1 dimensions $I(X^0,\mathbf{p})$ is logarithmically divergent, but in this dimensions we only need to consider the mass shift $\delta m^2_{\rm sun}$ in the estimation of $E_{\rm sun}(X^0)$ and $P_{\rm sun}(X^0)$ [8] shown as

$$E_{\rm sun}(X^0) \quad = -P_{\rm sun}(X^0) = \tfrac{1}{4}\textstyle\int\frac{d^dp}{(2\pi)^d}I(X^0,\mathbf{p}) + \frac{1}{2}\int\frac{d^dp}{(2\pi)^d}\delta m^2_{\rm sun}F(X^0,X^0,\mathbf{p}), \tag{114}$$

where

$$\delta m^2_{\rm sun} = -{\rm Re}\Sigma_R(p^0,\mathbf{p}) = \frac{\lambda^2}{6}\int\frac{d^dq}{(2\pi)^d}\int\frac{d^dk}{(2\pi)^d}\frac{1}{4\omega_{\mathbf{q}}\omega_{\mathbf{k}}\omega_{\mathbf{p-q-k}}}\frac{\omega_{\mathbf{q}}+\omega_{\mathbf{k}}+\omega_{\mathbf{p-q-k}}}{\left(\omega_{\mathbf{q}}+\omega_{\mathbf{k}}+\omega_{\mathbf{p-q-k}}\right)^2 - p_0^2}. \tag{115}$$

[8] In the case of $3+1$ dimensions, the renormalization of self-consistent theories is required and developed in [149].

3.4 Numerical simulation for scalar ϕ^4 theory in 1+1 dimensions

In this subsection we show numerical results for simulations with KB equations in the $\lambda\phi^4$ theory in 1+1 dimensions. We solve KB equations (60) with the self-energy functions (61), (63) and (64) numerically by setting $\phi = 0$. We use the initial conditions for the statistical and spectral functions (69), (70), (71) and (57) or its Fourier transformation:

$$\begin{aligned} \rho(x^0, y^0; \mathbf{p})\Big|_{x^0=y^0} &= 0 \\ \partial_{x^0}\rho(x^0, y^0; \mathbf{p})\Big|_{x^0=y^0} &= 1. \end{aligned} \tag{116}$$

We should put initial condition for the number distribution function $n_{\mathbf{p}}$. As a sample simulation, we prepare the two initial conditions for the distribution function. One is "tsunami" distribution function

$$n^T_{\mathbf{p}} = \frac{1}{\mathcal{N}_T} \exp\left[-\frac{(|p_x| - \mathbf{p}_T)^2}{2\sigma^2}\right] \tag{117}$$

where the number density is Gaussian function localized at $p_T = 7 \cdot 2\pi/L$ with width $\sigma^2/m^2 = 4.4 \times \left(\frac{2\pi}{mL}\right)^2$ and height $1/\mathcal{N}_T = 4.0$. The other is Woods-Saxon initial condition which has platt around $p_x = 0$ and damps exponentially for $p_x > p_{\rm WS}$:

$$n^{WS}_{\mathbf{p}} = \frac{1}{\mathcal{N}_{WS}} \frac{1}{e^{(\sqrt{\mathbf{p}^2+m^2} - p_{WS})/\kappa} + 1} \tag{118}$$

with $p_{WS}/m = 2.936$, $\kappa/m = 0.35$ and $\mathcal{N}_{WS} = 0.5$. In the case of tsunami initial condition we consider the collision processes of two nuclei with localized momentum distribution. The WS initial condition is used to check the initial condition dependence of our simulation. The parameters in WS initial condition are tuned so that both initial conditions give the same energy at $\lambda/m^2 = 4$. We varied the coupling $\lambda/m^2 = 4, 2$ and 1 without changing the above initial conditions to research the dependence of evolution on coupling strength.

In order to trace the time evolution of the Kadanoff-Baym equation, we use a normal lattice discretization with respect to momentum space[119]. The volume of the space is L in 1+1 dimensions. The lattice spacing is a_s, and N_s is the mesh size of the area, so that $L = 2N_s a_s$. Here $\mathbf{p}^2$ is discretized in the following,

$$\mathbf{p}^2 \to \Sigma_{i=1}^2 \frac{4}{a_s^2} \sin^2\left(\frac{a_s p_n}{2}\right) \tag{119}$$

where the momenta $\mathbf{p_n}$ are discretized according to $\mathbf{p_n} = \frac{2\pi \mathbf{n}}{L}$ with $n \in \{-N_s, -N_s+1, \cdots N_s-1, N_s\}$. In order to remove most of the lattice artifacts, we take $\mathbf{p}^2$ in this way . And we take the following replacement in integrating in the momentum space

$$\int \frac{dp}{(2\pi)} \to \frac{1}{L}\Sigma_{n\in\{-N_s,\cdots,N_s\}}. \tag{120}$$

For the numerical analysis we have used a space lattice with

$$ma_s = 0.3,\ a_t/a_s = 0.1,\ N_s = 40 \tag{121}$$

In Fig.7 the time evolution of number distribution $n(\omega_{\mathbf{p}})$ with tsunami initial conditions is shown. The top of the tsunami structure collapse and low momentum $\omega_{\mathbf{p}} \sim 0$ and high momentum $\omega_{\mathbf{p}} > 4$ start to grow up. At later times $mX^0 > 60$ the number distribution function approaches the Bose distribution function $n_{\mathbf{p}} = 1/(e^{\epsilon_{\mathbf{p}}/T} - 1)$ with the temperature $T/m \sim 2.5$ and zero chemical potential. This figure represents the reproduction of the results of Ref.[92]. In the similar way in Fig.8 we show the time evolution of number distribution function $n(\omega_{\mathbf{p}})$ with the WS initial

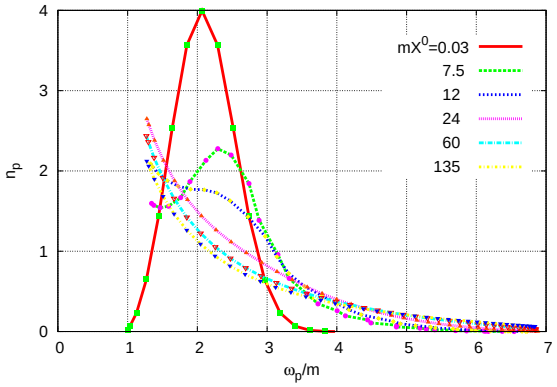

Figure 7: Evolution of the distribution function $n_{\mathbf{p}}(\tilde{\omega}_{\mathbf{p}}/m)$ from the tsunami initial condition ($\lambda/m^2 = 4$).

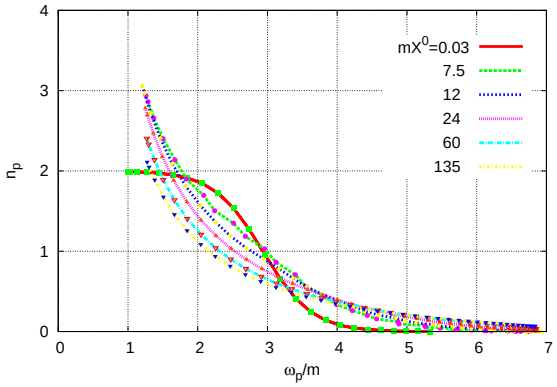

Figure 8: Evolution of the distribution function $n_{\mathbf{p}}(\tilde{\omega}_{\mathbf{p}}/m)$ from the WS initial condition ($\lambda/m^2 = 4$).

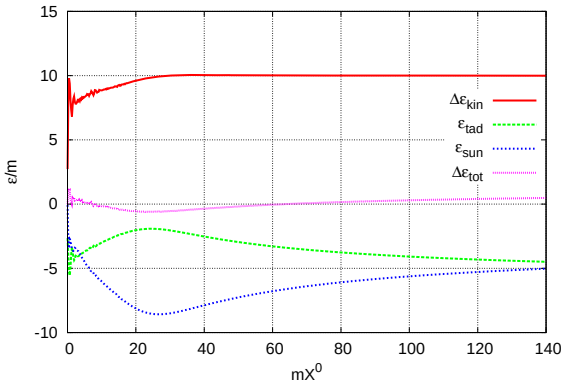

Figure 9: Evolution of energy content in units of m from the tsunami initial condition with $\lambda/m^2 = 4$; Kinetic $\Delta\epsilon_{\rm kin}/m = (\epsilon_{\rm kin}(t) - \epsilon_{\rm kin}(0))/m$ (solid), tadpole $\epsilon_{\rm tad}/m$ (dashed), sunset $\epsilon_{\rm sun}/m$ (dotted) and the total energy $\Delta\epsilon_{\rm tot}/m = (\epsilon_{\rm tot}(t) - \epsilon_{\rm tot}(0))/m$ (bold solid).

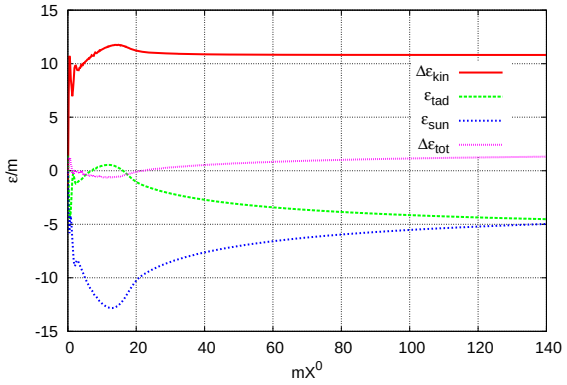

Figure 10: Evolution of energy content in units of m from the Woods-Saxon initial condition with $\lambda/m^2 = 4$; Kinetic $\Delta\epsilon_{\rm kin}/m = (\epsilon_{\rm kin}(t) - \epsilon_{\rm kin}(0))/m$ (solid), tadpole $\epsilon_{\rm tad}/m$ (dashed), sunset $\epsilon_{\rm sun}/m$ (dotted) and the total energy $\Delta\epsilon_{\rm tot}/m = (\epsilon_{\rm tot}(t) - \epsilon_{\rm tot}(0))/m$ (bold solid).

condition (118). Then $n(\omega_{\mathbf{p}})$ converges to the same thermal distribution as the one in the case of "tsunami" initial condition.

Next we show the energy conservation of the system. The expression of the energy is given in Sec.3.3. In Figs.9 and 10 we show the time evolution of kinetic (110a), tadpole (110c), sunset (110d) and total energy (109a) for the tsunami and WS initial conditions. As for the total and kinetic energies we plot their differences measured from the initial value of the total energy $\epsilon_{\rm tot}/m \sim 260$ in our discretization. The growth of the kinetic energy is canceled by the tadpole and the sunset energy to have a constant total energy for both initial conditions. The energy is conserved within 0.5 % percent for $0 \leq mX^0 \leq 140$ in the figures.

Next let us study the kinetic entropy (91) derived with the gradient expansion of the KB equation. In order to express the plot of the entropy we first examine the shape of the spectral function $\rho(X,p)$, which appears in Eq. (91) and is needed to compute the occupation number function $f(X,p)$ in σ. In Figs. 11, 12, 13 and 14 we show $\rho(X,p)$ for $p_x = 2\pi n/L$ with $n = 0$ and 10 for "tsunami" and WS initial conditions, respectively at several values of time mX^0. We can observe peak structures near $p^0 \sim \sqrt{p_x^2 + m^2}$ at later times in the figures.

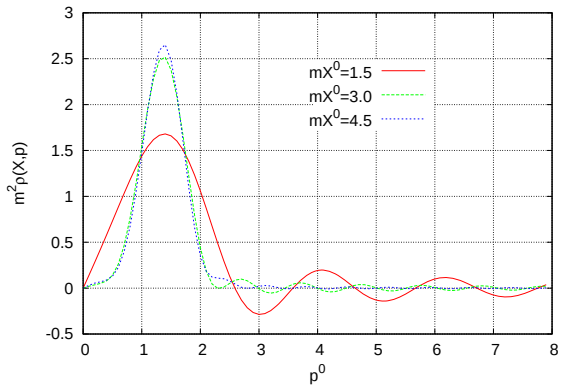

Figure 11: Spectral function $\rho(X, p^0, p_x)$ with $p_x = 0$ at $mX^0 = 1.5$, 3, and 4.5 for tsunami initial conditions in $\lambda/m^2 = 4$.

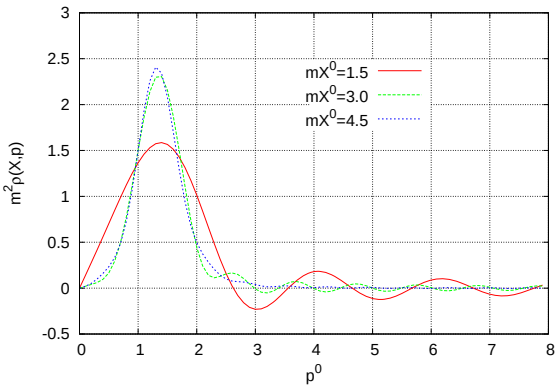

Figure 12: Spectral function $\rho(X, p^0, p_x)$ with $p_x = 0$ at $mX^0 = 1.5$, 3, and 4.5 for Woods-Saxon initial conditions in $\lambda/m^2 = 4$.

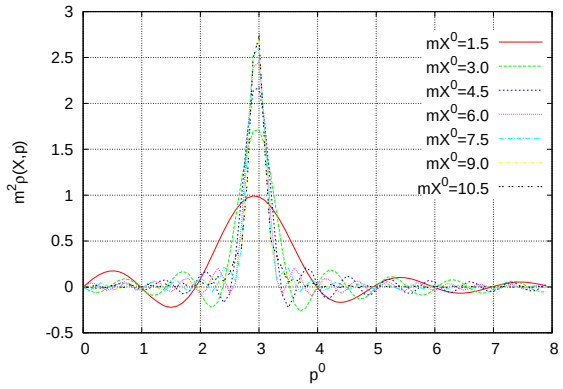

Figure 13: Spectral function $\rho(X, p^0, p_x)$ with $p_x = 2\pi \cdot 10/L$ at $mX^0 = 1.5, \cdots, 10.5$ for tsunami initial conditions in $\lambda/m^2 = 4$.

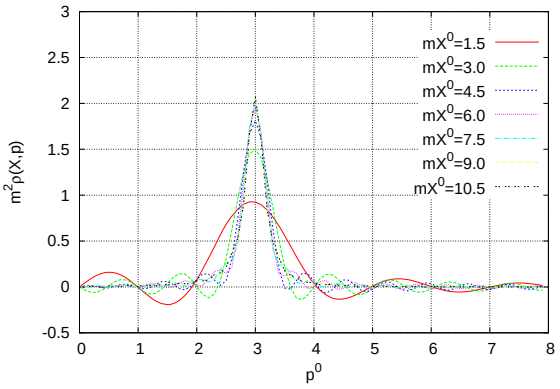

Figure 14: Spectral function $\rho(X, p^0, p_x)$ with $p_x = 2\pi \cdot 10/L$ at $mX^0 = 1.5, \cdots, 10.5$ for Woods-Saxon initial conditions in $\lambda/m^2 = 4$.

At early times, however, the spectral function $\rho(X,p)$ shows oscillatory behavior. This can be

understood as the uncertainty relation between the energy and the time. In the observation within a finite time interval $|x^0 - y^0| < X^0$, one can resolve the p^0 dependence of $\rho(X,p)$ on the scale larger than $1/X^0$, because we have an oscillating factor due to $\int_{-X_0}^{X^0} dt\ \exp(-ip^0 t) = 2\sin(p^0 X^0)/p^0$. We numerically confirmed that the oscillation frequency is indeed proportional to X^0. This means that any finer structure of $\rho(X,p)$ than $1/T$ is resolved only after the evolution time of $X^0 > T$. The sharper peak in the case of $p_x = 20\pi/L$ needs more time to be resolved as seen in Figs.13 and 14 . As time proceeds, the oscillation amplitude of $\rho(X,p)$ diminishes leaving $\rho(X,p)$ positive definite.

When the oscillating $\rho(X,p)$ near the initial time is given, we also have an oscillation for the occupation number function $f(X,p)$ accordingly. We thus encounter a problem in evaluating σ as it contains the logarithm of $f(X,p)$. Here We come to recognize that the form of the kinetic entropy (91) obtained in the leading-order gradient expansion cannot be applied in the early stage of the initial value problem, although the gradient expansion itself becomes unjustifiable there. The applicable range of the kinetic entropy [108, 109] has not yet been examined so far with using the numerical solution of the KB equation before this study.

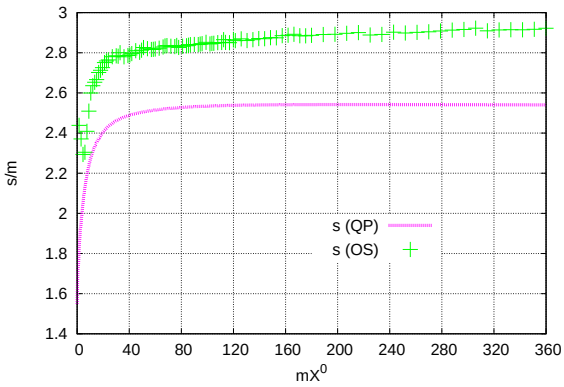

Figure 15: Time evolution of kinetic entropy (91) denoted in + and its quasi-particle approximation (95) shown in a curve for the "tsunami" initial condition with coupling $\lambda/m^2 = 4$.

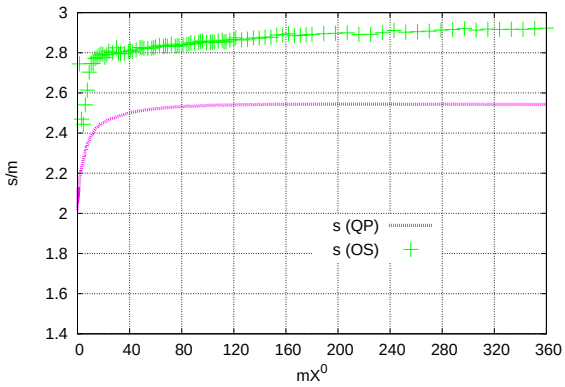

Figure 16: Time evolution of kinetic entropy (91) denoted in + and its quasi-particle approximation (95) shown in a curve for the "Woods-Saxon" initial condition with coupling $\lambda/m^2 = 4$.

In Fig. 15 and 16 we try evaluating the kinetic entropy (91) as a function of time X^0 for tsunami and WS initial conditions. It is easier to estimate this kinetic entropy with larger width of spectral functions in the range of stronger coupling. Crude as it is, we simply neglect the contributions from the region of p^0 where $\rho(X,p)$ has negative values. We obtain the entropy that decreases until $mX^0 \sim 10$. This peculiar behavior is presumably stemming from omitting the negative $\rho(X,p)$ contribution, which seems likely to overestimate the entropy. In the later stage, say $mX^0 > 20$, the kinetic entropy increases monotonically as time proceeds, which is expected from the fact that the kinetic entropy (91) satisfies the H-theorem. Asymptotic behavior of both entropy in this stage is independent of the initial conditions. This plot is one of the new results in our work [110].

In Fig. 17 we show the ratio between kinetic entropy (91) and its quasiparticle approximation (95) for tsunami and WS initial conditions. At early stage $mX^0 \sim 10$ the ratio has numerical artifact from the uncertainty principle of $\rho(X,p)$ and $f(X,p)$. At the middle stage $20 < mX^0 < 80$ the ratio becomes constant for both initial conditions. In this range it seems that the contributions to kinetic entropy around the peaks of spectral function are expressed by $12\% \sim 13\%$ of its quasiparticle approximation. At the late stage $mX^0 > 80$ the ratio starts to increase. This tendency can be explained from the behavior of time evolution of number density. In Fig. 18 we show the time evolution of total number density for tsunami and WS initial conditions with $\lambda = 4$. At the rate time $mX^0 > 80$ with $\lambda = 4$ the number density decreases continually. In addition the distribution

function shown in Figs. 7 and 8 has the small change for $mX^0 > 80$. Due to the decrease of number density and small change for $n_{\mathbf{p}}$ the entropy with quasiparticle approximation (95) increases weakly compared with the kinetic entropy (91).

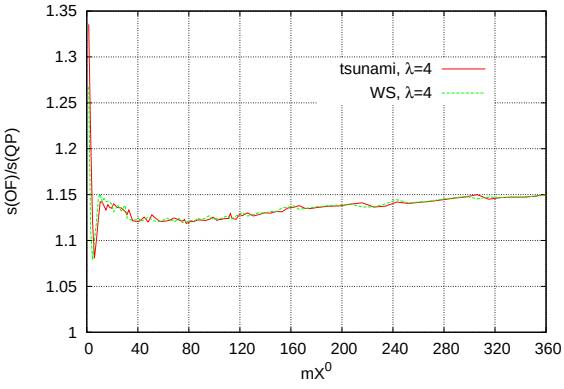

Figure 17: Time evolution of the ratio kinetic entropy $s(\text{Kinetic entropy with Off} - \text{Shellness})$ and $s(\text{Quasi} - \text{Particle approximation})$ for "tsunami" (solid) and Woods-Saxon (dotted) initial conditions with coupling $\lambda/m^2 = 4$.

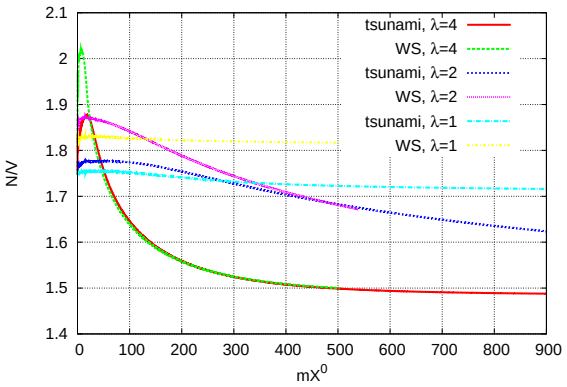

Figure 18: Time evolution of total number density for "tsunami" and Woods-Saxon initial conditions with coupling $\lambda/m^2 = 4$, 2 and 1.

As an alternative estimate for the entropy of the system, let us evaluate it in the quasi-particle (QP) approximation (95) with the number distribution $n_p(X^0)$ defined in Eq. (72). The quasi-particle approximation (95) may be reasonable because the spectral function is nicely peaked [92] near $\omega^2 \sim m^2 + \mathbf{p}^2$ as seen in Figs. 11, 12, 13 and 14. For the weaker coupling it is reasonable to use (95) since the width of spectral function is thinner to be approximated by delta function. We remark that $n_{\mathbf{p}}(X^0)$ is here obtained using the solution of the full KB equation via Eqs. (72) and (73). Since $n_{\mathbf{p}}(X^0)$ is defined locally at time $x^0 = y^0$ without the Fourier transformation, we have no computational difficulty even at the very early stage, in contrast to the kinetic entropy (91). Since the concept of entropy is hardly depicted with nonequilibrium KB simulation, the estimation in this subsection is also one of the new results in our work. We present the result in Figs. 15 and 16 in a solid curve.

Although the QP entropy (95) yields somewhat a smaller value as compared with the kinetic entropy (91), the evolution profiles of these entropies are quite similar to each other, except at the early times. Smaller value for the QP entropy (95) may be related to the fact that it neglects the finite width of the spectral distribution over p^0. With the QP approximation we see in Figs. 15 and 16 that the entropy production is concentrated at early times $mX^0 \lesssim 20$ and slows down at later times $mX^0 \gtrsim 20$, approaching an equilibrium value.

The entropy in the QP approximation is also written in term of $n(\tilde{\omega}_{\mathbf{p}})$. We can study which microscopic process contributes to the change of the distribution function $n(\tilde{\omega}_{\mathbf{p}})$ in course of the time evolution. Although the distribution $n(\tilde{\omega}_{\mathbf{p}})$ in Figs. 7 and 8 is computed using Eqs. (72) and (73), it seems instructive to evaluate the time derivative $dn_{\mathbf{p}}/dX^0$ in the quasi-particle approximation, which is given in Eq. (570) in Appendix D. Within this approximation we can clearly separate out the contributions of 0-to-4, 1-to-3, 2-to-2 and 3-to-1 processes. In Figs. 19, 20, 21 and 22 shown are the contributions of each microscopic process on the RHS of $dn_{\mathbf{p}}/dX^0$ Eq. (570) at the momentum $p_n = 2\pi n/(2L)$ with $n = 7$ and 0 for "tsunami" and WS initial conditions, respectively. We set $\lambda/m^2 = 4$. The mode with $\mathbf{p}$ is included as one of the three particles in the 1-to-3 process while it is formed from three particles in the 3-to-1 process.

Even in the quasi-particle approximation, the number changing processes are possible because

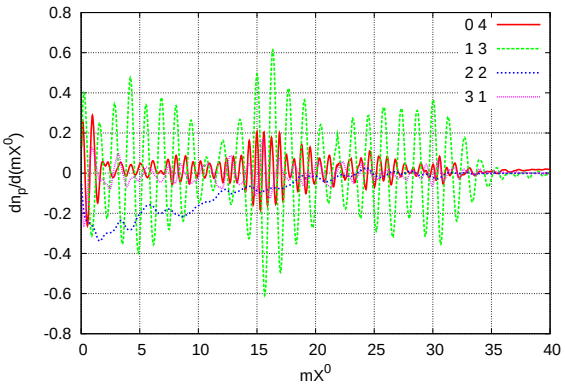

Figure 19: Microscopic contributions to $dn_{\mathbf{p}}/dX^0$ at $pL = 7 \cdot 2\pi$ as functions of mX^0 in the case of "tsunami" initial condition with $\lambda/m^2 = 4$. By integrating from $mX^0 = 0$ to $mX^0 = 35$ each contribution to $\delta n_{\mathbf{p}}$ is obtained to be 0.51, 0.62, -3.17 and -0.24 for 0-to-4, 1-to-3, 2-to-2 and 3-to-1 processes.

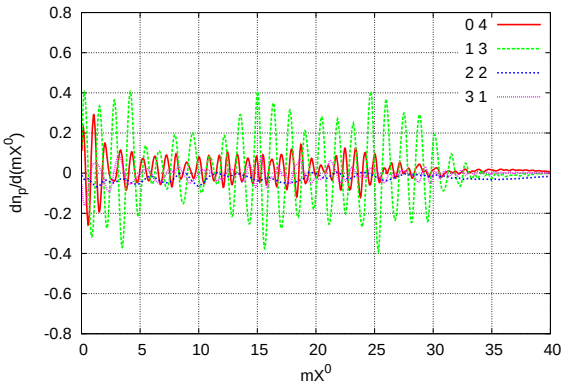

Figure 20: Microscopic contributions to $dn_{\mathbf{p}}/dX^0$ at $pL = 7 \cdot 2\pi$ as functions of time mX^0 in the case of the WS initial condition with $\lambda/m^2 = 4$. By integrating from $mX^0 = 0$ to $mX^0 = 35$ each contribution to $\delta n_{\mathbf{p}}$ is obtained to be 0.54, 0.75, -0.86 and -0.26 for 0-to-4, 1-to-3, 2-to-2 and 3-to-1 processes.

of the finite memory time as was studied in Ref. [173]. We see that at early times the number changing processes $1 \leftrightarrow 3$ contribute as well as $2 \leftrightarrow 2$ scattering processes. One should recall that $dn_{\mathbf{p}}/dX^0 = 0$ in the Boltzmann limit in 1+1 dimensions; even the 2-to-2 process is possible only when it keeps the particle momenta unchanged.

As is seen in Fig. 7, the momentum of $n = 7$ locates near the peak for the tsunami initial condition, and $n(\tilde{\omega}_{\mathbf{p}})$ decreases rapidly toward the equilibrium value. In the quasi-particle approximation shown in Fig. 19, the 2-to-2 process contributes largely to this decrease, although other number changing processes are also operative at early times, say $mX^0 < 35$. For the WS initial condition, the momentum of $n = 7$ locates near the shoulder position of the distribution and $n(\tilde{\omega}_{\mathbf{p}})$ decreases with time as seen in Fig. 8. In this case, the 2-to-2 and other processes seem equally contributing to $dn(\tilde{\omega}_{\mathbf{p}})/dX^0$. However, the 2-to-2 contribution is negative and rather non-oscillatory while others are fast oscillating.

In addition in Fig. 7, the mode with $n = 0$ is located at the tail of the Gaussian initial condition, and the number distribution function grows up rapidly. In the microscopic processes shown in Fig.21, the 2-to-2 scattering process contribute largely to this growth, and the other number changing processes are smaller contributions to this growth. For the WS initial condition, the mode with $n = 0$ is located in the flat regions and $n(\tilde{\omega}_{\mathbf{p}})$ increases with time as seen in Fig.8. In this case, the 1-to-3 processes have the largest contributions in all processes. (Although we might think that they are too large to achieve the Bose distribution function, they are cancelled by 3-to-1 processes ~ -8 given by integration from $mX^0 = 0$ to $mX^0 = 140$ in the end.) Here $n(\tilde{\omega}_{\mathbf{p}})$ around the lowest mode contribute to the growth of $n(\tilde{\omega}_{\mathbf{p}})$.

The above observations are in the quasi-particle approximation, while we evaluated $n(\tilde{\omega}_{\mathbf{p}})$ using the full solution of the KB equation which includes both the effects of the finite memory time and the spectral distribution $\rho(X, p)$. The latter is missed in the estimate with the quasi-particle approximation.

In the end we compare the evolutions of the QP entropy for λ/m^2=4, 2 and 1 with the tsunami and WS initial conditions, respectively, in Figs. 23 and 24. In these figures, we see that the larger is the coupling the faster is the entropy produced and saturated to the equilibrium value. In order to quantify the approach to the equilibrium value, we fit the entropy evolution with a simple functional

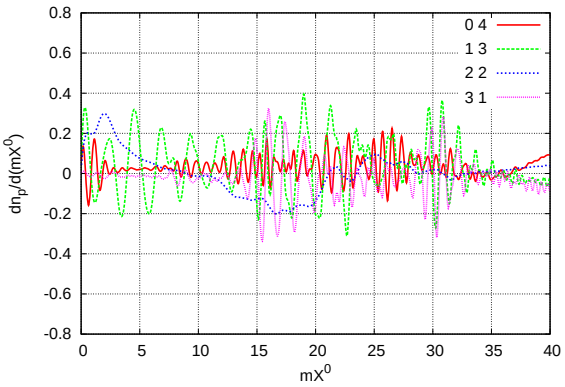

Figure 21: Microscopic contributions to $dn_{\mathbf{p}}/dX^0$ at $pL = 0 \cdot 2\pi$ as functions of mX^0 in the case of "tsunami" initial condition with $\lambda/m^2 = 4$. By integrating from $mX^0 = 0$ to $mX^0 = 35$ each contribution to $\delta n_{\mathbf{p}}$ is obtained to be 0.05, 0.12, -2.74 and -0.56 for 0-to-4, 1-to-3, 2-to-2 and 3-to-1 processes.

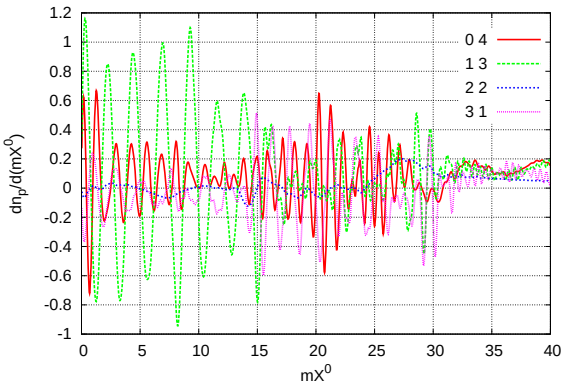

Figure 22: Microscopic contributions to $dn_{\mathbf{p}}/dX^0$ at $pL = 0 \cdot 2\pi$ as functions of time mX^0 in the case of the WS initial condition with $\lambda/m^2 = 4$. By integrating from $mX^0 = 0$ to $mX^0 = 35$ each contribution to $\delta n_{\mathbf{p}}$ is obtained to be 0.54, 10.49, -0.88 and -1.12 for 0-to-4, 1-to-3, 2-to-2 and 3-to-1 processes.

λ	γ_0	$s_{\max}$	A	γ	γ_0	$s_{\max}$	A	γ
4(OS)	-	2.93	0.16	0.0071	-	2.93	0.15	0.0071
4	0.24	2.54	0.16	0.030	0.14	2.54	0.14	0.030
2	0.084	2.48	0.10	0.0031	0.036	2.44	0.13	0.0031
1	0.027	2.39	0.17	0.0024	0.0085	2.39	0.19	0.0011

Table 1: Slope parameter γ_0 near $X^0 \sim 0$ and parameters in Eq. (122) for "tsunami" (left) and WS (right) initial conditions.

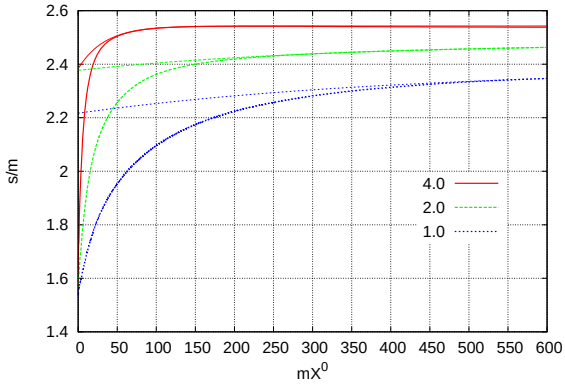

Figure 23: Entropy density s^0/m in the quasiparticle approximation for the "tsunami" initial condition with coupling λ/m^2 =4, 2 and 1. The exponential fit with (122) is denoted by a thin line in each case.

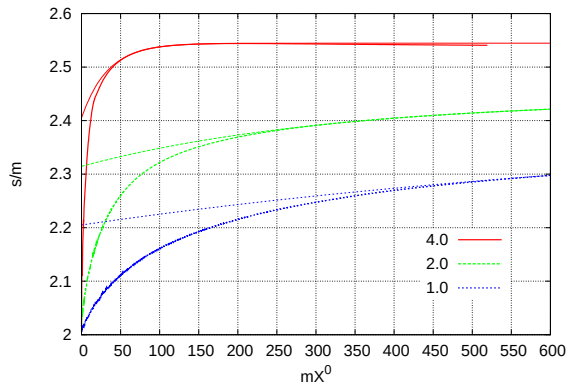

Figure 24: Entropy density s^0/m in the quasiparticle approximation for the WS initial condition with coupling λ/m^2 =4, 2 and 1. The exponential fit with (122) is denoted by a thin line in each case.

form

$$s(X^0) = s_{\max} - Ae^{-\gamma(mX^0)} \ , \tag{122}$$

where $s_{\max}$, A and γ are parameters. We chose to fit the evolution in the regions $100 \leq mX^0 \leq 150$, $300 \leq mX^0 \leq 600$ and $600 \leq mX^0 \leq 900$ for λ=4, 2 and 1, because the approach to equilibrium is slower for smaller λ. The resultant values for the parameters are summarized in Table. 1. Furthermore we add the fit of kinetic entropy (91) in the regions $120 \leq mX^0 \leq 360$ as a reference. The parameters γ and $s_{\max}$ take the same values independent of the initial conditions both for the coupling constants λ =4 and 2. This property is the same as the kinetic entropy (91) with $\lambda = 4$. The λ dependence of the parameter γ seems non-trivial, contrary to the λ^2 dependence naively inferred from(96). For λ=1, our fit seems still sensitive to the initial conditions. As shown in Fig.18, the total number density is dependent on the initial condition in $600 \leq mX^0 \leq 900$ although the number distribution functions are near the Bose distribution. Since the entropy (95) tends to be affected by the total number density and the total number density does not still lose its initial condition dependence for $\lambda = 1$, its asymptotic form depends on the initial conditions. At the later stage γ might coincide for both initial conditions, but in this range $mX^0 > 900$ we have energy errors more than 0.5%, so that we stop our simulation.

3.5 Numerical simulation for scalar ϕ^4 theory in 2+1 dimensions

In this subsection we present numerical analysis for 2+1 dimensions. This analysis is motivated from the Weibel instability which cause the isotropization of the system after heavy ion collisions. Here the isotropization is the process without entropy production. The isotropization is considered to help the rapid thermalization of gluons due to 2-to-3 scattering processes with entropy production and to explain the early thermalization $\tau_{\rm eq} = 0.6 \sim 1.0$ fm/c. However we have a question here. How much the isotropization help the thermalization. To answer this question we present two initial conditions. One is anisotropic initial condition which is before the instability has occurred. The other is the isotropic initial condition which is after the instability has occurred. Both energy density and entropy density are set to be the same value to make the comparison of the thermalization time to the same thermal equilibrium (Fig.25). Before analyzing in gluodynamics we should investigate

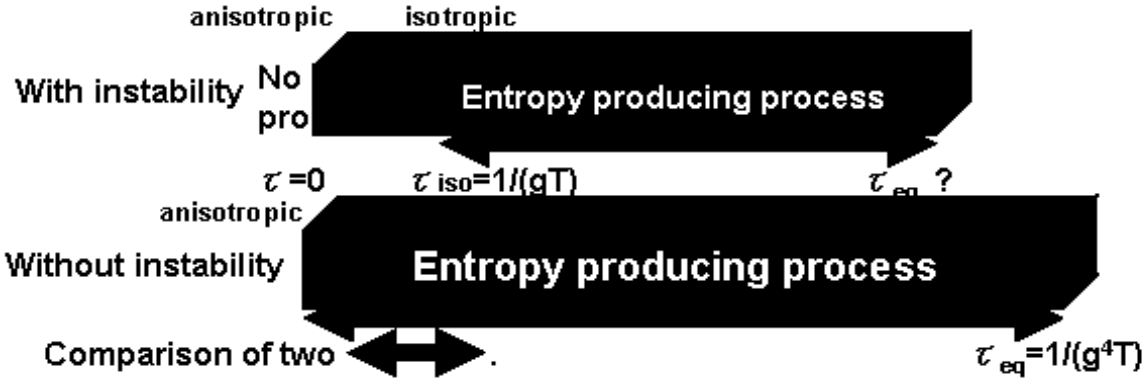

Figure 25: Comparison of the thermalization time from isotropic and anisotropic initial conditions.

the thermalization process and compare the speed of entropy production with two initial conditions in scalar field theory as a practice. In $O(\lambda^2)$ of scalar ϕ^4 theory we are only allowed to analyze 2-to-2 scattering processes which is significant for kinetic equilibrium and particle number changing processes 3-to-1 and 4-to-0 and inverse which play an important role in chemical equilibrium. We present the comparison of two initial conditions with the above scattering and particle number changing processes.

In order to trace the time evolution of statistical and spectral functions in the Kadanoff-Baym equation, we shall use a normal lattice discretization with respect to momentum space[119]. The edges of the square have length L, so that its area is $S = L^2$. The lattice spacing is a_s, and N_s is the mesh size of the area, so that $L = 2N_s a_s$. Here $\mathbf{k}^2$ is discretized in the following,

$$\mathbf{k}^2 \to \Sigma_{i=1}^2 \frac{4}{a_s^2} \sin^2\left(\frac{a_s k_n}{2}\right) \tag{123}$$

where the momenta $\mathbf{k_n}$ are discretized according to $\mathbf{k_n} = \frac{2\pi \mathbf{n}}{L}$ with $n \in \{-N_s, \cdots, N_s\}^2$. By taking $\mathbf{k}^2$ as the above way we can remove most of the lattice artifacts. And we take the following replacement in integrating in the momentum space

$$\int \frac{d^2p}{(2\pi)^2} \to \frac{1}{S} \Sigma_{n \in \{-N_s, \cdots, N_s\}^2}. \tag{124}$$

The mesh size N_s is sufficient to plot the momentum dependence of mode distribution function and to satisfy the conversions of the solutions in each momentum mode, which can be verified by increasing N_s. For the numerical analysis we have used a space lattice with

$$ma_s = 0.3,\ a_t/a_s = 0.1,\ N_s = 30. \tag{125}$$

Now we shall start the numerical simulation of KB equation in 2+1 dimensions. First in Fig.26 we present the anisotropic initial distribution function given by

$$n_{p,\mathrm{ani}} = \frac{1}{\mathcal{N}} \exp\left(-\frac{(p_x - p_t)^2}{2\sigma_1^2} - \frac{p_y^2}{2\sigma_2^2}\right) \tag{126}$$

with $\sigma_1^2/m^2 = 10.4 \times \left(\frac{2\pi}{mL}\right)^2$, $\sigma_2^2/m^2 = 100 \times \left(\frac{2\pi}{mL}\right)^2$, $p_t = 9.20 \cdot 2\pi/L$ and $\mathcal{N} = 0.25$. The distribution function is localized in $p_x = p_t, p_y = 0$ and has the Gaussian structure. Total energy is set to be $E_{\mathrm{tot}}/m = 18200$ and entropy density is set to be $s_0/m^2 = 5.9$.

The coupling constant is set to be $\lambda/m = 8$. As time goes by, the Gaussian structure of anisotropic initial condition collapse and becomes isotropic with entropy production (Figs.27 and 28). After the isotropization the distribution function becomes thermal equilibrium (Figs.29 and 30). In Fig.30 we present the logarithmic plot of distribution function $\log\left(1 + \frac{1}{n_p}\right)$. At kinetic equilibrium this function becomes $\frac{\epsilon_p}{T} - \frac{\mu}{T}$ where T is the temperature and μ is the chemical potential. In Fig.30 the plot seems to be on this straight line, so that we can see that kinetic equilibrium is achieved.

We expressed the kinetic energy $E_{\mathrm{kin}} - E_{\mathrm{tot}}|_{mX^0=0}$, tadpole energy E_{tad}, sunset energy E_{sun} and total energy $E_{\mathrm{tot}} - E_{\mathrm{tot}}|_{mX^0=0}$ in Fig.31. In the numerical simulation the energy is conserved in the error range of 0.5%.

Next let us prepare the isotropic initial condition which has the same energy and entropy density as the anisotropic initial conditions. We present the initial condition as

$$n_{p,\mathrm{iso}} = \frac{1}{\mathcal{N}_1} \exp\left(-\frac{{p_x}^2 + p_y^2}{2\sigma_3^2}\right) - \frac{1}{\mathcal{N}_2} \exp\left(-\frac{{p_x}^2 + p_y^2}{2\sigma_4^2}\right) \tag{127}$$

with $\sigma_3^2/m^2 = 48.0 \times \left(\frac{2\pi}{mL}\right)^2$, $\mathcal{N}_1 = 0.1326$, $\sigma_4^2/m^2 = 12.0 \times \left(\frac{2\pi}{mL}\right)^2$ and $\mathcal{N}_2 = 0.20$. Here we have set $1/\mathcal{N}_1 > 1/\mathcal{N}_2$ and $\sigma_3 > \sigma_4$. In Fig.32 we show the isotropic initial condition in momentum space. The coupling constant is set to be the same $\lambda/m = 8$ as the anisotropic case in the time evolution.

As time goes by, the distribution function approaches thermal equilibrium with maintaining its isotropy (Figs.33 and 34). At the late time ($mX^0 = 36$) we find that the distribution function is thermalized (Figs.35 and 36). In Fig.36 the logarithmic plot seems to be on the line of $\log\left(1 + \frac{1}{n_p}\right) = \frac{\epsilon_p}{T} - \frac{\mu}{T}$. Thus the kinetic equilibrium seems to be achieved.

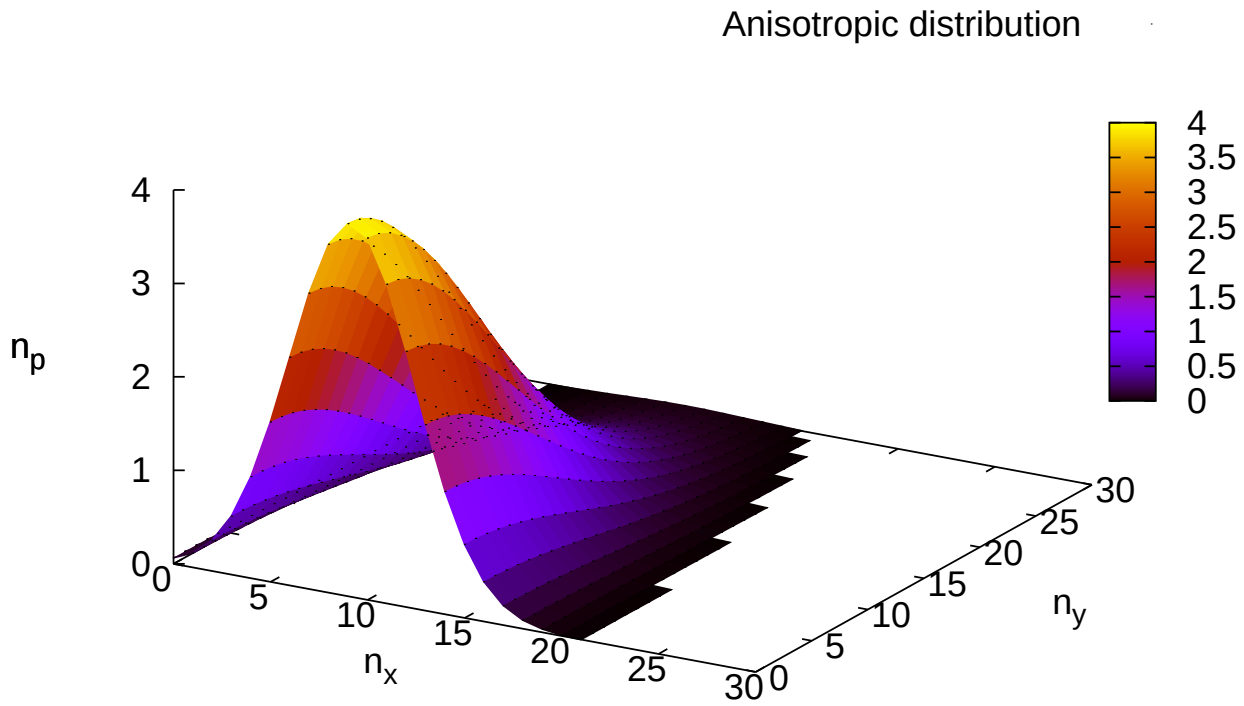

Figure 26: Anisotropic initial conditions in which the distribution function is localized in $p_x = p_t$.

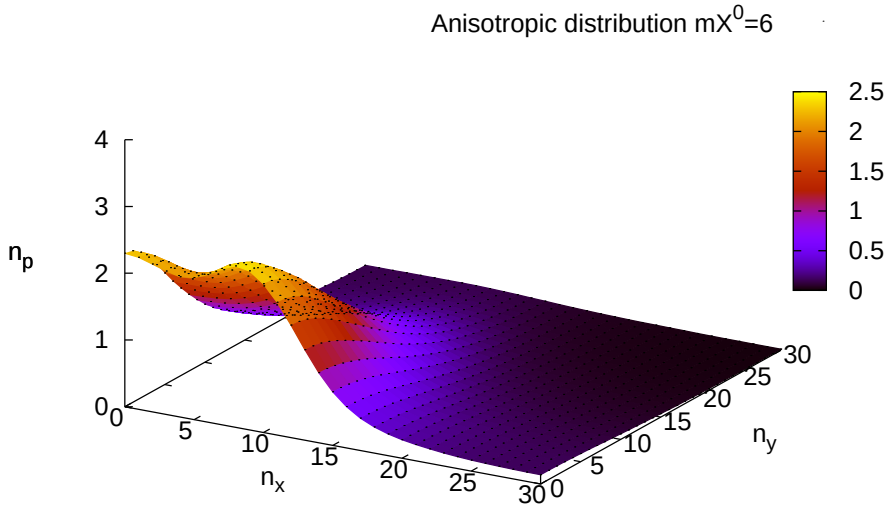

Figure 27: Anisotropic initial conditions at $mX^0 = 6$

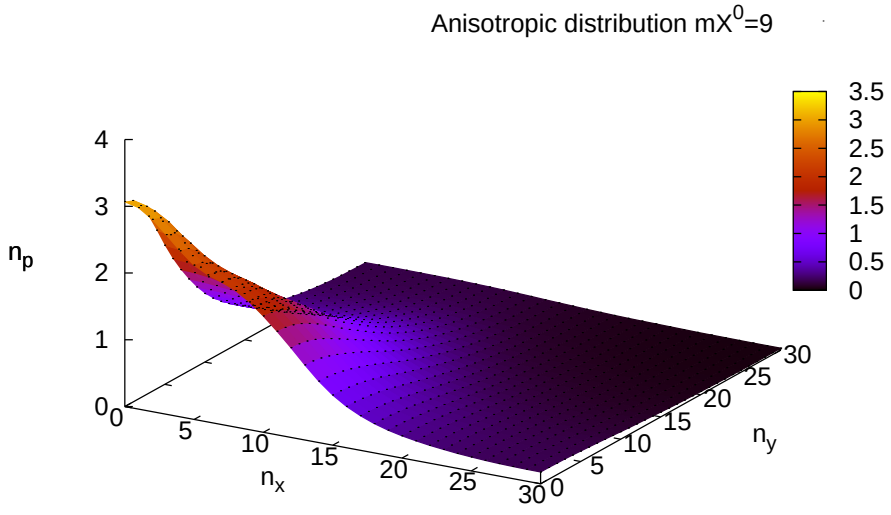

Figure 28: Anisotropic initial conditions at $mX^0 = 9$

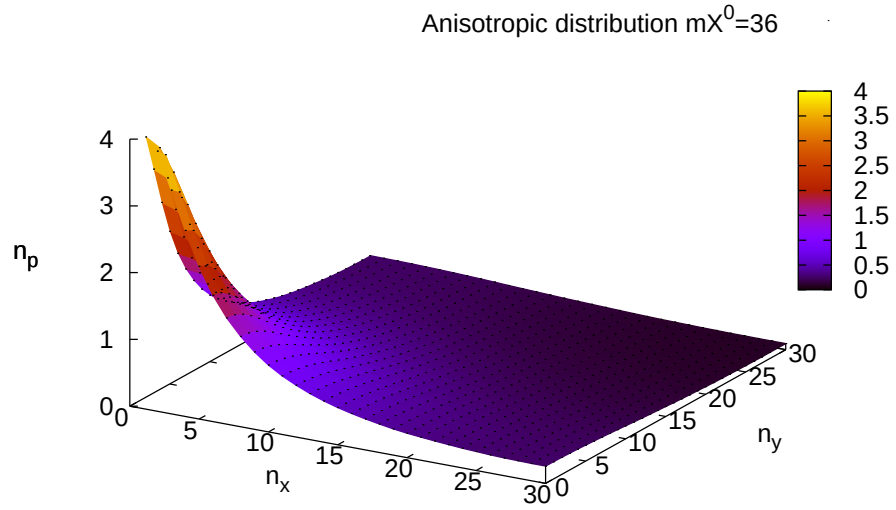

Figure 29: Anisotropic initial conditions at $mX^0 = 36$

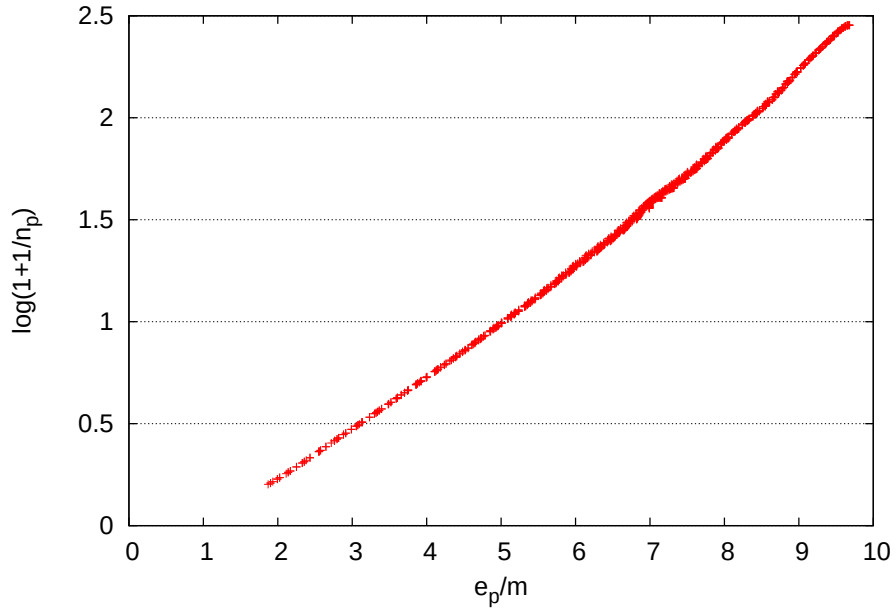

Figure 30: Logarithmic plot $\log(1 + 1/n_p)$ vs. ϵ_p/m at $mX^0 = 36$. The plot seems to be on the straight line with slope m/T.

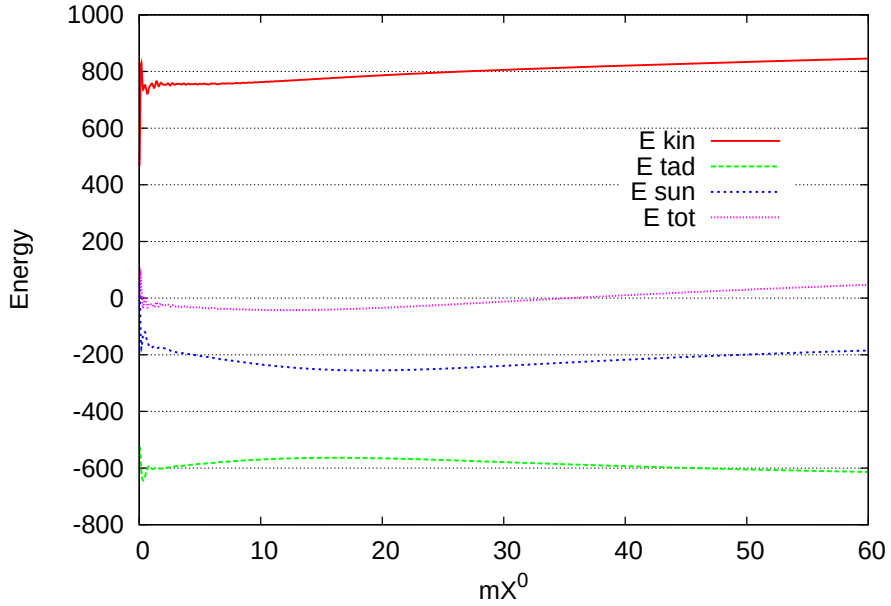

Figure 31: Kinetic, tadpole, sunset and total energies for the anisotropic initial condition in the range of $0 < mX^0 < 60$. The kinetic energy and total energy are represented with the difference from the initial total energy. The error of the total energy is 0.5%.

In Fig.37 we represent the kinetic energy $E_{\rm kin} - E_{\rm tot}|_{mX^0=0}$, tadpole energy $E_{\rm tad}$, sunset energy $E_{\rm sun}$ and total energy $E_{\rm tot} - E_{\rm tot}|_{mX^0=0}$. The kinetic energy and total energy is expressed as the difference from the initial total energy. The error of the total energy is 1% compared to the $E_tot|_{mX^0=0} = 18200$ in the range of $0 < mX^0 < 60$.

In Fig.38 we express the time evolution of total number density with respect to the anisotropic and isotropic initial condition. We can confirm whether the chemical equilibrium is achieved by investigating whether the total number density approaches the constant value. In this figure the two number densities seem to converge to the same value, but the value is not constant. We conclude if we prepare initial conditions with the same energy density, their distribution functions seem to converges the same chemical equilibrium, but at $mX^0 = 60$ the chemical equilibrium is not achieved.

Finally let us compare the speed of thermalization for two initial conditions by comparing the entropy production rate. In Fig.39 we represent the time evolution of entropy density with respect to the anisotropic and isotropic initial conditions. The definition of entropy density is $s^0 = \int_p [(1+n_p)\log(1+n_p) - n_p \log n_p]$ and we do not use the kinetic entropy with spectral width. Let us observe the two behavior in Fig.39. The initial entropy density is the same value, but at early time entropy density in isotropic case increased more rapidly. The difference of the entropy density converges to the constant value. By comparing the time where $s^0/m^2 = 8$ we conclude that the isotropic initial condition is earlier by 10%. If instability caused only 10% earlier thermalization, it would become useless. However discussion with comparison of isotropic and anisotropic initial condition is initial condition dependent. And we should have discussions with gauge theory where Weibel instability occurs. Therefore we should apply the above discussions to the analysis of gauge theory.

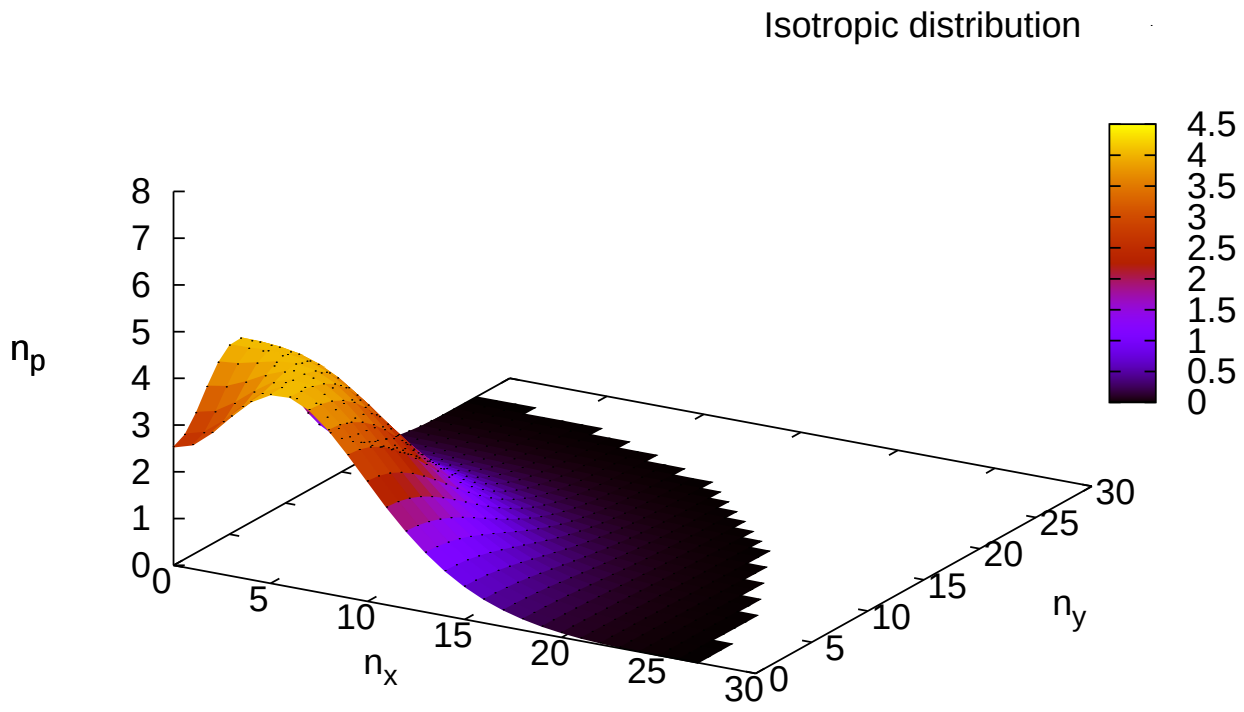

Figure 32: Isotropic initial conditions in which the distribution function is the difference of two Gaussian distribution function centered at $p_x = p_y = 0$.

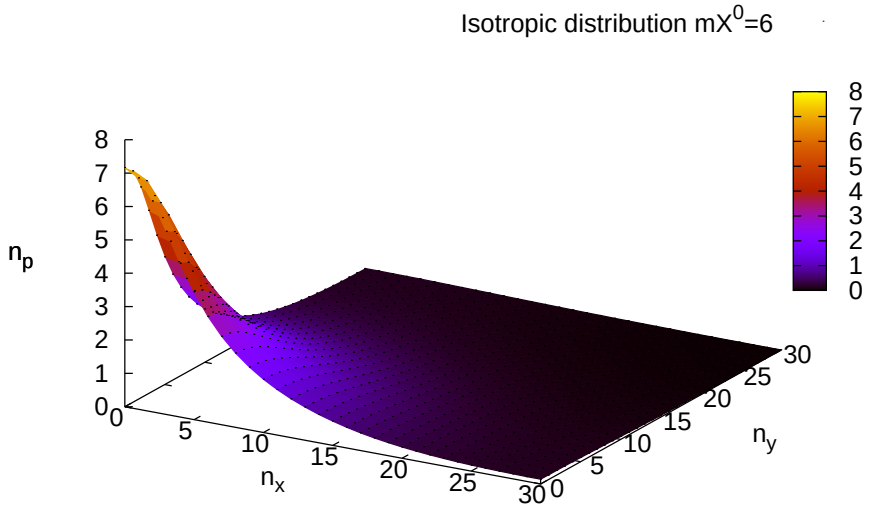

Figure 33: Isotropic initial conditions at $mX^0 = 6$.

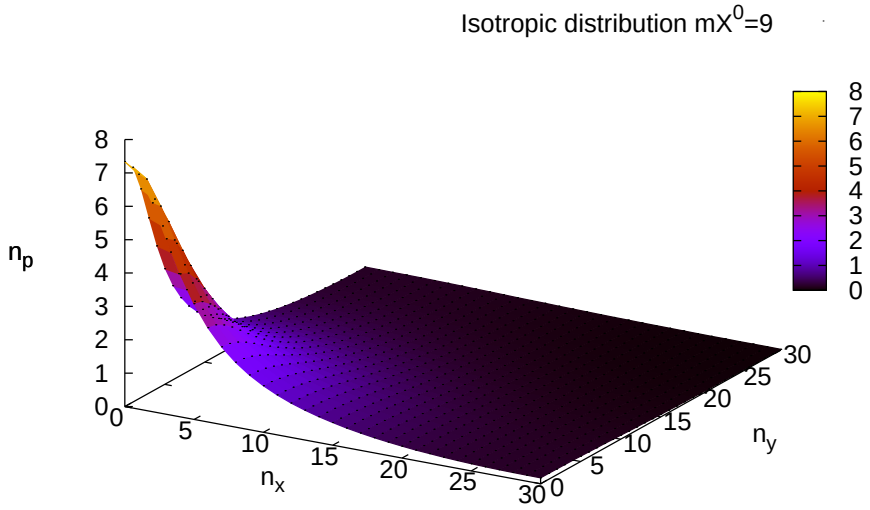

Figure 34: Isotropic initial conditions at $mX^0 = 9$.

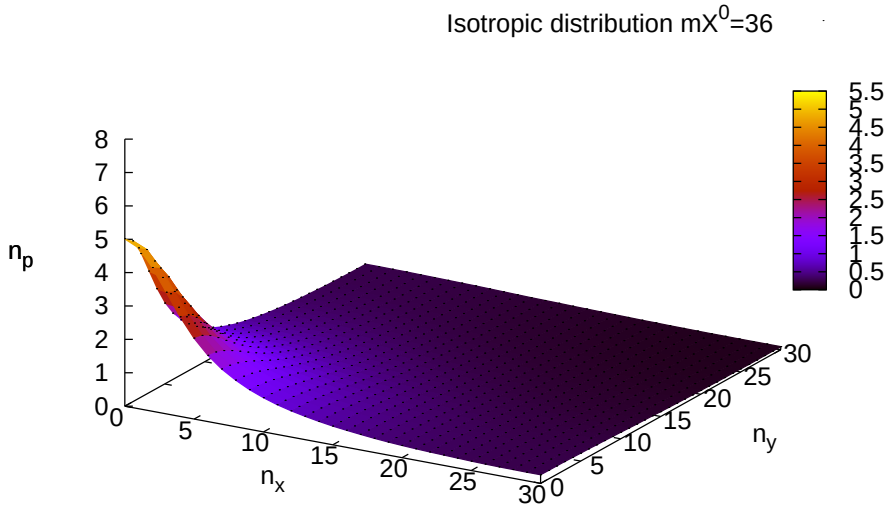

Figure 35: Isotropic initial conditions at $mX^0 = 36$.

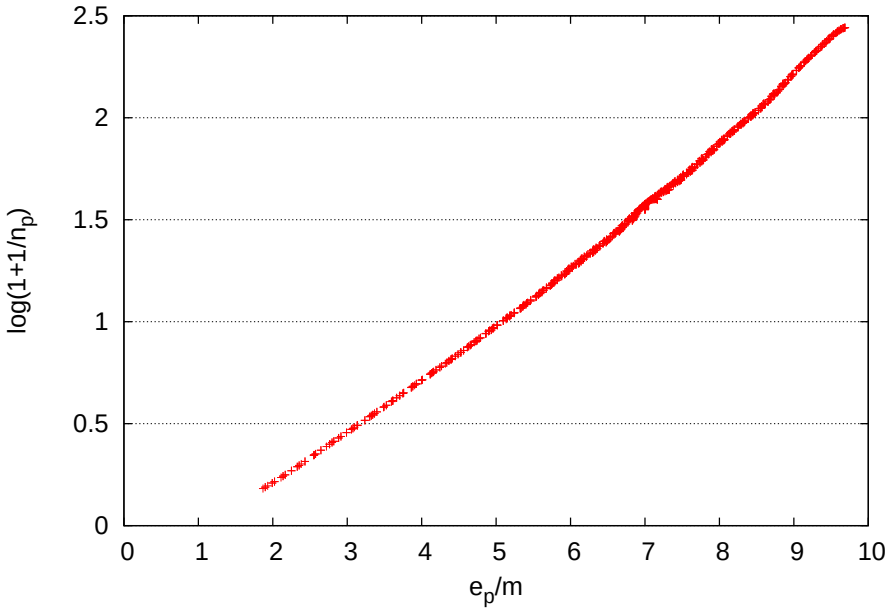

Figure 36: Logarithmic plot of distribution function vs. ϵ_p/m at $mX^0 = 36$. The plot seems to be on the straight line with slope m/T.

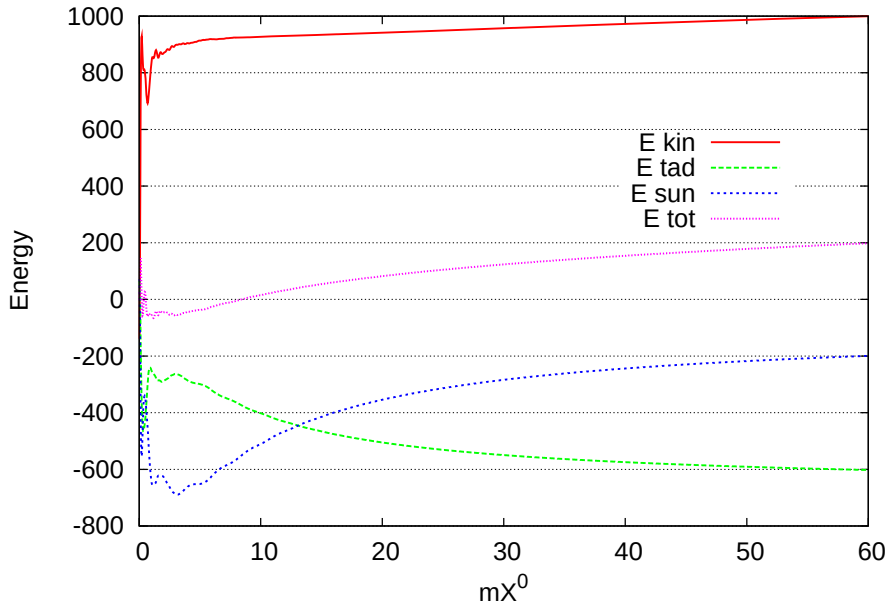

Figure 37: Kinetic, tadpole, sunset and total energy vs. time mX^0. Energy error is within 1%.

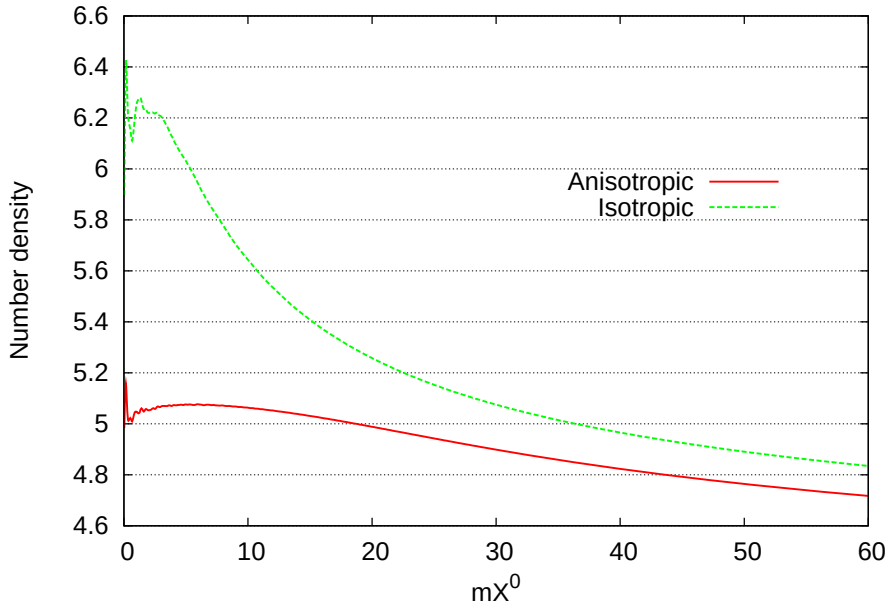

Figure 38: Comparison of time evolution of total number density with respect to isotropic and anisotropic initial condition.

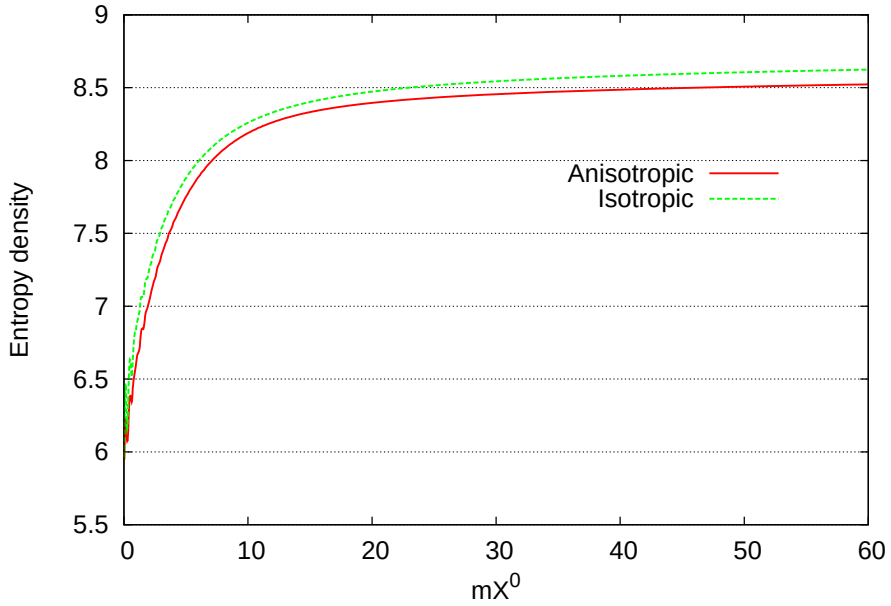

Figure 39: Comparison of time evolution of entropy density with respect to isotropic and anisotropic initial condition.

3.6 Discussion

In this section we have reviewed the derivation of Kadanoff-Baym equation with NLO self-energy of the coupling expansion. We have studied the time evolution of the $\lambda\phi^4$ theory in 1+1 and 2+1 dimensions in the framework of the KB equations with the statistical and spectral functions, $F(X,p)$ and $\rho(X,p)$, as basic ingredients. In this framework we can take into account two kinds of the "offshell" effects; one is the finite memory time effect and the other is the non-trivial form of the spectral functions $\rho(X,p)$.

We should note that no thermalization occurs in 1+1 dimensions with the Boltzmann approach with 2-to-2 collision processes, while it occurs with the KB approach even in 1+1 dimensions. We have seen that the particle number distribution $n(\tilde{\omega}_{\mathbf{p}})$, which is defined with the numerical solution of the KB equations, converges to the Bose distribution in the time evolution in 1+1 dimensions as well as 2+1 dimensions. We also showed that both the kinetic entropy (91) and the QP entropy (95) increase in course of the evolution. In order to understand the mechanism of the entropy production, we analyzed the microscopic processes within the quasi-particle approximation and found that the 2-to-2 scattering processes as well as the particle number changing processes are operative in the early stage of the evolution.

We have introduced formally the kinetic entropy (91) associated with the relativistic KB equations, to the 1st order in the gradient expansion. In general, the gradient expansion applies only when the X^0 dependence becomes gentle near equilibrium, otherwise the higher order terms can give substantial effects. Furthermore, we encountered a difficulty in evaluating the kinetic entropy (91) itself because of the fact that the spectral function $\rho(X,p)$ shows an oscillation in p^0 with the frequency proportional to $1/X^0$. This is understood as the uncertainty relation between the energy and the time. This yields negative values for the occupation number function $f(X,p)$, and invalidate the expression for the kinetic entropy (91) at early times. This has not been recognized before.

For a sufficiently later times so as to resolve the structure of the spectral function $\rho(X,p)$, we have $\rho(X,p)$ and $f(X,p)$ positive definite, and the resultant entropy monotonically increases in

time. In contrast, the QP entropy (95) is expressed in terms of the number distribution $n_{\mathbf{p}}$ obtained from the two-point function F without the Fourier transformation, and it shows a nonmonotonic increase in Figs. 15, 16, 23 and 24. Although the QP entropy has no strict justification in the context of the KB equation, its time evolution seems physically quite suitable as an indicator of the system entropy.

We have also analyzed and compared the behavior of kinetic entropy (91) and its quasiparticle approximation (95) in 1+1 dimensions. In the middle range of thermalization the ratio of both entropy becomes constant, so that entropy (95) is enough to monitor the thermalization. However at the asymptotic stage of thermalization due to the small change of $n_{\mathbf{p}}$ entropy (95) is affected by the behavior of total number density. Therefore entropy (95) has difficulty a little in estimating asymptotic behavior of the kinetic entropy (95) which is based on KB equation, but does not take so large difference.

4 Scalar $O(N)$ Field Theory

In this section let us review the nonequilibrium field theoretical approach in $O(N)$ scalar field theory. First we analyze the dynamics of the quantum field theoretical $O(N)$ model with $1/N$ expansion of the 2PI effective action to Next-to-Leading Order(NLO). Next we prove the H-theorem in the symmetric phase $\langle\phi\rangle = 0$ for KB equation with the NLO self-energy by use of first order gradient expansion. We simulate the time evolution of KB equation in 1+1 dimensions by assuming vanishing mean field and no expansion and discuss entropy production with the 2-point Green's functions.

The $O(N)$ model has been employed in the vacuum and thermal equilibrium analysis and several recent applications have studied in time dependent phenomena. It has been used in inflationary models of the early Universe, the formation of Bose-Einstein condensate in the laboratory and also in the analysis of chiral phase transition in heavy ion collisions. The dynamics of the chiral phase transition following the expansion of a quark-gluon plasma produced in relativistic heavy ion collisions has been analyzed by an $O(4)$ σ model at leading order in $1/N$ [120, 121]. Nonvanishing field expectation value is significant to describe the physics of heavy ion collisions, where the presence of a scalar quark-antiquark condensate signals the spontaneous symmetry breakdown of chiral symmetry like $\phi \sim \langle\bar{q}q\rangle$ in the the $O(4)$ model for two flavor QCD.

In the analysis of $O(N)$ model the large N approximation has been tried to study for a long time in both statistical mechanics and quantum field theory[122, 123, 124]. Recently this approximation has been applied to study the dynamical evolution of $O(N)$ model[99]. A $1/N$ expansion has the advantage over the loop expansion that it is not restricted to small couplings. In order to describe quantum scattering and thermalization we must include the Next-to-Leading Order (NLO) contribution of $1/N$ expansion. However the naive application of standard perturbation with $1/N$ expansion to the dynamical simulation breaks down by the problem that a secular (unbounded) time evolution prevents the description of the late-time behavior of quantum field[125, 126]. In addition the other application of 1PI effective action, which corresponds to the first Legendre transformation of the generating functional with respect to the expectation value of the field, is also plagued by the secular problems and unitarity violation, which means that $\langle\phi(x)^2\rangle$ can become negative in the late time behavior even when we begin with initial condition of the exact solution of large N in $O(N)$ model [125, 126].

Recently a systematic $1/N$ expansion of the 2PI effective action has been applied to a scalar $O(N)$ in the symmetric and broken phase[99, 98]. 2PI effective action is the resummation schemes of all 2 particle reducible diagrams and this approach can describe the time evolution without the secular problem and the unitarity violation in far-from-equilibrium dynamics[99].

4.1 2PI effective action of $O(N)$ model and the Equation of Motion for classical field and 2 point Green's functions

We analyze a real scalar N-component quantum field ϕ_a $(a = 1, \cdots, N)$ with an $O(N)$ invariant action

$$S[\hat{\phi}] = \int d^{d+1}x \left[\frac{1}{2}\partial\hat{\phi}_a\partial\hat{\phi}_a - \frac{1}{2}m^2\hat{\phi}_a\hat{\phi}_a - \frac{\lambda}{4!N}(\hat{\phi}_a\hat{\phi}_a)^2\right]. \tag{128}$$

The two-particle irreducible (2PI) effective action $\Gamma[\phi, G]$ is parameterized by the macroscopic field $\phi_a(x)$ and the 2 point correlation functions $G_{ab}(x, y)$ given by

$$\phi_a(x) = \langle\hat{\phi}_a(x)\rangle, \tag{129}$$

$$G_{ab}(x, y) = \langle T_C\hat{\phi}_a(x)\hat{\phi}_b(y)\rangle - \phi_a(x)\phi_b(y). \tag{130}$$

The brackets denote the expectation value with respect to the density matrix and T_C denotes time-ordering along a closed time contour.

The 2PI effective action can be derived with the methods used in Ref. [74, 114] as follows,

$$\Gamma_{\rm 2PI}[\phi, G] = S[\phi] + \frac{i}{2}{\rm Tr}\ln G^{-1} + \frac{i}{2}{\rm Tr}G_0^{-1}(\phi)G + \frac{1}{2}\Gamma_2[\phi, G] + {\rm const} \tag{131}$$

where we have used the inverse free Green's function iG_0^{-1} expressed as

$$\begin{aligned} iG_0^{-1}(x, y; \phi) &\equiv \frac{\delta^2 S[\phi]}{\delta\phi_a \delta\phi_b} \\ &= -\left[\left(\partial_x^2 + m^2 + \frac{\lambda}{6N}\phi_c(x)\phi_c(x)\right)\delta_{ab} + \frac{\lambda}{3N}\phi_a(x)\phi_b(y)\right]\delta_C(x-y). \end{aligned} \tag{132}$$

Dynamical equation for ϕ_a and G_{ab} can be derived by imposing the stationary condition of the 2PI effective action. When we have no external sources, physically meaningful solutions are derived with the constraints

$$\frac{\delta\Gamma_{\rm 2PI}[\phi, G]}{\delta\phi_a} = 0 \tag{133}$$

and

$$\frac{\delta\Gamma_{\rm 2PI}[\phi, G]}{\delta G_{ab}} = 0. \tag{134}$$

The first relation (133) leads to the evolution equation of the classical fields

$$-\left[\partial_x^2 + m^2 + \frac{\lambda}{6N}\left(\phi_b(x)\phi_b(x) + G_{bb}(x, x)\right)\right]\phi_a(x) = \frac{\lambda}{3N}\phi_b(x)G_{ba}(x, x) - \frac{1}{2}\frac{\delta\Gamma_2[\phi, G]}{\delta\phi_a(x)}, \tag{135}$$

where we have used (131) and the following relations;

$$\frac{\delta S}{\delta\phi_a(x)} = -\partial_x^2\phi_a(x) - m^2\phi_a(x) - \frac{\lambda}{3!N}\phi_a(x)\phi_b(x)\phi_b(x) \tag{136}$$

and

$$\frac{\delta}{\delta\phi_a}\left(\frac{i}{2}{\rm Tr}G_0^{-1}G\right) = -\frac{\lambda}{6N}\phi_a(x)G_{bb}(x, x) - \frac{\lambda}{3N}\phi_b(x)G_{ba}(x, x). \tag{137}$$

In addition to (135) we derive from the second relation (134) the following Schwinger-Dyson (SD) equation:

$$G_{ab}^{-1}(x, y) = G_{0,ab}^{-1}(x, y) - \Sigma_{ab}(x, y; \phi, G) \tag{138}$$

with the self-energy defined by

$$\Sigma_{ab}(x, y; \phi, G) \equiv i\frac{\delta\Gamma_2[\phi, G]}{\delta G_{ab}(x, y)}. \tag{139}$$

The relation (138) can be rewritten by multiplying the Green functions G from the right as

$$\begin{aligned} -\left[\partial_x^2 + m^2 + \frac{\lambda}{6N}\phi_c(x)\phi_c(x)\right]G_{ab}(x, y) &= \frac{\lambda}{3N}\phi_a(x)\phi_c(x)G_{cb}(x, y) \\ &\quad + i\int_C dz\Sigma_{ac}(x, z; \phi, G)G_{cb}(z, y) \\ &\quad + i\delta_{ab}\delta_C(x-y) \end{aligned} \tag{140}$$

where we have used (132). We can trace the dynamics of $O(N)$ model with classical field ϕ_a and fluctuations or 2 point Green's functions G_{ab} with (135) and (140).

4.1.1 Next to Leading Order of $1/N$ expansion for $O(N)$ model

In this subsection we give the detailed derivation of the $1/N$ expansion of the 2PI effective action proposed in Ref. [99, 98]. At first the interaction vertices can be derived in the following,

$$\mathcal{L}_{\rm int}(x;\phi,\hat{\phi}) = -\frac{\lambda}{6N}\phi_a(x)\hat{\phi}_a(x)\hat{\phi}_b(x)\hat{\phi}_b(x) - \frac{\lambda}{4!N}\left[\hat{\phi}_a(x)\hat{\phi}_a(x)\right]^2 \tag{141}$$

which are obtained by extracting cubic and quartic parts in $\hat{\phi}$ in the classical action after shifting the field $\hat{\phi} \to \phi + \hat{\phi}$.

With the above interaction vertices we will classify 2PI diagrams contributing to $\Gamma_2[\phi, G]$ in the following,

$$\frac{1}{2}\Gamma_2[\phi,G] = \frac{1}{2}\Gamma_2^{\rm LO}[G] + \frac{1}{2}\Gamma_2^{\rm NLO}[\phi,G] + \cdots \tag{142}$$

where $\Gamma_2^{\rm LO}$ denotes the Leading Order (LO) and $\Gamma_2^{\rm NLO}$ represents the Next-to-Leading Order (NLO) contributions of $1/N$ expansion. The LO contribution to $\Gamma_2[G]$ which is ϕ independent is depicted

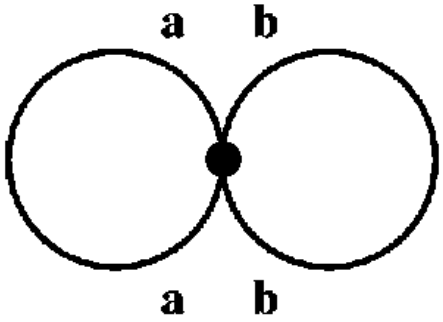

Figure 40: Leading order contribution of $1/N$ expansion for $O(N)$ theory [98].

in Fig.40, and written by the following equations:

$$\frac{1}{2}\Gamma_2^{\rm LO}[G] = \frac{1}{i}\left(\frac{-i\lambda}{4!N}\right)\int_C dx G_{aa}(x,x)G_{bb}(x,x). \tag{143}$$

This diagram contributes to the local part of the self-energy in SD equation.

The NLO contribution contains an infinite series of diagrams which are classified to 2 classes. The first class is contributions which are independent of ϕ and constructed only quartic vertices. All the contributions of this class are depicted in Fig. 41 and written by the equations

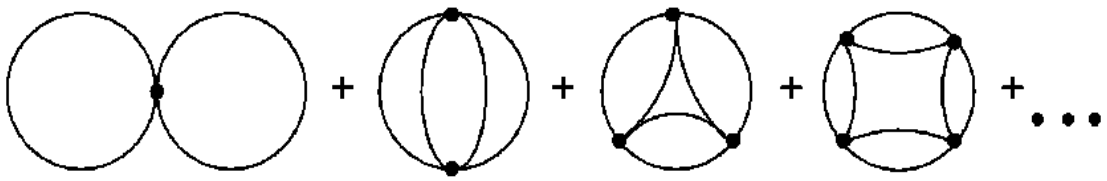

Figure 41: First class of Next-to-Leading Order diagrams [98].

$$
\begin{aligned}
\frac{1}{2}\Gamma_2^{\mathrm{NLO},1}[G] &= -\frac{1}{i}\frac{i\lambda}{4!N}2\int_C dx G_{ab}(x,x)G_{ba}(x,x) \\
&+ \frac{1}{i}\frac{1}{2}\left(\frac{-i\lambda}{4!N}\right)^2 2\cdot 2\cdot 2\int_C dxdy\ G_{ab}(x,y)G_{ab}(x,y)G_{cd}(y,x)G_{cd}(y,x) \\
&+ \frac{1}{i}\frac{1}{3!}\left(\frac{-i\lambda}{4!N}\right)^3 4\cdot 2\cdot 2\cdot 2\cdot 2\int_C dxdydz\ G_{ac}(x,y)G_{ac}(x,y) \\
&\times\ G_{be}(y,z)G_{be}(y,z)G_{df}(z,x)G_{df}(z,x) \\
&+ \cdots \\
&= \frac{i}{2}\Big[\frac{i\lambda}{6N}\int_C dx G_{ab}(x,x)G_{ab}(x,x) \\
&- \frac{1}{4}\left(\frac{i\lambda}{6N}\right)^2\int_C dxdy\ G_{ab}(x,y)G_{ab}(x,y)G_{cd}(y,x)G_{cd}(y,x) \\
&+ \frac{1}{6}\left(\frac{i\lambda}{6N}\right)^3\int_C dxdydz\ G_{ac}(x,y)G_{ac}(x,y)G_{be}(y,z)G_{be}(y,z)G_{df}(z,x)G_{df}(z,x) - \cdots\Big] \\
&= \frac{i}{2}\mathrm{Tr}\ln\left(B(G)\right), \qquad (144)
\end{aligned}
$$

where we have used the relation

$$
\ln(1+x) = x - \frac{1}{2}x^2 + \frac{1}{3}x^3 - \frac{1}{4}x^4 + \cdots, \qquad (145)
$$

and the definition

$$
B(x,y;G) = \delta_C(x-y) + \frac{i\lambda}{6N}G_{ab}(x,y)G_{ab}(x,y). \qquad (146)
$$

Here note that diagrams with the chain structure $\sim G_{a_1a_2}(x_1,x_2)G_{a_1a_2}(x_1,x_2)$ can be NLO contribution of $1/N$ expansion. This class contributes to both local and nonlocal part of the self-energy in SD equation. The nonlocal self-energy contributes to the collision term C of SD or KB equation in $O(N)$ theory as in scalar ϕ^4 theory.

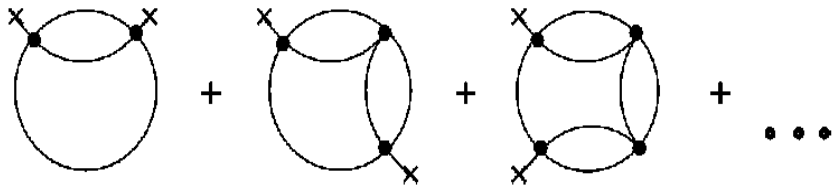

Figure 42: Second class of Next-to-Leading Order diagrams [98].

The second class of Γ_2^{NLO} is dependent on ϕ and contributes in the case of a nonzero classical

field. These series of diagrams are depicted in Fig. 42 and can be summed in the similar way as

$$\begin{aligned}
\frac{1}{2}\Gamma_2^{\mathrm{NLO},2}[\phi,G] &= +\frac{1}{i}\frac{1}{2}\left(\frac{i\lambda}{6N}\right)^2\cdot 2\int_C dxdy\phi_a(x)\phi_c(y)G_{ac}(x,y)G_{bd}(y,x)G_{bd}(y,x) \\
&+ \frac{1}{i}\frac{1}{3!}\left(\frac{-i\lambda}{4!N}\right)\left(\frac{-i\lambda}{6N}\right)^2\cdot 3\cdot 2\cdot 2\cdot 2\int_C dxdydz \\
&\times \phi_z(x)\phi_e(z)G_{ae}(x,z)G_{bc}(x,y)G_{bc}(x,y)G_{df}(y,z)G_{df}(y,z)+\cdots \\
&= -i\frac{i\lambda}{6N}\left[\frac{i\lambda}{6N}\int_C dxdy\ \phi_a(x)\phi_c(y)G_{ac}(x,y)G_{bd}(y,x)G_{bd}(y,x)\right. \\
&- \left.\left(\frac{i\lambda}{6N}\right)^2\int_C dxdydz\ \phi_a(x)\phi_e(z)G_{ae}(x,z)G_{bc}(x,y)G_{bc}(x,y)G_{df}(y,z)+\cdots\right] \\
&= \frac{i\lambda}{6N}\int_C dxdy\ [I(x,y;G)\phi_a(x)\phi_b(y)G_{ab}(x,y)] \qquad (147)
\end{aligned}$$

where we have used

$$\begin{aligned}
iI(x,y;G) &= \frac{i\lambda}{6N}G_{ab}(x,y)G_{ab}(x,y)-\left(\frac{i\lambda}{6N}\right)^2\int_C dzG_{ab}(x,z)G_{ab}(x,z)G_{cd}(z,y)G_{cd}(z,y)+\cdots \\
&= \frac{i\lambda}{6N}G_{ab}(x,y)G_{ab}(x,y)-\frac{i\lambda}{6N}\int_C dz\ iI(x,z;G)G_{cd}(z,y)G_{cd}(z,y). \qquad (148)
\end{aligned}$$

Here it is convenient to use the following relation for $I(x,y;G)$ (148) and $B(x,y;G)$ (146);

$$B^{-1}(x,y;G)=\delta_C(x-y)-iI(x,y;G) \qquad (149)$$

which is derived by use of Eq. (146) and

$$\begin{aligned}
B^{-1}=\frac{1}{1+\frac{i\lambda}{6N}GG} &= 1-\frac{i\lambda}{6N}GG+\left(\frac{i\lambda}{6N}GG\right)^2-\cdots \\
&= 1-\frac{i\lambda}{6N}GG\left(1-\frac{i\lambda}{6N}GG+\cdots\right) \\
&= 1-iI. \qquad (150)
\end{aligned}$$

As a result by summing (144) and (147) the $\Gamma_2^{\mathrm{NLO}}[\phi,G]$ can be derived as[9]

$$\begin{aligned}
\frac{1}{2}\Gamma_2^{\mathrm{NLO}}[\phi,G] &= \frac{1}{2}\Gamma_2^{\mathrm{NLO},1}[G]+\frac{1}{2}\Gamma_2^{\mathrm{NLO},2}[\phi,G] \\
&= \frac{i}{2}\mathrm{Tr}_C\ln[B(G)]+\frac{i\lambda}{6N}\int_C dxdy\ I(x,y;G)\phi_a(x)G_{ab}(x,y)\phi_b(y). \qquad (151)
\end{aligned}$$

4.1.2 Equation of Motion for NLO $1/N$ expansion

In this subsection we derive the equation of motion with respect to the classical fields ϕ and 2 point Green's functions with up to Γ_2^{NLO}.

First let us derive the equation of motion of classical field with NLO of $1/N$ expansion. The

[9] Although the $1/N$ expansion is simple in $O(N)$ theory, it is still very difficult to take $1/N_c$ expansion which sum over all of planar diagrams in gauge theory.

r.h.s. of (135) can be rewritten with (151) and (147) as

$$\begin{aligned}
\frac{\lambda}{3N}\phi_b(x)G_{ba}(x,x) - \frac{1}{2}\frac{\delta\Gamma_2[\phi,G]}{\delta\phi_a(x)} &= \frac{\lambda}{3N}\phi_b(x)G_{ba}(x,x) \\
&- \frac{i\lambda}{3N}\int dy I(x,y;G)G_{ab}(x,y)\phi_b(y) \\
&= \frac{\lambda}{3N}\int dy\left(\delta_C(x-y) - iI(x,y)\right)G_{ab}(x,y)\phi_b(y) \\
&= \frac{\lambda}{3N}\int dy B^{-1}(x,y)G_{ab}(x,y)\phi_b(y) \\
&= K_a(x,x;\phi,G) \qquad (152)
\end{aligned}$$

where we have used (149) and the definition

$$K_a(x,y;\phi,G) = \frac{\lambda}{3N}\int_C dz B^{-1}(x,z;G)G_{ab}(y,z)\phi_b(z). \qquad (153)$$

The equation of motion for the classical fields can be rewritten as

$$-\left[\partial_x^2 + m^2\frac{\lambda}{6N}\left(\phi_c(x)\phi_c(x) + G_{cc}(x,x)\right)\right]\phi_a(x) = K_a(x,x) \qquad (154)$$

Next we derive the equation of motion for the 2 point Green's functions from (140) with (143), (144), (147) and (151). The self energy of (138) can be derived with the differentiation of $\Gamma_2[\phi,G]$ with respect to 2 point Green's function. The LO of the self energy can be derived as

$$\Sigma_{ab}^{\rm LO}(x,y) = i\frac{\delta\Gamma_2^{\rm LO}[\phi,G]}{\delta G_{ab}(x,y)} = -\frac{i\lambda}{6N}\delta_{ab}G_{cc}(x,x)\delta_C(x-y) \qquad (155)$$

where we have used (143). In the similar way the NLO of the self energy can be derived with (151) as

$$\begin{aligned}
\Sigma_{ab}^{\rm NLO}(x,y) &= i\frac{\delta\Gamma_2^{\rm NLO}[\phi,G]}{\delta G_{ab}(x,y)} \\
&= -\frac{i\lambda}{3N}B^{-1}(x,y)G_{ab}(x,y) - \frac{\lambda}{3N}I(x,y)\phi_a(x)\phi_b(y) \\
&- \left(\frac{\lambda}{3N}\right)^2\int_C dzdw B^{-1}(x,z)G_{cd}(z,w)\phi_c(z)\phi_d(w)B^{-1}(w,y)G_{ab}(x,y) \qquad (156)
\end{aligned}$$

since

$$\begin{aligned}
\frac{1}{2}\frac{\delta\Gamma_2^{\rm NLO}[\phi,G]}{\delta G_{ab}(x,y)} &= \frac{i}{2}\int_C dudv B^{-1}(u,v)\frac{\delta B(u,v)}{\delta G_{ab}(x,y)} \\
&+ \frac{i\lambda}{6N}\int_C dzdw I(z,w)\phi_a(z)\phi_b(w)\delta_C(z-x)\delta_C(w-y) \\
&+ \frac{i\lambda}{6N}\int_C dzdw\frac{\delta I(z,w)}{\delta G_{ab}(x,y)}\phi_a(z)\phi_b(w)G_{ab}(z,w) \\
&= \frac{i}{2}B^{-1}(u,v)\frac{i\lambda}{3N}G_{ab}(x,y)\delta_C(u-x)\delta_C(v-y) + \\
&+ \frac{i\lambda}{6N}\int_C dzdw I(z,w)\phi_a(z)\phi_b(w)\delta_C(z-x)\delta_C(w-y) \\
&+ \frac{i\lambda}{6N}\int_C dzdw\frac{\lambda}{3N}B^{-1}(z,x)G_{ab}(x,y)B^{-1}(y,w)\phi_c(z)\phi_d(w)G_{cd}(z,w) \qquad (157)
\end{aligned}$$

where we have used the relation

$$\frac{\delta B(u,v;G)}{\delta G_{ab}(x,y)} = \frac{i\lambda}{3N} G_{ab}(x,y)\delta_C(u-x)\delta_C(v-y) \tag{158}$$

and

$$\begin{aligned}\frac{\delta I(u,v;G)}{\delta G_{ab}(x,y)} &= i\frac{B^{-1}(u,v;G)}{\delta G_{ab}(x,y)} \\ &= \frac{\lambda}{3N} B^{-1}(u,x;G)G_{ab}(x,y)B^{-1}(y,v;G).\end{aligned} \tag{159}$$

By use of the definition

$$D(x,y) \equiv \frac{i\lambda}{3N} B^{-1}(x,y;G) + \left(\frac{\lambda}{3N}\right)^2 \int_C dudv B^{-1}(x,y;G)\phi_a(u)G_{ab}(u,v)\phi_b(v)B^{-1}(v,y;G) \tag{160}$$

and the relations (149), (155) and (156) we can rewrite the (138) as

$$\begin{aligned}iG^{-1}_{ab}(x,y) &= -\left[\partial_x^2 + m^2 + \frac{\lambda}{6N}\left(\phi_c(x)\phi_c(x) + G_{cc}(x,x)\right)\right]\delta_{ab}\delta_C(x-y) \\ &- \frac{\lambda}{3N} B^{-1}(x,y;G)\phi_a(x)\phi_b(y) + iD(x,y)G_{ab}(x,y)\end{aligned} \tag{161}$$

Equations (154) and (161) with (153), (160), (148) and (149) form the complete set of equations which can trace the time evolution of classical fields and fluctuations at NLO in $1/N$ expansion. However (160) contains a double integration over the time contour C which makes the practical numerical calculation difficult. Then we can remove the double integration by exploiting the function K_a and rewriting from B and D to D and K_a.

Here D can be rewritten as

$$D(x,y) = i\frac{\lambda}{3N}\delta_C(x-y) + \frac{\lambda}{3N}K_a(x,y)\phi_a(x) - i\frac{\lambda}{6N}\int_C dz G_{ab}(x,z)G_{ab}(x,z)D(z,y) \tag{162}$$

since from (160), (153) and (149) D can be expanded as

$$\begin{aligned}D(x,y) &= i\frac{\lambda}{3N}B^{-1}(x,y) + \left(\frac{\lambda}{3N}\right)^2 \int_C dudv B^{-1}(x,u;G)\phi_a(u)G_{ab}(u,v)\phi_b(v)B^{-1}(v,y;G) \\ &= i\frac{\lambda}{3N}B^{-1}(x,y;G) + \frac{\lambda}{3N}\int_C du K_a(y,u)B^{-1}(x,u;G)\phi_a(u) \\ &= \frac{\lambda}{3N}\int_C du B^{-1}(x,u)\left[i\delta_C(y-u) + K_a(y,u)\phi_a(u)\right] \\ &= \frac{\mathbf{1}}{\mathbf{1} + i\frac{\lambda}{6N}G^2}\frac{\lambda}{3N}\left(i\mathbf{1} + K_a\phi_a\right) \\ &= i\frac{\lambda}{3N}\mathbf{1} + \frac{\lambda}{3N}K_a\phi_a - i\frac{\lambda}{6N}G^2\left(i\mathbf{1} + K_a\phi_a\right) + \left(-i\frac{\lambda}{6N}G^2\right)^2\left(i\mathbf{1} + K_a\phi_a\right) + \cdots \\ &= i\frac{\lambda}{3N}\mathbf{1} + \frac{\lambda}{3N}K_a\phi_a - i\frac{\lambda}{6N}\int_C dz G_{ab}(x,z)G_{ab}(x,z)D(z,y).\end{aligned} \tag{163}$$

In addition K_a can be rewritten as

$$K_a(x,y) = \frac{\lambda}{3N}\phi_b(x)G_{ba}(x,y) - i\frac{\lambda}{6N}\int_C dz G_{bc}(x,z)G_{bc}(x,z)K_a(z,y) \tag{164}$$

since from (153) and (149) K_a can be expanded as

$$\begin{aligned} K_a(x,y) &= \frac{\lambda}{3N}\int_C dz B^{-1}(x,z;G)G_{ab}(y,z)\phi_b(z) \\ &= \frac{\lambda}{3N}\frac{\mathbf{1}}{\mathbf{1}+i\frac{\lambda}{6N}G^2}G\phi \\ &= \frac{\lambda}{3N}G\phi - i\frac{\lambda}{6N}G^2\left(\frac{\lambda}{3N}G\phi\right)+\left(-i\frac{\lambda}{6N}G^2\right)\left(\frac{\lambda}{3N}G\phi\right)-\cdots \\ &= \frac{\lambda}{3N}G\phi - i\frac{\lambda}{6N}G^2K_a \\ &= \frac{\lambda}{3N}G_{ba}(x,y)\phi_b(x) - i\frac{\lambda}{6N}\int_C dz G_{bc}(x,z)G_{bc}(x,z)K_a(z,y). \end{aligned} \tag{165}$$

As a result B and B^{-1} are eliminated from the representation of D and K_a, and the D and K_a which have no double integration are left. In the end multiplying G from the left in (486) and by use of (153) we obtain

$$\begin{aligned} -\left[\partial_x^2 + m^2 + \frac{\lambda}{6N}\left(\phi_c(x)\phi_c(x) + G_{cc}(x,x)\right)\right]G_{ab}(x,y) &= i\delta_{ab}\delta_C(x-y) \\ +\phi_a(x)K_b(x,y) - i\int_C dz D(x,z)G_{ac}(x,z)G_{cb}(z,y). \end{aligned} \tag{166}$$

Finally we obtain the equations (154) and (166) with (164), (162) which can trace the dynamics of classical fields and fluctuations in the range of NLO of $1/N$ expansion without double integration of time contour.

4.1.3 Evolution Equations for the Spectral and Statistical functions

When we describe the nonequilibrium field dynamics we exploit the closed time contour in the path integral formulation. First the two-point function can be decomposed as

$$G_{ab}(x,y) = G^{21}_{ab}(x,y)\theta_C(x^0-y^0) + G^{12}_{ab}(x,y)\theta_C(y^0-x^0) \tag{167}$$

where $G^{21}_{ab}(x,y) = G^{12}_{ab}{}^*(x,y)$ are complex functions. We can express the evolution equations in terms of two independent real two-point functions which can be represented as the expectation values of the commutator and anti-commutator of two fields. We define

$$F_{ab}(x,y) = \frac{1}{2}\left(G^{21}_{ab}(x,y) + G^{12}_{ab}(x,y)\right) = \mathrm{Re}\left[G^{21}_{ab}(x,y)\right], \tag{168}$$

$$\rho_{ab}(x,y) = i\left(G^{21}_{ab}(x,y) - G^{12}_{ab}(x,y)\right) = -2\mathrm{Im}\left[G^{21}_{ab}(x,y)\right] \tag{169}$$

Here F is called the statistical function and ρ represents the spectral function, with properties $F^*_{ab}(x,y) = F_{ab}(x,y) = F_{ba}(y,x)$ and $\rho^*_{ab}(x,y) = \rho_{ab}(x,y) = -\rho_{ba}(y,x)$.

Next we have to separate the local part and non-local part of the self energies. As the first approach of the separation we separate the local part of D as

$$D(x,y) = \frac{\lambda}{3N}\left[i\delta_C(x-y) + \hat{D}(x,y)\right] \tag{170}$$

where

$$\hat{D}(x,y) = K_a(y,x)\phi_a(x) - \frac{\lambda}{3N}\Pi(x,y) + i\frac{\lambda}{3N}\int_C dz \Pi(x,z)\hat{D}(z,y) \tag{171}$$

since by equating (162) and (170) D can be expanded as

$$\begin{aligned} D(x,y) &= i\frac{\lambda}{3N}\delta_C(x-y)+\frac{\lambda}{3N}K_a(y,x)\phi_a(x) \\ &- i\frac{\lambda}{6N}\int_C dz G_{ab}(x,z)G_{ab}(x,z)\left[\frac{\lambda}{3N}\left(i\delta_C(z-y)+\hat{D}(z,y)\right)\right] \\ &= i\frac{\lambda}{3N}\delta_C(x-y)+\frac{\lambda}{3N}\hat{D}(x,y) \end{aligned} \tag{172}$$

and by eliminating $\delta_C(x-y)$ from the above equation $\hat{D}$ can be expressed as (171).

Let us define the statistical and spectral function for $K_a(x,y)$ and $\hat{D}(x,y)$ as

$$K_a^F(x,y)=\frac{1}{2}\left[K_a^{21}(x,y)+K_a^{12}(x,y)\right]=\mathrm{Re}\left[K_a^{21}(x,y)\right], \tag{173}$$

$$K_a^\rho(x,y)=i\left[K_a^{21}(x,y)-K_a^{12}(x,y)\right]=-2\mathrm{Im}\left[K_a^{21}(x,y)\right], \tag{174}$$

and

$$\hat{D}_F(x,y)=\frac{1}{2}\left[\hat{D}^{21}(x,y)+\hat{D}^{12}(x,y)\right]=\mathrm{Re}\left[\hat{D}^{21}(x,y)\right], \tag{175}$$

$$\hat{D}_\rho(x,y)=i\left[\hat{D}^{21}(x,y)-\hat{D}^{12}(x,y)\right]=-2\mathrm{Im}\left[\hat{D}^{21}(x,y)\right], \tag{176}$$

Now we have to express the time evolution equations for the classical fields and two-point Green's functions with respect to the spectral and statistical form. From (154) the time evolution equation for the classical field can be rewritten as

$$-\left[\partial_x^2+m^2+\frac{\lambda}{6N}\left(\phi_c(x)\phi_c(x)+F_{cc}(x,x)\right)\right]\phi_a(x)=K_a^F(x,x). \tag{177}$$

The functions $K_a^F(x,y)$ and $K_a^\rho(x,y)$ satisfy the equations

$$K_a^F(x,y)=\frac{\lambda}{3N}\phi_b(x)F_{ba}(x,y)+\frac{\lambda}{3N}\int_{t_0}^{x^0}dz\Pi_\rho(x,z)K_a^F(z,y)-\frac{\lambda}{3N}\int_{t_0}^{y^0}\Pi_F(x,z)K_a^\rho(z,y), \tag{178}$$

$$K_a^\rho(x,y)=\frac{\lambda}{3N}\phi_b(x)\rho_{ba}(x,y)+\frac{\lambda}{3N}\int_{y^0}^{x^0}\Pi_\rho(x,z)K_a^\rho(z,y) \tag{179}$$

where we have used the notation

$$\int_{t_0}^{x^0}dz\equiv\int_{t_0}^{x^0}dz^0\int d\mathbf{z}, \tag{180}$$

relations for arbitrary functions $X(x,y)$ and $Y(x,y)$

$$\begin{aligned} \left[\int_{t_0}^{\infty}X(x,z)Y(z,y)\right]_F &= i\int_{t_0}^{\infty}dz\left[X(x,z)Y(z,y)\theta(x^0-z^0)-X(x,z)Y(z,y)\theta(y^0-z^0)\right], \\ \left[\int_{t_0}^{\infty}X(x,z)Y(z,y)\right]_\rho &= i\int_{t_0}^{\infty}dzX(x,z)Y(z,y)\left[\theta(y^0-z^0)-\theta(x^0-z^0)\right], \end{aligned} \tag{181}$$

and

$$\Pi_F(x,y)=-\frac{1}{2}\left[F_{ab}(x,y)F_{ab}(x,y)-\frac{1}{4}\rho_{ab}(x,y)\rho_{ab}(x,y)\right], \tag{182}$$

$$\Pi_\rho(x,y) = -F_{ab}(x,y)\rho_{ab}(x,y). \tag{183}$$

Furthermore from (166) the evolution equation for the statistical function can be expressed as

$$-\left[\partial_x^2 + m^2 + \frac{\lambda}{6N}\left(\phi_c(x)\phi_c(x)F_{cc}(x,x)\right)\right]F_{ab}(x,y) = \frac{\lambda}{3N}F_{ac}(x,x)F_{cb}(x,y) + \phi_a(x)K_b^F(x,y) + \int_{t_0}^{x^0}\hat{\Sigma}_{ac}^\rho(x,z)F_{cb}(z,y) - \int_{t_0}^{y^0}\hat{\Sigma}_{ac}^F(x,z)\rho_{cb}(z,y), \tag{184}$$

and the evolution equation for the spectral function can be expressed as

$$-\left[\partial_x^2 + m^2 + \frac{\lambda}{6N}\left(\phi_c(x)\phi_c(x)F_{cc}(x,x)\right)\right]F_{ab}(x,y) = \frac{\lambda}{3N}F_{ac}(x,x)\rho_{cb}(x,y) + \phi_a(x)K_b^\rho(x,y) + \int_{y^0}^{x^0}\hat{\Sigma}_{ac}^\rho(x,z)\rho_{cb}(z,y), \tag{185}$$

where we have used (181) and the nonlocal self energies Σ_{ab}^F and Σ_{ab}^ρ expressed as

$$\hat{\Sigma}_{ab}^F(x,y) = -\frac{\lambda}{3N}\left[F_{ab}(x,y)\hat{D}_F(x,y) - \frac{1}{4}\rho_{ab}(x,y)\hat{D}_\rho(x,y)\right], \tag{186}$$

$$\hat{\Sigma}_{ab}^\rho(x,y) = -\frac{\lambda}{3N}\left[\rho_{ab}(x,y)\hat{D}_F(x,y) + F_{ab}(x,y)\hat{D}_\rho(x,y)\right] \tag{187}$$

with

$$\hat{D}_F(x,y) = K_a^F(y,x)\phi_a(x) - \frac{\lambda}{3N}\Pi_F(x,y) + \frac{\lambda}{3N}\int_{t_0}^{x^0}dz\Pi_\rho(x,z)\hat{D}_F(z,y) - \frac{\lambda}{3N}\int_{t_0}^{y^0}\Pi_F(x,z)\hat{D}_\rho(z,y), \tag{188}$$

$$\hat{D}_\rho(x,y) = -K_a^\rho(y,x)\phi_a(x) - \frac{\lambda}{3N}\Pi_\rho(x,y) + \frac{\lambda}{3N}\int_{y^0}^{x^0}\Pi_\rho(x,z)\hat{D}_\rho(z,y). \tag{189}$$

In the absence of classical fields ($\phi_a = 0$) we find that $K_a^F = K_a^\rho = 0$ and that only the equations for two-point Green's functions are left.

4.2 H-theorem in the symmetric phase for the NLO in the $1/N$ expansion

In this subsection we prove that the H-theorem is satisfied for the time evolution of KB equation and that the entropy defined in Sec. 3.2 is a monotonically increasing function when we consider the self-energies of the NLO in the $1/N$ expansion. We assume the zero classical fields ($\phi_a(x) = 0$) in the proof, that is we can neglect $K_a(x,y)$. Furthermore we assume two-point Green's functions are symmetric in the particle species ($G_{ab}(x,y) = \delta_{ab}G(x,y)$). Then the derivation of divergence of the entropy current is the same as that in the ϕ^4 theory. The problems are $\hat{\Sigma}_F(X,p)\rho(X,p) - \hat{\Sigma}_\rho(X,p)F(X,p)$ in the r.h.s. of (96) in which $\hat{\Sigma}_F(X,p)$ and $\hat{\Sigma}_\rho(X,p)$ should be represented by $F(X,p)$ and $\rho(X,p)$ or $G^{21}(X,p)$ and $G^{12}(X,p)$. In the (186) and (187) we find that self energies are represented $\hat{D}_F$ and $\hat{D}_\rho$. Thus we first express the Fourier transform of $\hat{D}_F(x,y)$ and $\hat{D}_\rho(x,y)$ with respect to the relative coordinate $x-y$ as functions of Fourier transformed $F(p)$ and $\rho(p)$.

In order to extract $\hat{D}_\rho(X,p)$ we derive $\hat{D}_R(X,p)$ and $\hat{D}_A(X,p)$ by multiplying $\theta(x^0-y^0)$ and $-\theta(y^0-x^0)$ in (189) and Fourier transform with respect to $x-y$. Then $\hat{D}_R(X,p)$ can be calculated

as

$$\begin{aligned}
\hat{D}_R(x,y) &\equiv \theta(x^0-y^0)\hat{D}_\rho(x,y) = -\frac{\lambda}{3N}\theta(x^0-y^0)\Pi_\rho(x,y) \\
&\quad +\frac{\lambda}{3N}\theta(x^0-y^0)\int_{y^0}^{x^0} dz\ \Pi_\rho(x,z)\hat{D}_\rho(z,y) \\
&= -\frac{\lambda}{3N}\theta(x^0-y^0)\Pi_\rho(x,y) \\
&\quad +\frac{\lambda}{3N}\theta(x^0-y^0)\int_{t_0}^{\infty} dz\ \Pi_\rho(x,z)\hat{D}_\rho(z,y)(\theta(x^0-z^0)-\theta(y^0-z^0)) \\
&= -\frac{\lambda}{3N}\theta(x^0-y^0)\Pi_\rho(x,y) \\
&\quad +\frac{\lambda}{3N}\int_{t_0}^{\infty} dz\ \Pi_\rho(x,z)\hat{D}_\rho(z,y)\left(\theta(x^0-y^0)\theta(x^0-z^0)-\theta(x^0-y^0)\theta(y^0-z^0)\right) \\
&\quad \left(\text{due to } \theta(x^0-y^0)\theta(x^0-z^0) = \theta(y^0-z^0)\theta(x^0-y^0)+\theta(z^0-y^0)\theta(x^0-z^0)\right) \\
&= -\frac{\lambda}{3N}\theta(x^0-y^0)\Pi_\rho(x,y) + \frac{\lambda}{3N}\int_{t_0}^{\infty} dz\ \Pi_\rho(x,z)\hat{D}_\rho(z,y)\theta(z^0-y^0)\theta(x^0-z^0) \\
&= -\frac{\lambda}{3N}\Pi_R(x,y) + \frac{\lambda}{3N}\int_{t_0}^{\infty} dz\ \Pi_R(x,z)\hat{D}_R(z,y).
\end{aligned} \tag{190}$$

By taking $t_0 \to -\infty$ and Fourier transforming with respect to $x-y$, $\hat{D}_R(p)$ can be written as

$$\hat{D}_R(X,p) = -\frac{\lambda}{3N}\Pi_R(X,p) + \frac{\lambda}{3N}\Pi_R(X,p)\hat{D}_R(X,p). \tag{191}$$

As a result we obtain $\hat{D}_R(X,p)$ can be derived as

$$\hat{D}_R(X,p) = \frac{-\frac{\lambda}{3N}\Pi_R(X,p)}{1-\frac{\lambda}{3N}\Pi_R(X,p)}. \tag{192}$$

In the similar way $D_A(X,p)$ can be written as

$$\hat{D}_A(X,p) = -\frac{\lambda}{3N}\Pi_A(X,p) + \frac{\lambda}{3N}\Pi_A(X,p)\hat{D}_A(X,p) \tag{193}$$

where we have used the relation $\theta(y^0-x^0)\theta(y^0-z^0) = \theta(x^0-z^0)\theta(y^0-x^0)+\theta(z^0-x^0)\theta(y^0-z^0)$. As a result we obtain

$$\hat{D}_A(X,p) = \frac{-\frac{\lambda}{3N}\Pi_A(X,p)}{1-\frac{\lambda}{3N}\Pi_A(X,p)}. \tag{194}$$

By using the relation $\hat{D}_\rho(X,p) = \hat{D}_R(X,p) - \hat{D}_A(X,p)$, (192) and (194), we obtain

$$\begin{aligned}
\hat{D}_\rho(X,p) = \hat{D}_R(X,p) - \hat{D}_A(X,p) &= \frac{-\frac{\lambda}{3N}\Pi_\rho(X,p)}{\left(1-\frac{\lambda}{3N}\Pi_R(X,p)\right)\left(1-\frac{\lambda}{3N}\Pi_A(X,p)\right)} \\
&= -\frac{\lambda_{\text{eff}}(X,p)}{3N}\Pi_\rho(X,p),
\end{aligned} \tag{195}$$

where we defined

$$\lambda_{\text{eff}}(X,p) = \frac{\lambda}{\left(1-\frac{\lambda}{3N}\Pi_R(X,p)\right)\left(1-\frac{\lambda}{3N}\Pi_A(X,p)\right)}. \tag{196}$$

In the similar way $\hat{D}_F(x,y)$ can be derived by rewriting as

$$\begin{aligned}\hat{D}_F(x,y) &= -\frac{\lambda}{3N}\Pi_F(x,y) \\ &\quad +\frac{\lambda}{3N}\int_{t_0}^{x^0} dz\ \Pi_\rho(x,z)\hat{D}_F(z,y) - \frac{\lambda}{3N}\int_{t_0}^{y^0} dz\Pi_F(x,z)\hat{D}_\rho(z,y) \\ &= -\frac{\lambda}{3N}\Pi_F(x,y) \\ &\quad +\frac{\lambda}{3N}\int_{t_0}^{\infty} dz\ \Pi_R(x,z)\hat{D}_F(z,y) + \frac{\lambda}{3N}\int_{t_0}^{\infty} dz\Pi_F(x,z)\hat{D}_A(z,y). \end{aligned} \tag{197}$$

Then $\hat{D}_F(X,p)$ is derived by taking $t_0 \to -\infty$ and Fourier transforming with respect to $x-y$ as

$$\begin{aligned}\hat{D}_F(X,p) &= -\frac{\lambda}{3N}\Pi_F(X,p) \\ &\quad +\frac{\lambda}{3N}\left(\Pi_R(X,p)\hat{D}_F(X,p) + \Pi_F(X,p)\hat{D}_A(X,p)\right) \\ \left(1-\frac{\lambda}{3N}\Pi_R(X,p)\right)\hat{D}_F(X,p) &= \frac{\lambda}{3N}\Pi_F(X,p)\left(\hat{D}_A(X,p)-1\right) \\ \hat{D}_F(X,p) &= \frac{-\frac{\lambda}{3N}\Pi_F(X,p)}{\left(1-\frac{\lambda}{3N}\Pi_R(X,p)\right)\left(1-\frac{\lambda}{3N}\Pi_A(X,p)\right)} \\ &= -\frac{\lambda_{\rm eff}(X,p)}{3N}\Pi_F(X,p), \end{aligned} \tag{198}$$

where we have used (194) and

$$\hat{D}_A(X,p)-1 = \frac{-\frac{\lambda}{3N}\Pi_A(X,p)}{1-\frac{\lambda}{3N}\Pi_A(X,p)} - \frac{1-\frac{\lambda}{3N}\Pi_A(X,p)}{1-\frac{\lambda}{3N}\Pi_A(X,p)} = \frac{-1}{1-\frac{\lambda}{3N}\Pi_A(X,p)}. \tag{199}$$

By use of (195) and (198) we obtain the following relations with respect to Fourier transformed $\Sigma_F(X,p)$ and $\Sigma_\rho(X,p)$ from (186) and (187) as

$$\begin{aligned}\hat{\Sigma}^F_{ab}(X,p) &= -\frac{\lambda}{3N}\int dq\left(F_{ab}(X,q)\hat{D}_F(X,p-q) - \frac{1}{4}\rho_{ab}(X,q)\hat{D}_\rho(X,p-q)\right) \\ &= -\frac{\lambda}{3N}\int dq\left(-\frac{\lambda_{\rm eff}(X,p-q)}{3N}\right) \\ &\quad \times\left(F_{ab}(X,q)\Pi_F(X,p-q) - \frac{1}{4}\rho_{ab}(X,q)\Pi_\rho(X,p-q)\right), \end{aligned} \tag{200}$$

and

$$\begin{aligned}\hat{\Sigma}^\rho_{ab}(X,p) &= -\frac{\lambda}{3N}\int dq\left(\rho_{ab}(X,q)\hat{D}_F(X,p-q) + F_{ab}(X,q)\hat{D}_\rho(X,p-q)\right) \\ &= -\frac{\lambda}{3N}\int dq\left(-\frac{\lambda_{\rm eff}(X,p)}{3N}\right) \\ &\quad \times\left(\rho_{ab}(X,q)\Pi_F(X,p-q) - F_{ab}(X,q)\Pi_\rho(X,p-q)\right), \end{aligned} \tag{201}$$

where $\Pi_F(X,p)$ and $\Pi_\rho(X,p)$ can be expressed from (182) and (183) as

$$\begin{aligned}\Pi_F(X,p) &= -\frac{1}{2}\int dq\left(F_{ab}(X,p-q)F_{ab}(X,q) - \frac{1}{4}\rho_{ab}(X,p-q)\rho_{ab}(X,q)\right) \\ &= -\frac{N}{2}\int dq\left(F(X,p-q)F(X,q) - \frac{1}{4}\rho(X,p-q),\rho(X,q)\right) \end{aligned} \tag{202}$$

and

$$\begin{aligned}\Pi_\rho(X,p) &= -\int dq\ F_{ab}(X,p-q)\rho_{ab}(X,q).\\ &= -N\int dq\ F(X,p-q)\rho(X,q). \end{aligned} \tag{203}$$

In the end $\hat{\Sigma}^F_{ab}(X,p)=\delta_{ab}\hat{\Sigma}^F(X,p)$ and $\hat{\Sigma}^\rho_{ab}(X,p)=\delta_{ab}\hat{\Sigma}^\rho(X,p)$ can be reexpressed by use of (202) and (203) as

$$\begin{aligned}\hat{\Sigma}^F(X,p) &= -\frac{\lambda}{3N}\int dq\left(F(X,q)\hat{D}_F(X,p-q)-\frac{1}{4}\rho(X,q)\hat{D}_\rho(X,p-q)\right)\\ &= -\frac{\lambda}{3N}\int dqdl\frac{\lambda_{\rm eff}(X,p-q)}{6}\Big[F(X,q)F(X,l)F(X,p-q-l)\\ &\quad -\frac{1}{4}F(X,q)\rho(X,l)\rho(X,p-q-l)-\frac{1}{2}\rho(X,q)F(X,l)\rho(X,p-q-l)\Big], \end{aligned} \tag{204}$$

and

$$\begin{aligned}\hat{\Sigma}^\rho(X,p) &= -\frac{\lambda}{3N}\int dqdl\left[\rho(X,q)\hat{D}_F(X,p-q)+F(X,q)\hat{D}_\rho(X,p-q)\right]\\ &= -\frac{\lambda}{3N}\int dqdl\frac{\lambda_{\rm eff}(X,p-q)}{6}\Big[\rho(X,q)F(X,l)F(X,p-q-l)\\ &\quad -\frac{1}{4}\rho(X,q)\rho(X,l)\rho(X,p-q-l)+2F(X,q)F(X,l)\rho(X,p-q-l)\Big] \end{aligned} \tag{205}$$

Finally we obtain the following relation with respect to $\hat{\Sigma}_\rho(X,p)F(X,p)-\Sigma_F(X,p)\rho(X,p)$ as

$$\begin{aligned}\hat{\Sigma}_\rho(X,p)F(X,p)-\Sigma_F(X,p)\rho(X,p) &= \frac{1}{i}\cdot\frac{\lambda}{18N}\int dqdldr\ \delta^{d+1}(p+q-l-r)\lambda_{\rm eff}(X,p+q)\\ &\quad \left(G^{12}(X,q)G^{12}(X,p)G^{21}(X,l)G^{21}(X,r)-G^{21}(X,q)G^{21}(X,p)G^{12}(X,l)G^{12}(X,r)\right), \end{aligned} \tag{206}$$

where we have used the self-energy (204), (205),

$$\begin{aligned}\hat{\Sigma}_\rho(X,p)F(X,p)-\Sigma_F(X,p)\rho(X,p) &= \frac{\lambda}{36N}\int dqdldr\ \delta^{d+1}(p+q-l-r)\lambda_{\rm eff}(X,p+q)\\ &= \Bigg[2\left(\rho(q)F(p)+F(q)\rho(p)\right)\left(F(l)F(r)-\frac{1}{4}\rho(l)\rho(r)\right)\\ &\quad -2\left(\rho(l)F(r)+F(l)\rho(r)\right)\left(F(q)F(p)-\frac{1}{4}\rho(q)\rho(p)\right)\Bigg] \end{aligned} \tag{207}$$

and

$$\begin{aligned}F(l)F(r)-\frac{1}{4}\rho(l)\rho(r) &= \frac{1}{2}\left[G^{12}(l)G^{12}(r)+G^{21}(l)G^{21}(r)\right],\\ \rho(l)F(r)+F(l)\rho(r) &= i\left[G^{21}(l)G^{21}(r)-G^{12}(l)G^{12}(r)\right] \end{aligned} \tag{208}$$

with the relations (168), (169) and their Fourier transformed. As a result the divergence of the

entropy current can be written as

$$\begin{aligned}
\partial_\mu s^\mu(X) &= \frac{N}{2}\int dp \left(\ln\frac{G^{12}(X,p)}{G^{21}(X,p)}\right) i\left(\Sigma_\rho(X,p)F(X,p)-\Sigma_F(X,p)\rho(X,p)\right) \\
&= \frac{\lambda}{36}\int dpdqdldr\ \delta^{d+1}(p+q-l-r)\lambda_{\rm eff}(p+q) \\
&\times \left(G^{12}(X,q)G^{12}(X,p)G^{21}(X,l)G^{21}(X,r)-G^{21}(X,q)G^{21}(X,p)G^{12}(X,l)G^{12}(X,r)\right) \\
&\times \ln\left(\frac{G^{12}(X,p)}{G^{21}(X,p)}\right) \\
&= \frac{\lambda}{36}\cdot\frac{1}{2}\int dpdqdldr\delta^{d+1}(p+q-l-r)\lambda_{\rm eff}(p+q) \\
&\times \left(G^{12}(X,q)G^{12}(X,p)G^{21}(X,l)G^{21}(X,r)-G^{21}(X,q)G^{21}(X,p)G^{12}(X,l)G^{12}(X,r)\right) \\
&\times \ln\left(\frac{G^{12}(X,p)G^{12}(X,q)}{G^{21}(X,p)G^{21}(X,q)}\right) \\
&= \frac{\lambda}{36}\cdot\frac{1}{4}\int dpdqdldr\delta^{d+1}(p+q-l-r)\lambda_{\rm eff}(p+q) \\
&\times \left(G^{12}(X,q)G^{12}(X,p)G^{21}(X,l)G^{21}(X,r)-G^{21}(X,q)G^{21}(X,p)G^{12}(X,l)G^{12}(X,r)\right) \\
&\times \ln\left(\frac{G^{12}(X,p)G^{12}(X,q)G^{21}(X,r)G^{21}(X,r)}{G^{21}(X,p)G^{21}(X,q)G^{12}(X,l)G^{12}(X,r)}\right)\geq 0 \qquad (209)
\end{aligned}$$

where we have used the change of the variables $p\leftrightarrow q$ and $p\leftrightarrow l, q\leftrightarrow r$ and inequality $(x-y)\ln(x/y)\geq 0$. Hence we have proved the H-theorem for the NLO of $1/N$ expansion in the range of 1st order gradient expansion. We can see that any change of Green's functions with nonzero collision term $C=i\left[\Sigma_\rho F-\Sigma_F\rho\right]\neq 0$ contributes to entropy production.

4.3 Numerical Analysis for the $O(N)$ model in 1+1 dimensions

In this section we simulate the time evolution of the 2-point Green's functions in the NLO of $1/N$ expansion. In order to trace the time evolution of Green's functions we have to give the initial conditions at $x^0=y^0=t_0$. The initial values for the spectral functions are completely fixed by the equal-time properties

$$\begin{aligned}
\rho_{ab}(x,y)\Big|_{x^0=y^0} &= 0 \\
\partial_{x^0}\rho_{ab}(x,y)\Big|_{x^0=y^0} &= \delta_{ab}\delta^d(\mathbf{x}-\mathbf{y}) \qquad (210)
\end{aligned}$$

or its Fourier transformed functions with respect to $\mathbf{x}-\mathbf{y}$ are given as

$$\begin{aligned}
\rho_{ab}(x^0,y^0;\mathbf{p})\Big|_{x^0=y^0} &= 0 \\
\partial_{x^0}\rho_{ab}(x^0,y^0;\mathbf{p})\Big|_{x^0=y^0} &= \delta_{ab}. \qquad (211)
\end{aligned}$$

Information for the initial distribution functions is contained in the statistical functions at initial time

$$F_{ab}(x,y)\Big|_{x^0=y^0=t_0}, \partial_{x^0}F_{ab}(x,y)\Big|_{x^0=y^0=t_0}, \text{and } \partial_{x^0}\partial_{y^0}F_{ab}(x,y)\Big|_{x^0=y^0=t_0}. \qquad (212)$$

We assume the spatially homogeneous systems and diagonal Green's functions in particle components $G_{ab}=\delta_{ab}G$ and use the Fourier transformed two Green's functions with respect to $\mathbf{x}-\mathbf{y}$ and

put initial conditions as

$$\begin{aligned} F_{ab}(x^0,y^0;\mathbf{p})\Big|_{x^0=y^0=t_0} &= \delta_{ab}\frac{1}{\sqrt{\mathbf{p}^2+M_0^2}}\left(\frac{1}{2}+n_{\mathbf{p}}\right) \\ \partial_{x^0}F_{ab}(x^0,y^0;\mathbf{p})\Big|_{x^0=y^0=t_0} &= 0 \\ \partial_{x^0}\partial_{y^0}F_{ab}(x^0,y^0;\mathbf{p})\Big|_{x^0=y^0=t_0} &= \delta_{ab}\sqrt{\mathbf{p}^2+M_0^2}\left(\frac{1}{2}+n_{\mathbf{p}}\right) \end{aligned} \tag{213}$$

where M_0^2 is self-consistently determined by

$$M_0^2 = m^2 + \frac{\lambda}{6}\int\frac{d^dp}{(2\pi)}F(t_0,t_0,\mathbf{p}). \tag{214}$$

Here we must subtract $\frac{\lambda}{6}\int\frac{d^dp}{(2\pi)}\frac{1}{2\sqrt{\mathbf{p}^2+m^2}}$ in the R.H.S. for renormalization of tadpole mass shift.

We consider the spatially homogeneous system, so that it is convenient to consider the Fourier transformed KB equation with respect to relative coordinate $\mathbf{x}-\mathbf{y}$. When we assume the spatially homogeneous system and only consider the symmetric phase $\phi_a = 0$ with diagonal Green's functions for particle components, we can write down the Fourier transformed KB equation for $F(x^0,y^0;\mathbf{p})$ and $\rho(x^0,y^0;\mathbf{p})$ from (184) and (185) as,

$$\begin{aligned} \left(\partial_{x^0}^2+\mathbf{p}^2+M(x^0;F)^2\right)F(x^0,y^0;\mathbf{p}) &= -\int_{t_0}^{x^0}\hat{\Sigma}_\rho(x^0,z^0;\mathbf{p})F(z^0,y^0;\mathbf{p}) \\ &\quad +\int_{t_0}^{y^0}\hat{\Sigma}_F(x^0,z^0;\mathbf{p})\rho(z^0,y^0;\mathbf{p}), \end{aligned} \tag{215}$$

$$\left(\partial_{x^0}^2+\mathbf{p}^2+M(x^0;F)^2\right)\rho(x^0,y^0;\mathbf{p}) = -\int_{y^0}^{x^0}\hat{\Sigma}_\rho(x^0,z^0;\mathbf{p})\rho(z^0,y^0;\mathbf{p}) \tag{216}$$

where

$$M(x^0;F)^2 = m^2+\lambda\frac{N+2}{6N}\int\frac{d^d\mathbf{k}}{(2\pi)^d}F(x^0,x^0;\mathbf{k}), \tag{217}$$

from (186) and (187)

$$\begin{aligned} \hat{\Sigma}_F(x^0,y^0;\mathbf{p}) &= -\frac{\lambda}{3N}\int\frac{d^d\mathbf{k}}{(2\pi)^d}\Bigg(F(x^0,y^0;\mathbf{p}-\mathbf{k})\hat{D}_F(x^0,y^0;\mathbf{k}) \\ &\quad -\frac{1}{4}\rho(x^0,y^0;\mathbf{p}-\mathbf{k})\hat{D}_\rho(x^0,y^0;\mathbf{k})\Bigg) \end{aligned} \tag{218}$$

and

$$\begin{aligned} \hat{\Sigma}_\rho(x^0,y^0;\mathbf{p}) &= -\frac{\lambda}{3N}\int\frac{d^d\mathbf{k}}{(2\pi)^d}\Bigg(F(x^0,y^0;\mathbf{p}-\mathbf{k})\hat{D}_\rho(x^0,y^0;\mathbf{k}) \\ &\quad +\rho(x^0,y^0;\mathbf{p}-\mathbf{k})\hat{D}_F(x^0,y^0;\mathbf{k})\Bigg). \end{aligned} \tag{219}$$

Here from (188) and (189)

$$\hat{D}_F(x^0,y^0;\mathbf{q}) = \frac{\lambda}{6}\Bigg[F(x^0,y^0;\mathbf{q}-\mathbf{k})F(x^0,y^0;\mathbf{k}) - \frac{1}{4}\rho(x^0,y^0;\mathbf{q}-\mathbf{k})\rho(x^0,y^0;\mathbf{k}) - \int_{t_0}^{x^0} dz\hat{D}_\rho(x^0,z^0;\mathbf{q}) \times \left(F(z^0,y^0;\mathbf{q}-\mathbf{k})F(z^0,y^0;\mathbf{k}) - \frac{1}{4}\rho(z^0,y^0;\mathbf{q}-\mathbf{k})\rho(z^0,y^0;\mathbf{k})\right) + 2\int_{t_0}^{y^0}\hat{D}_F(x^0,z^0;\mathbf{q})F(z^0,y^0;\mathbf{q}-\mathbf{k})\rho(z^0,y^0;\mathbf{k})\Bigg], \tag{220}$$

$$\hat{D}_\rho(x^0,y^0;\mathbf{q}) = \frac{\lambda}{3}\int\frac{d^d\mathbf{k}}{(2\pi)^d}\Bigg[F(x^0,y^0;\mathbf{q}-\mathbf{k})\rho(x^0,y^0;\mathbf{k}) - \int_{y^0}^{x^0}\hat{D}_\rho(x^0,z^0;\mathbf{q})F(z^0,y^0;\mathbf{q}-\mathbf{k})\rho(z^0,y^0;\mathbf{k})\Bigg], \tag{221}$$

where we have used (182) and (183) and $\hat{D}_F(x,y) = \hat{D}_F(y,x), \hat{D}_\rho(x,y) = -\hat{D}_\rho(y,x)$ for the convenience of numerical analyses.

Now let us begin the numerical simulation with (215) and (216) with (217), (218), (219), (220) and (221). We discretize the space $L = 2Na_s$ into $2N$ grid points $x_n = na_s$ ($n = -N, -N+1, \cdots, N-1, N$) with a_s the lattice spacing and apply the periodic boundary condition. Then the momentum is discretized as $p_n = \frac{2\pi n}{L}$, and $-\partial_x^2$ is set $\mathbf{p}^2 = \frac{4}{a_s^2}\sin^2\left(\frac{a_s p_n}{2}\right)$, which removes much of the lattice artifacts. We set $N = 40$ which is sufficient to study the momentum dependence. We confirmed that the simulation with $N = 80$ has no appreciable differences numerically. We set the mass $ma_s = 0.3$ and solve the evolution with time step $a_t/a_s = 0.25$. We varied the coupling $\lambda^2/m^2 = 40$ and 30 and particle components $N = 10, 5$ and 3. In the same way as simulations in ϕ^4 (Sec. 3.4), we prepared the two different types of the initial conditions, "tsunami" distribution and the Woods-Saxon (WS) distribution in (213), respectively,

$$n_{\mathbf{p}}^T = \frac{1}{\mathcal{N}_T}\exp\left[-\frac{(|p_x| - p_T)^2}{2\sigma^2}\right] \tag{222}$$

with $\sigma^2/m^2 = 6.0 \times \left(\frac{2\pi}{mL}\right)^2$, $p_T = 9\cdot 2\pi/L$ and $\mathcal{N}_T = 0.25$ and

$$n_{\mathbf{p}}^{WS} = \frac{1}{\mathcal{N}_{WS}}\frac{1}{e^{(\sqrt{\mathbf{p}^2+m^2}-p_{WS})/\kappa}+1} \tag{223}$$

with $p_{WS}/m = 3.4$, $\kappa/m = 0.45$ and $\mathcal{N}_{WS} = 0.5$. The "tsunami" initial condition with two peaks $\pm p_T$ may be regarded as a toy model of the nuclear collisions. The WS initial condition is prepared to investigate the sensitivity of the evolution to the initial condition. The above parameters in the WS case are tuned so that both the initial conditions give the same energy for $\lambda/m^2 = 40$ and $N = 10$. Later in this subsection, we change the coupling constant λ and the number of particle components N with other parameters fixed, in order to see how the evolution depends on λ and N.

In Fig. 43, we show the time evolution of the number distribution $n(\tilde{\omega}_{\mathbf{p}})$ defined in Eqs. (72) and (73) with $\lambda/m^2 = 40$ and $N = 10$, starting from the tsunami initial condition in (4.3). This figure shows that our simulation reproduces the results of Ref. [99]. The peak of Gaussian distribution damps rapidly and the values at high and low momentum regions grow up gradually with time. In the end the number distribution function approaches the Bose distribution function $n_{\mathbf{p}}^{\rm eq} = 1/(e^{(\tilde{\omega}_{\mathbf{p}}-\mu)/T}-1)$ with $T/m = 2.06$ and $\mu/m = 0.801$. Similarly in Fig. 44 we show the time evolution of number distribution $n(\tilde{\omega}_{\mathbf{p}})$ with the WS initial condition (223). From this figure we can

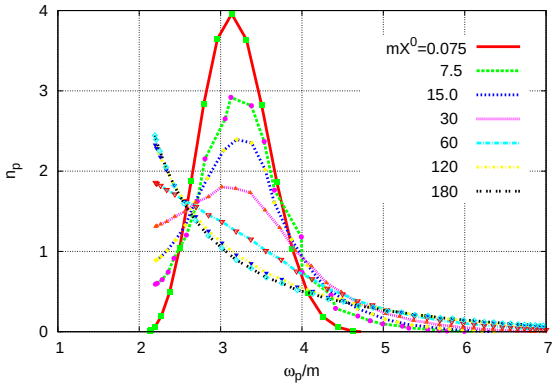

Figure 43: Evolution of the distribution function $n_{\mathbf{p}}(p_x)$ from the tsunami initial condition ($\lambda/m^2 = 40,\ N = 10$).

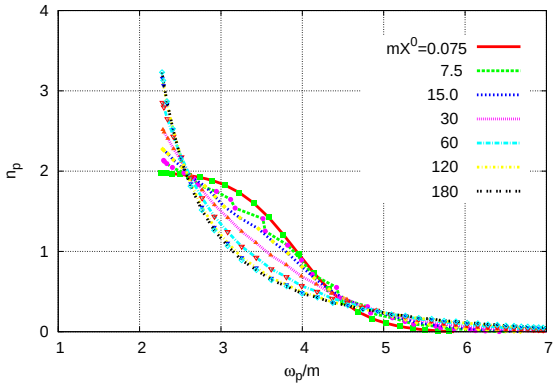

Figure 44: Evolution of the distribution function $n_{\mathbf{p}}(p_x)$ from the WS initial condition ($\lambda/m^2 = 40,\ N = 40$).

see that from WS initial conditions $n(\tilde{\omega}_{\mathbf{p}})$ also converges to the Bose distribution function with time. Here we should comment on the mass shift and the initial condition in (213) with (214). In Figs. 43 and 44, we can notice that each mode starts from its minimum value $\tilde{\omega}_{\mathbf{p}=\mathbf{0}} \sim \sqrt{m^2 + \frac{\lambda}{6}\int_{\mathbf{p}} F} \sim 2m$. This means that the mass shift is comparable with the bare mass: $\frac{\lambda}{6}\int_{\mathbf{p}} F \sim 3m^2$, which arises by setting large coupling $\lambda/m^2 = 40$ in $O(N)$. If we suddenly switch-on the coupling at $x^0, y^0 > t_0$ from zero coupling $\lambda = 0$ at $x^0 = y^0 = t_0$, this mass shift comparable with the bare mass causes various problems in numerical analyses, such as the energy momentum conservation around initial time t_0. Therefore in order to avoid problems, we prepared initial conditions (213) with (214) which already involve the mass shift from the LO of $1/N$ expansion[10].

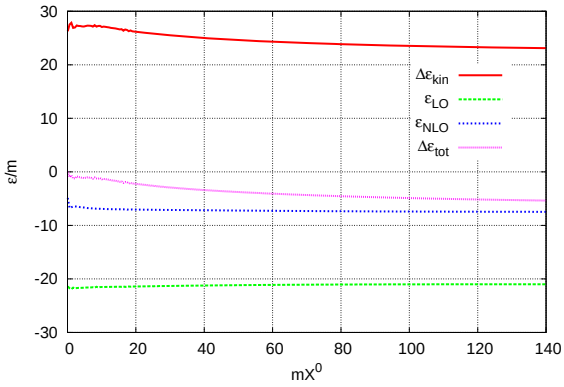

Figure 45: Evolution of kinetic energy, LO potential, NLO potential energy and total energy for the tsunami initial condition ($\lambda/m^2 = 40$, $N = 10$). Error of total energy is about 2%.

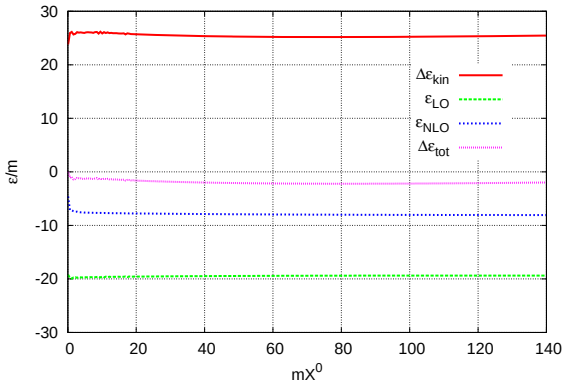

Figure 46: Evolution of kinetic energy, LO potential, NLO potential energy and total energy for the WS initial condition ($\lambda/m^2 = 40$, $N = 10$). Error of total energy is about 1%.

Next we study the energy content of the system. The explicit expression of the energy per particle component is given by replacing the self-energy in Sec. 3.3 by that for LO NLO of $1/N$ expansion in $O(N)$ theory. Figs. 45 and 46 show the kinetic, LO, NLO and total energy as a

[10] In the simulations of ϕ^4 model, mass shift from the tadpole diagram is sufficiently small for $\lambda/m^2 = 4$ compared with the bare mass. Hence we have not prepared initial conditions with tadpole mass shift.

function of time X^0 for the tsunami and WS initial conditions with $\lambda/m^2 = 40$ and $N = 10$. Here we have classified the potential energy by the order of $1/N$ expansion, where NLO contains both a local tadpole and a nonlocal part. Strictly speaking, kinetic and total energy here represent the difference of true kinetic and total energy minus initial total energy true $\epsilon_{kin,tot} - \epsilon_{tot,initial}$. True $\epsilon_{tot}/m \sim 275$ and $\epsilon_{kin}/m = 300$ in our lattice spacing. We can find that the growth of the kinetic energy is cancelled by the LO and the NLO energy to have a constant total energy. The energy is conserved within 2% in Fig. 45 and 1% in Fig. 46.

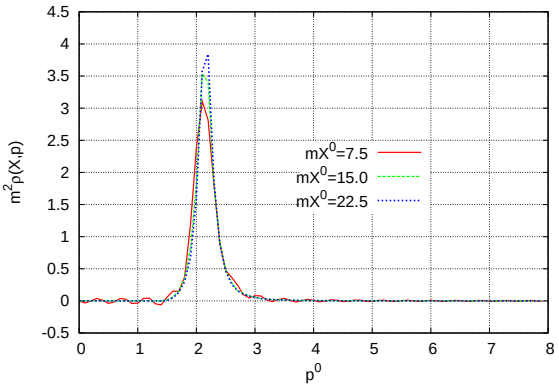

Figure 47: Evolution of the spectral function $\rho(X^0, p_0, p_x)$ at $p_x = 0$ for the tsunami initial condition ($\lambda/m^2 = 40$, $N = 10$).

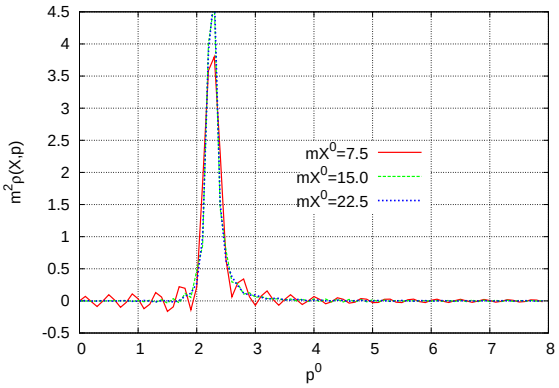

Figure 48: Evolution of the spectral function $\rho(X^0, p_0, p_x)$ at $p_x = 0$ for the WS initial condition ($\lambda/m^2 = 40$, $N = 10$).

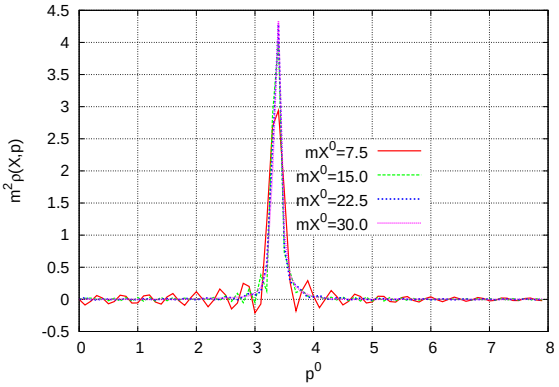

Figure 49: Evolution of the spectral function $\rho(X^0, p_0, p_x)$ at $p_x = 2\pi \cdot 10/L$ for the tsunami initial condition ($\lambda/m^2 = 40$, $N = 10$).

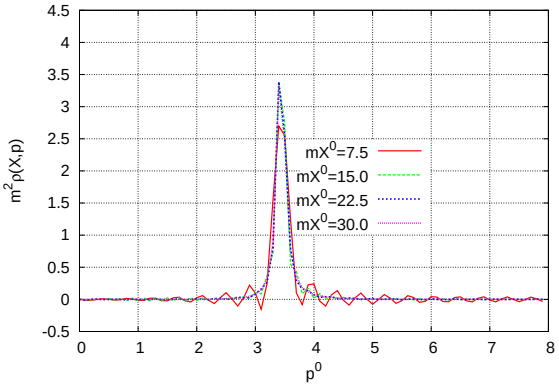

Figure 50: Evolution of the spectral function $\rho(X^0, p_0, p_x)$ at $p_x = 2\pi \cdot 10/L$ for the WS initial condition ($\lambda/m^2 = 40$, $N = 10$).

We shall study the kinetic entropy (91) derived with the gradient expansion of the KB equation. In order to estimate the entropy we have to examine the shape of the spectral function in (91), which is needed to compute $f(X, p)$ in σ. We show the spectral functions $\rho(X, p)$ in Figs. 47, 48, 49 and 50 for $p_x = 2\pi n/L$ with $n = 0$ and 10 for the tsunami and the WS initial condition at several values of time X^0. We can see that peak structures near $p^0/m \sim \sqrt{m^2 + (\text{mass shift}) + p_x^2}/m$ at later times for four figures, where (mass shift) $\sim 3m^2$ is comparable to the squared bare mass due to the large coupling $\lambda/m^2 = 40$.

At early times $mx^0, my^0 \sim O(1)$, the spectral function $\rho(X, p)$ has oscillatory behavior. As we have discussed in Sec. 3.4, within a finite time interval $|x^0 - y^0| < X^0$, we can resolve the p^0

dependence of $\rho(X,p)$ on the scale larger than $1/X^0$, because we have an oscillating factor due to $\int_{-X^0}^{X^0} dt \exp\left(-ip^0 t\right) = 2\sin(p^0 X^0)/p^0$. Indeed the oscillation frequency is proportional to X^0 and independent of the model. Since any finer structure of $\rho(X,p)$ than a scale $1/T$ can be resolved only after the evolution time of $X^0 > T$, the sharper the peak structure is, the longer time it needs to be resolved. In the case of $O(N)$ theory with $\lambda/m^2 = 40$ and $N = 10$, the width of the spectral function in Figs. 47-50 is about twice narrower than that of ϕ^4 theory with $\lambda/m^2 = 4$ which is shown in Figs. 11-14. This is because the width is suppressed by the factor $1/\sqrt{N}$. Hence at least twice longer time is required to resolve the peak structure of $\rho(X,p)$ compared with ϕ^4 theory with $\lambda/m^2 = 4$. (Here we can see the width of the spectral functions are sufficiently narrow compared to the position of the peak of Breit-Wigner function. Then the quasiparticle picture might be approximately appropriate in this case.) The same oscillatory behavior at early times and the narrower width also occur in the statistical function $F(X,p)$ and the occupation number function $f(X,p)$. We thus encounter a problem in evaluating σ as it contains the logarithm of $f(X,p)$. In addition because of twice narrower width of $\rho(X,p)$ and $f(X,p)$, twice longer time is necessary to resolve the peak structure of $\rho(X,p)$ and $f(X,p)$ and to estimate the kinetic entropy (91).

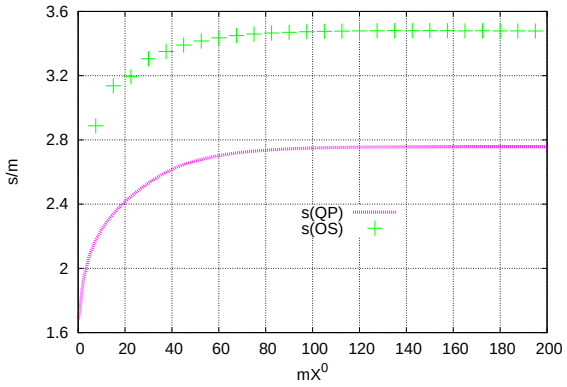

Figure 51: Evolution of entropy density $s(\mathrm{OS})$ (91) denoted in + and its quasiparticle approximation $s(\mathrm{QP})$ (95) shown in a curve for the tsunami initial condition ($\lambda/m^2 = 40$, $N = 10$).

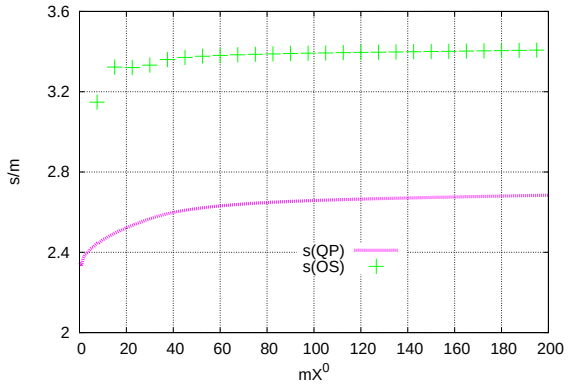

Figure 52: Evolution of entropy density $s(\mathrm{OS})$ (91) denoted in + and its quasiparticle approximation $s(\mathrm{QP})$ (95) shown in a curve for the WS initial condition ($\lambda/m^2 = 40$, $N = 10$).

We shall start the estimation of the kinetic entropy (91) in $O(N)$ theory. In Figs. 51 and 52 we show the kinetic entropy (91) as a function of time X^0 for the tsunami and the WS initial condition. As an exploratory estimation we simply neglect the contributions from the region of p^0 where $\rho(X,p)$ has negative values. In the later stage $mX^0 > 20$ the kinetic entropy increases monotonically as time proceeds in both figures, (while the monotonical increasing behavior starts from about $mX^0 > 10$ in ϕ^4 theory with $\lambda/m^2 = 4$ as shown in Figs. 15 and 16) which is the expected result from the H-theorem. Asymptotic behavior of both entropy in this stage is still a little dependent on initial conditions, where the deviation is about $s^{\mathrm{tsunami}}(OS)/s^{\mathrm{WS}}(OS) = 1.017$ at $mX^0 = 260$. The reason of this result is analyzed later.

Here we also use the quasiparticle (QP) approximation (95) with the number distribution $n_{\mathbf{p}}(X^0)$ defined in Eq. (72). Since the spectral function is nicely peaked near $p^0 \sim m^2 + (\text{mass shift}) + \mathbf{p}^2$ as seen in Figs. 47-50, the quasiparticle approximation (95) may be reasonable although it is not based on the H-theorem of KB equation with the finite spectral width. Asymptotic behavior of this entropy $s(QP)$ (95) is also a little dependent on initial conditions. The deviation is about $s^{\mathrm{tsunami}}(QP)/s^{\mathrm{WS}}(QP) = 1.018$ at $mX^0 = 300$, which is almost the same as the asymptotic value of $s^{\mathrm{tsunami}}(OS)/s^{\mathrm{WS}}(OS)$. Let us compare kinetic entropy $s(OS)$ (91) and its quasiparticle approximation $s(QP)$ by taking its ratio $s(OS)/s(QP)$. The ratio is shown in Figs. 53 for two

initial conditions. Until $mX^0 \sim 20$ the ratio contains numerical artifact in $\rho(X,p)$ and $F(X,p)$ as explained above. In the late time region $mX^0 > 60$ the ratio becomes constant for both initial condition but two lines has a little deviation. However two lines are approaching and the deviation tends to disappear as time proceeds. At $mX^0 = 260$ the deviation is about $(s(OS)/s(QP))^{\rm tsunami}/(s(OS)/s(QP))^{\rm WS} = 0.995$. The percentage of entropy components from the spectral width is less dependent on initial conditions.

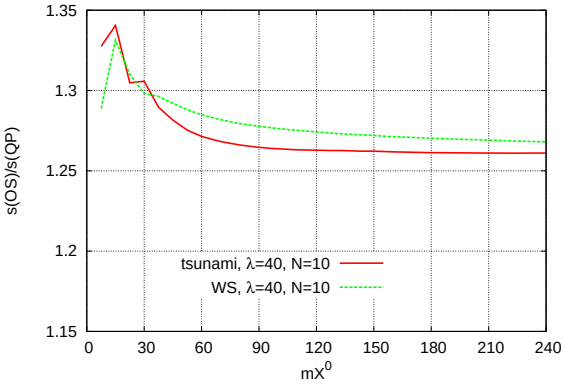

Figure 53: Evolution of the ratio $s(\mathrm{OS})/s(\mathrm{QP})$ for the tsunami (red line) and the WS initial condition (green line) ($\lambda/m^2 = 40$, $N = 10$).

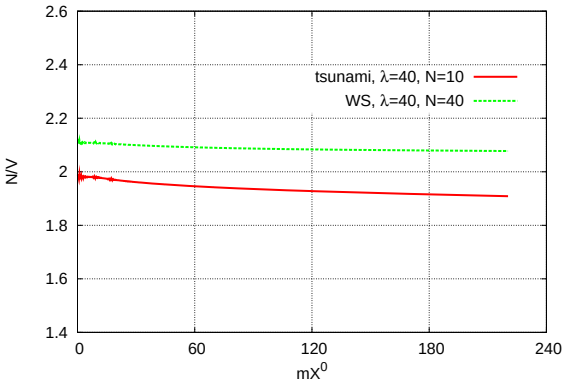

Figure 54: Evolution of the total number density for tsunami (red line) and WS initial condition (green line) ($\lambda/m^2 = 40$, $N = 10$).

Next we should analyze the reason why asymptotic behavior of entropy is a little dependent on initial conditions. Fig. 54 shows a time evolution of the total number for two initial conditions with $\lambda/m^2 = 40$ and $N = 10$. The total number density does not change dynamically and remains nearly constant as the large time goes by. This behavior is explained by the spectral function. In Figs. 47-50 we observe the spectral functions with narrower width than those of ϕ^4 theory with $\lambda/m^2 = 4$ in Figs. 11-14 since the width is suppressed by the factor $1/\sqrt{N}$. This width does not change dynamically as time goes by. Then the particle number changing processes are suppressed in the time evolution, so that the change of the total number density becomes very moderate. As a result it takes longer times for total number density for tsunami and WS initial condition to converges to the same asymptotic value. Even in the later time $mX^0 \sim 200$ the deviation about 10% remains, so that the system for tsunami initial condition and that for WS initial condition have the same total energy but the different total number density. These behaviors of total number density might affect the asymptotic behavior of entropy. (Since the total number density is different for two initial conditions, the asymptotic values of entropy for two become different in Figs. 51 and 52.) We can confirm later that kinetic entropy at thermal equilibrium becomes independent of initial conditions when the total number density is independent of initial conditions.

When the spectral width is suppressed by the factor $1/\sqrt{N} = 1/\sqrt{10}$ particle number changing processes are suppressed and the deviation of total number density is hard to disappear. This also causes the deviation of temperature and chemical potential derived from the Bose distribution function appearing at later time. Figs. 55 and 56 show the logarithmic plots of the distribution function for the tsunami and the WS initial condition. Judging from these figures, we see that the logarithmic plots for both cases are around on the line $\ln\left(1 + \frac{1}{n_{\mathbf{p}}}\right) = \frac{\omega_{\mathbf{p}}}{T} - \frac{\mu}{T}$, which means that both distribution functions are approaching to the Both distribution function $1/(e^{\frac{\omega_{\mathbf{p}} - \mu}{T}} - 1)$. We can estimate the temperature and chemical potential from the slope and the intercept of the logarithmic plot. Then at $mX^0 = 180$ the temperature becomes $T/m = 2.06$ for tsunami and $T/m = 1.70$ for WS initial condition, and the chemical potential is $\mu/m = 1.65$ for tsunami and $\mu/m = 1.98$ for WS initial condition. They might be dependent on initial conditions at $mX^0 = 180$. As time goes by, the temperature and the chemical potential for both cases tend to approach the

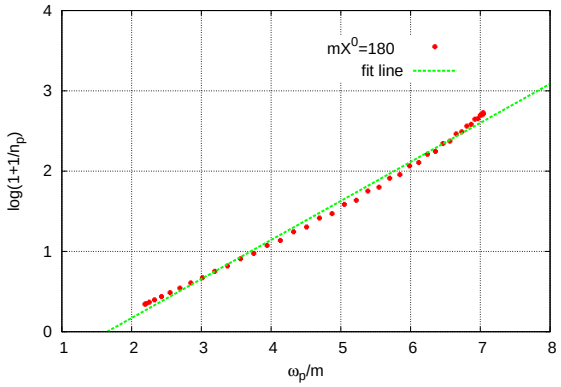

Figure 55: Logarithmic plot of number distribution function at $mX^0 = 180$ for the tsunami initial condition ($\lambda/m^2 = 40$, $N = 10$). The straight line is $y = \frac{\omega_p}{T} - \frac{\mu}{T}$ with $\frac{m}{T} = 0.486$ and $\frac{\mu}{T} = 0.801$.

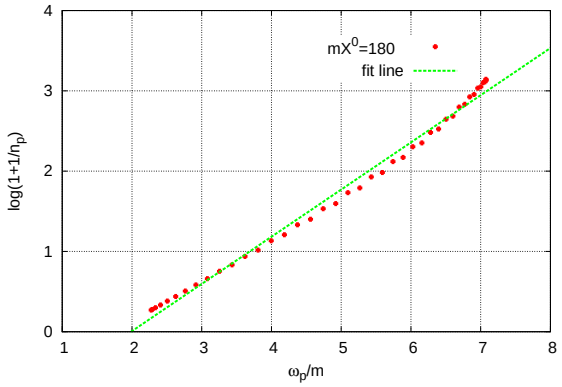

Figure 56: Logarithmic plot of number distribution function at $mX^0 = 180$ for the WS initial condition ($\lambda/m^2 = 40$, $N = 10$). The straight line is $y = \frac{\omega_p}{T} - \frac{\mu}{T}$ with $\frac{m}{T} = 0.588$ and $\frac{\mu}{T} = 1.17$.

same values very moderately and initial condition dependence might disappear. However since the spectral width is narrower than the cases in Sec. 3.4 and particle number changing processes are suppressed, it takes much longer time for the initial condition dependence of total number density, the temperature, the chemical potential and kinetic entropy to disappear.

In order to confirm that initial condition dependence disappears at later times we can perform two types of simulations. One is to perform longer time simulation for $N = 10$ although it is time-consuming approach. The other is the simulation for smaller N. The smaller N becomes, the wider the spectral width (which is $\sim \frac{1}{\sqrt{N}}$) becomes as shown in Fig. 57 and the less particle number changing processes are suppressed. As a result it is expected that the total number density

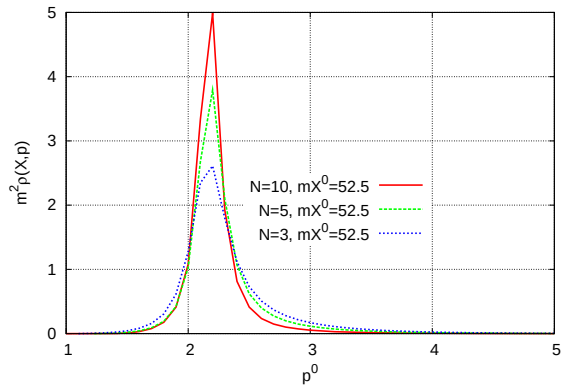

Figure 57: Spectral function $\rho(p^0, p_x = 0)$ at $mX^0 = 52.5$ for $N = 10$, 5 and 3 for tsunami initial condition with $\lambda/m^2 = 40$.

approaches the same value faster and that the deviation of temperature, chemical potential and entropy might disappear. We shall select the latter approach.

In Figs. 58 and 59, we show the evolution of kinetic entropy (91) and its quasiparticle approximation (95) for the tsunami and the WS initial condition with $\lambda/m^2 = 40$ and $N = 5$. After sufficiently large time $mt > 200$ the kinetic entropy (91) for both initial conditions seem to converge

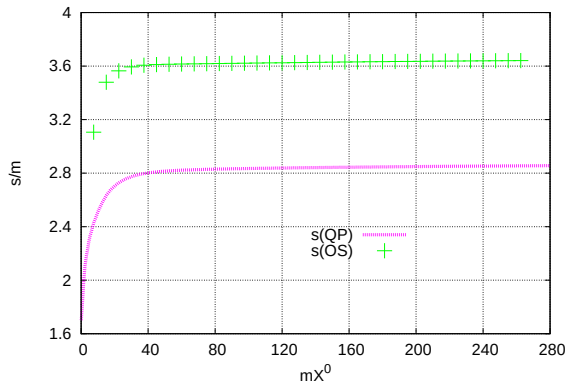

Figure 58: Evolution of s^0(OS) (91) denoted by + and its quasiparticle approximation s^0(QP) (95) (red line) for the tsunami initial condition ($\lambda/m^2 = 40$, $N = 5$).

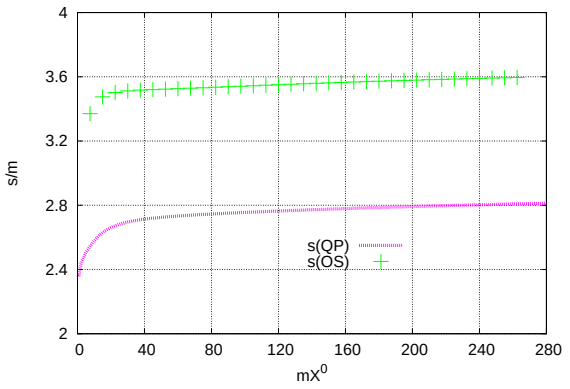

Figure 59: Evolution of s^0(OS) (91) denoted by + and its quasiparticle approximation s^0(QP) (95) (red line) for the WS initial condition ($\lambda/m^2 = 40$, $N = 5$).

to the same value and the deviation between two initial condition seem to be improved by preparing smaller N, but still a little dependent on initial conditions. The initial condition dependence

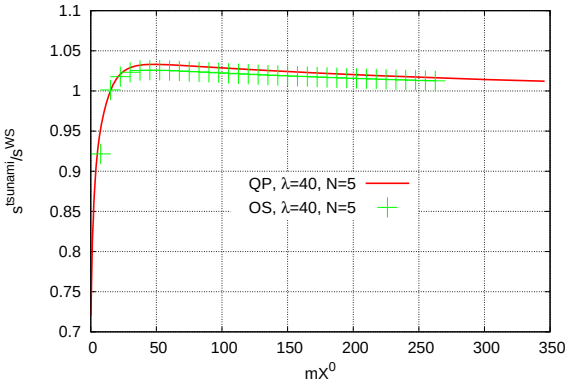

Figure 60: Evolution of the ratios $s^{\rm tsunami}$(OS)/$s^{\rm WS}$(OS) and $s^{\rm tsunami}$(QP)/$s^{\rm WS}$(QP) with $\lambda/m^2 = 40$ and $N = 5$.

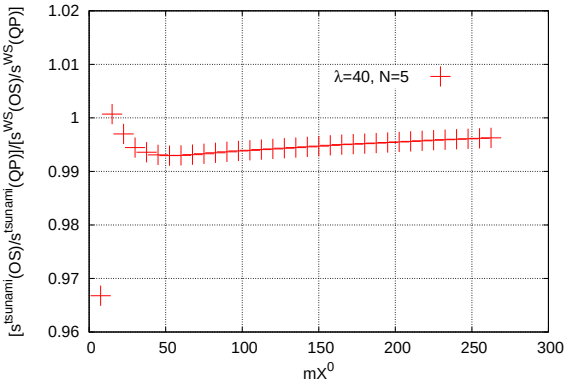

Figure 61: Evolution of $[(s^{\rm tsunami}$(OS) $/s^{\rm tsunami}$(QP)) $/(s^{\rm WS}$(OS) $/s^{\rm WS}$(QP))] with $\lambda/m^2 = 40$ and $N = 5$.

of entropy is estimated by taking the ratios $s^{\rm tsunami}$(OS)/$s^{\rm WS}$(OS) and $s^{\rm tsunami}$(QP)/$s^{\rm WS}$(QP). In Fig. 60 we show the time evolution of ratios with $\lambda/m^2 = 40$ and $N = 5$. The ratio $s^{\rm tsunami}/s^{\rm WS}$ is ~ 1.012 at $mX^0 = 350$ for quasiparticle approximation (95) and approaches 1 at $mX^0 > 50$ for both (91) and (95). Initial condition dependence tends to disappear at the later times. In addition we can notice that $s^{\rm tsunami}$(OS)/$s^{\rm WS}$(OS) = $[(s^{\rm tsunami}$(OS)/$s^{\rm tsunami}$(QP)) $/(s^{\rm WS}$(OS)/$s^{\rm WS}$(QP))] $\times s^{\rm tsunami}$(QP)/$s^{\rm WS}$(QP) is near $s^{\rm tsunami}$(QP) $/s^{\rm WS}$(QP). This is because the percentage of entropy components from the width is less dependent on initial conditions than the ratio $s^{\rm tsunami}/s^{\rm WS}$ (also in $N = 5$), that is $0.993 \leq [(s^{\rm tsunami}$(OS)/$s^{\rm tsunami}$(QP)) $/(s^{\rm WS}$(OS)/$s^{\rm WS}$(QP))] ≤ 1.001 at $mX^0 \geq 15$, which is confirmed in Fig. 61.

Then let us see the time evolution of total number density for the tsunami and the WS initial condition with $\lambda/m^2 = 40$ and $N = 5$. It is shown in Fig. 62. Two lines of the total number density are decreasing as time goes by, and approaching each other. The deviation of two lines

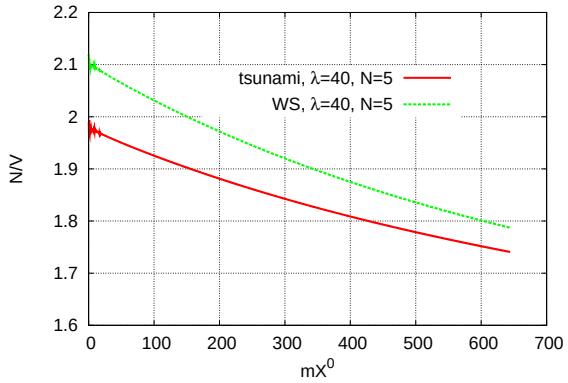

Figure 62: Evolution of the total number density with $\lambda/m^2 = 40$ and $N = 5$.

becomes less than that in the case of $N = 10$ (Fig. 54), but it still remains even at $mX^0 = 350$. Two distribution functions near thermal equilibrium at $mX^0 \sim 350$ are expected to have different properties since two systems have the same energy density and the different total number density.

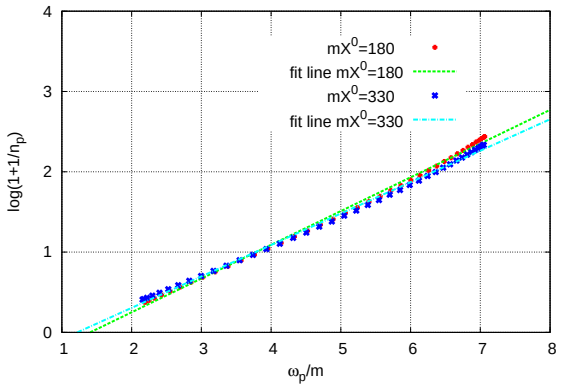

Figure 63: Logarithmic plot of number distribution function at $mX^0 = 180$ and 330 for the tsunami initial condition ($\lambda/m^2 = 40$, $N = 5$). The slope line is $y = \frac{\omega_p}{T} - \frac{\mu}{T}$ with $\frac{m}{T} = 0.420$ and $\frac{\mu}{T} = 0.590$ (dashed-line) for $mX^0 = 180$ and that with $\frac{m}{T} = 0.392$ and $\frac{\mu}{T} = 0.478$ (dot-dashed-line) for $mX^0 = 330$.

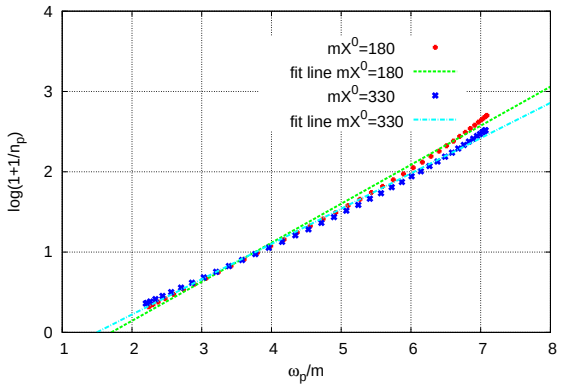

Figure 64: Logarithmic plot of number distribution function at $mX^0 = 180$ and 330 for the WS initial condition ($\lambda/m^2 = 40$, $N = 5$). The slope lines are $y = \frac{\omega_p}{T} - \frac{\mu}{T}$ with $\frac{m}{T} = 0.486$ and $\frac{\mu}{T} = 0.828$ (dashed-line) for $mX^0 = 180$ and that with $\frac{m}{T} = 0.439$ and $\frac{\mu}{T} = 0.657$ (dot-dashed-line) for $mX^0 = 330$.

Next let us see that the initial condition dependence still remains in the distribution functions at late times $180 \leq mX^0 \leq 330$ even in $N = 5$. Initial condition dependence remains in the temperature and the chemical potential derived from the logarithmic plot of distribution function. In Figs. 63 and 64 we show the logarithmic plot $\ln\left(1 + \frac{1}{n_{\mathbf{p}}}\right)$ for both initial conditions at $mX^0 = 180$ and $mX^0 = 330$. Even at $mX^0 = 180$ the distribution functions for both initial conditions are on the straight line, that is $n_{\mathbf{p}} \sim 1/(e^{(\omega_{\mathbf{p}}-\mu)/T} - 1)$. But the temperature and the chemical potential are still dependent on initial conditions as expected from evolution of total number density. In Figs. 65 and 66 we show the time evolution of temperature and chemical potential derived from the logarithmic plot. Although they seem to approach moderately as time proceeds, the deviations

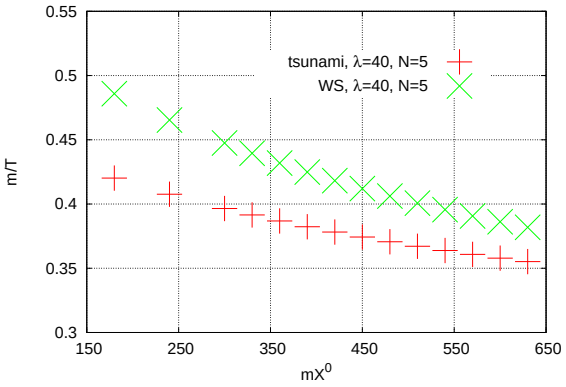

Figure 65: Evolution of m/T derived from the logarithmic plot of $n_{\mathbf{p}}(p_x)$ at $mX^0 > 180$ for the tsunami and the WS initial condition with $\lambda/m^2 = 40$ and $N = 5$.

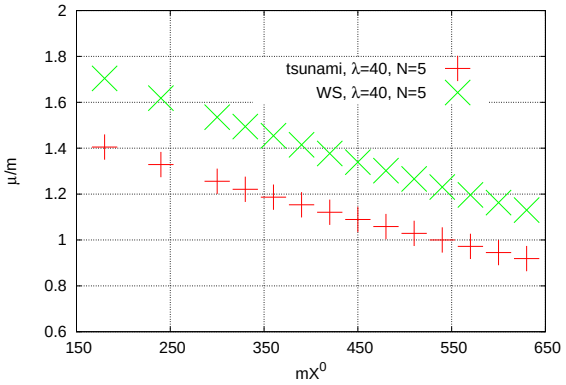

Figure 66: Evolution of the chemical potential μ/m derived from the logarithmic plot of $n_{\mathbf{p}}(p_x)$ at $mX^0 > 180$ for the tsunami and the WS initial condition with $\lambda/m^2 = 40$ and $N = 5$.

of them still remain even at $mX^0 = 600$.

We shall confirm that initial condition dependence of temperature and chemical potential disappears and that entropy converges to the same value when systems have the same energy and number density. In Fig. 67, we show the evolution of the ratio $s^{\rm tsunami}/s^{\rm WS}$ for (91) and (95) with

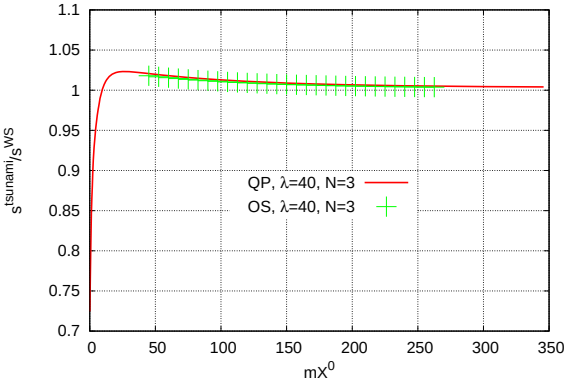

Figure 67: Evolution of the ratios $s^{\rm tsunami}({\rm OS})/s^{\rm WS}({\rm OS})$ and $s^{\rm tsunami}({\rm QP})/s^{\rm WS}({\rm QP})$ with $\lambda/m^2 = 40$ and $N = 3$.

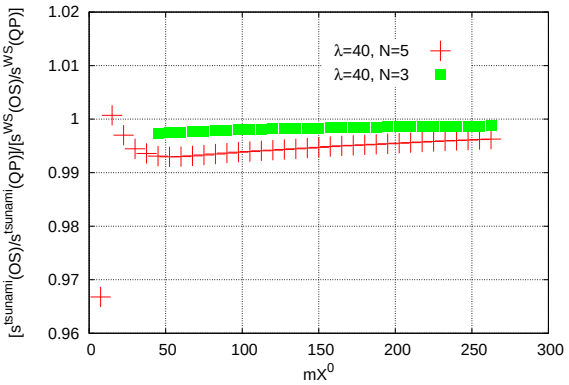

Figure 68: Evolution of $[(s^{\rm tsunami}({\rm OS})/s^{\rm tsunami}({\rm QP}))/(s^{\rm WS}({\rm OS})/s^{\rm WS}({\rm QP}))]$ with $N = 5$ and $N = 3$ for $\lambda/m^2 = 40$.

$\lambda/m^2 = 40$ and $N = 3$. We can see that both ratios converge to 1 rapidly compared with the case $N = 5$ in Fig. 60. The ratio for kinetic entropy (91) is 1.004 for $N = 3$ at $mX^0 = 260$ which is improved from 1.013 for $N = 5$ at the same time. Furthermore the ratio for quasiparticle approximation (95) is 1.004 for $N = 3$ at $mX^0 = 350$ which is also improved from 1.012 for $N = 5$ at the same time. Initial condition dependence of both (91) and (95) disappears faster for smaller N. In addition the ratio $s^{\rm tsunami}({\rm OS})/s^{\rm WS}({\rm OS}) = [(s^{\rm tsunami}({\rm OS})/s^{\rm tsunami}({\rm QP}))/(s^{\rm WS}({\rm OS})/s^{\rm WS}({\rm QP}))] \times s^{\rm tsunami}({\rm QP})/s^{\rm WS}({\rm QP})$ for (91) is almost on the line $s^{\rm tsunami}({\rm QP})/s^{\rm WS}({\rm QP})$ for quasiparticle approximation (95) for $N = 3$. The reason why two ratios are near is that the percentage of entropy components from the width is less dependent on initial condition than the ratio $s^{\rm tsunami}/s^{\rm WS}$, that

is $|[(s^{\rm tsunami}({\rm OS})/s^{\rm tsunami}({\rm QP}))\ /(s^{\rm WS}({\rm OS})/s^{\rm WS}({\rm QP}))]-1| < |s^{\rm tsunami}/s^{\rm WS}-1|$, which is the common property with $N = 10$ and 5. We can also notice that two ratios for $N = 3$ in Fig. 67 are nearer to 1 than those in Fig. 60. This is because the smaller N becomes, the faster the initial condition dependence of $[(s^{\rm tsunami}({\rm OS})/s^{\rm tsunami}({\rm QP}))\ /(s^{\rm WS}({\rm OS})/s^{\rm WS}({\rm QP}))]$ also disappears. This is confirmed in Fig. 68, that is $0.997 < [(s^{\rm tsunami}({\rm OS})/s^{\rm tsunami}({\rm QP}))\ /(s^{\rm WS}({\rm OS})/s^{\rm WS}({\rm QP}))] < 1.000$ at $mX^0 \geq 45$ for $N = 3$ in Fig. 67 is nearer to 1 than $0.993 < [(s^{\rm tsunami}({\rm OS})/s^{\rm tsunami}({\rm QP}))\ /(s^{\rm WS}({\rm OS})/s^{\rm WS}({\rm QP}))] < 1.001$ at $mX^0 \geq 45$ for $N = 5$.

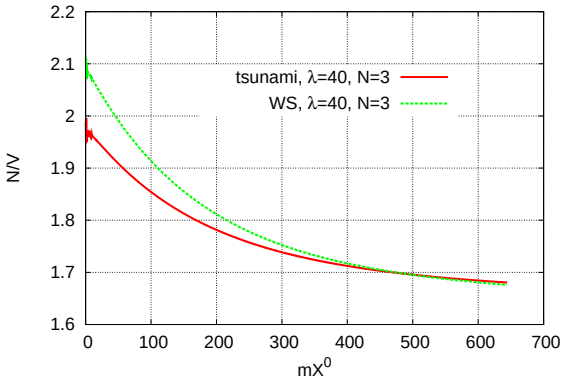

Figure 69: Evolution of the total number density with $\lambda/m^2 = 40$ and $N = 3$.

Then let us investigate whether the initial condition dependence of total number density disappears as time proceeds for $N = 3$. In Fig. 69 we show the evolution of total number density with $\lambda/m^2 = 40$ and $N = 3$. Here we can see that initial condition dependence of the total number density seem to disappear at around $mX^0 = 350$. As time goes by, two systems for tsunami and WS initial condition tend to have the same energy and number density. Then we can confirm that as the initial condition dependence of total number density disappears gradually in Fig. 69, that of entropy density also disappears in Fig. 67.

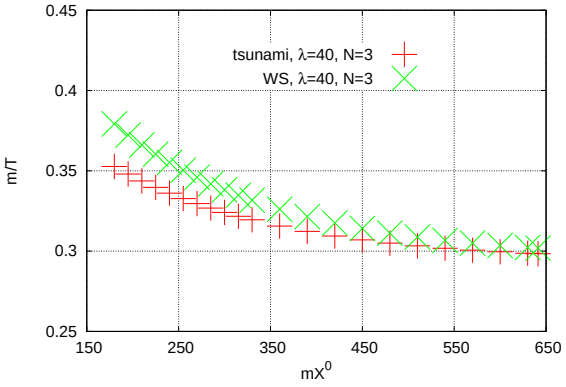

Figure 70: Evolution of m/T derived from the logarithmic plot of $n_{\mathbf{p}}(p_x)$ at $mX^0 > 180$ for the tsunami and the WS initial condition with $\lambda/m^2 = 40$ and $N = 3$.

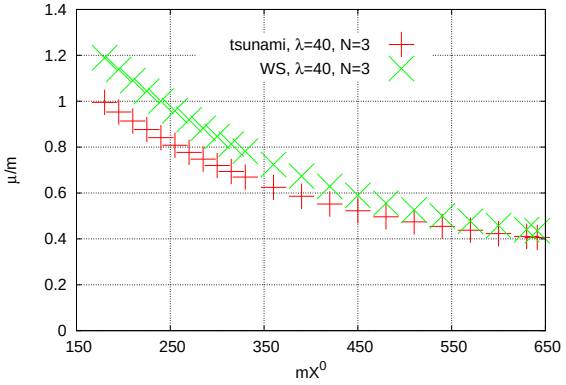

Figure 71: Evolution of the chemical potential μ/m derived from the logarithmic plot of $n_{\mathbf{p}}(p_x)$ at $mX^0 > 180$ for the tsunami and the WS initial condition with $\lambda/m^2 = 40$ and $N = 3$.

When total energy and number density become less dependent on initial conditions, the initial

condition dependence of the temperature and the chemical potential derived from the logarithmic plot $\ln\left(1+\frac{1}{n_{\rm p}}\right)$ near Bose distribution are also expected to become less as that of entropy does. We show the evolution of the inverse of temperature in Fig. 70. Here we can observe that the deviation of the temperature T becomes improved and both T tend to converge to the same value as time proceeds. The ratio of both temperature is $T^{\rm tsunami}/T^{\rm WS} = 1.037$ at $mX^0 = 350$, but the deviation still remains. Since number and entropy density is expected to be proportional to T^d simply in massless and $\lambda \to 0$ limit where d is the dimension of space, we might guess that the $T^{\rm tsunami}/T^{\rm WS}$ is near $N^{\rm tsunami}/N^{\rm WS}$ (~ 0.994) or $s^{\rm tsunami}({\rm QP})\ /s^{\rm WS}({\rm QP})$ (~ 1.004) at $mX^0 = 350$ in 1+1 dimensions. However the deviation of temperature is much larger than that of entropy density, and appears to be inversely proportional to that of number density. Thus the simple analysis cannot be applied. This might show that the thermodynamic variables which do not lose initial condition dependence completely, given by solutions of nonlinear SD equation with large mass shift $> m^2$ in $1/N$ expansion, spectral width, memory effects, and so forth, can not be simply related to each other as we have done in naive perturbation theory near thermal equilibrium. Here we observe that the deviation of temperature is less improved than that of entropy and number density.

Next let us analyze the behavior of the chemical potential shown in Fig. 71. We observe that it is monotonically decreasing and at $mX^0 = 350$ reduces to about 2/3 of that at $mX^0 = 180$ for both initial conditions as time proceeds. Initial condition dependence of the chemical potential tends to disappear, and at the later times it might converge to the same asymptotic value or might vanish as the chemical potential does for particle number nonconserving system in ϕ^4 theory (Sec. 3.4). In order to confirm this we should perform longer time simulation.

In the end we compare the evolution of QP entropy (95) for two values of the coupling, $\lambda/m^2 = 40$ and 30 for $N = 3$ with tsunami and WS initial conditions, respectively, in Figs, 72 and 73. (Here we comment that the deviation of total energy density is still less $\epsilon_{\rm tot}^{\rm tsunami}/\ \epsilon_{\rm tot}^{\rm WS} \sim 1.003$ at $\lambda/m^2 = 40$ and $N = 3$.) In these two figures, we see that the larger is the coupling the faster is the entropy produced and saturated to the equilibrium value as ϕ^4 theory in Sec. 3.4. In order to quantify the approach to the equilibrium value, as we have done in Sec. 3.4 we shall fit the entropy evolution with

$$s(X^0) = s_{\rm max} - Ae^{-\gamma(mX^0)}, \tag{224}$$

where $s_{\rm max}$, A and γ are parameters. The regions of the fit is chosen as $70 \le mX^0 \le 120$ and $100 \le mX^0 \le 180$ for $\lambda/m^2 = 40$ and 30, because of the behavior of slower approach to equilibrium for smaller coupling. The resultant values for the parameters are expressed in Table. 2. The parameter $s_{\rm max}$ take the same value and is independent of the initial conditions both for the coupling constants $\lambda/m^2 = 40$ and 30. The parameter γ is independent of initial conditions for $\lambda/m^2 = 40$, but still dependent on initial conditions for $\lambda/m^2 = 30$. As shown in the proof of H-theorem, it might be inferred that the entropy production rate is proportional to $\lambda\lambda_{\rm eff}/N \sim \lambda^2/N$. The λ dependence of the parameter γ might be consistent to the proof, that is $\gamma \propto \lambda^2$, although for $\lambda/m^2 = 30$ the parameter is still sensitive to the initial conditions.

λ	N	$s_{\rm max}$	A	γ	$s_{\rm max}$	A	γ
40 (QP)	3	2.91	0.078	0.012	2.90	0.16	0.012
30 (QP)	3	2.89	0.063	0.0084	2.88	0.15	0.0071

Table 2: Parameters in Eq. (224) for "tsunami" (left) and WS (right) initial conditions with $\lambda/m^2 = 40$ and 30 for $N = 3$.

We shall do the similar analysis of the QP entropy (95) for two values of the number of particle components, N =3 and 5 and $\lambda/m^2 = 40$ with the tsunami and WS initial conditions, respectively. In Fig. 74 and 75 we show the evolutions of QP entropy with two values of N for both initial conditions and their fit lines with (224). In these figures, we can see that the smaller is the N is the faster is the entropy saturated. The fit parameters are given in Table. 3 and the regions of the fit is

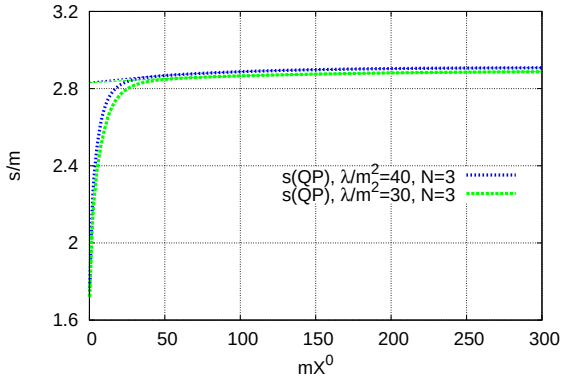

Figure 72: Entropy density $s^0(\mathrm{QP})/m$ in the quasiparticle approximation for the "tsunami" initial condition with the coupling λ/m^2 =40 and 30 for $N = 3$. The exponential fit with (224) is denoted by a thin line in each case.

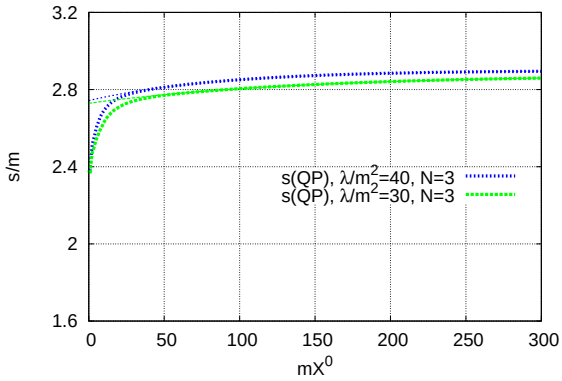

Figure 73: Entropy density $s^0(\mathrm{QP})/m$ in the quasiparticle approximation for the WS initial condition with the coupling λ/m^2 =40 and 30 for $N = 3$. The exponential fit with (224) is denoted by a thin line in each case.

$70 \leq mX^0 \leq 120$ and $100 \leq mX^0 \leq 180$. The parameters $s_{\max}$ take the same values independent of the initial conditions both for the number of particle components $N = 3$ and 5. The parameter γ is a little dependent on initial conditions for $N = 5$. As shown in the proof of H-theorem, γ is inferred to be proportional to $1/N$. The parameter γ in Table. 3 seems nontrivial although initial condition dependence still remains for $N = 5$.

N	λ	$s_{\max}$	A	γ	$s_{\max}$	A	γ
3(OS)	40	3.76	0.087	0.011	3.75	0.18	0.011
5(OS)	40	3.67	0.067	0.0035 ± 0.0001	3.67	0.17	0.0035 ± 0.0001
3(QP)	40	2.91	0.078	0.012	2.90	0.16	0.012
5(QP)	40	2.86	0.058	0.0064	2.86	0.16	0.0043

Table 3: Parameters in Eq. (224) for "tsunami" (left) and WS (right) initial conditions for $N = 3$ and 5 with $\lambda/m^2 = 40$.

Figs. 76 and 77 show the evolutions of entropy density $s^0(\mathrm{OS})/m$ for three values of N, that is N =3, 5, 10, with the tsunami and the WS initial condition, respectively. The smaller N becomes, (the larger spectral width becomes,) the larger values the kinetic entropy (91) take in the evolution and the faster it saturates, so that thermalization occurs earlier for smaller N. Moreover for smaller $N = 3$ and 5, the spectral function with wider width is resolved at the earlier times than $N = 10$, so that kinetic entropy (91) monotonically increases even at earlier times $mX^0 \sim 5$. We estimated the fit parameter in (224) in the similar way to the above analyses. We chose to fit the evolution in the regions $70 \leq mX^0 \leq 120$ and $100 \leq mX^0 \leq 180$ for $N = 3$ and 5. This fit regions are the same as those of $s(\mathrm{QP})$ for $N = 3$ and 5 with $\lambda/m^2 = 40$. The resultant values for the parameters are summarized in Table. 3. Here note that there are a few plots for (91) because large memories in PC are necessary to calculate each plot. This causes error bar of the parameters especially in γ. We find that both the parameters γ and $s_{\max}$ are independent of the initial conditions both for $N = 3$ and 5. Initial condition dependence of γ for $N = 5$ does not appear in the asymptotic behavior of the kinetic entropy $s(\mathrm{OS})$ (91) although it appears in the behavior of (95). The N dependence of the parameter γ seems non-trivial, contrary to the $1/N$ dependence naively inferred from the H-theorem in $O(N)$ theory.

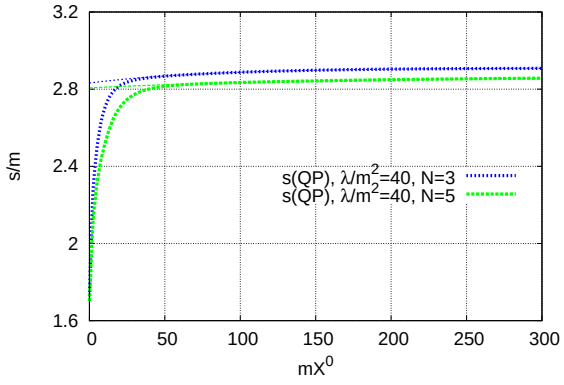

Figure 74: Entropy density $s^0(\mathrm{QP})/m$ in the quasiparticle approximation for the "tsunami" initial condition with the number of particle components N =3 and 5 and the coupling $\lambda/m^2 = 40$. The exponential fit with (224) is denoted by a thin line in each case.

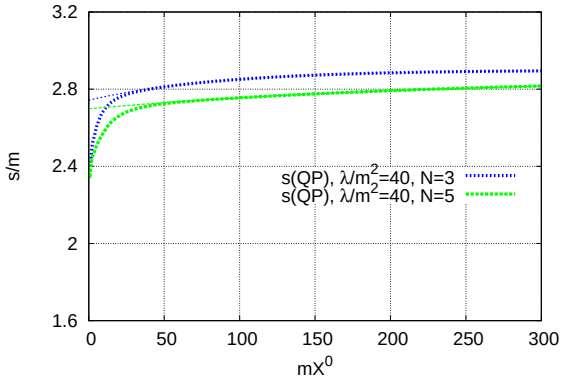

Figure 75: Entropy density $s^0(\mathrm{QP})/m$ in the quasiparticle approximation for the WS initial condition with the number of particle components N =3 and 5 and the coupling $\lambda/m^2 = 40$. The exponential fit with (224) is denoted by a thin line in each case.

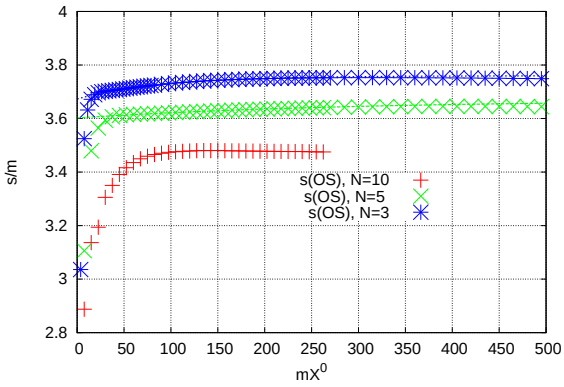

Figure 76: Entropy density $s^0(\mathrm{OS})/m$ (91) for the "tsunami" initial condition with the number of particle components N =3 and 5 for $\lambda/m^2 = 40$. The exponential fit with (224) is denoted by a thin line for $N = 3$ and 5.

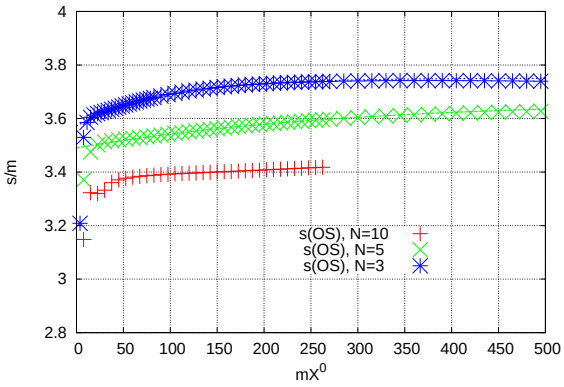

Figure 77: Entropy density $s^0(\mathrm{OS})/m$ (91) for the WS initial condition with the number of particle components N =3 and 5 for $\lambda/m^2 = 40$. The exponential fit with (224) is denoted by a thin line for $N = 3$ and 5.

4.4 Nonthermal fixed point

When we consider strongly correlated systems far from equilibrium, we notice that the system shows scaling solutions for the correlation functions and stationary relations in the nonthermal point. In this subsection we present the nonthermal fixed point where time evolution of number distribution function shows zero in the Boltzmann equation and the point where stationary relation $\Sigma_F(p)\rho(p) - \Sigma_\rho(p)F(p) = 0$ is satisfied in the KB equation. The derivation refers the lecture note [127] and Refs. [128, 129, 130]. We can find the nonthermal fixed point by seeking the scale invariant energy or number flux in the momentum space in the Boltzmann case. We find the fixed point in the KB case by searching the looser condition of the stationary solution $\Sigma_F\rho - \Sigma_\rho F = 0$. In the following analysis, we will restrict ourselves to the systems with spatially isotropic and homogeneous distribution functions.

In the far-from-equilibrium dynamics we find the scaling solution $n(\mathbf{p}) \sim \frac{1}{p^{5/3}}$ or $n(\mathbf{p}) \sim \frac{1}{p^{4/3}}$ for $d = 3$ under the condition $n \gg 1$ in the Boltzmann approach. However normally in the Boltzmann equation the system must be dilute $n \ll 1$, so that its derivation may have contradiction with the condition[11]. Next we consider the case of KB equation based on field theoretical approach which can deal with the dense systems. When we use the above stationary relation in the KB equation, we obtain the scaling solution $n(\mathbf{p}) \sim \frac{1}{p^{5/3}}$ or $n(\mathbf{p}) \sim \frac{1}{p^{4/3}}$ for $d = 3$ in the scalar ϕ^4 theory. We give the numerical results with the scaling solution in $d = 2$ in the later section. In addition we can extend the analysis for large N expansion to next-to-leading order in $O(N)$ scalar field theory. Then we obtain the scaling solution $n(\mathbf{p}) \sim \frac{1}{p^{5/3}}$ or $n(\mathbf{p}) \sim \frac{1}{p^{4/3}}$ in the UV region and $n(\mathbf{p}) \sim \frac{1}{p^4}$ or $n(\mathbf{p}) \sim \frac{1}{p^5}$ in the IR region. The numerical analyses of the nonthermal fixed point with the scaling solution of number distribution function are given in Refs. [131, 132].

4.4.1 Nonthermal fixed point for the Boltzmann equation

First let us consider the scalar ϕ^4 field theory. Then the expression of the Boltzmann equation for bosons containing up to 2 to 2 scattering processes is given in the following

$$\partial_t n_p(t) = \int d\Omega(\mathbf{p},\mathbf{l},\mathbf{q},\mathbf{r})\left[(1+n_{\mathbf{p}}(t))\,(1+n_{\mathbf{l}}(t))\,n_{\mathbf{q}}(t)n_{\mathbf{r}}(t) - n_{\mathbf{p}}(t)n_{\mathbf{l}}(t)\,(1+n_{\mathbf{q}}(t))\,(1+n_{\mathbf{r}}(t))\right] \quad (225)$$

where

$$\int d\Omega(\mathbf{p},\mathbf{l},\mathbf{q},\mathbf{r}) = \lambda^2 \int_{\mathbf{l},\mathbf{q},\mathbf{r}} \frac{1}{2\omega_p 2\omega_l 2\omega_q 2\omega_r}(2\pi)^d\delta^{(d)}(\mathbf{p}+\mathbf{l}-\mathbf{q}-\mathbf{r})\mathbf{2}\pi\delta(\omega_{\mathbf{p}}+\omega_{\mathbf{l}}-\omega_{\mathbf{q}}-\omega_{\mathbf{r}}). \quad (226)$$

$d\Omega$ contains δ functions which imposes the energy-momentum conservation, the coupling constant λ^2 of the corresponding process and integration measure over the momentum space with respect to $\mathbf{l},\mathbf{q},\mathbf{r}$.

Here we rewrite the above relation as

$$\begin{aligned} \partial_t n_{\mathbf{p}} &= I_{\mathbf{p}}[n] \\ I_{\mathbf{p}}[n] &= \int d\Omega(\mathbf{p},\mathbf{l},\mathbf{q},\mathbf{r})L(\mathbf{p},\mathbf{l},\mathbf{q},\mathbf{r}) \\ L(\mathbf{p},\mathbf{l},\mathbf{q},\mathbf{r}) &= \left[(1+n_{\mathbf{p}}(t))\,(1+n_{\mathbf{l}}(t))\,n_{\mathbf{q}}(t)n_{\mathbf{r}}(t) - n_{\mathbf{p}}(t)n_{\mathbf{l}}(t)\,(1+n_{\mathbf{q}}(t))\,(1+n_{\mathbf{r}}(t))\right]. \end{aligned} \quad (227)$$

The effects of the interactions is described by the collision integral $I_{\mathbf{p}}[n]$. The collision integral is a function of the target momentum $\mathbf{p}$ and a functional of the distribution function n. $I_{\mathbf{p}}$ is described by the integral $\int d\Omega L(\mathbf{p},\mathbf{l},\mathbf{q},\mathbf{r})$ where $\mathbf{p}$ is the target momentum and $\mathbf{l},\mathbf{q},\mathbf{r}$ refer to momenta over which the integration is carried out. In the classical statistical limit $n \gg 1$, $O(n^2)$ terms can be neglected and L is a sum of $O(n^3)$ terms

$$L(\mathbf{p},\mathbf{l},\mathbf{q},\mathbf{r}) = (n_{\mathbf{p}}+n_{\mathbf{l}})n_{\mathbf{q}}n_{\mathbf{r}} - n_{\mathbf{p}}n_{\mathbf{l}}(n_{\mathbf{q}}+n_{\mathbf{r}}) \quad (228)$$

[11] We try to derive the scaling solutions with Boltzmann equation in the next subsection to compare with results of KB equation although its derivation might be meaningless.

where $O(n^4)$ terms are canceled and the power of n in the collision term becomes the number of external line minus one.

A collision integral conserves several quantities. The energy density

$$\epsilon = \int_{\mathbf{p}} \omega_{\mathbf{p}} n_{\mathbf{p}}(t) \tag{229}$$

conserves due to the δ function of the Boltzmann eq and the number density also does

$$n = \int_{\mathbf{p}} n_{\mathbf{p}}(t). \tag{230}$$

Conservation of ϵ and n can be expressed as a continuity equation in Fourier space, e.g.

$$\partial_t(\omega_{\mathbf{p}} n_{\mathbf{p}}) + \bigtriangledown_{\mathbf{p}} \cdot j_{\mathbf{p}} = 0. \tag{231}$$

The case of conserved number can be easily obtained by a formal substitution $\omega_{\mathbf{p}} = 1$. We restrict ourselves to systems which are homogeneous in coordinate space and isotropic in momentum space. Then number distribution function $n_{\mathbf{p}}$ depend only on the absolute value of momenta only. Thus we only have to consider the radial component of the flux density $j_{\mathbf{p}}$ and obtain the energy flux $S^{\epsilon}(K)$ thorough the sphere of radius K

$$\begin{aligned}(2\pi)^d S^{\epsilon}(K) \equiv \int_{\mathbf{p}}^{K} \bigtriangledown_{\mathbf{p}} \cdot j_{\mathbf{p}} &= -\int^{K} d^d p\ \omega_{\mathbf{p}} \partial_t n_{\mathbf{p}} \\ &= -\frac{\pi^{d/2}}{\Gamma\left(1+\frac{d}{2}\right)} \int^{K} dp p^{d-1} \omega_{\mathbf{p}} I_{\mathbf{p}}[n] \end{aligned} \tag{232}$$

Next let us seek the solution $n_{\mathbf{p}}$ where the flux $S^{\epsilon}(K)$ is scale independent, i.e. the integral does not depend on the integration limit K. Let us assume the scaling relation

$$\begin{aligned} n(s\mathbf{p}) &= s^{-\kappa} n(\mathbf{p}), \text{ that is} \\ n(p) &= |\mathbf{p}|^{-\kappa} n(1), \end{aligned} \tag{233}$$

then we obtain the following scaling relation for the time derivative of $n(\mathbf{p})$

$$\begin{aligned} \partial_t n(s\mathbf{p}) &= s^{-\kappa(m-1)+\mu} \partial_t n(\mathbf{p}) \text{that is} \\ \partial_t n(\mathbf{p}) &= |\mathbf{p}|^{-\kappa(m-1)+\mu} \partial_t n(1), \end{aligned} \tag{234}$$

since we have the following scaling relation

$$\omega(s\mathbf{p}) = s\omega(\mathbf{p}) \text{ that is } \omega(\mathbf{p}) = |\mathbf{p}|\omega_1 \tag{235}$$

and from (235)

$$\begin{aligned} d\Omega(s\mathbf{p}, s\mathbf{l}, s\mathbf{q}, s\mathbf{r}) &= \lambda^2 \int \frac{d(s\mathbf{l})}{(2\pi)^d} \frac{d(s\mathbf{q})}{(2\pi)^d} \frac{d(s\mathbf{r})}{(2\pi)^d} \frac{1}{2\omega_{s\mathbf{p}} 2\omega_{s\mathbf{l}} 2\omega_{s\mathbf{q}} 2\omega_{s\mathbf{r}}} \\ &\quad (2\pi)^d \delta^{(d)}(s\mathbf{p} + s\mathbf{l} - s\mathbf{q} - s\mathbf{r}) 2\pi\delta(\omega_{s\mathbf{p}} + \omega_{s\mathbf{l}} - \omega_{s\mathbf{q}} - \omega_{s\mathbf{r}}) \\ &= s^d \cdot s^d \cdot s^d \cdot s^{-4} \cdot s^{-d-1} d\Omega(\mathbf{p}, \mathbf{l}, \mathbf{q}, \mathbf{r}) \\ &= s^{d(m-1)} \cdot s^{-m} \cdot s^{-d-1} d\Omega(\mathbf{p}, \mathbf{l}, \mathbf{q}, \mathbf{r}) \\ &= s^{\mu} d\Omega(\mathbf{p}, \mathbf{l}, \mathbf{q}, \mathbf{r}), \quad \mu = d(m-1) - m - d - 1 \end{aligned} \tag{236}$$

where m is the number of external lines e.g. $m = 4$ for 2 to 2 scattering $m = 3$ for 1 to 2 or 2 to 1

scattering, and finally we obtain

$$\begin{aligned}
\partial_t n(s\mathbf{p}) &= \int d\Omega(s\mathbf{p},\mathbf{l},\mathbf{q},\mathbf{r})\left[(n(s\mathbf{p})+n(\mathbf{l}))\,n(\mathbf{q})n(\mathbf{r})-n(s\mathbf{p})n(\mathbf{l})\,(n(\mathbf{q})+n(\mathbf{r}))\right] \\
&= \int d\Omega(s\mathbf{p},s\mathbf{l},s\mathbf{q},s\mathbf{r})\left[(n(s\mathbf{p})+n(s\mathbf{l}))\,n(s\mathbf{q})n(s\mathbf{r})-n(s\mathbf{p})n(s\mathbf{l})\,(n(s\mathbf{q})+n(s\mathbf{r}))\right] \\
&= \int s^{\mu} d\Omega(\mathbf{p},\mathbf{l},\mathbf{q},\mathbf{r}) s^{-3\kappa}\left[(n(\mathbf{p})+n(\mathbf{l}))\,n(\mathbf{q})n(\mathbf{r})-n(\mathbf{p})n(\mathbf{l})\,(n(\mathbf{q})+n(\mathbf{r}))\right] \\
&= s^{\mu-(m-1)\kappa}\partial_t n(\mathbf{p}). \qquad (237)
\end{aligned}$$

As a result we obtain the energy flux $S^{\epsilon}(K)$ in the following way:

$$\begin{aligned}
S^{\epsilon}(K) &= -\frac{\pi^{d/2}}{\Gamma\left(1+\frac{d}{2}\right)}\cdot\frac{1}{(2\pi)^d}\int_0^K dp\; p^{d-1}\omega(\mathbf{p})\partial_t n(\mathbf{p}) \\
&= -\frac{1}{2^d\pi^{d/2}\Gamma\left(1+\frac{d}{2}\right)}\int_0^K dp\; p^{d-1}(p\;\omega_1)(p^{-\kappa(m-1)+\mu}\partial_t n_1) \\
&= -\frac{1}{2^d\pi^{d/2}\Gamma\left(1+\frac{d}{2}\right)}\int_0^K p^{d-\kappa(m-1)+\mu}\omega_1\partial_t n_1 \\
&= -\frac{\omega_1\partial_t n_1}{2^d\pi^{d/2}\Gamma\left(1+\frac{d}{2}\right)}\cdot\frac{K^{d+1-\kappa(m-1)+\mu}}{d+1-\kappa(m-1)+\mu}. \qquad (238)
\end{aligned}$$

When we impose the scale invariance on $S^{\epsilon}(K)$, we notice that we have to impose the following relation

$$d+1-\kappa(m-1)+\mu=0,\;\text{ or }\;\kappa=\frac{d+1+\mu}{m-1}. \qquad (239)$$

When we impose (239) on (238), we notice that only the logarithmic dependence of $S^{\epsilon}(K)$ is left. When the scale invariance on $S^{\epsilon}(K)$ is imposed, we notice that

$$\frac{\omega_1\partial_t n_1}{d+1-\kappa(m-1)+\mu},\quad\text{for}\quad d+1-\kappa(m-1)+\mu=0 \qquad (240)$$

must be finite since the energy flux must be finite. This is a sufficient condition for the existence of a stationary solution. Therefore

$$\omega_1\partial_t n_1=0 \qquad (241)$$

can be derived under the condition (239). This relation means that the collision integral must have a zero of first degrees in $d-\kappa(m-1)+\mu$ and that the number distribution function $n(\mathbf{p})$ is time independent.

For 2 to 2 scattering in the $d=3$ dimensions we obtain the following scaling solution for $n(\mathbf{p})$

$$\begin{aligned}
\mu &= d(m-1)-m-d-1=d(4-1)-4-d-1=2d-5 \\
\kappa &= \frac{d+1+\mu}{m-1}=\frac{d+1+2d-5}{4-1}=\frac{3+1+2\cdot 3-5}{4-1}=\frac{5}{3} \\
&\quad (\text{ 2 to 2 scattering in } d=3 \text{ from scale invariance of energy flux}). \qquad (242)
\end{aligned}$$

When $n(\mathbf{p})$ has the scaling solution $\frac{1}{p^{5/3}}$, time evolution of the number distribution function stops under 2 to 2 scattering processes for $d=3$.

Here we can trially consider 1 to 2 or 2 to 1 scattering processes which means that

$$\begin{aligned}
L(\mathbf{p},\mathbf{l},\mathbf{q})[n] &= \left[(1+n(\mathbf{p})n(\mathbf{l})n(\mathbf{q})-n(\mathbf{p})(1+n(\mathbf{l}))(1+n(\mathbf{q}))\right] \\
&= \left[n(\mathbf{l})n(\mathbf{q})-n(\mathbf{p})n(\mathbf{l})-n(\mathbf{p})n(\mathbf{q})\right] \\
&\quad \text{for the classical statistical limit } n\gg 1. \qquad (243)
\end{aligned}$$

These collision processes are forbidden due to the energy momentum conservation in the Boltzmann equation. However later we consider the case when these 1 to 2 or 2 to 1 scattering processes appears in KB equation in the gauge field theory. To make a comparison with that we consider the scaling solution of 1 to 2 or 2 to 1 scattering processes. For 1 to 2 scattering or 2 to 1 scattering in the $d = 3$ dimensions we obtain

$$\begin{aligned} \mu &= d(m-1) - m - d - 1 = d(3-1) - 3 - d - 1 = d - 4 \\ \kappa &= \frac{d+1+\mu}{m-1} = \frac{d+1+d-4}{3-1} = \frac{3+1+3-4}{3-1} = \frac{3}{2} \\ &\quad (\text{ 1 to 2 or 2 to 1 scattering in } d = 3 \text{ from scale invariance of energy flux}). \end{aligned} \tag{244}$$

In addition another scaling solution for the number distribution function can be derived from the scale dependence of the number flux, that is the scale invariance of

$$\begin{aligned} S^n(K) &= -\frac{\pi^{d/2}}{\Gamma\left(1+\frac{d}{2}\right)} \cdot \frac{1}{(2\pi)^d} \int_0^K dp\ p^{d-1} \partial_t n(\mathbf{p}) \\ &= -\frac{1}{2^d \pi^{d/2} \Gamma\left(1+\frac{d}{2}\right)} \int_0^K dp\ p^{d-1-\kappa(m-1)+\mu} \partial_t n_1 \\ &= -\frac{\partial_t n_1}{2^d \pi^{d/2} \Gamma\left(1+\frac{d}{2}\right)} \cdot \frac{K^{d-\kappa(m-1)+\mu}}{d+1-\kappa(m-1)+\mu}. \end{aligned} \tag{245}$$

Therefore scaling relation for the number flux can be obtained in the following

$$d - \kappa(m-1) + \mu = 0, \text{ or } \kappa = \frac{d+\mu}{m-1}. \tag{246}$$

As a result for 2 to 2 scattering in $d = 3$ we obtain

$$\begin{aligned} \kappa = \frac{d+\mu}{m-1} = \frac{d+2d-5}{4-1} = \frac{3+2\cdot 3-5}{4-1} = \frac{4}{3} \\ (\text{ 2 to 2 scattering in } d = 3 \text{ from scale invariance of number flux}). \end{aligned} \tag{247}$$

On the other hand since the particle number density is not conserved for 1 to 2 or 2 to 1 scattering processes,

$$\begin{aligned} \kappa \neq \frac{d+\mu}{m-1} = \frac{d+d-4}{3-1} = \frac{3+3-4}{3-1} = 1 \quad (\text{for } d = 3) \\ (\text{ 1 to 2 or 2 to 1 scattering in } d = 3 \text{ from scale invariance of number flux}) \end{aligned} \tag{248}$$

can not be the solution. When the above scaling solutions are satisfied for $n(\mathbf{p})$, time evolution of number distribution function stops.

4.4.2 Nonthermal fixed point for the scalar ϕ^4 theory

The dilute gas approximation underlying the Boltzmann equation becomes invalid for high occupation numbers $n(\mathbf{p}) \sim \frac{1}{p^\kappa}$. Therefore we have to confirm the above scaling relation with KB equation which can treat the dense systems.

In this subsection we derive the scaling solution for the correlation functions by using the looser relation of the stationary condition $\Sigma_F \rho - \Sigma_\rho F = 0$. In the scalar ϕ^4 theory we consider up to 3 loop expansion of the coupling λ. Then we derive the scaling solution of the correlation functions. In Sec. 3.1 we obtained the following relation

$$\begin{aligned} &\left[2ip \cdot \frac{\partial}{\partial X} - \frac{i}{2} \cdot \frac{\lambda}{2} \int \frac{d^{d+1}k}{(2\pi)^{d+1}} \left(\frac{\partial G^{aa}(X,k)}{\partial X} + \frac{\partial G^{bb}(X,k)}{\partial X} \right) \cdot \frac{\partial}{\partial p} \right] G^{ab} \\ &= i \int d(x-y) e^{ip\cdot(x-y)} \int dz (\Sigma^{ac}_{\rm nonl}(x,z) c^{cd} G^{db}(z,y) - G^{ac}(x,z) c^{cd} \Sigma^{db}_{\rm nonl}(z,y)) , \end{aligned} \tag{249}$$

on the way of deriving the entropy with off-shellness from the Schwinger-Dyson equation. By summing or differentiating $(1,2)$ and $(2,1)$ components in the above equation we obtain the following relation:

$$\left[2p^\mu \partial_{X^\mu} + (\partial_{X^\mu} M^2(X))\partial_{p^\mu}\right] F(X,p) = \Sigma_\rho(X,p)F(X,p) - \Sigma_F(X,p)\rho(X,p) \tag{250}$$

and

$$\left[2p^\mu \partial_{X^\mu} + (\partial_{X^\mu} M^2(X))\partial_{p^\mu}\right] \rho(X,p) = 0. \tag{251}$$

where we have left up to the 1st order of the gradient expansion.

From the relations (250) and (251) we can interpret that the stationary relation is found to be

$$\Sigma_\rho(X,p)F(X,p) - \Sigma_F(X,p)\rho(X,p) = 0. \tag{252}$$

For the thermal equilibrium we have the fluctuating-dissipation relation (FDR) as

$$\begin{aligned} F(p) &= \left(f_{BE}(p^0) + \frac{1}{2}\right)\rho(p) \\ \Sigma_F(p) &= \left(f_{BE}(p^0) + \frac{1}{2}\right)\Sigma_\rho(p) \end{aligned} \tag{253}$$

where $f_{BE}(p^0) = \frac{1}{e^{\beta p^0}-1}$. Under the condition (253) the stationary condition (252) is satisfied, so that when the FDR is satisfied the system is stationary.

However we can find the state where stationary relation is approximately satisfied even in far from equilibrium. In this subsection we seek the nonthermal fixed point with the looser relation of stationary relation (252).

In the similar way of the previous subsection let us use the scaling solution of correlation functions. The scaling relation of the statistical function can be written as

$$F(p) = s^{2+\kappa}F(sp) \tag{254}$$

since we consider $F(p) = \rho(p)\left(fp + \frac{1}{2}\right) \sim \rho(p)f(p)$ for $f(p) \gg 1$ where we use the scaling relation

$$\rho(p) = s^2 \mathrm{sgn}(s)\rho(sp), \quad \left(\text{and } G^{R,A}(p) = s^2 G^{R,A}(sp)\right) \tag{255}$$

which is the analogy of $\rho(p) = 2\pi\epsilon(p^0)\delta(p^2) = s^2\mathrm{sgn}(s)\cdot 2\pi\epsilon(sp^0)\delta(s^2p^2) = s^2\mathrm{sgn}(s)\rho(sp)$ and the assumption $f(p) = s^\kappa f(sp)$ as in the previous subsection.

Then the scaling relation of the self energy can be derived in the following way,

$$\begin{aligned} \Sigma_F(p) &= -\frac{\lambda^2}{6}\int \frac{d^{d+1}l}{(2\pi)^{d+1}}\frac{d^{d+1}q}{(2\pi)^{d+1}}F(p-l-q)\left(F(l)F(q) - \frac{3}{4}\rho(l)\rho(q)\right) \\ &= -\frac{\lambda^2}{6}s^{-2(d+1)}\int \frac{d^{d+1}(sl)}{(2\pi)^{d+1}}\frac{d^{d+1}(sq)}{(2\pi)^{d+1}}s^{2+\kappa}F(s(p-l-q)) \\ &\quad \times \left(s^{2(2+\kappa)}F(sl)F(sq) - \frac{3}{4}s^4\rho(sl)\rho(sq)\right) \\ &\simeq -s^{-2(d+1)}\cdot s^{3(2+\kappa)}\cdot\frac{\lambda^2}{6}\int \frac{d^{d+1}(sl)}{(2\pi)^{d+1}}\frac{d^{d+1}(sq)}{(2\pi)^{d+1}}F(s(p-l-q))F(sl)F(sq) \\ &= s^{-2(d+1)+3(2+\kappa)}\Sigma_F(sp), \end{aligned} \tag{256}$$

and

$$\begin{aligned}
\Sigma_\rho(p) &= -\frac{\lambda^2}{2}\int \frac{d^{d+1}l}{(2\pi)^{d+1}}\frac{d^{d+1}q}{(2\pi)^{d+1}}\rho(p-l-q)\left(F(l)F(q)-\frac{1}{12}\rho(l)\rho(q)\right) \\
&= -\frac{\lambda^2}{2}s^{-2(d+1)}\int \frac{d^{d+1}l}{(2\pi)^{d+1}}\frac{d^{d+1}q}{(2\pi)^{d+1}}s^2\rho(s(p-l-q)) \\
&\quad \times\left(s^{2(2+\kappa)}F(sl)F(sq)-\frac{1}{12}s^4\rho(sl)\rho(sq)\right) \\
&\simeq -s^{-2(d+1)}\cdot s^{2(2+\kappa)}\cdot\frac{\lambda^2}{2}\int\frac{d^{d+1}(sl)}{(2\pi)^{d+1}}\frac{d^{d+1}(sq)}{(2\pi)^{d+1}}s^2\rho(s(p-l-q))F(sl)F(sq) \\
&= s^{-2(d+1)+2+2(2+\kappa)}\Sigma_\rho(sp). \qquad (257)
\end{aligned}$$

In the process of seeking the power scaling with dominant contributions, we can approximately write $\Sigma_F(p)\rho(p)$ as

$$\Sigma_F(p)\rho(p) = -\frac{\lambda^2}{6}\int\frac{d^{d+1}l}{(2\pi)^{d+1}}\frac{d^{d+1}q}{(2\pi)^{d+1}}F(p-l-q)F(l)F(q)\rho(p), \qquad (258)$$

and $\Sigma_\rho(p)F(p)$ as

$$\begin{aligned}
\Sigma_\rho(p)F(p) &= -\frac{\lambda^2}{2}\int\frac{d^{d+1}l}{(2\pi)^{d+1}}\frac{d^{d+1}q}{(2\pi)^{d+1}}\rho(p-l-q)F(l)F(q)F(p) \\
&= -\frac{\lambda^2}{2}\int\frac{d^{d+1}l}{(2\pi)^{d+1}}\frac{d^{d+1}q}{(2\pi)^{d+1}}\frac{d^{d+1}r}{(2\pi)^{d+1}}\delta^{d+1}(r-p+q+l)\rho(r)F(l)F(q)F(p) \\
&= -\frac{\lambda^2}{6}\int\frac{d^{d+1}l}{(2\pi)^{d+1}}\frac{d^{d+1}q}{(2\pi)^{d+1}}\Big(\rho(p-l-q)F(l)F(q)F(p) \\
&\quad +F(p-l-q)\rho(q)F(l)F(p)+F(p-l-q)F(q)\rho(l)F(p)\Big). \qquad (259)
\end{aligned}$$

By equating (258) and (259) as

$$\begin{aligned}
\int_{q,l}F(p-l-q)F(l)F(q)\rho(p) &= \int_{q,l}\Big[\rho(p-l-q)F(l)F(q)F(p) \\
&\quad +F(p-l-q)F(l)\rho(q)F(p) \\
&\quad +F(p-l-q)\rho(l)F(q)F(p)\Big], \qquad (260)
\end{aligned}$$

or

$$\begin{aligned}
\int_{q,l,r}\delta(p+l-q-r)\Big\{&\left[F(p)\rho(l)+\rho(p)F(l)\right]F(q)F(r) \\
&-F(p)F(l)\left[F(q)\rho(r)+\rho(q)F(r)\right]\Big\}=0, \qquad (261)
\end{aligned}$$

where we have used the relation $F(l)=F(-l)$, $\rho(l)=-\rho(-l)$, we seek the solution of the (252).

However it is difficult to find the solutions of (261) analytically. Therefore we use the looser equation of (261). Looser equation is the integrated version over spatial component $\mathbf{p}$ as

$$\begin{aligned}
\int_{\mathbf{p},q,l,r}\delta(p+l-q-r)\Big[&F(p)\rho(l)F(q)F(r)+\rho(p)F(l)F(q)F(r) \\
&-F(p)F(l)F(q)\rho(r)-F(p)F(l)\rho(q)F(r)\Big]=0. \qquad (262)
\end{aligned}$$

In Eq. (262) the functions of 2nd, 3rd and 4th terms in the bracket can be changed to be the same without coefficients as the 1st term. The change of the second term of the bracket in (262) is

$$l\to\frac{p^0}{l^0}p,\ q\to\frac{p^0}{l^0}q,\ r\to\frac{p^0}{l^0}r,\ p\to\frac{p^0}{l^0}l. \qquad (263)$$

We can notice that p^0 component does not change in (263). By use of the (263), the Jacobian of the $\left(\frac{(p^0)^2}{l^0}, \frac{p^0 q^0}{l^0}, \frac{p^0 r^0}{l^0}\right)$:

$$\left| \begin{array}{ccc} -\left(\frac{p^0}{l^0}\right)^2 & -\frac{p^0 q^0}{(l^0)^2} & -\frac{p^0 r^0}{(l^0)^2} \\ 0 & \frac{p^0}{l^0} & 0 \\ 0 & 0 & \frac{p^0}{l^0} \end{array} \right| = \left(\frac{p^0}{l^0}\right)^4 \tag{264}$$

and the scaling relations (254) and (255), we can rewrite the second term of (262) as

$$\begin{aligned} & \int_{\mathbf{p},l,q,r} \delta^{d+1}(p+l-q-r)\rho(p)F(l)F(q)F(r) \\ = & \left(\frac{p^0}{l^0}\right)^{4(d+1)} \int_{\mathbf{p},l,q,r} \delta\left(\frac{p^0}{l^0}(p+l-q-r)\right) \rho\left(\frac{p^0}{l^0}l\right) F\left(\frac{p^0}{l^0}p\right) F\left(\frac{p^0}{l^0}q\right) F\left(\frac{p^0}{l^0}r\right) \\ = & \left(\frac{p^0}{l^0}\right)^{4(d+1)} \left(\frac{p^0}{l^0}\right)^{-(d+1)} \left(\frac{p^0}{l^0}\right)^{-2} \left(\frac{p^0}{l^0}\right)^{-3(2+\kappa)} \mathrm{sgn}\left(\frac{p^0}{l^0}\right) \\ \times & \int_{\mathbf{p},l,q,r} \delta^{d+1}(p+l-q-r)\rho(l)F(p)F(q)F(r) \\ = & \left(\frac{p^0}{l^0}\right)^{3(d+1)-3(2+\kappa)-2} \mathrm{sgn}\left(\frac{p^0}{l^0}\right) \int_{\mathbf{p},l,q,r} \delta^{d+1}(p+l-q-r)\rho(l)F(p)F(q)F(r). \end{aligned} \tag{265}$$

By use of the change of variables in the third term in (262) as

$$l \to \frac{p^0}{r^0}q,\ q \to \frac{p^0}{r^0}p,\ r \to \frac{p^0}{r^0}l,\ p \to \frac{p^0}{r^0}r, \tag{266}$$

and the scaling relation (254) and (255), we can obtain

$$\begin{aligned} & \int_{\mathbf{p},l,q,r} \delta^{d+1}(p+l-q-r)F(p)F(l)F(q)\rho(r) \\ = & \left(\frac{p^0}{r^0}\right)^{3(d+1)-3(2+\kappa)-2} \mathrm{sgn}\left(\frac{p^0}{r^0}\right) \int_{\mathbf{p},l,q,r} \delta^{d+1}(p+l-q-r)\rho(l)F(p)F(q)F(r). \end{aligned} \tag{267}$$

Finally the fourth term can be transformed by the change of variables as

$$l \to \frac{p^0}{q^0}r,\ q \to \frac{p^0}{q^0}l,\ r \to \frac{p^0}{q^0}p,\ p \to \frac{p^0}{q^0}q \tag{268}$$

to

$$\begin{aligned} & \int_{\mathbf{p},l,q,r} \delta^{d+1}(p+l-q-r)F(p)F(l)\rho(q)F(r) \\ = & \left(\frac{p^0}{q^0}\right)^{3(d+1)-3(2+\kappa)-2} \mathrm{sgn}\left(\frac{p^0}{q^0}\right) \int_{\mathbf{p},l,q,r} \delta^{d+1}(p+l-q-r)\rho(l)F(p)F(q)F(r). \end{aligned} \tag{269}$$

As a result the Eq. (262) can be rewritten by use of (265), (267) and (269) as

$$\begin{aligned} 0 = & \int_{\mathbf{p},l,q,r} \delta^{d+1}(p+l-q-r)F(p)\rho(l)F(q)F(r) \\ \times & \left[1 + \left|\frac{p^0}{l^0}\right|^{\bar{\Delta}} \mathrm{sgn}\left(\frac{p^0}{l^0}\right) - \left|\frac{p^0}{r^0}\right|^{\bar{\Delta}} \mathrm{sgn}\left(\frac{p^0}{r^0}\right) - \left|\frac{p^0}{q^0}\right|^{\bar{\Delta}} \mathrm{sgn}\left(\frac{p^0}{q^0}\right)\right] \end{aligned} \tag{270}$$

where

$$\tilde{\Delta} = 3(d+1) - 3(2+\kappa) - 2 = 3d - 5 - 3\kappa. \tag{271}$$

The one solution of the (270) is $\tilde{\Delta} = -1$ because of the relation

$$\delta^{d+1}(p+l-q-r) \times \left[1 + \frac{l^0}{p^0} - \frac{r^0}{p^0} - \frac{q^0}{p^0}\right] = 0 \tag{272}$$

in (270). When $\tilde{\Delta} = -1$, we obtain

$$\tilde{\Delta} = 3d - 5 - 3\kappa = -1, \text{ or } \kappa = d - \frac{4}{3} = \frac{5}{3} \text{ for } d = 3. \tag{273}$$

This result corresponds to the relations derived from the restriction of the scale invariant energy flux the Boltzmann equation in the previous subsection.

Another solution of the Eq. (270) is $\tilde{\Delta} = 0$. It is because for $\tilde{\Delta} = 0$ the relation (262) can be rewritten as

$$\begin{aligned}
&\int_{\mathbf{p},l,q,r} \delta^{d+1}(p+l-q-r)\left[1 + \mathrm{sgn}\left(\frac{p^0}{l^0}\right) - \mathrm{sgn}\left(\frac{p^0}{r^0}\right) - \mathrm{sgn}\left(\frac{p^0}{q^0}\right)\right] \\
(\text{for } p^0 > 0), \quad = \quad &\int_{\mathbf{p},\mathbf{l},\mathbf{q},\mathbf{r}} \int_0^\infty \frac{dl^0}{2\pi} \int_0^\infty \frac{dq^0}{2\pi} \int_0^\infty \frac{dr^0}{2\pi} \delta^d(\mathbf{p}+\mathbf{l}-\mathbf{q}-\mathbf{r}) \\
&\Big(0 \cdot \delta(p^0 + l^0 - q^0 - r^0) - 2 \cdot \delta(p^0 - l^0 - q^0 - r^0) + 2 \cdot \delta(p^0 + l^0 + q^0 - r^0) \\
&+2 \cdot \delta(p^0 + l^0 - q^0 + r^0) + 0 \cdot \delta(p^0 - l^0 - q^0 - r^0) + 0 \cdot \delta(p^0 - l^0 - q^0 + r^0) \\
&+4 \cdot \delta(p^0 + l^0 + q^0 + r^0) + 2 \cdot \delta(p^0 - l^0 + q^0 + r^0)\Big).
\end{aligned} \tag{274}$$

In (274) we can notice that only particle number changing processes could lead to nonzero contributions. In the massless case $p^0 = |\mathbf{p}|$ energy momentum conservation restricts 1 to 3 processes to be collinear momenta only, which are suppressed in the phase space. As a result $\tilde{\Delta} = 0$ can be the solution of the stationary condition (252). For $\tilde{\Delta} = 0$, we find

$$\tilde{\Delta} = 3d - 5 - 3\kappa = 0, \text{ or } \kappa = d - \frac{5}{3} = \frac{4}{3} \text{ for } d = 3. \tag{275}$$

This result corresponds to the relations derived from the restriction of the scale invariant number flux the Boltzmann equation in the previous subsection. Thus in this subsection we have reproduced the same scaling solution of statistical function or number distribution function in the KB equation as those in Boltzmann equation.

In the end let us confirm that entropy production is suppressed in the evolution from the initial condition with scaling solution. We perform the KB simulation in $2+1$ dimensions to reduce the numerical cost. We prepared the two different types of the initial condition, isotropic distribution (127) in Sec. 3.5 and the scaling distribution, respectively,

$$n_{\mathbf{p}}^{NTF} = \frac{1}{\mathcal{N}_{NTF}} \left(\frac{m}{\sqrt{\mathbf{p}^2 + m^2}}\right)^{\frac{2}{3}} \tag{276}$$

where $\mathcal{N}_{NTF} = 3.22$ and the factor $\frac{2}{3}$ is the scaling in Eq. (273) with $d = 2$. This parameter in $n_{\mathbf{p}}^{NTF}$ is tuned so that both the initial conditions give the same energy for the evolution with the coupling $\lambda/m = 8$, which is the same as that in Sec. 3.5.

In Fig. 78 we show the time evolution of $n(\tilde{\omega}_{\mathbf{p}})$ with the isotropic initial condition (127). We can see that the peak of Gaussian distribution disappears rapidly and that the values at low and high momentum regions grow up drastically until $mX \sim 9$. At the later times $mX^0 \geq 9$ the values

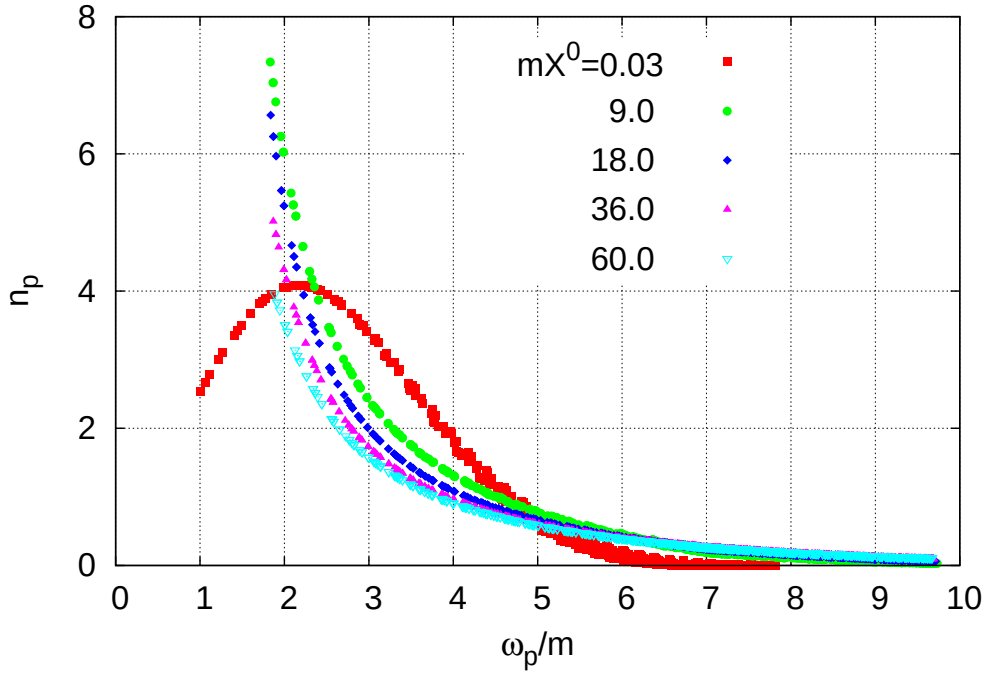

Figure 78: Evolution of the distribution function $n_{\mathbf{p}}(\tilde{\omega}_{\mathbf{p}}/m)$ from the isotropic initial condition $(\lambda/m^2 = 8)$ in Sec.3.5.

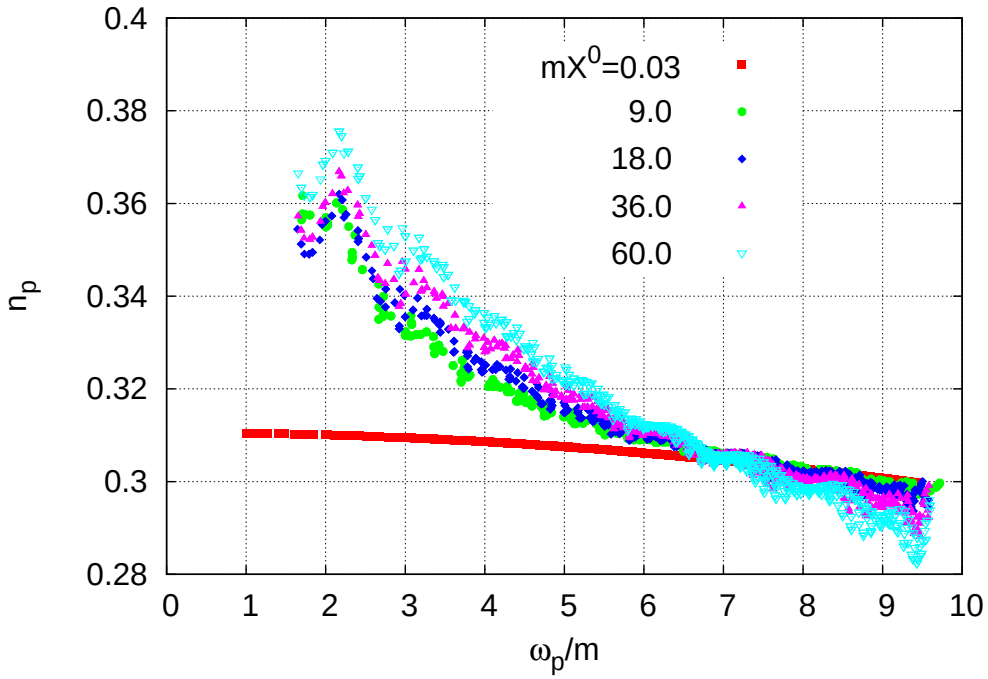

Figure 79: Evolution of the distribution function $n_{\mathbf{p}}(\tilde{\omega}_{\mathbf{p}}/m)$ from the initial condition with the scaling solution $(\lambda/m^2 = 8)$.

at low momentum regions decreases gradually, and the distribution function at high momentum changes moderately. As a result the particle number distribution approaches the Bose distribution. Similarly we show the time evolution of number distribution function $n(\tilde{\omega}_{\mathbf{p}})$ with the scaling initial condition (276). From this figure we see that until $mX^0 \sim 9$ the values at high momentum $\tilde{\omega}_{\mathbf{p}}/m \geq 7$ regions in the distribution function change little. In addition those at low momentum $\tilde{\omega}_{\mathbf{p}}/m < 7$ regions do not grow up so drastically although they grow up gradually. At the low momentum regions the values in $n(\tilde{\omega}_{\mathbf{p}})$ still increases monotonically at the later times $mX^0 \geq 9$, and those at the low momentum regions decreases monotonically too. The distribution function $n_{\mathbf{p}}$ is expected to approach the Bose distribution function with the same temperature and chemical potential as that with isotropic initial condition (127) shown in Fig. 78 since the total energy density for both initial conditions are set to take the same value. However as can be seen in $n_{\mathbf{p}}$ in Fig. 79 at the later times, the change of the values in $n_{\mathbf{p}}$ is very moderate.

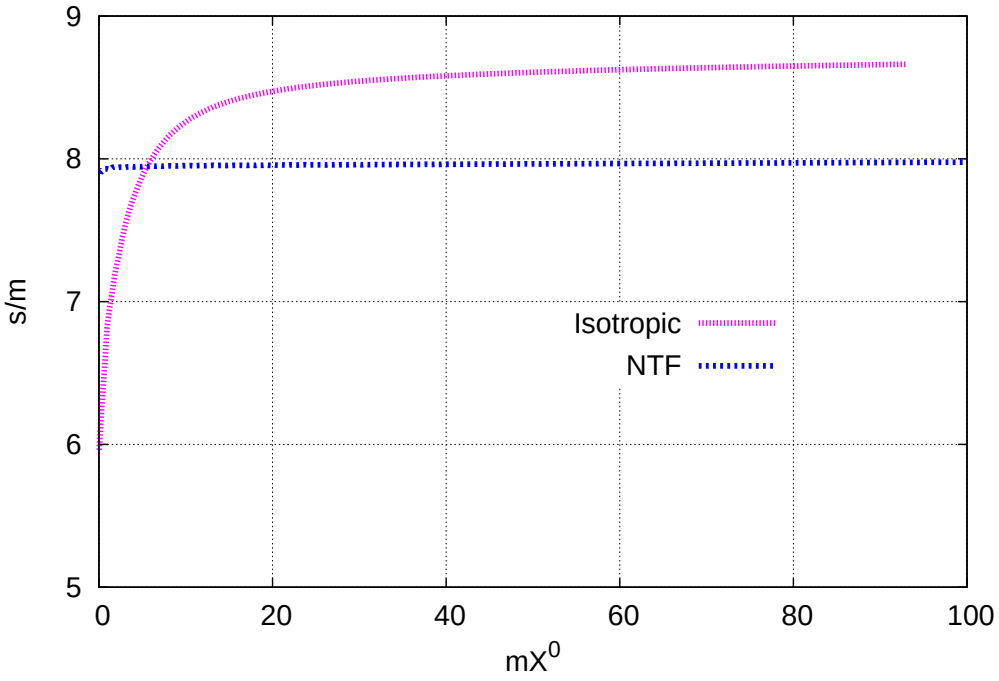

Figure 80: Evolution of the QP entropy (95) from the isotropic initial condition in Sec. 3.5 and initial condition with the scaling solution ($\lambda/m^2 = 8$).

As a result entropy production with the scaling distribution (276) is suppressed compared with the isotropic one (127). We show the QP entropy density for both initial conditions in Fig. 80 as a function of time X^0. In this figure until $mX^0 \sim 9$ the entropy density for the isotropic initial condition (127) increases rapidly. In the later times $mX^0 > 9$ the entropy production for this initial condition is saturated. Meanwhile as we can see this figure the entropy density for the scaling initial condition increases little. Thus we can confirm that entropy production is suppressed for initial conditions with the scaling solution.

4.4.3 Nonthermal fixed point for $O(N)$ theory in the symmetric phase

When the order of the number density becomes $n_{\mathbf{p}} \sim O\left(\frac{1}{\lambda}\right)$ with the coupling constant λ, some processes in the higher order of the coupling can be the same order as the leading collision processes, which causes strongly correlated systems even in $\lambda \ll 1$. In this case the expansion of λ in ϕ^4 theory

is no longer correct. Therefore we should use the $1/N$ expansion instead of the coupling expansion so as to classify diagrams. In this subsection we present the derivation of the scaling solution in the $O(N)$ scalar field theory by use of $1/N$ expansion. The derivation for $O(N)$ theory is based on lectures by J. Berges [127].

First we shall also assume the scaling relation of the statistical (254) and spectral function (255). From these scaling relations we can derive the scaling relations of the self-energy $\Sigma_F(p)$ and $\Sigma_\rho(p)$. The self energy that is given by taking NLO of $1/N$ expansion in symmetric phase ($\langle\phi\rangle = 0$) as

$$\Sigma_F(p) = -\frac{1}{3N}\int_q \lambda_{\rm eff}(p-q)\left[\Pi_F(p-q)F(q) - \frac{1}{4}\Pi_\rho(p-q)\rho(q)\right], \tag{277}$$

and

$$\Sigma_\rho(p) = -\frac{1}{3N}\int_q \lambda_{\rm eff}(p-q)\left[\Pi_F(p-q)\rho(q) + \Pi_\rho(p-q)F(q)\right] \tag{278}$$

where

$$\Pi^{R,A}(p) = \frac{\lambda}{3}\int_q F(p-q)G^{R,A}(q), \quad \Pi_\rho(p) = \Pi^R(p) - \Pi^A(p), \tag{279}$$

$$\Pi_F(p) = \frac{\lambda}{6}\int_q \left[F(p-q)F(q) - \frac{1}{4}\rho(p-q)\rho(q)\right] \tag{280}$$

and the effective coupling

$$\lambda_{\rm eff}(p) = \frac{\lambda}{[1+\Pi^R(p)]\,[1+\Pi^A(p)]}. \tag{281}$$

Here scaling relations of Π_F and $\Pi^{R,A}$ are given by

$$\Pi^{R,A}(p) = s^{3-d+\kappa}\Pi^{R,A}(sp) \tag{282}$$

since $\Pi_{R,A}$ is rewritten as

$$\begin{aligned}
\Pi^{R,A}(sp) &= \frac{\lambda}{3}\int\frac{d^{d+1}q}{(2\pi)^{d+1}}F(sp-q)G^{R,A}(q) \\
&= \frac{\lambda}{3}\int\frac{d^{d+1}(sq)}{(2\pi)^{d+1}}F(sp-sq)G^{R,A}(sq) \\
&= \frac{\lambda}{3}s^{d+1}\int\frac{d^{d+1}q}{(2\pi)^{d+1}}s^{-2-\kappa}F(p-q)s^{-2}G^{R,A}(q) \\
&= s^{d-3-\kappa}\cdot\frac{\lambda}{3}\int\frac{d^{d+1}q}{(2\pi)^{d+1}}F(p-q)G^{R,A}(q) \\
&= s^{d-3-\kappa}\Pi^{R,A}(p), \\
\Pi^{R,A}(p) &= s^{3-d+\kappa}\Pi^{R,A}(sp), \quad \Pi_\rho(p) = s^{\kappa-d+3}\Pi_\rho(sp)
\end{aligned} \tag{283}$$

where in the third line we have used the scaling relation (254) and (255), and Π_F is

$$\begin{aligned}
\Pi_F(p) &= \frac{\lambda}{6}\int\frac{d^{d+1}q}{(2\pi)^{d+1}}\left(F(p-q)F(q) - \frac{1}{4}\rho(p-q)\rho(q)\right) \\
&= \frac{\lambda}{6}\int\frac{d^{d+1}q}{(2\pi)^{d+1}}\left(s^{4+2\kappa}F(s(p-q))F(sq) - \frac{1}{4}s^4\rho(s(p-q))\rho(sq),\right),
\end{aligned} \tag{284}$$

and by assuming $\kappa > 0$ and taking only low momenta (large s), then

$$\begin{aligned}\Pi_F(p) &\simeq \frac{\lambda}{6} s^{-d-1} \frac{d^{d+1}(sq)}{(2\pi)^{d+1}} s^{4+2\kappa} F(s(p-q)) F(sq) \\ &= s^{3+2\kappa-d} \Pi_F(sp). \end{aligned} \tag{285}$$

In addition the scaling relation of $\lambda_{\rm eff}$ can be written as

$$\begin{aligned}\lambda_{\rm eff}(p) &= \frac{\lambda}{[1+\Pi^R(p)]\,[1+\Pi^A(p)]} \\ &= \frac{\lambda}{[1+s^{3-\kappa-d}\Pi^R(sp)]\,[1+s^{3-\kappa-d}\Pi^A(sp)]} \\ &= \begin{cases} s^{-2(3-\kappa-d)}\lambda_{\rm eff}(sp) & (sp=1,\ \text{low momenta } p,\ \text{or large } s) \\ \lambda & (sp=1,\ \text{high momenta } p,\ \text{or small } s) \end{cases}. \end{aligned} \tag{286}$$

As a result the scaling relation of the self energy for low momenta (large s) can be derived as

$$\begin{aligned}\Sigma_F(p) &= -\frac{1}{3N}\int \frac{d^{d+1}q}{(2\pi)^{d+1}} \lambda_{\rm eff}(p-q) \left[\Pi^F(p)F(q) - \frac{1}{4}\Pi^\rho(p-q)\rho(q)\right] \\ &= -\frac{1}{3N} s^{-d-1} \int \frac{d^{d+1}(sq)}{(2\pi)^{d+1}} s^{-2(3-\kappa-d)} \lambda_{\rm eff}(s(p-q)) \\ &\quad \left[s^{3-d+2\kappa}\Pi^F(sp) s^{2+\kappa} F(sq) - \frac{1}{4} s^{3-d+\kappa}\Pi^\rho(s(p-q)) s^2 \rho(sq)\right] \\ &\simeq -\frac{1}{3N} s^{-d-1} \int \frac{d^{d+1}(sq)}{(2\pi)^{d+1}} s^{-2(3-\kappa-d)} \lambda_{\rm eff}(s(p-q)) s^{3-d+2\kappa}\Pi^F(sp) s^{2+\kappa} F(sq) \\ &= s^{2\kappa+2-(3-d+\kappa)-d-1}\Sigma_F(sp) \end{aligned} \tag{287}$$

where in the second and third line we have used (254), (255), (283),(285) and (286), and

$$\begin{aligned}\Sigma_\rho(p) &= -\frac{1}{3N}\int \frac{d^{d+1}q}{(2\pi)^{d+1}} \lambda_{\rm eff}(p-q) \left[\Pi_F(p-q)\rho(q) + \Pi_\rho(p-q)F(q)\right] \\ &= -\frac{1}{3N} s^{-d-1} \int \frac{d^{d+1}(sq)}{(2\pi)^{d+1}} s^{-2(3-\kappa-d)} \lambda_{\rm eff}(s(p-q)) \\ &\quad \left[s^{3-d+2\kappa}\Pi_F(s(p-q)) s^2 \rho(sq) + s^{3-d+\kappa}\Pi_\rho(s(p-q)) s^{2+\kappa} F(sq)\right] \\ &= -s^{\kappa+2-(3-d+\kappa)-d-1} \cdot \frac{1}{3N} \int \frac{d^{d+1}(sq)}{(2\pi)^{d+1}} \lambda_{\rm eff}(s(p-q)) \\ &\quad \left[\Pi_F(s(p-q))\rho(sq) + \Pi_\rho(s(p-q))F(sq)\right] \\ &= s^{\kappa+2-(3-d+\kappa)-d-1}\Sigma_\rho(sp). \end{aligned} \tag{288}$$

Here in the second and third line we have used (254), (255), (283),(285) and (286). When the power scaling of $\Sigma_F(p)$ is estimated, only $O(F^2)$ terms are left. On the other hand all terms of $\Sigma_\rho(p)$ show the same power scaling.

By estimating the power scaling in the self energy we can extract the dominant part of self energy. By extracting the dominant part we can write the $\Sigma_F(p)\rho(p)$ in (252) as

$$\Sigma_F(p)\rho(p) = -\frac{\lambda}{18N}\int \frac{d^{d+1}q}{(2\pi)^{d+1}} \frac{d^{d+1}l}{(2\pi)^{d+1}} \lambda_{\rm eff}(p-l) F(p-l-q) F(q) F(l) \rho(p). \tag{289}$$

In the similar way we can write the $\Sigma_\rho(p)F(p)$ as

$$\begin{aligned}\Sigma_\rho(p)F(p) = -\frac{\lambda}{18N}\int \frac{d^{d+1}q}{(2\pi)^{d+1}} \frac{d^{d+1}l}{(2\pi)^{d+1}} \lambda_{\rm eff}(p-l) \Big[&F(p-l-q)F(q)\rho(l)F(p) \\ &+F(p-l-q)\rho(q)F(l)F(p) \\ &+\rho(p-l-q)F(q)F(l)F(p)\Big]. \end{aligned} \tag{290}$$

By equating the (289) and (290) we seek the scaling solution of correlation functions where the looser relation of stationary relation (252) is satisfied. The stationary relation can be written as

$$\int \frac{d^{d+1}q}{(2\pi)^{d+1}}\frac{d^{d+1}l}{(2\pi)^{d+1}}\frac{d^{d+1}r}{(2\pi)^{d+1}}\delta^{d+1}(p+l-q-r)\lambda_{\rm eff}(p+l)$$
$$\Big\{\,[F(p)\rho(l)+\rho(p)F(l)]\,F(q)F(r)-F(p)F(l)\,[F(q)\rho(r)+\rho(q)F(r)]\,\Big\} \;=\; 0 \qquad (291)$$

where we have used the relation $F(p)=F(-p)$ and $\rho(p)=-\rho(-p)$.

By integrating in terms of spatial components $\mathbf{p}$ and transforming the variables of the second, third and fourth terms in (291), we derive the power $\tilde{\Delta}$ as in the case of ϕ^4 theory. The difference between (262) in ϕ^4 theory and (291) in $O(N)$ theory is the effective coupling $\lambda_{\rm eff}(p+l)$ in (291). Therefore when we derive the stationary solution of (291) we must be careful only for the scaling relation of $\lambda_{\rm eff}(p+l)$.

In the high momentum p regions we have $\lambda_{\rm eff}(p-l)\simeq\lambda$ as (286), so that the scaling solution is

$$\kappa=\frac{4}{3},\ \text{or}\ \frac{5}{3}. \qquad (292)$$

This is the same as the solutions of both KB and Boltzmann equation in the ϕ^4 theory.

On the other hand in the low momentum p regions we must take into account the scaling of the $\lambda_{\rm eff}(p-l)$. Then $\tilde{\Delta}$ becomes the value which is (271) plus the factor $2(3-d+\kappa)$ in (286), so that

$$\tilde{\Delta}=3d-5-3\kappa+2(3-d+\kappa)=d-\kappa+1. \qquad (293)$$

Therefore by imposing $\tilde{\Delta}=-1,0$, the scaling κ in the low momentum regions can be derived as

$$\kappa=d+2\ \text{for}\ \tilde{\Delta}=-1,\ \text{that is}\ \kappa=5, \qquad (294)$$

and

$$\kappa=d+1\ \text{for}\ \tilde{\Delta}=0,\ \text{that is}\ \kappa=4. \qquad (295)$$

We have derived the new scaling solution $\kappa=4,5$ in the low momentum regions which is peculiar in the KB equation with NLO self-energy of $1/N$ expansion in $O(N)$ theory.

4.5 Discussion

In this section we have considered the Kadanoff-Baym equation with NLO self-energy of $1/N$ expansion in the $O(N)$ theory and the time evolution in 1+1 dimensions in the framework of the KB simulation with statistical and spectral functions, $F(X,p)$ and $\rho(X,p)$. The merit of solving this equation is that we can take into account two kinds of the "offshell" effects; one is the memory time effect and the other is the spectral functions $\rho(X,p)$ with its decay width. It is nontrivial whether the dynamics with these effects contribute to thermalization. Next we have introduced kinetic entropy based on KB equation with gradient expansion and proven the H-theorem for two point Green's functions in KB equation with NLO self-energy of $1/N$ expansion in the symmetric phase $\langle\phi\rangle=0$ within 1st order gradient expansion. This result means that entropy production occurs for any change of two point Green's functions $F(X,p)$ and $\rho(X,p)$ (or $G^{12}(X,p)$ and $G^{21}(X,p)$) with nonzero collision term $C\neq 0$, which effectively contains particle number changing processes, such as 0-to-4, 1-to-3 and 3-to-1, as well as 2-to-2 scattering processes, in any dimensions if the gradient expansion is a proper approximation.

We have done the numerical simulation of KB equation in $O(N)$ theory in 1+1 dimensions to confirm the H-theorem. In 1+1 dimensions no thermalization or entropy production occurs in Boltzmann approach without offshell effects due to its energy-momentum conservation, while it occurs in the KB simulation with nonzero $C\neq 0$, which contains particle number changing processes as well as 2-to-2 scattering processes. We have seen that the number distribution function $n(\tilde{\omega}_{\mathbf{p}})$

defined with statistical function converges to the Bose distribution in the time evolution. Here we have also confirmed that both the kinetic entropy (91) and its quasiparticle approximation (95) increase monotonically in the evolution. This numerical result in $1+1$ dimension is consistent to the H-theorem for KB equation.

We have also compared the behavior of kinetic entropy (91) and the QP entropy (95). In the middle range of thermalization the ratio of both entropy becomes constant, so that the QP entropy (95) is a useful indicator of the thermalization. Furthermore we have investigated initial condition dependence of both entropy by changing the number of particle components N. We found that it remains even at asymptotic stage of thermalization when initial condition dependence of the total number density remain. The larger N is, the narrower the spectral width becomes, then the total number density is hard to change since the particle number changing processes are suppressed. By choosing the smaller N we can observe that the total number density tends to lose its initial condition dependence. Then both entropy becomes independent of initial conditions as total number density for two initial conditions approaches.

In the end we have seen the derivation of nonthermal fixed point in scalar theories with both Boltzmann and KB equation by assuming the scaling relation with respect to momentum in the particle number distribution (or statistical function) and the spectral function. In the Boltzmann equation we have used the continuity equation based on total energy and number conservation in the derivation. Here we have estimated both 2-to-2 scattering processes and 1-to-2 particle number changing processes. The former processes are estimated to compare with KB equation in scalar theories, while the latter ones are to be compared with KB equation in gauge theories. Meanwhile in KB equation we have adopted the stationary relation integrated by spatial components of momentum. As a result we can find that the same scaling solutions for the statistical function in ϕ^4 theory appear in both Boltzmann and KB equation. Here we have confirmed that entropy production is suppressed with the scaling solutions in KB simulation. In the case of $O(N)$ theory the solutions have different scaling between low and high momentum regions. The statistical function has the same scaling as ϕ^4 theory in high momentum regions, while it has the different scaling in low momentum regions due to the scaling of momentum dependent coupling $\lambda_{\rm eff}(p)$. Here we have, however, not explicitly mentioned how long the time scale of suppression of entropy production is and whether this scaling solution can appear on the way to thermalization without using another initial condition. We have not investigated whether this solution really interferes with thermalization of gluons in relativistic heavy ion collision. They are still remaining problems.

5 Thermal Gauge Theory

Much of the interest for studying heavy-ion collisions at ultra-relativistic energies is paid since matter at high temperature or density becomes simple due to the asymptotic freedom of QCD [1, 2, 3]. We guess that if the weakly coupled quark-gluon matters are created in the experiments, the properties are determined by a weak coupling expansion in the high energy regimes.

However many difficulties are in front of us in investigating thermal field theories with naive perturbation theory. Since QCD is too complicated to estimate the specific problems of perturbative approach, we first study the difficulties appearing thermal scalar field theories in this section and consider the application of various techniques adopted in the analysis of them to QCD. We give the merit and limitations of various techniques which go beyond the perturbative analysis in the soft sector, such as optimized perturbation theory [133], mass-screened perturbation theory [134, 135], hard-thermal-loop (HTL) perturbation and resummation technique [136]-[146] and Φ-derivable approximation [72]. Before we use Φ-derivable approximation, we review the perturbative analyses and the above theoretical techniques at thermal equilibrium.

First let us consider the problems appearing in naive perturbative analyses [147]. As a example we shall consider massless ϕ^4 theory. What determines the accuracy of a weak coupling calculation in thermal field theories is not only the strength of the coupling constant, but also the temperature of the system. The criteria of whether the weak coupling expansion is proper is comparing the kinetic terms of the Lagrangian and interaction term. For the interaction term $g^2\phi^4$ for the relativistic scalar field theory, the thermal fluctuation which should be compared to $\partial^2 \sim k^2$ is $g^2\langle\phi^2\rangle$ where

$$\langle\phi^2\rangle_T = \int \frac{d^3k}{(2\pi)^3}\frac{n(\epsilon)}{\epsilon_k}. \tag{296}$$

Here $n(\epsilon_k) = 1/(e^{\beta\epsilon_k} - 1)$ is the Bose-Einstein distribution function.

For the plasma particles $\epsilon_k = k \sim T$, then we find $\langle\phi^2\rangle_T \sim T^2$. By comparing the kinetic part $\partial^2 \sim k^2$ and $g^2\langle\phi^2\rangle_T \sim g^2T^2$, we can conclude that in the short wavelength or hard fluctuating regions the perturbative analysis is proper.

Next let us consider the fluctuations at the soft regions $k \sim gT \ll T$ for weak coupling regimes. In these regions the associated occupation number $n(\epsilon_k)$ can be replaced by T/ϵ_k in Eq. (296). By giving an upper cut-off gT in the momentum integral, we get:

$$\langle\phi^2\rangle_{gT} \sim \int^{gT} d^3k\frac{T}{\epsilon_k} \sim gT^2. \tag{297}$$

Thus $g^2\langle\phi^2\rangle_{gT} \sim g^3T^2 \ll k^2 \sim (gT)^2$ is still perturbative. However when we consider the soft kinetic regime $k \sim gT$, we have contributions which are not analytic in g^2 in estimating the energy density. They are shown to be of the order g^3 as:

$$\epsilon^{(3)} \sim \int_0^{gT} d^3k\epsilon_k n(\epsilon_k) = \int_0^{gT} d^3k\epsilon_k\frac{T}{\epsilon_k} \sim T(gT)^3 \sim g^3T^4. \tag{298}$$

Here we find that g^3 term in energy appears by treating the soft mode. This is the origin of the $O(g^3)$ term in the naive perturbation theory.

Finally we shall estimate the ultrasoft momentum scale $k \sim g^2T$ (magnetic screening scale in QCD analysis). Then we have

$$\langle\phi^2\rangle_{g^2T} \sim \int_0^{g^2T} d^3k\frac{T}{\epsilon^2} \sim g^2T^2, \tag{299}$$

so that $g^2\langle\phi^2\rangle_{g^2T} \sim g^4T^2 \sim k^2 \sim (g^2T)^2$. We encounter the breakdown of naive perturbative expansion. Moreover let us estimate the energy density. It is calculated as

$$\epsilon^{(6)} \sim \int_0^{(g^2T)} \sim T(g^2T)^3 \sim g^6T^4. \tag{300}$$

Notice that this calculation is in the regions where the perturbative expansion is completely broken. Therefore we can not calculate higher order energy density than $O(g^6)$ order perturbatively. If the above order estimation is adopted for QCD, similar problems will occur in $O(g^6)$. In fact the famous 'Linde problem' occurs [8].

In addition naive perturbation theory has a problem of poor convergence of thermodynamic variables in the coupling expansion. In order to overcome the poor convergence property of perturbation theory, we need to some elegant techniques, such as screened perturbation theory or HTL perturbation theory and Φ-derivable approximations. Most of the review focus on purely analytical resummation techniques which have been proposed to improve naive perturbation theory in the soft sector.

Among these the simplest theory which tries to estimate nonperturbatively for the effects in the soft sector, is so-called "screened perturbation theory". This is to solve the gap equation of mass shift;

$$m^2 = \frac{\lambda(N+2)}{6N}\left(\int_P \frac{1}{P^2+m^2} + \frac{m^2}{16\pi^2}\left(\frac{1}{\epsilon} + \ln\frac{\bar{\mu}^2}{T^2}\right)\right) \tag{301}$$

where $\bar{\mu}$ is the $\overline{MS}$ scale. The above case is the example of mass screening of tadpole diagrams $O(N)$ symmetric theory. The mass shift is obtained self-consistently from the above gap equation. Then convergence of thermodynamic quantities such as pressure and entropy is estimated, and quite stable convergence properties are shown in this technique. However this technique has a drawback that ultraviolet divergences for the mass shift becomes temperature dependent.

As another strategy to thermal gauge theory is HTL perturbation technique. This technique is applied to the aim of constructing effective theories for temperature dependent massive quasiparticles. There we first calculate the HTL by "standard" perturbation theory. The particular contribution of the one-loop self energy Π of the gluon propagation is an example of what has been called a "hard thermal loop" (HTL). Hard-thermal-loop perturbation theory is a reorganization of the perturbation series for finite temperature QCD.

$$\begin{aligned}\mathcal{L} &= (\mathcal{L}_{0,\mathrm{QCD}} + \mathcal{L}_{\mathrm{HTL}}) - \mathcal{L}_{\mathrm{HTL}} + \mathcal{L}_{\mathrm{int,QCD}}. \\ &= \mathcal{L}'_{0,\mathrm{QCD}} + \mathcal{L}'_{\mathrm{int,QCD}}\end{aligned} \tag{302}$$

where

$$\mathcal{L}_{\mathrm{HTL}} = -\frac{1}{2}(1-\delta)\, m_D^2 \mathrm{Tr}\left((\partial_\mu A_\alpha - \partial_\alpha A_\mu)\langle\frac{y^\alpha y^\beta}{(y\cdot D)^2}\rangle(\partial^\mu A_\beta - \partial_\beta A^\mu)\right) \tag{303}$$

where $y^\mu = (1, \hat{\mathbf{y}})$ is a light-like four-vector, and $\langle\cdots\rangle$ represents the average over the directions of $\hat{\mathbf{y}}$. Hard thermal perturbation theory is defined by treating δ as a formal expansion parameter. Then propagators and vertices corrected by the HTL are adopted to perturbative expansion for the remaining $\mathcal{L}'_{int}$. However perturbative expansion in this method is very complicated and it is necessary to introduce temperature dependent counter terms for the ultraviolet divergence. (In the case when no optimization for the loop expansion is adopted.[12]) In addition in far-from-equilibrium case this method still lacks the proof of conservation law (for energy-momentum, charge ,and so on) , so that this approach have not been applied to non-equilibrium system up to now.

In the end we introduce Φ-derivable approximation (2PI technique) in thermal field theory. It uses the Schwinger-Dyson (SD) equation with respect to the propagator:

$$G^{-1} = G_0^{-1} - \Sigma(G). \tag{304}$$

We can see that the propagator is determined self-consistently from this equation. The rules for the loop expansion of $\Sigma(G)$ is similar to the standard perturbation theory, and simplifications in calculation for the thermodynamic quantities are achieved. As a result we obtain good convergences for them by solving the above SD equation [148]. This approach provide a more natural

[12]Temperature dependent divergences can be removed by some optimization of loop expansion.[133]

approach to renormalization of ultraviolet divergences than above techniques. It is proven that ultraviolet divergences are temperature independent for any loop order[149]. With regard to far-from-equilibrium case the conservation law is achieved from the symmetry of 2PI effective action. However in the case of gauge theory we encounter a drawback of this approach. This approach has difficulty in satisfying the Ward Identity for finite order self-energy. For leading order of the loop expansion for $\Pi = \frac{\delta\Gamma_2}{\delta D}$ where D is the gluon propagator and Π is the polarization vector we obtain in the limit $k_0 \to 0$, and then $\mathbf{k} \to 0$,

$$\frac{k^\mu k^\nu}{k^2}\Pi_{\mu\nu}(k) = \frac{2}{3}g^2 NT\Sigma_n \int \frac{d^d p}{(2\pi)^d}\big[D_L(p) + (d-1)D_T(p) - 2\mathbf{p}^2 D_T^2(p) \\ -\mathbf{p}^2 D_L(p)D_T(p) + \mathbf{p}^2 D_L(p)^2\big] \tag{305}$$

where we have used the gluon propagator for the temporal axial gauge

$$D_{00}(p) = D_{0i}(p) = D_{i0}(p) = 0, \quad D_{ij}(p) = \left(\delta_{ij} - \frac{p_i p_j}{\mathbf{p^2}}\right) D_T(p) + \frac{p_i p_j}{\mathbf{p^2}} D_L(p). \tag{306}$$

The Ward identity should be satisfied for any order of perturbation theory. As an example when we substitute the perturbative thermal propagator (no resummation), the Ward identity is satisfied due to the form

$$\Pi_{\mu\nu}(k) = m_D^2 \left[-\delta_{0\mu}\delta_{0\nu} + k^0 \int \frac{d\Omega}{4\pi} \frac{v_\mu v_\nu}{k^0 - \mathbf{v}\cdot\mathbf{k} + i\epsilon}\right], \tag{307}$$

which is given in Appendix B. The reason why the Ward identity is not satisfied is because the propagator (Green's function) D is resumed propagator of all the 1PI diagrams and leading order of coupling expansion in $\Pi(D)$ is the infinite summations of 1PI diagrams only and throws away the others. With respect to all summations of 2PI diagrams in $\Pi(D)$ we will reproduce the Ward identity.

6 Nonequilibrium dynamics of gauge fields

Collisions of heavy ion (Au+Au, Pb+Pb) at RHIC have been exploited for decades to search for and study the phase transition of hadronic matter to QGP[11, 14, 15, 16]. The dynamical evolution of this hot and dense medium has various stages, which start with some initial state concentrated at mid-rapidity, are followed by a thermalization of partons (formation of QGP), a hydrodynamical expansion and hadronization of QGP, a kinetic freeze-out and the observation of hadrons in a detector.

In the above stages we are in particular interested in the stage of formation of QGP in the early stage of the heavy ion collisions. The data in the heavy-ion experiments to search for and study QGP at RHIC are interpreted as the evidence that the matter constituted by partons (quarks and gluons) are produced, it thermalizes ($\tau_{\rm eq} = 0.6 \sim 1$ fm/c) and its behavior is quantitatively well described by the perfect-fluid hydrodynamics [23, 24, 27, 28]. The problem appears in the explanation of its thermalization time in the early stage. The thermalization time $\tau_{\rm eq} = 0.6 \sim 1$ fm/c is very fast compared with the perturbative analysis [36][13]. There are various theoretical studies on the possibility for this short time thermalization, some of which rely on the instabilities in the plasma [60, 62, 63, 64, 150, 151, 152], and some others include the 2-to-3 processes in parton cascade simulations [153].

In this paper we would like to study one candidate which may explain the above early thermalization of partons (in particular gluons). The author conjectures that the thermalization time due to the scattering processes can be decreased by considering particle number changing processes 1-to-2 and 1-to-3 scattering processes in addition to the above collision processes. These particle number changing processes where initial and ending state of particles are off-shell are forbidden in the normal Boltzmann's analysis due to its on-shell particle picture and not considered in [36]. This off-shell dynamics can help the more entropy production and may explain the early thermalization of partons. One of the methods which can trace these off-shell dynamics is Kadanoff-Baym approach. In this section we would like to review the derivation of the KB equation of gauge fields and try to prove the H-theorem for LO self-energy of the coupling expansion which contains 1-to-2 particle number changing processes.

6.1 Generating functional of gauge field theory

All physical quantities derived in QCD must be gauge invariant and independent of the particular gauge chosen. The original Lagrangian for the gauge field exposes a exact gauge invariance. However, when we quantize the gauge theory in a particular gauge, we have to give the gauge fixing term and the Fadeev-Popov ghost term which break the exact gauge invariance of the original Lagrangian. Thus we have to introduce the background (BG) field method which is a technique that allows a gauge fixing without losing the classical gauge invariance. [14]

When we employ the BG field method, we can express the gluon field as a sum of a classical background field A and a quantum fluctuation a. The remarkable property of this method is the fact that this gauge-fixing term does not break gauge invariance relative to the transformations of the background field A; it fixes only the gauge of the quantized field a. Then we encounter the

[13] However recently it has been claimed that complete thermal equilibrium may not be necessary for the application of hydrodynamics[105, 161]. Nonequilibrium instabilities in anisotropic plasmas which may be identified as the fastest processes may help to explain a rapid isotropization of the equation of state $\Theta_{ij} \simeq P\delta_{ij}$ relevant for near-perfect fluid descriptions [161, 61, 62, 63, 64, 150, 151]. The isotropization of the equation of state may be sufficient for the descriptions of near-perfect fluid. On the other hand in this case viscous hydrodynamics may be necessary for the description of fluid since partons are not completely thermalized.

[14] We use the BG gauge in Sec. 6.1, 6.2 and 6.4 in order to respect classical gauge invariance and match to another nonequilibrium approach to gauge theory. However we show that thermodynamic variables derived from the effective action have controlled gauge dependence at equilibrium and that we can analyze with arbitrary gauge in the estimation of such variables in Sec. 6.4. Hence we use temporal axial gauge in the analysis in the analysis of entropy production. When one wants to know our new results only, skip Sec. 6.1, 6.2 and 6.4.

following action[154, 155, 156, 157, 158];

$$\begin{aligned}
S &= S_0 + S_{\rm fix} + S_{\rm ghost} + S_{\rm source}, \\
S_0 &= -\frac{1}{4}\int d^{d+1}x \left(F^a_{\mu\nu}[A] + D^{ab}_\mu[A]a^b_\nu - D^{ab}_\nu a^b_\mu + g f^{abc} a^b_\mu a^c_\nu\right)^2, \\
S_{\rm fix} &= -\frac{1}{2\alpha}\int d^{d+1}x \left(D^{ab}_\mu a^{\mu,b}\right)^2, \\
S_{\rm ghost} &= \int d^{d+1}x \overline{C}^a D^{ab}_\mu D^{\mu,bc}[A+a]C^c, \\
S_{\rm source} &= \int d^{d+1}x \left(J^a_\mu a^{\mu,a} + \overline{\xi}^a C^a + \overline{C}^a \xi^a\right) \\
&\quad + \frac{1}{2}\int d^{d+1}x d^{d+1}y \left(a^{\mu,a}(x) K^{ab}_{\mu\nu}(x,y) a^{\nu,b}(y) + \overline{C}^a(x)\Xi^{ab}(x,y)C^b(y)\right)
\end{aligned} \tag{308}$$

where f^{abc} is the structure constant of the gauge group $SU(3)$, $C^a, \overline{C}^a$ are the ghost and antighost field, J^a_μ is the external sources of the quantum fluctuations, $\overline{\xi}, \xi$ are the external sources multiplying the ghost and antighost fields, respectively, and

$$F^a_{\mu\nu}[A] = \partial_\mu A^a_\nu - \partial_\nu A^a_\mu + g f^{abc} A^b_\mu A^c_\nu, \tag{309}$$

$$D^{ab}_\mu[A] = \left(\partial_\mu \delta^{ab} + g f^{acb} A^c_\mu\right). \tag{310}$$

The generating functional for the gauge field becomes

$$Z[A, J, \xi, \overline{\xi}, K, \Xi] = \int DaDCD\overline{C} \exp\left(iS\right) \tag{311}$$

where we should notice that quantum fluctuations a^a_μ of the gluon field are the integration variables in the functional integral. In addition the generating functional for the connected Green's functions W is expressed as

$$W[A, J, \xi, \overline{\xi}, K, \Xi] = -i \ln Z[A, J, \xi, \overline{\xi}, K, \Xi] \tag{312}$$

Then we have two types of gauge transformations that leave Z invariant[157]. In this article we shall employ the type I transformations which are given by

$$\begin{aligned}
A'_\mu = UA_\mu U^{-1} + \frac{i}{g} U\partial_\mu U^{-1}, a'_\mu = Ua_\mu U^{-1}, J'_\mu = UJ_\mu U^{-1}, \\
C'_\mu = UCU^{-1}, \overline{\xi}' = U\overline{\xi}U^{-1}, \overline{C}' = U\overline{C}U^{-1}, \xi' = U\xi U^{-1}, \\
K'_{\mu\nu}(x,y) = U(x)K_{\mu\nu}(x,y)U^{-1}(y), \Xi'(x,y) = U(x)\Xi(x,y)U^{-1}(y),
\end{aligned} \tag{313}$$

where $U(x) = \exp(ig\omega^a(x)T^a)$. For an infinitesimal gauge transformation the fields and sources transform as

$$\begin{aligned}
\delta A^a_\mu = D^{ab}_\mu[A]\omega^b,\ \delta a^a_\mu = g f^{abc} a^b_\mu \omega^c,\ \delta J^a_\mu = g f^{abc} J^b_\mu \omega^c, \delta C^a = g f^{abc} C^b \omega^c, \\
\delta\overline{\xi}^a = g f^{abc}\overline{\xi}^b\omega^c,\ \delta\overline{C}^a = g f^{abc}\overline{C}^b\omega^c,\ \delta\xi^a = g f^{abc}\xi^b\omega^c, \\
\delta K^{ab}_{\mu\nu}(x,y) = -g f^{acd}\omega(x)^c K^{db}_{\mu\nu}(x,y) - g f^{bcd}\omega^c(y) K^{ad}_{\mu\nu}(x,y) \\
\delta\Xi^{ab}(x,y) = -g f^{acd}\omega(x)^c \Xi^{db}(x,y) - g f^{bcd}\omega^c(y)\Xi^{ad}(x,y).
\end{aligned} \tag{314}$$

We notice that Z is invariant under type I transformations, if all sources, except A, belong to the adjoint representation.

6.2 2PI effective action for gauge fields in the background gauge

By introducing the effective action Γ let us reexpress the classical action S with the notation of DeWitt[159, 160].

$$
\begin{aligned}
S &= S_0 + S_{\rm source} \\
S_0 &= \frac{1}{2}\Gamma^{(0)}_{mn}(A^2)A_mA_n + \frac{1}{6}\Gamma^{(0)}_{mnp}(A^3)A_mA_nA_p + \frac{1}{24}\Gamma^{(0)}_{mnpq}(A^4)A_mA_nA_pA_q \\
&\quad + \frac{1}{2}\Gamma^{(0)}_{mn}(a^2)a_ma_n + \frac{1}{6}\Gamma^{(0)}_{mnp}(a^3)a_ma_na_p + \frac{1}{24}\Gamma^{(0)}_{mnpq}(a^4)a_ma_na_pa_q \\
&\quad + \Gamma^{(0)}_{mn}(Aa)A_ma_n + \frac{1}{2}\Gamma^{(0)}_{mnp}(Aa^2)A_ma_na_p + \frac{1}{2}\Gamma^{(0)}_{mnp}(A^2a)A_mA_na_p \\
&\quad + \frac{1}{6}\Gamma^{(0)}_{mnpq}(A^3a)A_mA_nA_pa_q + \frac{1}{6}\Gamma^{(0)}_{mnpq}(Aa^3)A_ma_na_pa_q \\
&\quad + \frac{1}{4}\Gamma^{(0)}_{mnpq}(A^2a^2)A_mA_na_pa_q \\
&\quad + \Gamma^{(0)}_{mn}(\overline{C}C)\overline{C}_mC_n + \Gamma^{(0)}_{mnp}(\overline{C}CA)\overline{C}_mC_nA_p + \Gamma^{(0)}_{mnp}(\overline{C}Ca)\overline{C}_mC_na_p \\
&\quad + \Gamma^{(0)}_{mnpq}(\overline{C}CAa)\overline{C}_mC_nA_pa_q + \frac{1}{2}\Gamma^{(0)}_{mnpq}(\overline{C}Ca^2)\overline{C}_mC_na_pa_q, \\
S_{\rm source} &= J_ma_m + \overline{\xi}_mC_m + \overline{C}_m\xi_m.
\end{aligned}
\tag{315}
$$

Here we have used

$$
\begin{aligned}
\Gamma^{(0)}_{mn}(A^2) &= \frac{\delta^2 S_0}{\delta A^{\mu,a}(x_1)\delta A^{\nu,b}(x_2)} \\
&= \delta^{ab}\int d^{d+1}u\ \delta^{d+1}(x_1-u)\left[g_{\mu\nu}\partial_u^2 - \partial_{u\mu}\partial_{u\nu}\right]\delta^{d+1}(x_2-u),
\end{aligned}
\tag{316}
$$

$$
\begin{aligned}
\Gamma^{(0)}_{mn}(a^2) &= \frac{\delta^2 S_0}{\delta a^{\mu,a}(x_1)\delta a^{\nu,b}(x_2)} \\
&= \delta^{ab}\int d^{d+1}u\ \delta^{d+1}(x_1-u)\left[g_{\mu\nu}\partial_u^2 - \partial_{u\mu}\partial_{u\nu} + \frac{1}{\alpha}\partial_{u\mu}\partial_{u\nu}\right]\delta^{d+1}(x_2-u),
\end{aligned}
\tag{317}
$$

where $m=(\mu,a,x_1)$ and $n=(\nu,b,x_2)$;

$$
\begin{aligned}
\Gamma^{(0)}_{mnp}(A^3) = \Gamma^{(0)}_{mnp}(a^3) &= \frac{\delta^3 S_0}{\delta a^{\mu a}(x_1)\delta a^{\nu b}(x_2)\delta a^{\lambda c}(x_3)} \\
&= -gf^{abc}\left[g_{\mu\lambda}(\partial_3-\partial_1)_\nu + g_{\mu\nu}(\partial_1-\partial_2)_\lambda + g_{\lambda\nu}(\partial_2-\partial_3)_\mu\right] \\
&\quad \times\int d^{d+1}u\ \delta^{d+1}(x_1-u)\delta^{d+1}(x_2-u)\delta^{d+1}(x_3-u),
\end{aligned}
\tag{318}
$$

$$
\begin{aligned}
\Gamma^{(0)}_{mnp}(Aa^2) &= \frac{\delta^3 S_0}{\delta a^{\mu a}(x_1)\delta A^{\nu b}(x_2)\delta a^{\lambda c}(x_3)} \\
&= -gf^{abc}\left[g_{\mu\lambda}(\partial_3-\partial_1)_\nu + g_{\mu\nu}\left(\partial_1 - \partial_2\frac{1}{\alpha}\partial_3\right)_\lambda\right. \\
&\quad \left. + g_{\lambda\nu}\left(\partial_2-\partial_3-\frac{1}{\alpha}\partial_1\right)_\mu\right] \\
&\quad \times\int d^{d+1}u\ \delta^{d+1}(x_1-u)\delta^{d+1}(x_2-u)\delta^{d+1}(x_3-u),
\end{aligned}
\tag{319}
$$

where $m=(\mu,a,x_1)$, $n=(\nu,b,x_2)$, $p=(\lambda,c,x_3)$ and $\partial_{1\mu}\equiv\partial\delta(x_1-u)/\partial x_1^\mu$;

$$\begin{aligned}\Gamma^{(0)}_{mnpq}(A^4) &= \Gamma^{(0)}_{mnpq}(Aa^3)=\Gamma^{(0)}_{mnpq}(a^4)\\ &= \frac{\delta^4 S_0}{\delta a^{\mu a}(x_1)\delta a^{\nu b}(x_2)\delta a^{\lambda c}(x_3)\delta a^{\sigma d}(x_4)}\\ &= \big[-g^2 f^{lda}f^{lcb}(g_{\sigma\lambda}g_{\mu\nu}-g_{\nu\sigma}g_{\mu\lambda})\\ &\quad -g^2 f^{lca}f^{ldb}(g_{\sigma\lambda}g_{\mu\nu}-g_{\mu\sigma}g_{\nu\lambda})\\ &\quad -g^2 f^{lcd}f^{lab}(g_{\mu\lambda}g_{\sigma\nu}-g_{\mu\sigma}g_{\nu\lambda})\big]\\ &\quad \times\int d^{d+1}u\ \delta^{d+1}(x_1-u)\delta^{d+1}(x_2-u)\delta^{d+1}(x_3-u)\delta^{d+1}(x_4-u),\end{aligned}\tag{320}$$

$$\begin{aligned}\Gamma^{(0)}_{mnpq}(A^2a^2) &= \frac{\delta^4 S_0}{\delta a^{\mu a}(x_1)\delta a^{\nu b}(x_2)\delta A^{\lambda c}(x_3)\delta A^{\sigma d}(x_4)}\\ &= \Bigg[-g^2 f^{lda}f^{lcb}\left(g_{\sigma\lambda}g_{\mu\nu}-g_{\nu\sigma}g_{\mu\lambda}+\frac{1}{\alpha}g_{\lambda\nu}g_{\mu\sigma}\right)\\ &\quad -g^2 f^{lca}f^{ldb}\left(g_{\sigma\lambda}g_{\mu\nu}-g_{\mu\sigma}g_{\nu\lambda}+\frac{1}{\alpha}g_{\sigma\nu}g_{\mu\lambda}\right)\\ &\quad -g^2 f^{lcd}f^{lab}(g_{\mu\lambda}g_{\sigma\nu}-g_{\mu\sigma}g_{\nu\lambda})\Bigg]\\ &\quad \times\int d^{d+1}u\ \delta^{d+1}(x_1-u)\delta^{d+1}(x_2-u)\delta^{d+1}(x_3-u)\delta^{d+1}(x_4-u),\end{aligned}\tag{321}$$

where $m=(\mu,a,x_1)$,$n=(\nu,b,x_2)$,$p=(\lambda,c,x_3)$ and $q=(\sigma,d,x_4)$. Furthermore we have used

$$\begin{aligned}\Gamma^{(0)}_{mn}(\overline{C}C) &= \frac{\delta^2 S_0}{\delta C^b(x_2)\delta\overline{C}^a(x_1)}\\ &= g\delta^{ab}\int d^{d+1}u\ \delta^{d+1}(x_1-u)\partial_u^2\delta^{d+1}(x_2-u),\end{aligned}\tag{322}$$

where $m=(a,x_1)$ and $n=(b,x_2)$;

$$\begin{aligned}\Gamma^{(0)}_{mnp}(\overline{C}Ca) &= \frac{\delta^3 S_0}{\delta C^b(x_2)\delta\overline{C}^a(x_1)\delta a^{\rho c}(x_3)}\\ &= gf^{acb}\int d^{d+1}u\ \delta^{d+1}(x_1-u)\left(\partial_{u\rho}\delta^{d+1}(x_2-u)\right)\delta^{d+1}(x_3-u),\end{aligned}\tag{323}$$

$$\begin{aligned}\Gamma^{(0)}_{mnp}(\overline{C}CA) &= \frac{\delta^3 S_0}{\delta C^b(x_2)\delta\overline{C}^a(x_1)\delta A^{\rho c}(x_3)}\\ &= gf^{acb}\int d^{d+1}u\ \left\{\delta^{d+1}(x_1-u)\partial_{u\rho}\left[\delta^{d+1}(x_2-u)\delta^{d+1}(x_3-u)\right]\right.\\ &\quad \left.+\delta^{d+1}(x_1-u)\delta^{d+1}(x_3-u)\left[\partial_{u\rho}\delta^{d+1}(x_2-u)\right]\right.,\end{aligned}\tag{324}$$

where $m=(a,x_1)$, $n=(b,x_2)$ and $p=c,\rho,x_3$;

$$\begin{aligned}\Gamma^{(0)}_{mnpq}(\overline{C}CAa) &= \frac{\delta^4 S_0}{\delta C^b(x_2)\delta\overline{C}^a(x_1)\delta A^{\rho c}(x_3)\delta a^{\eta d}(x_4)}\\ &= g^2 f^{ace}f^{edb}g_{\rho\eta}\int d^{d+1}u\ \delta^{d+1}(x_1-u)\delta^{d+1}(x_2-u)\\ &\quad \times\delta^{d+1}(x_3-u)\delta^{d+1}(x_4-u),\end{aligned}\tag{325}$$

where $m=(a,x_1)$, $n=(b,x_2)$, $p=(c,\rho,x_3)$ and $q=(d,\eta,x_4)$;

$$\begin{aligned}\Gamma^{(0)}(\overline{C}CA^2) &= \frac{\delta^4 S_0}{\delta C^b(x_2)\delta\overline{C}^a(x_1)\delta A^{\rho c}(x_3)\delta A^{\eta d}(x_4)} \\ &= g^2\left(f^{ace}f^{edb}+f^{ade}f^{ecb}\right)g_{\rho\eta} \\ &\quad\times\int d^{d+1}u\;\delta^{d+1}(x_1-u)\delta^{d+1}(x_2-u)\delta^{d+1}(x_3-u)\delta^{d+1}(x_4-u) \end{aligned} \tag{326}$$

where $m=(a,x_1)$, $n=(b,x_2)$, $p=(c,\rho,x_3)$ and $q=(d,\eta,x_4)$.

When we use the classical action (315) and the Legendre transform of generating functional W as

$$\begin{aligned}\Gamma_{2PI}[A,D,\Delta] &= W[A,J,\xi,\overline{\xi},K,\Xi]-\frac{\delta W}{\delta J}\cdot J-\frac{\delta W}{\delta\xi}\cdot\xi-\frac{\delta W}{\delta\overline{\xi}}\cdot\overline{\xi}-\frac{\delta W}{\delta K}\cdot K-\frac{\delta W}{\delta\Xi}\cdot\Xi \\ &= W-\langle a\rangle\cdot J-\langle\overline{C}\rangle\cdot\xi-\overline{\xi}\cdot\langle C\rangle \\ &\quad -\frac{1}{2}(D+\langle a\rangle\langle a\rangle)\cdot K-\frac{1}{2}(\Delta+\langle\overline{C}\rangle\langle C\rangle)\cdot\Xi \end{aligned} \tag{327}$$

where dot represents the trace over all internal degrees of freedom and integration in the coordinate, $D(x,y)$ and $\Delta(x,y)$ represents the 2 point connected Green's function of fluctuation of the gauge fields and FP ghost. The $\langle\cdot\rangle$ represents the expectation value expressed as

$$\langle\cdot\rangle=\frac{\int DaD\overline{C}DC\cdot\exp\left(iS_0\right)}{Z}. \tag{328}$$

Here $\langle a\rangle$ can be set to zero by setting background field A to be the classical field[68]. In addition we assume the expectation value of ghost field $\langle\overline{C}\rangle$ and $\langle C\rangle$ to be zero.

Then we obtain the following 2PI effective action for the gauge field

$$\begin{aligned}\Gamma_{2PI}[A,D,\Delta] &= S_0|_{\langle a\rangle=0,\langle\overline{C}\rangle=0,\langle C\rangle=0}[A]+\frac{i}{2}\mathrm{Tr}\ln D^{-1}+\frac{i}{2}D_0^{-1}[A]D \\ &\quad -i\mathrm{Tr}\ln\Delta^{-1}-i\mathrm{Tr}\Delta_0^{-1}[A]\Delta+\Gamma_2[A,D,\Delta] \end{aligned} \tag{329}$$

where

$$\begin{aligned}S_0|_{\langle a\rangle=0,\langle\overline{C}\rangle=0,\langle C\rangle=0} &= \frac{1}{2}\Gamma^{(0)}_{mn}(A^2)A_mA_n+\frac{1}{6}\Gamma^{(0)}_{mnp}(A^3)A_mA_nA_p+\frac{1}{24}\Gamma^{(0)}_{mnpq}(A^4)A_mA_nA_pA_q \\ &= -\frac{1}{4}F^a_{\mu\nu}(x)F^{a\mu\nu}(x), \end{aligned} \tag{330}$$

$$\begin{aligned}iD_0^{-1}{}_{mn}[A] &= \left.\frac{\delta^2 S_0}{\delta a_m\delta a_n}\right|_{a=0} \\ &= \Gamma^{(0)}_{mn}(a^2)+\Gamma^{(0)}_{pmn}(Aa^2)A_p+\frac{1}{2}\Gamma^{(0)}_{pqmn}(A^2a^2)A_pA_q \\ &= \Bigg[g_{\mu\nu}D^{ac}_\tau[A(x)]D^{\tau cb}[A(x)]-D^{ac}_\nu[A(x)]D^{cb}_\mu[A(x)] \\ &\quad +\frac{1}{\alpha}D^{ac}_\mu[A(x)]D^{cb}_\nu[A(x)]+gf^{acb}F^c_{\mu\nu}[A(x)]\Bigg]\delta^{d+1}(x-y), \end{aligned} \tag{331}$$

and

$$\begin{aligned}i\Delta_0^{-1\;ab}[A](x,y) &= \left.\frac{\delta^2 S_0}{\delta C_n\delta\overline{C}_m}\right|_{a=0,\overline{C}=0,C=0} \\ &= \Gamma^{(0)}_{mn}(\overline{C}C)+\Gamma^{(0)}_{mnp}(\overline{C}CA)A_p \\ &= \left[\delta^{ab}\partial_x^2+gf^{acb}\left(A^{\rho c}(y)\partial_{x\rho}-A^{\rho c}(x)\partial_{\rho y}\right)\right]\delta^{d+1}(x-y). \end{aligned} \tag{332}$$

When we estimate physical variables, we should investigate the gauge invariance of the above effective action, which we will remark in the next subsection. There we will see that the gauge dependence appears at higher order than the truncated order.

6.3 Controlled gauge dependence of NPI effective action

In this subsection we give general analysis of gauge dependence for the 1PI and 2PI effective action. For recent decades much interest has grown to the possibility of creating quark-gluon plasma in heavy-ion collision experiments at Brookhaven and CERN. Besides a lot of progress has been achieved in the research of the quantum dynamics in and far from equilibrium. In equilibrium the HTL effective theory is studied in a gauge invariant way to describe collective phenomena. This method can however not be extended to far from equilibrium case since an arbitrary resummation scheme will not guarantee the conservation law of the original theory. On the other hand, in far from equilibrium we have 2PI effective action method as a very attractive mathematical framework for the analyses of properties of high energy plasmas. A way to solve problems by formulating action functional respects the symmetries of the original theory. Then the preserved symmetries of the original theory guarantee the conservation law in the dynamics.

The 2PI effective action technique adopts the dressed versions of condensate and quantum fluctuations. These dressed quantities are obtained by use of nonperturbative resummation schemes, in which a set of self-consistent equations are solved. However arbitrarily dressed propagators do not satisfy the Ward identities, which implies that thermodynamical quantities computed within these approximations may suffer from dependence on the choice of gauge-condition. The gauge dependence of functional methods has been studied since in 1975. First Nielsen has shown the gauge parameter independence of effective potential[162]. Next Fukuda and Kugo have shown that the exact 1PI effective action and effective potential become gauge invariant at any stationary point[163]. The exact 2PI effective action is also gauge invariant at its stationary point.

In practical calculations we use the approximate, or truncated, version of effective action, which complicates the problem of gauge invariance. By use of the expression for the exact effective action we can analyze the gauge dependence of the truncated effective action. Then we can show that the gauge dependence always occurs at higher order and can be controlled.

In this subsection we review the gauge fixing dependence of the exact 1PI and 2PI effective action. Then we review the way to prove the gauge invariance of the action with Nielsen identity[165] instead of the one with BRST symmetry[164][15]. Next we investigate the gauge dependence of truncated effective action with the Nielsen identity.

6.3.1 Gauge invariance of the exact NPI effective action

Let us review the proof to show gauge invariance of the exact NPI effective action. First we show the proof of gauge invariance of 1PI effective action. The partition function of the pure Yang Mills theory is given by

$$Z_{1PI}[J] = \int \mathcal{D}\mathcal{A}\mathrm{Det}\left|\frac{\delta F^\alpha}{\delta \mathcal{A}_m} D_{m\beta}[\mathcal{A}]\right| \exp\left[i(S_{\mathrm{YM}} + S_{\mathrm{gf}})\right] \tag{333}$$

where m represents (μ, a, x) and $S_{\mathrm{gf}} = \frac{1}{2\alpha} F_\alpha F^\alpha$ ($F^\alpha = \partial^\mu \mathcal{A}^a_\mu$ for example) need not to be that of back ground gauge. We use the notation $\mathcal{A}$ for the gauge field and $\bar{A} \equiv \langle \mathcal{A} \rangle$ for its expectation value in this section with distinguishing the background and quantum fields in the previous section. 1PI effective action is defined by the Legendre transformation of the generating functional $W[J] = -i \ln Z$,

$$\Gamma_{1\mathrm{PI}}[\bar{A}] = W[J] - J_m \frac{\delta W}{\delta J_m} = W[J] - J_m \bar{A}_m, \tag{334}$$

[15] Discussion in the background field gauge is given in Ref. [166].

which satisfies

$$\frac{\delta\Gamma_{1\mathrm{PI}}[\bar{A}]}{\delta\bar{A}_m} = -J_m. \tag{335}$$

Next we estimate the gauge dependence of the effective action. Under an infinitesimal change of the gauge condition:

$$F_\alpha \to F_\alpha + \delta F_\alpha, \tag{336}$$

we will have the change of the generating functional,

$$\delta W = W[F^\alpha + \delta F^\alpha] - W[F^\alpha]. \tag{337}$$

The infinitesimal change of the gauge fixing condition in the action $S_{\mathrm{YM}} + S_{\mathrm{gf}}$ can be cancelled by the infinitesimal gauge transformation of $\mathcal{A}$:

$$\mathcal{A} \to \mathcal{A} + \delta\mathcal{A}. \tag{338}$$

We define $\delta\mathcal{A}$ through the equation

$$\delta(F[\mathcal{A}]) = F[\mathcal{A} + \delta\mathcal{A}] + \delta F[\mathcal{A} + \delta\mathcal{A}] - F[\mathcal{A}] = 0. \tag{339}$$

Then the leading order of δF can be represented by

$$\frac{\delta F^\alpha}{\delta\mathcal{A}_m}\delta\mathcal{A}_m = -\delta F^\alpha[\mathcal{A}] \tag{340}$$

where $\delta\mathcal{A}_m$ has the unique solution $\delta\mathcal{A}_m = -D_{m\alpha}(1/[(\delta F/\delta\mathcal{A})D[\mathcal{A}])_{\alpha\beta}\delta F^\beta[\mathcal{A}]$. Under the gauge transformation (336) and (338), the action $S_{\mathrm{YM}} + S_{\mathrm{gf}}$ and the measure $\mathcal{D}\mathcal{A}\mathrm{Det}\left|\frac{\delta F}{\delta\mathcal{A}}D\right|$ will be invariant. The only contribution to δW and $\delta\Gamma_{1\mathrm{PI}}$ comes from the source term. As a result we can obtain

$$\begin{aligned}
\delta W|_{J=\mathrm{const}} &= W[F^\alpha + \delta F^\alpha] - W[F^\alpha] = J_m\langle\delta\mathcal{A}_m\rangle, \\
\delta\Gamma_{1\mathrm{PI}}|_{J=\mathrm{const}} &= \delta W|_{J=\mathrm{const}} - J_m\delta\bar{A}_m, \\
\delta\bar{A}_m &= \langle\delta\mathcal{A}_m\rangle + iJ_n\langle\delta\mathcal{A}_n\mathcal{A}_m\rangle - iJ_n\langle\delta\mathcal{A}_n\rangle\bar{A}_m
\end{aligned} \tag{341}$$

where the second and third term come from the elements of the exponential in the numerator and denominator since $\bar{A} = \int\mathcal{D}\mathcal{A}\mathcal{A}e^{i(S+J\mathcal{A})}/\int\mathcal{D}\mathcal{A}e^{i(S+J\mathcal{A})}$. By combining the above equations we obtain the Nielsen identity for the 1PI effective action

$$\delta\Gamma_{1\mathrm{PI}} = -i\frac{\delta\Gamma_{1\mathrm{PI}}}{\delta\bar{A}_m}\frac{\delta\Gamma_{1\mathrm{PI}}}{\delta\bar{A}_n}\langle(\mathcal{A}_m - \bar{A}_m)\delta\mathcal{A}_n\rangle. \tag{342}$$

Hence at the stationary point where $J_m = -\frac{\delta\Gamma_{1\mathrm{PI}}}{\delta\bar{A}_m} = 0$ the 1PI effective action is gauge invariant.

The above analysis can be easily applied to 2PI effective action by use of the generalized version of Nielsen identity. First the partition function of the pure Yang-Mills theory can be prepared by

$$Z_{2\mathrm{PI}}[J,K] = \int\mathcal{D}\mathcal{A}\mathrm{Det}\left|\frac{\delta F^\alpha[\mathcal{A}]}{\delta\mathcal{A}_m}D_{m\beta}[\mathcal{A}]\right|\exp\left[i\left(S_{\mathrm{YM}} + S_{\mathrm{gf}} + J_m\mathcal{A}_m + \frac{1}{2}\mathcal{A}_mK_{mn}\mathcal{A}_n\right)\right]. \tag{343}$$

The next step is to calculate the change of the generating functional $W[J,K] = -\ln Z_{2\mathrm{PI}}[J,K]$ under the transformation (336) and (338). In the similar way to the 1PI effective action $S_{\mathrm{YM}} + S_{\mathrm{gf}}$ and $\mathcal{D}\mathcal{A}\mathrm{Det}\left|\frac{\delta F}{\delta\mathcal{A}}D[\mathcal{A}]\right|$ are invariant under the transformation. This implies that the change of $W[J,K]$ comes from the source terms. Under the transformation with the fixed J,K the change of $W[J,K]$ and $\Gamma_{2\mathrm{PI}}$ can be obtained as

$$\begin{aligned}
\delta W[J,K]|_{J,K=\mathrm{const}} &= W[F^\alpha + \delta F^\alpha] - W[F^\alpha] = J_m\langle\delta\mathcal{A}_m\rangle + \frac{K_{mn}}{2}\left[\langle\delta\mathcal{A}_m\mathcal{A}_n\rangle + \langle\mathcal{A}_m\delta\mathcal{A}_n\rangle\right] \\
\delta\Gamma_{2\mathrm{PI}}|_{J,K=\mathrm{const}} &= \delta W|_{J,K=\mathrm{const}} - J_m\delta\bar{A}_m - \frac{K_{mn}}{2}\delta\langle\mathcal{A}_m\mathcal{A}_n\rangle
\end{aligned} \tag{344}$$

where

$$\begin{aligned} \delta\bar{A}_m &= \langle\delta\bar{A}_m\rangle + i\langle\mathcal{A}_m\mathcal{R}\rangle - i\bar{A}_m\langle\mathcal{R}\rangle, \\ \delta\langle\mathcal{A}_m\mathcal{A}_n\rangle &= \langle\mathcal{A}_m\delta\mathcal{A}_n + \delta\mathcal{A}_m\mathcal{A}_n\rangle + i\langle\mathcal{A}_m\mathcal{A}_n\mathcal{R}\rangle - i\langle\mathcal{A}_m\mathcal{A}_n\rangle\langle\mathcal{R}\rangle \end{aligned} \tag{345}$$

where $\mathcal{R}$ that comes from the source terms in the exponential of the partition function is defined

$$\mathcal{R} = J_m\delta\mathcal{A}_m + \frac{K_{mn}}{2}(\mathcal{A}_m\delta\mathcal{A}_n + \delta\mathcal{A}_m\mathcal{A}_n). \tag{346}$$

As a result by combining the above equations we obtain

$$\begin{aligned} \delta\Gamma_{\rm 2PI} &= \left\langle \left[J_m\xi_m + \frac{K_{mn}}{2}\left(\mathcal{A}_m\mathcal{A}_n - \langle\mathcal{A}_m\mathcal{A}_n\rangle\right)\right]\mathcal{R}\right\rangle \\ &= i\left\langle \left(\frac{\delta\Gamma_{\rm 2PI}}{\delta\bar{A}_m}\xi_m + \frac{\delta\Gamma_{\rm 2PI}}{\delta D_{mn}}\tilde{D}_{mn}\right)\left(\frac{\delta\Gamma_{\rm 2PI}}{\delta\bar{A}_m}\delta\mathcal{A}_m + \frac{\delta\Gamma_{\rm 2PI}}{\delta D_{mn}}\left(\delta\mathcal{A}_m\xi_n + \xi_m\delta\mathcal{A}_n\right)\right)\right\rangle \end{aligned} \tag{347}$$

where $\xi_m \equiv \mathcal{A}_m - \bar{A}_m$ and $\tilde{D}_{mn} \equiv \xi_m\xi_n - D_{mn}$ and we have used

$$\frac{\delta\Gamma_{\rm 2PI}}{\delta\bar{A}_m} = -J_m - K_{mn}\bar{A}_n, \quad \frac{\delta\Gamma_{\rm 2PI}}{\delta D_{mn}} = -\frac{1}{2}K_{mn}. \tag{348}$$

We have obtained the generalized Nielsen identity. Under the gauge transformation $\Gamma_{\rm 2PI}$ is gauge invariant at the stationary point.[16]

6.3.2 Gauge dependence of the truncated effective action

In the previous subsection we have seen the exact 1PI and 2PI effective actions which contain all orders in the expansion parameter. The stationary relations are given and at that point the effective action is found to be gauge independent. In this subsection we discuss below the truncation of the exact 1PI and 2PI effective action and show that truncations have a controlled gauge-fixing dependence, i.e. the gauge-dependent terms appear at higher order.

First let us investigate the gauge dependence of the truncated 1PI effective action. We separate the truncated action Γ_L which contain up to L loops and the remainder $\Gamma_{\rm ex}$:

$$\Gamma_{\rm 1PI} = \Gamma_L + \Gamma_{\rm ex} \tag{349}$$

where $\Gamma_L \sim O(g^{2L-2})$ and $\Gamma_{\rm ex} = O(g^{2L})$. When we use the truncated action and its stationary solution in practice, $\bar{A}^0_L$ can be determined from the stationary relation of the Γ_L,

$$\left.\frac{\delta\Gamma_L[\bar{A}]}{\delta\bar{A}}\right|_{\bar{A}^0_L} = 0. \tag{350}$$

By use of (350) we obtain

$$\left.\frac{\delta\Gamma_{\rm 1PI}}{\delta\bar{A}}\right|_{\bar{A}^0_L} = \left.\frac{\delta\Gamma_{\rm ex}}{\delta\bar{A}}\right|_{\bar{A}^0_L} \sim \Gamma_{\rm ex} \sim g^{2L} \tag{351}$$

since $\Gamma_{\rm ex}$ and the derivative are of the same order in the expansion. Due to the Nielsen identities (342) $\delta\Gamma_{1PI} \sim \frac{\delta\Gamma_{\rm 1PI}}{\delta\bar{A}}\frac{\delta\Gamma_{\rm 1PI}}{\delta\bar{A}} \times \cdots$ and

$$\delta(\Gamma_L + \Gamma_{\rm ex}) \sim g^{4L}, \tag{352}$$

[16] This result is obvious since the exact 2PI effective action which contains all order of quantum loop diagrams corresponds to the exact 1PI effective action.

and

$$\delta\Gamma_L = \Gamma_{\rm ex} + O(g^{4L}) \sim \Gamma_{\rm ex} + O(g^{4L}) \sim g^{2L}. \tag{353}$$

Therefore we obtain

$$\delta\Gamma_L \sim g^2\Gamma_L, \tag{354}$$

which shows that the gauge dependence of the 1PI effective action at the stationary point occurs at higher order than the order of truncation.

Next let us consider the case of 2PI effective action. In the previous subsection we see that the exact 2PI effective action is the same as 1PI effective action and independent of the gauge fixing. We have problems when we try to work with the truncated action practically. Then the stationary relation we use is

$$\left.\frac{\delta\Gamma_L}{\delta\bar{A}}\right|_{\bar{A}_L^0, D_L^0} = 0; \quad \left.\frac{\delta\Gamma_L}{\delta D}\right|_{\bar{A}_L^0, D_L^0} = 0. \tag{355}$$

By use of the above relation we obtain

$$\begin{aligned} \left.\frac{\delta\Gamma_{\rm 2PI}}{\delta\bar{A}}\right|_{\bar{A}_L^0, D_L^0} &= \left.\frac{\delta\Gamma_{\rm ex}}{\delta\bar{A}}\right|_{\bar{A}_L^0, D_L^0} \sim \Gamma_{\rm ex} \sim g^{2L} \\ \left.\frac{\delta\Gamma_{\rm 2PI}}{\delta D}\right|_{\bar{A}_L^0, D_L^0} &= \left.\frac{\delta\Gamma_{\rm ex}}{\delta D}\right|_{\bar{A}_L^0, D_L^0} \sim \Gamma_{\rm ex} \sim g^{2L} \end{aligned} \tag{356}$$

since the differentiation will not change the order of $\Gamma_{\rm ex}$. In the end by use of the Nielsen identities (347) we obtain

$$\delta(\Gamma_L + \Gamma_{\rm ex}) \sim g^{4L}, \tag{357}$$

which gives

$$\delta\Gamma_L \sim \delta\Gamma_{\rm ex} + O(g^{4L}) \sim \Gamma_{\rm ex} + O(g^{4L}) \sim g^{2L}. \tag{358}$$

Thus we obtain the same result as in the 1PI case:

$$\delta\Gamma_L \sim g^2\Gamma_L, \tag{359}$$

which shows that the gauge dependence of the truncated 2PI effective action always occurs at higher order than the order of truncation. And gauge-fixing dependent artifacts would appear at higher orders of the truncation, thus making the approximation with the truncation controllable. This means that thermodynamic variables at equilibrium derived from the effective actions, such as total energy E, pressure P and entropy S which is derived by differentiating the action $\Gamma_{\rm 2PI}$ with temperature T, have gauge dependence which is always higher order of the truncation and that they are reliable in the truncated order.

6.4 Yang-Mills equation and Kadanoff-Baym equation for gluons and ghosts

In this subsection we derive the Yang-Mills equation for the classical fields and Kadanoff-Baym equations for quantum fluctuations for gluons and FP ghosts by differentiating $\Gamma_{\rm 2PI}[A, D, \Delta]$ with respect to A, D and Δ in the background gauge. The non-equilibrium quantum field dynamics is usually described in the CTP formalism, and in this case the variables A, D and Δ are on this CTP.

First we derive the Yang-Mills equation which represents the dynamics of the classical fields which has sources expressed with Green's functions for gluons and ghosts by use of $\frac{\delta\Gamma_{\rm 2PI}}{\delta A}=0$. We obtain the relations

$$D^{\mu da}[A(z)]F^a_{\mu\rho}[A(z)]-j^d_\rho(z)=0 \tag{360}$$

where

$$-j^d_\rho(z)=\frac{\delta}{\delta A^{\rho d}(z)}\left(-i{\rm Tr}\Delta_0^{-1}[A]\Delta+\frac{i}{2}{\rm Tr}D_0^{-1}[A]D+\frac{1}{2}\Gamma_2[A,D,\Delta]\right), \tag{361}$$

$$\frac{\delta}{\delta A^{\rho d}(z)}\left(-i{\rm Tr}\Delta_0^{-1}[A]\Delta\right)=gf^{adb}\left(\partial_{\rho x}\Delta^{ba}(z,x)\Big|_{x=z}-\partial_{\rho x}\Delta^{ba}(x,z)\Big|_{x=z}\right), \tag{362}$$

$$\begin{aligned}
\frac{\delta}{\delta A^{\rho d}(z)}\left(\frac{i}{2}{\rm Tr}D_0^{-1}[A]D\right) &= \frac{1}{2}gf^{adb}\left(\partial_{\rho y}D^{\mu ba}_\mu(y,z)\Big|_{y=z}-\partial_{\rho x}D^{\mu ba}_\mu\Big|_{x=z}\right)\\
&+\frac{1}{2}g^2A^e_\rho\left(f^{adc}f^{ceb}D^{\mu ba}_\mu(z,z)+f^{aec}f^{cdb}D^{\mu ba}_\mu(z,z)\right)\\
&-\frac{1}{2}gf^{adb}\left(\partial^\mu_y D^{ba}_{\rho\mu}(y,z)\Big|_{y=z}-\partial^\nu_x D^{ba}_{\nu\rho}(z,x)\Big|_{x=z}\right)\\
&-\frac{1}{2}g^2f^{adc}f^{ceb}A^{\mu e}D^{ba}_{\rho\mu}(z,z)-\frac{1}{2}g^2f^{aec}f^{cdb}A^{\nu e}D^{ba}_{\nu\rho}(z,z)\\
&+\frac{1}{2\alpha}\Big\{gf^{adc}\left[\left(\partial^\mu_y\delta^{cb}+gf^{ceb}A^{\mu e}(y)\right)D^{ba}_{\mu\rho}(y,z)\right]_{y=z}\\
&+gf^{bdc}\left[\left(\partial^\nu_x\delta^{ca}+gf^{cea}A^{\nu e}(x)\right)D^{ba}_{\rho\nu}(z,x)\right]_{x=z}\Big\}\\
&+\frac{1}{2}gf^{adb}\left(-\partial^\mu_z D^{ba}_{\rho\mu}(z,z)+\partial^\nu_z D^{ba}_{\nu\rho}(z,z)\right)\\
&-\frac{1}{2}g^2f^{acb}\left(f^{ced}A^{\nu e}(z)D^{ba}_{\nu\rho}(z,z)-f^{ced}A^{\mu e}(z)D^{ba}_{\rho\mu}(z,z)\right).
\end{aligned} \tag{363}$$

Next the Kadanoff-Baym equation for the gluons are given by $\frac{\delta\Gamma_{\rm 2PI}}{\delta D}=0$ in the following way:

$$\begin{aligned}
&-\frac{i}{2}D^{-1}+\frac{1}{2}D_0^{-1}+\frac{1}{2}\frac{\delta\Gamma_2}{\delta D}=0\\
&\to iD^{-1}_{0mp}D_{pq}+i\Pi_{mp}D_{pq}=i\delta_{mq}
\end{aligned} \tag{364}$$

where $\Pi=i\frac{\delta\Gamma_2}{\delta D}$ and

$$\begin{aligned}
iD^{-1}_{0mp}=iD^{-1ab}_{0\mu\nu}(x,y)=\Big(&g_{\mu\nu}D^{ac}_\tau[A(x)]D^{\tau cb}[A(x)]-D^{ac}_\nu[A(x)]D^{cb}_\mu[A(x)]\\
&+\frac{1}{\alpha}D^{ac}_\mu[A(x)]D^{cb}_\nu[A(x)]+gf^{acb}F^c_{\mu\nu}[A(x)]\Big)\delta^{d+1}(x-y).
\end{aligned} \tag{365}$$

Here $\{m,p\}$ represents $m=(\mu,a)$ and $p=(\nu,b)$. Due to the gauge fixing condition

$$D^{cb}_\nu[A(x)]D^{\nu\rho\ bd}(x,y)=D^{\mu\nu\ ab}(x,y)D^{\dagger\ bc}_\nu[A(y)]=0, \tag{366}$$

the term proportional to $\frac{1}{\alpha}$ disappears in (364). The KB equation (364) should be solved under the condition (366).

Then when we define the statistical and spectral function in the following way:

$$\begin{aligned}
F_{pq}(x,y) &\equiv \frac{1}{2}\left(D^{21}_{pq}(x,y)+D^{12}_{pq}(x,y)\right),\\
\rho_{pq}(x,y) &\equiv i\left(D^{21}_{pq}(x,y)-D^{12}_{pq}(x,y)\right),
\end{aligned} \tag{367}$$

and we can obtain the different representations for KB equation as

$$\begin{aligned} iD_{0mp}^{-1}F_{pq}(x,y) &= -\int_{t_0}^{x^0} dz\Pi_{\rho\ mp}(x,z)F_{pq}(z,y) + \int_{t_0}^{y^0} \Pi_{F\ mp}(x,z)\rho_{pq}(z,y) \\ iD_{0mp}^{-1}\rho_{pq}(x,y) &= \int_{x^0}^{y^0} \Pi_{\rho\ mp}(x,z)\rho_{pq}(z,y) \end{aligned} \tag{368}$$

where we have defined

$$\begin{aligned} \Pi_{F\ mp}(x,y) &= \frac{1}{2}\left(\Pi_{mp}^{21}(x,y) + \Pi_{mp}^{12}(x,y)\right) \\ \Pi_{\rho\ mp}(x,y) &= i\left(\Pi_{mp}^{21}(x,y) - \Pi_{mp}^{12}(x,y)\right). \end{aligned} \tag{369}$$

In the similar way by differentiating $\Gamma_{\rm 2PI}$ by Δ we obtain

$$i\Delta^{-1} - i\Delta_0^{-1} + i\Sigma = 0 \tag{370}$$

where $\Sigma = -\frac{i}{2}\frac{\delta\Gamma_2}{\delta\Delta}$ and

$$\Delta_0^{-1ab}(x,y) = \left[\delta^{ab}\partial_x^2 + gf^{acb}\left(A^{\rho c}(y)\partial_{x\rho} - A^{\rho c}(x)\partial_{y\rho}\right)\right]\delta^{d+1}(x-y). \tag{371}$$

When we define

$$\begin{aligned} \Delta_F^{ab}(x,y) &\equiv \frac{1}{2}\left(\Delta^{21\ ab}(x,y) + \Delta^{12\ ab}(x,y)\right), \\ \Delta_\rho^{ab}(x,y) &\equiv i\left(\Delta^{21\ ab}(x,y) - \Delta^{12\ ab}(x,y)\right), \end{aligned} \tag{372}$$

we can derive the Kadanoff-Baym equation for the fluctuations of FP ghost as

$$\begin{aligned} \Delta_0^{-1ac}\Delta_F^{cb}(x,y) &= -\int_{t_0}^{x^0} \Sigma_\rho^{ac}(x,z)\Delta_F^{cb}(z,y) + \int_{t_0}^{y^0} dz\Sigma_F^{ac}(x,z)\Delta_\rho^{cb}(z,y) \\ \Delta_0^{-1ac}\Delta_\rho^{cb}(x,y) &= \int_{x^0}^{y^0} dz\Sigma_\rho^{ac}(x,z)\Delta_\rho^{cb}(z,y). \end{aligned} \tag{373}$$

$$\begin{aligned} \Sigma_F^{ab}(x,y) &\equiv \frac{1}{2}\left(\Sigma^{21\ ab}(x,y) + \Sigma^{12\ ab}(x,y)\right) \\ \Sigma_\rho^{ab}(x,y) &\equiv i\left(\Sigma^{21\ ab}(x,y) - \Sigma^{12\ ab}(x,y)\right). \end{aligned} \tag{374}$$

When we trace the dynamics of the gauge fields, we solve the Yang-Mills equations (360) with (361), (362) and (363) and Kadanoff-Baym equations for gluons (368) with (365) and (369) and ghosts (373) with (371) and (374).

6.5 KB equation for gluons in TAG

In this subsection we derive the Kadanoff-Baym equation for gluons in temporal axial gauge (TAG) $A^0 = 0$. This subsection focuses on the practical use of the KB equation. Let us neglect the classical field $\langle A\rangle = 0$ and concentrate on the quantum fluctuations only. We start with the Lagrangian density

$$\mathcal{L} = \frac{1}{2}(\mathbf{E}^a)^2 - \frac{1}{2}(\mathbf{B}^a)^2 \tag{375}$$

where $E_i^a = \partial_0 a_i^a$ and $B_i^a = \epsilon_{ijk}(\partial_j a_k^a - \partial_k a_j^a + gf^{abc}a_j^b a_k^c)$. Then the 2PI effective action with vanishing classical field is written as

$$\Gamma[D] = \frac{i}{2}{\rm Tr}\ln(D)^{-1} + \frac{i}{2}D_0^{-1}D + \frac{1}{2}\Gamma_2[D]. \tag{376}$$

Here $iD_0^{-1} = -(\delta_{ij}\partial_x^2 - \partial_{x,i}\partial_{x,j})\delta^{ab}\delta_{\mathcal{C}}(x-y)$ is the free Green's function and D is the full Green's function, both of which are defined on the closed time path $\mathcal{C}$. The remaining functional $\frac{1}{2}\Gamma_2[D]$ in (376) is a sum of the all possible 2PI graphs written with respect to D which remains connected upon cutting two Green's function lines. The stationary relation for the effective action (376)

$$\frac{\delta\Gamma}{\delta D} = 0 \tag{377}$$

gives the Schwinger-Dyson equation for the Green's function $D(x,y)$

$$D^{-1}(x,y) = D_0^{-1}(x,y) - \Pi(x,y) \tag{378}$$

with the proper self-energy defined as $\Pi = 2i\delta\Gamma_2[D]/\delta D$. The self-energy is expressed as

$$\Pi = \Pi_{\rm loc} + \Pi_{\rm nonl} \tag{379}$$

where the local part $\Pi_{\rm loc}$ contributes to the mass shift while the non-local part $\Pi_{\rm nonl}$ induces the mode-coupling between the different wavenumbers.

We shall decompose the two-point function $D_{ij}^{ab}(x,y)$ into two real functions, the statistical $F_{ij}^{ab}(x,y)$ and the spectral function $\rho_{ij}^{ab}(x,y)$ defined, respectively, as

$$F_{ij}^{ab}(x,y) = \frac{1}{2}\langle\{a_i^a(x), a_j^b(y)\}\rangle = \frac{1}{2}\left[D_{ij}^{21,ab}(x,y) + D_{ij}^{12,ab}(x,y)\right] \tag{380}$$

and

$$\rho_{ij}^{ab}(x,y) = i\langle[a_i^a(x), a_j^b(y)]\rangle = i\left[D_{ij}^{21,ab}(x,y) - D_{ij}^{12,ab}(x,y)\right], \tag{381}$$

where $\langle\cdots\rangle$ represents the expectation value taken over a certain density matrix. The indices 1 and 2 specify the branch of the contour $\mathcal{C}$ in the Schwinger-Keldysh formalism. The Schwinger-Dyson equation (378) can be equivalently rewritten in terms of $F_{ij}^{ab}(x,y)$ and $\rho_{ij}^{ab}(x,y)$ as coupled integro-differential equations

$$\begin{aligned}\left[(\delta_{ij}\partial_x^2 - \partial_{x,i}\partial_{x,j})\delta^{ab} + \Pi_{\rm loc,ij}^{ab}(x)\right] F_{jk}^{bc}(x,y) &= \int_{t_0}^{y^0} dz \Pi_{F,ij}^{ab}(x,z)\rho_{jk}^{bc}(z,y) \\ &\quad - \int_{t_0}^{x^0} dz \Pi_{\rho,ij}^{ab}(x,z)F_{jk}^{bc}(z,y),\end{aligned} \tag{382}$$

$$\left[(\delta_{ij}\partial_x^2 - \partial_{x,i}\partial_{x,j})\delta^{ab} + \Pi_{\rm loc,ij}^{ab}(x)\right] \rho_{jk}^{bc}(x,y) = -\int_{y^0}^{x^0} dz \Pi_{\rho,ij}^{ab}(x,z)\rho_{jk}^{bc}(z,y) \tag{383}$$

where t_0 is the initial time. The non-local self-energy has been reexpressed similarly as

$$\begin{aligned}\Pi_{F,ij}^{ab}(x,y) &= \frac{1}{2}\left[\Pi_{{\rm nonl},ij}^{21,ab} + \Pi_{{\rm nonl},ij}^{12,ab}\right], \\ \Pi_{\rho,ij}^{ab}(x,y) &= i\left[\Pi_{{\rm nonl},ij}^{21,ab} - \Pi_{{\rm nonl},ij}^{12,ab}\right].\end{aligned} \tag{384}$$

The set of equations (382) and (383) is the Kadanoff-Baym equation of the gauge theory, which describes the time evolution of the fluctuations with F and ρ. At each time step the spectral function $\rho_{ij}^{ab}(x,y)$ must satisfy the conditions following from the commutation relations:

$$\begin{aligned}\rho_{ij}^{ab}(x,y)|_{x^0\to y^0} &= 0, \\ \partial_{x^0}\rho_{ij}(x,y)|_{x^0\to y^0} &= \delta^d(\mathbf{x}-\mathbf{y}), \\ \partial_{x^0}\partial_{y^0}\rho(x,y)|_{x^0\to y^0} &= 0.\end{aligned} \tag{385}$$

In this paper we restrict ourselves to the spatially homogeneous situation. From the translational invariance, the statistical function $F^{ab}_{ij}(x,y) = F^{ab}_{ij}(x^0.y^0, \mathbf{x}-\mathbf{y})$ and the spectral function $\rho^{ab}_{ij}(x,y) = \rho^{ab}_{ij}(x^0,y^0,\mathbf{x}-\mathbf{y})$ can be Fourier transformed to $F^{ab}_{ij}(x^0,y^0;\mathbf{k})$ and $\rho^{ab}_{ij}(x^0,y^0;\mathbf{k})$. Furthermore we restrict ourselves to the color isotropic case $F^{ab}, \rho^{ab} \sim \delta^{ab}$ and then $\Pi^{ab}_F, \Pi^{ab}_\rho \sim \delta^{ab}$ and divide the transverse and longitudinal part of D and Π as

$$
\begin{aligned}
D^{ab}_{ij}(x^0,y^0;\mathbf{k}) &= \delta^{ab}\left[\left(\delta_{ij}-\frac{k_ik_j}{\mathbf{k}^2}\right)D_T(x^0,y^0;\mathbf{k}) + \frac{k_ik_j}{\mathbf{k}^2}D_L(x^0,y^0;\mathbf{k})\right], && (386)\\
\Pi^{ab}_{ij}(x^0,y^0;\mathbf{k}) &= \delta^{ab}\left[\left(\delta_{ij}-\frac{k_ik_j}{\mathbf{k}^2}\right)\Pi_T(x^0,y^0;\mathbf{k}) + \frac{k_ik_j}{\mathbf{k}^2}\Pi_L(x^0,y^0;\mathbf{k})\right], && (387)
\end{aligned}
$$

or

$$
\begin{aligned}
F^{ab}_{ij}(x^0,y^0;\mathbf{k}) &= \delta^{ab}\left[\left(\delta_{ij}-\frac{k_ik_j}{\mathbf{k}^2}\right)F_T(x^0,y^0;\mathbf{k}) + \frac{k_ik_j}{\mathbf{k}^2}F_L(x^0,y^0;\mathbf{k})\right]\\
\rho^{ab}_{ij}(x^0,y^0;\mathbf{k}) &= \delta^{ab}\left[\left(\delta_{ij}-\frac{k_ik_j}{\mathbf{k}^2}\right)\rho_T(x^0,y^0;\mathbf{k}) + \frac{k_ik_j}{\mathbf{k}^2}\rho_L(x^0,y^0;\mathbf{k})\right] && (388)\\
\Pi^{ab}_{F,ij}(x^0,y^0;\mathbf{k}) &= \delta^{ab}\left[\left(\delta_{ij}-\frac{k_ik_j}{\mathbf{k}^2}\right)\Pi_{F,T}(x^0,y^0;\mathbf{k}) + \frac{k_ik_j}{\mathbf{k}^2}\Pi_{F,L}(x^0,y^0;\mathbf{k})\right]\\
\Pi^{ab}_{\rho,ij}(x^0,y^0;\mathbf{k}) &= \delta^{ab}\left[\left(\delta_{ij}-\frac{k_ik_j}{\mathbf{k}^2}\right)\Pi_{\rho,T}(x^0,y^0;\mathbf{k}) + \frac{k_ik_j}{\mathbf{k}^2}\Pi_{\rho,L}(x^0,y^0;\mathbf{k})\right] && (389)
\end{aligned}
$$

Then the KB equations of the transverse part are simplified in the momentum space as

$$
\begin{aligned}
\left(\partial^2_{x,0}+\mathbf{k}^2+\Pi_{\mathrm{loc},T}(x^0)\right)F_T(x^0,y^0,\mathbf{k}) = &\int_{t_0}^{y^0} dz^0\Pi_{F,T}(x^0,z^0;\mathbf{k})\rho_T(z^0,y^0;\mathbf{k})\\
&-\int_{t_0}^{x^0} dz^0\Pi_{\rho,T}(x^0,z^0;\mathbf{k})F_T(z^0,y^0;\mathbf{k}) \qquad (390a)
\end{aligned}
$$

$$
\left(\partial^2_{x,0}+\Pi_{\mathrm{loc},T}(x^0)\right)\rho_T(x^0,y^0;\mathbf{k}) = -\int_{y^0}^{x^0}\Pi_{\rho,T}(x^0,z^0;\mathbf{k})\rho_T(z^0,y^0;\mathbf{k}), \qquad (390b)
$$

and the KB equations of the longitudinal part are

$$
\begin{aligned}
\left(\partial^2_{x,0}+\mathbf{k}^2+\Pi_{\mathrm{loc},L}(x^0)\right)F_L(x^0,y^0,\mathbf{k}) = &\int_{t_0}^{y^0} dz^0\Pi_{F,L}(x^0,z^0;\mathbf{k})\rho_L(z^0,y^0;\mathbf{k})\\
&-\int_{t_0}^{x^0} dz^0\Pi_{\rho,L}(x^0,z^0;\mathbf{k})F_L(z^0,y^0;\mathbf{k}) \qquad (391a)
\end{aligned}
$$

$$
\left(\partial^2_{x,0}+\Pi_{\mathrm{loc},L}(x^0)\right)\rho_L(x^0,y^0;\mathbf{k}) = -\int_{y^0}^{x^0}\Pi_{\rho,L}(x^0,z^0;\mathbf{k})\rho_L(z^0,y^0;\mathbf{k}). \qquad (391b)
$$

We approximate $\frac{1}{2}\Gamma_2[D]$ with the skeleton diagrams obtained at the leading order in g^2 which is depicted in Fig.81. Then we obtain

$$
\begin{aligned}
\Sigma^{mn}_{\mathrm{LO,loc}} &= -\frac{1}{2}\Gamma^{(0)}_{mnpq}(a^4)D_{pq}, && (392)\\
\Sigma^{mn}_{\mathrm{LO,nonl}} &= -\frac{1}{2}\Gamma^{(0)}_{mpq}(a^3)\Gamma^{(0)}_{nrs}(a^3)D_{pr}D_{qs} && (393)
\end{aligned}
$$

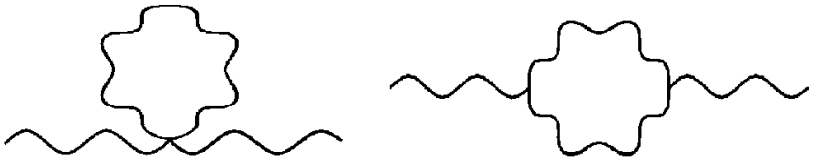

Figure 81: Leading order self energy for gluons [68].

where m, n, p, q, r and s represents the coordinate, color and polarization indices. The local part $\Sigma_{\rm LO,loc}$ can be Fourier transformed and divided into transverse and longitudinal parts and written explicitly in terms of D_T and D_L as

$$\Pi^{ab}_{{\rm LO,loc},ij}(x^0) = \delta^{ab}\left[\left(\delta_{ij} - \frac{k_i k_j}{\mathbf{k}^2}\right)\left(\Pi_{{\rm loc},ll} - \Pi_{{\rm loc},L}\right) + \frac{k_i k_j}{\mathbf{k}^2}\Pi_{{\rm loc},L}\right], \tag{394}$$

where

$$\Pi_{{\rm loc},ii}(x^0) = g^2 N \int \frac{d^d p}{(2\pi)^d}\left[(d-1)^2 D_T(x^0,x^0;\mathbf{p}) + (d-1) D_L(x^0,x^0;\mathbf{p})\right], \tag{395}$$

$$\Pi_{{\rm loc},L}(x^0) = g^2 N \left[\left(d-2+\frac{(\mathbf{p}\cdot\mathbf{k})^2}{\mathbf{p}^2\mathbf{k}^2}\right) D_T(x^0,x^0;\mathbf{p}) + \left(1-\frac{(\mathbf{p}\cdot\mathbf{k})^2}{\mathbf{p}^2\mathbf{k}^2}\right) D_L(x^0,x^0;\mathbf{p})\right] \tag{396}$$

Similarly the nonlocal part $\Sigma_{\rm LO,nonl}$ can be Fourier transformed and divided into transverse and longitudinal parts and written explicitly in terms of D_T and D_L as

$$\Pi^{ab}_{{\rm LO,nonl},ij}(x^0,y^0;\mathbf{k}) = \delta^{ab}\left[\left(\delta_{ij} - \frac{k_i k_j}{\mathbf{k}^2}\right)\Pi_{{\rm nonl},T} + \frac{k_i k_j}{\mathbf{k}^2}\Pi_{{\rm nonl},L}\right](x^0,y^0;\mathbf{k}), \tag{397}$$

where we define $\Pi_{{\rm nonl},T} \equiv (\Pi_{{\rm nonl},ii} - \Pi_{{\rm nonl},L})/(d-1)$ and $\Pi_{{\rm nonl},ii}$ and $\Pi_{{\rm nonl},L}$ have the following components

$$\begin{aligned}\Pi_{{\rm nonl},ii}(x^0,y^0;-\mathbf{k}) = \frac{1}{2}g^2 N \int \frac{d^d p}{(2\pi)^d}\Big[& f_1(\mathbf{k}+\mathbf{p},\mathbf{p}) D_T(x^0,y^0;\mathbf{p}) D_T(x^0,y^0;-\mathbf{p}-\mathbf{k}) \\ & + f_2(\mathbf{k}+\mathbf{p},\mathbf{p}) D_L(x^0,y^0;\mathbf{p}) D_T(x^0,y^0;-\mathbf{p}-\mathbf{k}) \\ & + f_3(\mathbf{k}+\mathbf{p},\mathbf{p}) D_T(x^0,y^0;\mathbf{p}) D_L(x^0,y^0;-\mathbf{p}-\mathbf{k}) \\ & + f_4(\mathbf{k}+\mathbf{p},\mathbf{p}) D_L(x^0,y^0;\mathbf{p}) D_L(x^0,y^0;-\mathbf{p}-\mathbf{k})\Big],\end{aligned} \tag{398}$$

and

$$\begin{aligned}\Pi_{{\rm nonl},L}(x^0,y^0;-\mathbf{k}) = \frac{1}{2}g^2 N \int \frac{d^d p}{(2\pi)^d}\Big[& g_1(\mathbf{k}+\mathbf{p},\mathbf{p}) D_T(x^0,y^0;\mathbf{p}) D_T(x^0,y^0;-\mathbf{p}-\mathbf{k}) \\ & + g_2(\mathbf{k}+\mathbf{p},\mathbf{p}) D_L(x^0,y^0;\mathbf{p}) D_T(x^0,y^0;-\mathbf{p}-\mathbf{k}) \\ & + g_3(\mathbf{k}+\mathbf{p},\mathbf{p}) D_T(x^0,y^0;\mathbf{p}) D_L(x^0,y^0;-\mathbf{p}-\mathbf{k}) \\ & + g_4(\mathbf{k}+\mathbf{p},\mathbf{p}) D_L(x^0,y^0;\mathbf{p}) D_L(x^0,y^0;-\mathbf{p}-\mathbf{k})\Big],\end{aligned} \tag{399}$$

Here f_i $(i = 1,2,3,4)$ can be expressed as

$$\begin{aligned} f_1(\mathbf{p}+\mathbf{k},\mathbf{p}) = & -(2\mathbf{p}+\mathbf{k})^2\left(d-2+\frac{\left[\mathbf{p}\cdot(\mathbf{k}+\mathbf{p})\right]^2}{(\mathbf{k}+\mathbf{p})^2\mathbf{p}^2}\right) \\ & - 4(d-1)\left[\left(\mathbf{p}^2 - \frac{\left[\mathbf{p}\cdot(\mathbf{k}+\mathbf{p})\right]^2}{(\mathbf{k}+\mathbf{p})^2}\right) + \left((\mathbf{k}+\mathbf{p})^2 - \frac{\left[\mathbf{p}\cdot(\mathbf{k}+\mathbf{p})\right]^2}{\mathbf{p}^2}\right)\right], \end{aligned} \tag{400a}$$

$$f_2(\mathbf{p}+\mathbf{k},\mathbf{p}) = -(2\mathbf{p}+\mathbf{k})^2\left(1-\frac{[\mathbf{p}\cdot(\mathbf{k}+\mathbf{p})]^2}{(\mathbf{k}+\mathbf{p})^2\mathbf{p}^2}\right)+2\left(\mathbf{p}^2-\frac{[\mathbf{p}\cdot(\mathbf{k}+\mathbf{p})]^2}{(\mathbf{k}+\mathbf{p})^2}\right) -(d-1)\frac{[\mathbf{p}\cdot(\mathbf{2k}+\mathbf{p})]^2}{\mathbf{p}^2} \quad (400b)$$

$$f_3(\mathbf{p}+\mathbf{k},\mathbf{p}) = -(2\mathbf{p}+\mathbf{k})^2\left(1-\frac{[\mathbf{p}\cdot(\mathbf{k}+\mathbf{p})]^2}{(\mathbf{k}+\mathbf{p})^2\mathbf{p}^2}\right)+2\left((\mathbf{k}+\mathbf{p})^2-\frac{[\mathbf{p}\cdot(\mathbf{k}+\mathbf{p})]^2}{\mathbf{p}^2}\right) -(d-1)\frac{[(\mathbf{p}+\mathbf{k})\cdot(\mathbf{p}-\mathbf{k})]^2}{(\mathbf{k}+\mathbf{p})^2} \quad (400c)$$

$$f_4(\mathbf{p}+\mathbf{k},\mathbf{p}) = -\mathbf{k}^2\left[1-\frac{[\mathbf{p}\cdot(\mathbf{k}+\mathbf{p})]^2}{\mathbf{p}^2(\mathbf{k}+\mathbf{p})^2}\right] \quad (400d)$$

where the above functions satisfy the following relations

$$\begin{aligned} f_1(\mathbf{k}+\mathbf{p},\mathbf{p}) &= f_1(-\mathbf{p},-\mathbf{k}-\mathbf{p}) \\ f_2(\mathbf{k}+\mathbf{p},\mathbf{p}) &= f_3(-\mathbf{p},-\mathbf{k}-\mathbf{p}) \\ f_3(\mathbf{k}+\mathbf{p},\mathbf{p}) &= f_2(-\mathbf{p},-\mathbf{k}-\mathbf{p}) \\ f_4(\mathbf{k}+\mathbf{p},\mathbf{p}) &= f_4(-\mathbf{p},-\mathbf{k}-\mathbf{p}). \end{aligned} \quad (401)$$

This relation (401) is required in the change of variables $\mathbf{p} \leftrightarrow \mathbf{p}+\mathbf{k}$ in the integration of (398). Next g_i $(i=1,2,3,4)$ are

$$\mathbf{k}^2 g_1(\mathbf{p}+\mathbf{k},\mathbf{p}) = -[\mathbf{k}\cdot\mathbf{2p}+\mathbf{k}]^2\left(d-2+\frac{[\mathbf{p}\cdot(\mathbf{k}+\mathbf{p})]^2}{(\mathbf{k}+\mathbf{p})^2\mathbf{p}^2}\right) \quad (402a)$$

$$\begin{aligned} \mathbf{k}^2 g_2(\mathbf{p}+\mathbf{k},\mathbf{p}) &= -(\mathbf{k}+\mathbf{p})^2\left[(\mathbf{k}+\mathbf{p})^2-\frac{[\mathbf{p}\cdot(\mathbf{k}+\mathbf{p})]^2}{\mathbf{p}^2}\right] \\ &= -(\mathbf{k}+\mathbf{p})^2\left[\mathbf{k}^2-\frac{[\mathbf{k}\cdot\mathbf{p}]^2}{\mathbf{p}^2}\right] \end{aligned} \quad (402b)$$

$$\begin{aligned} \mathbf{k}^2 g_3(\mathbf{p}+\mathbf{k},\mathbf{p}) &= -\mathbf{p}^2\left[\mathbf{p}^2-\frac{[\mathbf{p}\cdot(\mathbf{k}+\mathbf{p})]^2}{(\mathbf{k}+\mathbf{p})^2}\right] \\ &= -\mathbf{p}^2\left[\mathbf{k}^2-\frac{[\mathbf{k}\cdot(\mathbf{k}+\mathbf{p})]^2}{(\mathbf{k}+\mathbf{p})^2}\right] \end{aligned} \quad (402c)$$

$$\mathbf{k}^2 g_4(\mathbf{p}+\mathbf{k},\mathbf{p}) = 0, \quad (402d)$$

where these functions satisfy the following relations

$$\begin{aligned} g_1(\mathbf{k}+\mathbf{p},\mathbf{p}) &= g_1(-\mathbf{p},-\mathbf{k}-\mathbf{p}) \\ g_2(\mathbf{k}+\mathbf{p},\mathbf{p}) &= g_3(-\mathbf{p},-\mathbf{k}-\mathbf{p}) \\ g_3(\mathbf{k}+\mathbf{p},\mathbf{p}) &= g_2(-\mathbf{p},-\mathbf{k}-\mathbf{p}) \\ g_4(\mathbf{k}+\mathbf{p},\mathbf{p}) &= g_4(-\mathbf{p},-\mathbf{k}-\mathbf{p}). \end{aligned} \quad (403)$$

In the limit of $k_0 \to 0$, and then $\mathbf{k} \to 0$, we can reproduce the mass shift

$$\begin{aligned} \Pi_{\mathrm{LO},ii}(x^0,y^0) &= g^2 N\int\frac{d^dp}{(2\pi)^d}(d-1)\Big[(d-1)\delta(x^0-y^0)D_T(x^0,x^0;\mathbf{p}) \\ &\quad +\delta(x^0-y^0)D_L(x^0,x^0;\mathbf{p})-2\mathbf{p}^2D_T(x^0,y^0;\mathbf{p})D_T(x^0,y^0;\mathbf{p}) \\ &\quad -\mathbf{p}^2D_T(x^0,y^0;\mathbf{p})D_L(x^0,y^0;\mathbf{p})\Big], \end{aligned} \quad (404)$$

which is derived in Ref. [167].

In the end we consider the NLO self-energy of the coupling which is depicted in Fig. 82. We can represent the self-energy in the equation as

$$\Pi^{mn}_{\rm NLO} = -\frac{1}{2}\Gamma^{(0)}_{mpqr}\Gamma^{(0)}_{nstu}D_{ps}D_{qt}D_{ru}. \tag{405}$$

If we assume $D_T = D_L$, we obtain the Fourier transformation in relative space $\mathbf{x}-\mathbf{y}$ as

$$\begin{aligned}\Pi^{ab}_{{\rm NLO},ij}(x^0,y^0;\mathbf{k}) &= -\frac{3}{2}g^4N^2(N-1)\delta^{ab}\delta_{ij}\int\frac{d^dp}{(2\pi)^d}\frac{d^dq}{(2\pi)^d} \\ &\quad\times D(x^0,y^0;\mathbf{p})D(x^0,y^0;\mathbf{q})D(x^0,y^0;\mathbf{k}-\mathbf{p}-\mathbf{q}).\end{aligned} \tag{406}$$

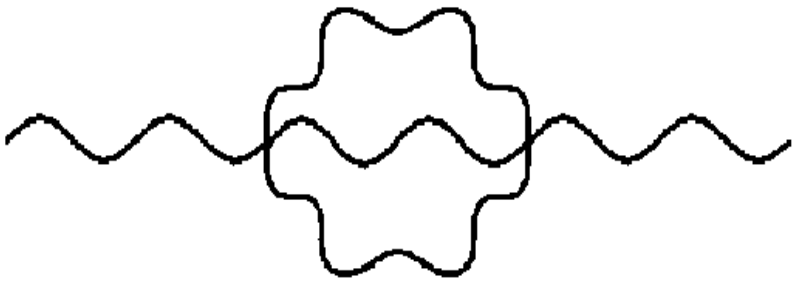

Figure 82: Next to leading order self energy for gluons [68].

The above form is the same as the NLO of ϕ^4 theory, so that the proof of H-theorem is trivial in the case of NLO.

6.6 Trial to prove the H-theorem for the non-Abelian gauge theory in $\bar{A}=0$

In this subsection we derive the expression for the kinetic entropy in terms of the two-point Green's functions $D(x,y)$ for the non-Abelian gauge theory. We shall investigate the case with vanishing classical fields $\bar{A}=0$ and isotropic Green's functions $D^{ab}(x,y)=\delta^{ab}D(x,y)$ in the temporal axial gauge $A^a_0=0$. Then we find that the kinetic entropy satisfies the H-theorem unless the Ward identity is satisfied and the gauge dependence of that is controlled in thermal equilibrium within the range of leading order coupling expansion $O(g^2)$ of the Φ-derivable approximation.

We begin with the Schwinger-Dyson equation (378). In the similar way as Sec. 3.2 we obtain the following relations with respect to the Fourier transformations $D(X,k)=\int d(x-y)\,e^{ip\cdot(x-y)}D(x,y)$ where $X=\frac{x+y}{2}$ is the "center-of-mass" coordinate.

$$\partial_\mu s^\mu(X) = \frac{1}{2}\int\frac{d^{d+1}k}{(2\pi)^{d+1}}(d-1)C_T\log\frac{D^{12}_T}{D^{21}_T} + \frac{1}{2}\int\frac{d^{d+1}k}{(2\pi)^{d+1}}C_L\log\frac{D^{12}_L}{D^{21}_L} \tag{407}$$

In deriving of the above relation we have used gradient expansion and taken the 1st order of the approximation. (We may have the singularity in 1st order gradient expansion for the longitudinal mode. This problem which is serious in the proof of the H-theorem is discussed in the subsection.) Here the term C represents the collision terms,

$$\begin{aligned}C_T(X,k) &= i\left(\Pi_{T,\rho}(X,k)F_T(X,k) - \Pi_{T,F}(X,k)\rho_T(X,k)\right) \\ C_L(X,k) &= i\left(\Pi_{L,\rho}(X,k)F_L(X,k) - \Pi_{L,F}(X,k)\rho_L(X,k)\right)\end{aligned} \tag{408}$$

and the form of kinetic entropy current in the gauge theory with temporal axial gauge is given by

$$
\begin{aligned}
s^\mu \equiv & \int \frac{d^{d+1}k}{(2\pi)^{d+1}}(d-1)\left[\left(k^\mu - \frac{1}{2}\frac{\partial \mathrm{Re}\ \Pi_{T,\mathrm{Re}}}{\partial k_\mu}\right)\frac{\rho_T}{i} + \frac{1}{2}\frac{\partial \mathrm{Re}\ D_{T,\mathrm{Re}}}{\partial k_\mu}\frac{\Pi_{\rho,T}}{i}\right]\sigma[f_T](X,k) \\
& + \int \frac{d^{d+1}k}{(2\pi)^{d+1}}\left[\left(k^0\delta^{\mu 0} - \frac{1}{2}\frac{\partial \mathrm{Re}\ \Pi_{L,\mathrm{Re}}}{\partial k_\mu}\right)\frac{\rho_L}{i} + \frac{1}{2}\frac{\partial \mathrm{Re}\ D_{L,\mathrm{Re}}}{\partial k_\mu}\frac{\Pi_{\rho,L}}{i}\right]\sigma[f_L](X,k) \qquad (409)
\end{aligned}
$$

where

$$
\sigma[f_{T,L}] \equiv (1+f_{T,L})\log(1+f_{T,L}) - f_{T,L}\log f_{T,L}. \qquad (410)
$$

The difference from the scalar theory is that the kinetic entropy is the sum of the transverse and the longitudinal part.

The remaining work is to prove that the R.H.S. of (407) is positive definite. Next it is convenient to rewrite $(d-1)\Pi_T(X,k) = \Pi^{ii}(X,k) - \Pi_L(X,k)$ in the collision term of (407). The transverse part can be derived by subtracting $\Pi_L(x^0,y^0,\mathbf{k})$ (399) from $\Pi^{ii}(x^0,y^0,\mathbf{k})$ (398) and Fourier transforming with respect to the relative coordinate x^0-y^0. Then $\Pi_T(X,k)$ is given by

$$
\begin{aligned}
(d-1)\Pi_T(X,-k) = & \frac{1}{2}g^2\int\frac{d^{d+1}k}{(2\pi)^{d+1}}\Big[\left(f_1(\mathbf{k}+\mathbf{p},\mathbf{p}) - g_1(\mathbf{k}+\mathbf{p},\mathbf{p})\right)D_T(X,p)D_T(X,-p-k) \\
& + \left(f_2(\mathbf{k}+\mathbf{p},\mathbf{p}) - g_2(\mathbf{k}+\mathbf{p},\mathbf{p})\right)D_L(X,p)D_T(X,-p-k) \\
& + \left(f_3(\mathbf{k}+\mathbf{p},\mathbf{p}) - g_3(\mathbf{k}+\mathbf{p},\mathbf{p})\right)D_T(X,p)D_L(X,-p-k) \\
& + \left(f_4(\mathbf{k}+\mathbf{p},\mathbf{p}) - g_4(\mathbf{k}+\mathbf{p},\mathbf{p})\right)D_L(X,p)D_L(X,-p-k)\Big]. \qquad (411)
\end{aligned}
$$

Here $f_1 - g_1$ can be simplified from (400a) and (402a) to

$$
\begin{aligned}
-\left[f_1(\mathbf{k}+\mathbf{p},\mathbf{p}) - g_1(\mathbf{k}+\mathbf{p},\mathbf{p})\right] = & 4(d-1)\left[\left(\mathbf{p}^2 - \frac{(\mathbf{k}\cdot\mathbf{p})^2}{\mathbf{k}^2}\right) + \left(\mathbf{k}^2 - \frac{(\mathbf{k}\cdot(\mathbf{k}+\mathbf{p}))^2}{(\mathbf{k}+\mathbf{p})^2}\right)\right. \\
& \left. + \left((\mathbf{k}+\mathbf{p})^2 - \frac{(\mathbf{p}\cdot(\mathbf{k}+\mathbf{p}))^2}{\mathbf{p}^2}\right)\right] \\
& -\frac{4}{3}\left[\mathbf{p}^2\left(1 - \frac{(\mathbf{k}\cdot\mathbf{p})^2}{\mathbf{k}^2\mathbf{p}^2}\right)\left(1 - \frac{((\mathbf{p}+\mathbf{k})\cdot\mathbf{p})^2}{(\mathbf{p}+\mathbf{k})^2\mathbf{p}^2}\right)\right. \\
& +\mathbf{k}^2\left(1 - \frac{(\mathbf{k}\cdot(\mathbf{k}+\mathbf{p}))^2}{\mathbf{k}^2(\mathbf{k}+\mathbf{p})^2}\right)\left(1 - \frac{(\mathbf{k}\cdot\mathbf{p})^2}{\mathbf{k}^2\mathbf{p}^2}\right) \\
& \left. +(\mathbf{k}+\mathbf{p})^2\left(1 - \frac{((\mathbf{p}+\mathbf{k})\cdot\mathbf{p})^2}{(\mathbf{p}+\mathbf{k})^2\mathbf{p}^2}\right)\left(1 - \frac{((\mathbf{p}+\mathbf{k})\cdot\mathbf{k})^2}{(\mathbf{p}+\mathbf{k})^2\mathbf{k}^2}\right)\right] \\
\geq & \ 0 \quad (\text{for } d \geq 2) \qquad (412)
\end{aligned}
$$

We can notice that $f_1 - g_1$ is symmetric for any exchange of the variables $r = -k-p$, k and p. In deriving the above relation we have used the identities

$$
\begin{aligned}
\mathbf{p}^2 - \frac{(\mathbf{k}\cdot\mathbf{p})^2}{\mathbf{k}^2} &= (\mathbf{k}+\mathbf{p})^2 - \frac{(\mathbf{k}\cdot(\mathbf{k}+\mathbf{p}))^2}{\mathbf{k}^2} \\
\mathbf{p}^2 - \frac{(\mathbf{p}\cdot(\mathbf{k}+\mathbf{p}))^2}{(\mathbf{k}+\mathbf{p})^2} &= \mathbf{k}^2 - \frac{(\mathbf{k}\cdot(\mathbf{k}+\mathbf{p}))^2}{(\mathbf{k}+\mathbf{p})^2} \\
(\mathbf{k}+\mathbf{p})^2 - \frac{(\mathbf{p}\cdot(\mathbf{k}+\mathbf{p}))^2}{\mathbf{p}^2} &= \mathbf{k}^2 - \frac{(\mathbf{k}\cdot\mathbf{p})^2}{\mathbf{p}^2} \qquad (413)
\end{aligned}
$$

without the change of the integration variables.

Similarly $f_2 - g_2$ and $f_3 - g_3$ can be expanded from (400b), (402b), (400c) and (402c) by using (413) in the following:

$$-(f_2 - g_2) = \frac{[\mathbf{p}\cdot(\mathbf{k}-(-\mathbf{p}-\mathbf{k}))]^2}{\mathbf{p}^2}\left[d-2+\frac{[\mathbf{k}\cdot(\mathbf{k}+\mathbf{p})]^{\mathbf{2}}}{\mathbf{k^2}(\mathbf{k}+\mathbf{p})^{\mathbf{2}}}\right] \geq 0 \text{ (for } d \geq 2), \tag{414}$$

and

$$-(f_3 - g_3) = \frac{[(-\mathbf{p}-\mathbf{k})\cdot(\mathbf{p}-\mathbf{k})]^2}{(\mathbf{p}+\mathbf{k})^2}\left[d-2+\frac{(\mathbf{k}\cdot\mathbf{p})^{\mathbf{2}}}{\mathbf{k^2}\mathbf{p^2}}\right] \geq 0 \text{ (for } d \geq 2). \tag{415}$$

We can notice that g_1 (402a), $f_2 - g_2$ and $f_3 - g_3$ has symmetries with respect to $r = -p - k$, p and k. For $p \leftrightarrow k$ we have $f_2 - g_2 \leftrightarrow g_1$, for $r \leftrightarrow k$ $f_3 - g_3 \leftrightarrow g_1$, for $r \leftrightarrow k$ $f_2 - g_2 \leftrightarrow f_2 - g_2$ and for $p \leftrightarrow k$ $f_3 - g_3 \leftrightarrow f_3 - g_3$. This symmetry is very useful to prove the positive definite of R.H.S. of (407).

In the similar way the longitudinal part $\Pi_L(X,k)$ can be expressed by changing $D(x^0,y^0,\mathbf{p})D(x^0,y^0;-\mathbf{p}-\mathbf{k})$ to $\int \frac{dp^0}{(2\pi)} D(X,p)D(X,-p-k)$ in (399). Furthermore we have similar symmetries with respect to f_4 (400d), g_2 (402b) and g_3 (402c) which are also useful to prove the H-theorem. (For $r \leftrightarrow k$ we have $f_4 \leftrightarrow g_2$, for $p \leftrightarrow k$ $f_4 \leftrightarrow g_3$, for $k \leftrightarrow p$ $g_2 \leftrightarrow g_2$ and for $k \leftrightarrow r$ $g_3 \leftrightarrow g_3$.)

In the end we can expand the R.H.S. of (407) by reexpressing with respect to $D^{12}_{T,L}$ and $D^{21}_{T,L}$:

$$\begin{aligned}
\partial_\mu s^\mu &= -\frac{g^2}{4}\int \frac{d^{d+1}k}{(2\pi)^{d+1}}\frac{d^{d+1}p}{(2\pi)^{d+1}}\frac{d^{d+1}r}{(2\pi)^{d+1}}(2\pi)^{d+1}\delta^{d+1}(p+k+r) \\
&\times \Big[(f_1(-\mathbf{r},\mathbf{p}) - g_1(-\mathbf{r},\mathbf{p}))\left(D^{12}_T(X,p)D^{12}_T(X,r)D^{12}_T(X,k) - D^{21}_T(X,p)D^{21}_T(X,r)D^{21}_T(X,k)\right) \\
&\quad +(f_2(-\mathbf{r},\mathbf{p}) - g_2(-\mathbf{r},\mathbf{p}))\left(D^{12}_L(X,p)D^{12}_T(X,r)D^{12}_T(X,k) - D^{21}_L(X,p)D^{21}_T(X,r)D^{21}_T(X,k)\right) \\
&\quad +(f_3(-\mathbf{r},\mathbf{p}) - g_3(-\mathbf{r},\mathbf{p}))\left(D^{12}_T(X,p)D^{12}_L(X,r)D^{12}_T(X,k) - D^{21}_T(X,p)D^{21}_L(X,r)D^{21}_T(X,k)\right) \\
&\quad +f_4(-\mathbf{r},\mathbf{p})\left(D^{12}_L(X,p)D^{12}_L(X,r)D^{12}_T(X,k) - D^{21}_L(X,p)D^{21}_L(X,r)D^{21}_T(X,k)\right)\Big] \\
&\times \ln\frac{D^{12}_T(X,k)}{D^{21}_T(X,k)} \\
&\quad -\frac{g^2}{4}\int \frac{d^{d+1}k}{(2\pi)^{d+1}}\frac{d^{d+1}p}{(2\pi)^{d+1}}\frac{d^{d+1}r}{(2\pi)^{d+1}}(2\pi)^{d+1}\delta^{d+1}(p+k+r) \\
&\times \Big[g_1(-\mathbf{r},\mathbf{p})\left(D^{12}_T(X,p)D^{12}_T(X,r)D^{12}_L(X,k) - D^{21}_T(X,p)D^{21}_T(X,r)D^{21}_L(X,k)\right) \\
&\quad +g_2(-\mathbf{r},\mathbf{p})\left(D^{12}_L(X,p)D^{12}_T(X,r)D^{12}_L(X,k) - D^{21}_L(X,p)D^{21}_T(X,r)D^{21}_L(X,k)\right) \\
&\quad +g_3(-\mathbf{r},\mathbf{p})\left(D^{12}_T(X,p)D^{12}_L(X,r)D^{12}_L(X,k) - D^{21}_T(X,p)D^{21}_L(X,r)D^{21}_L(X,k)\right) \\
&\quad \Big]\ln\frac{D^{12}_L(X,k)}{D^{21}_L(X,k)}
\end{aligned} \tag{416}$$

where we have used $D^{21}_{T,L}(X,-k) = D^{12}_{T,L}(X,k)$. In R.H.S. of (416) we have three type of three gluon interaction processes, that is three transverse (TTT), two transverse and one longitudinal (TTL) and one transverse and two longitudinal processes (TLL) in two brackets $[\cdots]$. We have no three longitudinal processes which do not exist for any dimensions since $g_4 = 0$.

For three transverse (TTT) processes we can change in the following from the R.H.S. of (416) by use of the symmetry of $f_1 - g_1$ (412), the change of variables $k \to p$ and $k \to r$ and averaging:

$$\begin{aligned}
\text{(TTT term)} &= -\frac{g^2}{12}\int \frac{d^{d+1}k}{(2\pi)^{d+1}}\frac{d^{d+1}p}{(2\pi)^{d+1}}\frac{d^{d+1}r}{(2\pi)^{d+1}}(2\pi)^{d+1}\delta^{d+1}(p+k+r) \\
&\times (f_1(-\mathbf{r},\mathbf{p}) - g_1(-\mathbf{r},\mathbf{p}))\big(D^{12}_T(X,p)D^{12}_T(X,r)D^{12}_T(X,k) \\
&\quad -D^{21}_T(X,p)D^{21}_T(X,r)D^{21}_T(X,k)\big)\ln\frac{D^{12}_T(X,k)D^{12}_T(X,p)D^{12}_T(X,r)}{D^{21}_T(X,k)D^{21}_T(X,p)D^{21}_T(X,r)} \geq 0
\end{aligned} \tag{417}$$

because of $-(f_1-g_1)\geq 0$ in (412). (Here note that entropy production is zero for three gluons with collinear momenta due to the form of f_1-g_1.)

For (TTL) processes we can expand in the following by use of the symmetry in f_2-g_2, f_3-g_3 and g_1, the change of variables $k\to p$ and $k\to r$ and averaging:

$$
\begin{aligned}
\text{(TTL term)} &= -\frac{g^2}{4}\int\frac{d^{d+1}k}{(2\pi)^{d+1}}\frac{d^{d+1}p}{(2\pi)^{d+1}}\frac{d^{d+1}r}{(2\pi)^{d+1}}(2\pi)^{d+1}\delta^{d+1}(p+k+r)\\
&\times \Big[\frac{1}{2}(f_2(-\mathbf{r},\mathbf{p})-g_2(-\mathbf{r},\mathbf{p}))\big(D_L^{12}(X,p)D_T^{12}(X,r)D_T^{12}(X,k)\\
&\quad -D_L^{21}(X,p)D_T^{21}(X,r)D_T^{21}(X,k)\big)\ln\frac{D_T^{12}(X,k)D_T^{12}(X,r)}{D_T^{21}(X,k)D_T^{21}(X,r)}\\
&\quad +\frac{1}{2}(f_3(-\mathbf{r},\mathbf{p})-g_3(-\mathbf{r},\mathbf{p}))\big(D_T^{12}(X,p)D_L^{12}(X,r)D_T^{12}(X,k)\\
&\quad -D_T^{21}(X,p)D_L^{21}(X,r)D_T^{21}(X,k)\big)\ln\frac{D_T^{12}(X,k)D_T^{12}(X,p)}{D_T^{21}(X,k)D_T^{21}(X,p)}\\
&\quad +g_1(-\mathbf{r},\mathbf{p})\big(D_T^{12}(X,p)D_T^{12}(X,r)D_L^{12}(X,k)\\
&\quad -D_T^{21}(X,p)D_T^{21}(X,r)D_L^{21}(X,k)\big)\ln\frac{D_L^{12}(X,k)}{D_L^{21}(X,k)}\Big]\\
&= -\frac{g^2}{4}\int\frac{d^{d+1}k}{(2\pi)^{d+1}}\frac{d^{d+1}p}{(2\pi)^{d+1}}\frac{d^{d+1}r}{(2\pi)^{d+1}}(2\pi)^{d+1}\delta^{d+1}(p+k+r)\\
&\times \Big[\frac{1}{2}(f_2(-\mathbf{r},\mathbf{p})-g_2(-\mathbf{r},\mathbf{p}))\big(D_L^{12}(X,p)D_T^{12}(X,r)D_T^{12}(X,k)\\
&\quad -D_L^{21}(X,p)D_T^{21}(X,r)D_T^{21}(X,k)\big)\ln\frac{D_T^{12}(X,k)D_T^{12}(X,r)D_L^{12}(X,p)}{D_T^{21}(X,k)D_T^{21}(X,r)D_L^{21}(X,p)}\\
&\quad +\frac{1}{2}(f_3(-\mathbf{r},\mathbf{p})-g_3(-\mathbf{r},\mathbf{p}))\big(D_T^{12}(X,p)D_L^{12}(X,r)D_T^{12}(X,k)\\
&\quad -D_T^{21}(X,p)D_L^{21}(X,r)D_T^{21}(X,k)\big)\ln\frac{D_T^{12}(X,k)D_T^{12}(X,p)D_L^{12}(X,r)}{D_T^{21}(X,k)D_T^{21}(X,p)D_L^{21}(X,r)}\\
&\geq 0
\end{aligned}
\tag{418}
$$

because of $-(f_2-g_2)\geq 0$ (414) in (414) and $-(f_3-g_3)\geq 0$ in (415). In the second equality we have used the symmetry relation for the change of variables, $f_2-g_2\leftrightarrow g_1$ for $p\leftrightarrow k$ and $f_3-g_3\leftrightarrow g_1$ for $r\leftrightarrow k$,

$$
\begin{aligned}
& g_1(-\mathbf{r},\mathbf{p})\big(D_T^{12}(X,p)D_T^{12}(X,r)D_L^{12}(X,k)-D_T^{21}(X,p)D_T^{21}(X,r)D_L^{21}(X,k)\big)\ln\frac{D_L^{12}(X,k)}{D_L^{21}(X,k)}\\
\to\ & (f_2(-\mathbf{r},\mathbf{p})-g_2(-\mathbf{r},\mathbf{p}))\\
& \times\big(D_L^{12}(X,p)D_T^{12}(X,r)D_T^{12}(X,k)-D_L^{21}(X,p)D_T^{21}(X,r)D_T^{21}(X,k)\big)\ln\frac{D_L^{12}(X,p)}{D_L^{21}(X,p)}\\
\to\ & (f_3(-\mathbf{r},\mathbf{p})-g_3(-\mathbf{r},\mathbf{p}))\\
& \times\big(D_T^{12}(X,p)D_L^{12}(X,r)D_T^{12}(X,k)-D_T^{21}(X,p)D_L^{21}(X,r)D_T^{21}(X,k)\big)\ln\frac{D_L^{12}(X,r)}{D_L^{21}(X,r)}\\
\to\ & \text{(Average over the above two terms).}
\end{aligned}
\tag{419}
$$

For (TLL) processes we can expand in the following by use of the symmetry in f_4, g_2 and g_3,

the change of variables $k \to p$ and $k \to r$ and averaging:

$$
\begin{aligned}
\text{(TLL term)} &= -\frac{g^2}{4}\int \frac{d^{d+1}k}{(2\pi)^{d+1}}\frac{d^{d+1}p}{(2\pi)^{d+1}}\frac{d^{d+1}r}{(2\pi)^{d+1}}(2\pi)^{d+1}\delta^{d+1}(p+k+r) \\
&\times \Big[\frac{1}{2}g_2(-\mathbf{r},\mathbf{p})\big(D_L^{12}(X,p)D_T^{12}(X,r)D_L^{12}(X,k) \\
&\quad -D_L^{21}(X,p)D_T^{21}(X,r)D_L^{21}(X,k)\big)\ln\frac{D_L^{12}(X,k)D_L^{12}(X,p)}{D_L^{21}(X,k)D_L^{21}(X,p)} \\
&\quad +\frac{1}{2}g_3(-\mathbf{r},\mathbf{p})\big(D_T^{12}(X,p)D_L^{12}(X,r)D_L^{12}(X,k) \\
&\quad -D_T^{21}(X,p)D_L^{21}(X,r)D_L^{21}(X,k)\big)\ln\frac{D_L^{12}(X,k)D_L^{12}(X,r)}{D_L^{21}(X,k)D_L^{21}(X,r)} \\
&\quad +f_4(-\mathbf{r},\mathbf{p})\big(D_L^{12}(X,p)D_L^{12}(X,r)D_T^{12}(X,k) \\
&\quad -D_L^{21}(X,p)D_L^{21}(X,r)D_T^{21}(X,k)\big)\ln\frac{D_T^{12}(X,k)}{D_T^{21}(X,k)}\Big] \\
&= -\frac{g^2}{4}\int \frac{d^{d+1}k}{(2\pi)^{d+1}}\frac{d^{d+1}p}{(2\pi)^{d+1}}\frac{d^{d+1}r}{(2\pi)^{d+1}}(2\pi)^{d+1}\delta^{d+1}(p+k+r) \\
&\times \Big[\frac{1}{2}g_2(-\mathbf{r},\mathbf{p})\big(D_L^{12}(X,p)D_T^{12}(X,r)D_L^{12}(X,k) \\
&\quad -D_L^{21}(X,p)D_T^{21}(X,r)D_L^{21}(X,k)\big)\ln\frac{D_L^{12}(X,k)D_T^{12}(X,r)D_L^{12}(X,p)}{D_L^{21}(X,k)D_T^{21}(X,r)D_L^{21}(X,p)} \\
&\quad +\frac{1}{2}g_3(-\mathbf{r},\mathbf{p})\big(D_T^{12}(X,p)D_L^{12}(X,r)D_L^{12}(X,k) \\
&\quad -D_T^{21}(X,p)D_L^{21}(X,r)D_L^{21}(X,k)\big)\ln\frac{D_L^{12}(X,k)D_L^{12}(X,r)D_T^{12}(X,p)}{D_L^{21}(X,k)D_L^{21}(X,r)D_T^{21}(X,p)} \\
&\geq 0
\end{aligned}
\tag{420}
$$

because of $g_2 \geq 0$ in (402b) and $g_3 \geq 0$ in (402c). In the second equality we have used the following transformation in the change of integration variables,

$$
\begin{aligned}
& f_4(-\mathbf{r},\mathbf{p})\big(D_L^{12}(X,p)D_L^{12}(X,r)D_T^{12}(X,k) - D_L^{21}(X,p)D_L^{21}(X,r)D_T^{21}(X,k)\big)\ln\frac{D_T^{12}(X,k)}{D_T^{21}(X,k)} \\
\to\ & g_2(-\mathbf{r},\mathbf{p})\big(D_L^{12}(X,p)D_T^{12}(X,r)D_L^{12}(X,k) - D_L^{21}(X,p)D_T^{21}(X,r)D_L^{21}(X,k)\big)\ln\frac{D_T^{12}(X,r)}{D_T^{21}(X,r)} \\
\to\ & g_3(-\mathbf{r},\mathbf{p})\big(D_T^{12}(X,p)D_L^{12}(X,r)D_L^{12}(X,k) - D_T^{21}(X,p)D_L^{21}(X,r)D_L^{21}(X,k)\big)\ln\frac{D_T^{12}(X,p)}{D_T^{21}(X,p)} \\
\to\ & \text{(Average over the above two terms)}
\end{aligned}
\tag{421}
$$

because of the symmetry $f_4 \leftrightarrow g_2$ for $k \leftrightarrow r$ and $f_4 \leftrightarrow g_3$ for $k \leftrightarrow p$. (Here we can find that entropy production is zero for three gluons with collinear momenta.)

As a result the divergence of the entropy current for the non-Abelian gauge theory in the temporal axial gauge appears to be positive definite:

$$
\partial_\mu s^\mu = (\text{TTT} : (417)) + (\text{TTL} : (418)) + (\text{TLL} : (420)) \geq 0. \tag{422}
$$

Therefore in TAG $0 \leftrightarrow 3$ and $1 \leftrightarrow 2$ processes of gluons may appear to help the thermalization in the LO gradient expanded KB equation. (To complete the proof we need to solve the problem described in the next subsection.)

In the end let us discuss the gauge dependence of the kinetic entropy (409). In far from equilibrium we have not proven the gauge invariance of s^0 (409), but at thermal equilibrium we

can prove that the gauge dependence of (409) with constant factor which is time and temperature independent is controlled in LO of the coupling expansion. We can explain this in the following.

At thermal equilibrium we have another definition of the entropy density $\mathcal{S} = -\frac{\partial \Omega/V}{\partial T}$, where Ω is the thermodynamic potential, that is explained in Appendix E. By extending the discussion in the appendix to the gauge theory, we find that $\mathcal{S}$ per color of gluons is given by

$$\begin{aligned}
\mathcal{S} &= s^0_{\rm eq} + \mathcal{S}' - \mathcal{S}^{(0)}_L \\
&= \int \frac{d^{d+1}k}{(2\pi)^{d+1}}(d-1)\left[\left(k^0 - \frac{1}{2}\frac{\partial {\rm Re}\ \Pi_{T,R}}{\partial k_0}\right)\rho_T + \frac{1}{2}\frac{\partial {\rm Re}\ D_{T,R}}{\partial k_0}\Pi_{\rho,T}\right]\sigma[f](k) \\
&\quad + \int \frac{d^{d+1}k}{(2\pi)^{d+1}}\left[\left(k^0 - \frac{1}{2}\frac{\partial {\rm Re}\ \Pi_{L,R}}{\partial k_0}\right)\rho_L + \frac{1}{2}\frac{\partial {\rm Re}\ D_{L,R}}{\partial k_0}\Pi_{\rho,L}\right]\sigma[f](k) + \mathcal{S}' - \mathcal{S}^{(0)}_L \\
&= \int \frac{d^{d+1}k}{(2\pi)^{d+1}}(d-1)\left[-{\rm Im}\log D^{-1}_{T,R} + {\rm Im}\Pi_{T,R}{\rm Re}D_{T,R}\right]\frac{\partial f^{\rm eq}}{\partial T} \\
&\quad + \int \frac{d^{d+1}k}{(2\pi)^{d+1}}\left[-{\rm Im}\log\left(\frac{\mathbf{k}^2}{(k^0+i\epsilon)^2}D^{-1}_{L,R}\right) + {\rm Im}\Pi_{L,R}{\rm Re}D_{L,R}\right]\frac{\partial f^{\rm eq}}{\partial T} + \mathcal{S}' \qquad (423)
\end{aligned}$$

where we have used $f^{\rm eq} = 1/(e^{k^0/T}-1)$, $\frac{\partial f^{\rm eq}(k^0)}{\partial T} = -\frac{\partial \sigma(k^0)}{\partial k^0}$, $D_R = D_{0,R} - \Pi_R$, $2i{\rm Im}D_R = \rho$, $2i{\rm Im}\Pi_R = \Pi_\rho$ and $\mathcal{S}' = 0$ for leading order (two-loop order) $O(g^2)$[170, 171]. The coupling dependence is in ρ, G_R, Π_R, Π_ρ and f. Here $\mathcal{S}^{(0)}_L$ comes from the functional integral of longitudinal mode in the calculation of Ω and is given by

$$\mathcal{S}^{(0)}_L = \int \frac{d^{d+1}k}{(2\pi)^{d+1}} 2\pi k^0 \epsilon(k^0)\delta\left((k^0)^2\right)\sigma[f(k^0/T)]. \qquad (424)$$

This constant (temperature independent) factor cancels longitudinal contribution in the entropy density at $g = 0$ and $\mathcal{S} = \pi^2 T^4/45$ is given in $d = 3$.

When we restrict ourselves to $O(g^2)$ case, we notice that $s^0 - \mathcal{S}^{(0)}_L$ is equivalent to $\mathcal{S}$

$$s^0 - \mathcal{S}^{(0)}_L = \mathcal{S} = -\frac{\delta\Omega}{\delta T} \qquad (425)$$

at thermal equilibrium. (In the proof of H-theorem we can not derive the time independent contribution, such as $\mathcal{S}^{(0)}_L$, to the entropy density s^0. In order to compare $s^0(X)$ with $\mathcal{S}$, we have to subtract some time independent function which cancels longitudinal contribution at $g = 0$. If we estimate $s^0(X)$ numerically in the future analysis, we might have to subtract this temperature independent factor $\mathcal{S}^{(0)}_L$ from $s^0(X)$ in order to compare with $\mathcal{S}$.) Therefore the gauge dependence of $s^0 - \mathcal{S}^{(0)}_L$ at thermal equilibrium can be determined by the gauge dependence of Ω. The thermodynamic potential Ω in the appendix E is equivalent to 2PI effective action $\Gamma_{\rm 2PI}$. In Sec. 6.3, the gauge dependence of $\Gamma_{\rm 2PI}$ is proven to be the higher order of the coupling at the stationary point $\delta\Gamma/\delta A = 0$, $\delta\Gamma/\delta D = 0$,

$$\delta\Gamma_{L=2} \sim g^2\Gamma_{L=2}. \qquad (426)$$

Hence we can conclude that $s^0 - \mathcal{S}^{(0)}_L$ at thermal equilibrium has the gauge dependence which is higher order $O(g^4)$ and that gauge invariance is guaranteed in the leading order $O(g^2)$. [17]

6.6.1 Singularity of longitudinal Green's function and the H-theorem

Here we shall discuss the influence of singularity in longitudinal Green's function D_L to the proof of H-theorem.

[17] This discussion of gauge dependence can not be extended to all order of the coupling since $\mathcal{S}'$ will not necessarily vanish. When we consider the gauge invariance of entropy at thermal equilibrium for any order, we should confirm $\mathcal{S}' = 0$ order by order in addition to proving H-theorem in the order.

First let us consider what the singularity of the Green's function is. From the 0th order of the gradient expansion in (378) the retarded Green's function can be written as

$$D_{L,R}(X,\omega\mathbf{k}) = -\frac{1}{\omega^2 - \mathrm{Re}\Pi_{L,R} - \frac{1}{2}\Pi_{L,\rho}}. \tag{427}$$

$$\rho_L(X,\omega,k) = 2i\mathrm{Im}D_{L,R} = -\frac{\Pi_{L,\rho}}{\left(\omega^2 - \mathrm{Re}\Pi_{L,R}\right)^2 - \frac{1}{4}\Pi_{L,\rho}^2} \tag{428}$$

where $\Pi_{L,\rho}$ is pure imaginary function.

For the transverse Green's function, the self-energy is written as $\Pi_{T,R} = m_D^2 + \cdots$ at thermal equilibrium and $\Pi_{T,R} = g^2 \times$ (total number) $+ \cdots$ for far from equilibrium in the estimation of tadpole diagram. This mass-shift (k-independent) factor plays a role of infrared cutoff, and then the difference from ϕ^4 and $O(N)$ model will not appear.

Next let us consider the longitudinal Green's function with the following type of self-energy

$$\Pi_L(X,\omega,\mathbf{k}) = \frac{\omega^2}{\mathbf{k}^2}\Sigma(X,\omega,\mathbf{k}) \tag{429}$$

where $\Sigma(X,\omega,\mathbf{k})$ has no singularity $\lim_{\omega\to 0}\Sigma =$ finite and $\lim_{\omega\to 0}\partial\Sigma/\partial X =$ finite, that is $\Sigma = a(X,\omega,\mathbf{k}) + b(X,\omega,\mathbf{k})\omega^2 + \cdot\cdot$ and so on. If the Ward identity is satisfied, this relation appears due to $\omega^2\Pi^{00} = \omega k^i\Pi^{0i} = k^ik^j\Pi^{ij} = \mathbf{k}^2\Pi_L$, that is $\Sigma = \Pi^{00}$ here. The subscript 'L' is omitted in the following discussions. By substituting (429) for (427) we obtain

$$D_R = -\frac{\mathbf{k}^2}{(\omega + i\epsilon)^2}\frac{1}{(\mathbf{k}^2 - \mathrm{Re}\Sigma_R) - \frac{1}{2}\Sigma_\rho}. \tag{430}$$

Then we find that this Green's function is singular at $\omega \to 0$. In the remainig part of this subsection we shall consider how the singularity of the Green's function affects the proof of H-theorem.

In the proof of H-theorem we first use 1st order of the gradient expansion of SD equation for D^{12} and D^{21}. They are given by

$$\begin{aligned}\left[i\left(\omega\delta^{\mu 0} - \frac{\partial \mathrm{Re}\Pi_R}{\partial k^\mu}\right)\frac{\partial}{\partial X_\mu} + \frac{i}{2}\frac{\partial \mathrm{Re}\Pi_R}{\partial X^\mu}\cdot\frac{\partial}{\partial k_\mu}\right] D^{12}(X,\omega,\mathbf{k}) & \\ -\frac{i}{2}\left[\frac{\partial \Pi^{12}}{\partial p^\mu}\cdot\frac{\partial}{\partial X_\mu} + \frac{\partial \Pi^{12}}{\partial X^\mu}\cdot\frac{\partial}{\partial p_\mu}\right]\mathrm{Re}D_R &= -iC(X,\omega,\mathbf{k})\end{aligned} \tag{431}$$

and

$$\begin{aligned}\left[i\left(\omega\delta^{\mu 0} - \frac{\partial \mathrm{Re}\Pi_R}{\partial k^\mu}\right)\frac{\partial}{\partial X_\mu} + \frac{i}{2}\frac{\partial \mathrm{Re}\Pi_R}{\partial X^\mu}\cdot\frac{\partial}{\partial k_\mu}\right] D^{21}(X,\omega,\mathbf{k}) & \\ -\frac{i}{2}\left[\frac{\partial \Pi^{21}}{\partial p^\mu}\cdot\frac{\partial}{\partial X_\mu} + \frac{\partial \Pi^{21}}{\partial X^\mu}\cdot\frac{\partial}{\partial p_\mu}\right]\mathrm{Re}D_R &= -iC(X,\omega,\mathbf{k})\end{aligned} \tag{432}$$

where C represents the collision term:

$$\begin{aligned}C(X,\omega,\mathbf{k}) &= i\left(\Pi_\rho(X,\omega,\mathbf{k})F(X,\omega,\mathbf{k}) - \Pi_F(X,\omega,\mathbf{k})\rho(X,\omega,\mathbf{k})\right) \\ &= \rho\Pi_\rho(f-\gamma)(X,\omega,\mathbf{k}).\end{aligned} \tag{433}$$

Here we have used the another representation of the self-energy and Green's function with $\Pi^{12} = -i\Pi_\rho\gamma$ and $\Pi^{21} = -i\Pi_\rho(1+\gamma)$ and $D^{12} = -i\rho f$ and $D^{21} = -i\rho(1+f)$ that are the Kadanoff-Baym Ansatz.

Next we shall consider the singularity in both sides of (431) and (432). In the R.H.S. in (431) and (432) the factor $\rho\Pi_\rho$

$$\rho\Pi_\rho = -\frac{\frac{\Pi_\rho^2}{2}}{(\omega^2 - \mathrm{Re}\Pi_R)^2 - \frac{1}{4}\Pi_\rho^2} = -\frac{\frac{\Sigma_\rho^2}{2}}{(\mathbf{k}^2 - \mathrm{Re}\Sigma_R)^2 - \frac{1}{4}\Sigma_\rho^2} \tag{434}$$

is finite for $\omega \to 0$. It is also finite for any type of self-energy, which is confirmed by use of 0-th order of the gradient expansion of the SD equation. For arbitrary $(\omega, \mathbf{k})$ we might have zero or infinity in $(\omega^2 - \mathrm{Re}\Pi_R)$ or Π_ρ, but $\rho\Pi_\rho$ is necessarily finite due to the relations

$$\begin{aligned} \rho\Pi_\rho &\to 0 \quad \text{for } \Pi_\rho/(\omega^2 - \mathrm{Re}\Pi_R) \to 0 \\ &\to \text{finite} \quad \text{for } \Pi_\rho/(\omega^2 - \mathrm{Re}\Pi_R) \sim 1 \\ &\to 2 \quad \text{for } (\omega^2 - \mathrm{Re}\Pi_R)/\Pi_\rho \to 0. \end{aligned} \tag{435}$$

Singularity in the R.H.S. is in $f - \gamma$ which is comparable to the L.H.S. $\omega\frac{\partial D}{\partial X} + \cdots \sim \frac{1}{\omega} \times f$ due to $D^{12} = -i\rho f$, $D^{21} = -i\rho(1+f)$ and $\rho \propto \frac{1}{\omega^2}$ if the Ward identity is satisfied. The derivative $\omega\frac{\partial}{\partial X}$ comparable to $\sim 1/\omega$ in L.H.S. may represent the breakdown of the gradient expansion around $\omega \sim 0$.

In the end we shall investigate the integrability of equation in the derivation of H-theorem. Let us subtract (432) multiplied by $\ln\frac{iD^{21}}{\rho}$ from (431) multiplied by $\ln\frac{iD^{12}}{\rho}$ and integrate with $(\omega, \mathbf{k})$. Then we obtain

$$\begin{aligned} \int \frac{d\omega}{(2\pi)}\frac{d^dk}{(2\pi)^d}\left[\text{(L.H.S.) in (431)} \times \ln\frac{iD^{12}}{\rho} - \text{(L.H.S.) in (432)} \times \ln\frac{iD^{21}}{\rho}\right] \\ = -i\int \frac{d\omega}{(2\pi)}\frac{d^dk}{(2\pi)^d} C \ln\frac{f}{1+f}, \end{aligned} \tag{436}$$

where L.H.S. normally the divergence of entropy current. Whether the above equation is integrable for momentum $(\omega, \mathbf{k})$ after multiplied $\ln\frac{D^{12}}{D^{21}} = \ln\frac{f}{1+f}$ is determined by whether the R.H.S. $C\ln\frac{f}{1+f}$ has singularity or not. The singularity of $C\ln\frac{f}{1+f}$ can be estimated as

$$C\ln\frac{f}{1+f} \sim (f-\gamma)\ln\frac{f}{1+f} \sim \frac{1}{\omega} \times f\ln\left(1+\frac{1}{f}\right), \tag{437}$$

where we have used (433), $\rho\Pi_\rho =$ finite and $f - \gamma \sim \frac{1}{\omega}f$ in (431) and (432). The singular factor $\frac{1}{\omega}$ still remains. In order to integrate $C\ln\frac{f}{1+f}$ we must restrict the occupation number function f into

$$f \sim \omega^\alpha \qquad ? \tag{438}$$

with $\alpha > 0$ around $\omega \sim 0$. It is ridiculous to restrict f into (438) since we can not discuss entropy production near thermal equilibrium where $f \sim \frac{1}{\omega} \sim \frac{1}{e^{\beta\omega}-1}$ around $\omega \sim 0$.

Fortunately the LO self-energy derived from truncation of 2PI diagrams $\Phi[G]$ does not satisfy the Ward identity. The longitudinal self-energy $\Pi_L \propto g^2 \times$ (Total Number of Particles) becomes infrared cutoff due to the local tadpole diagram in the similar way to the transverse self-energy, and it does not have the form $\frac{\omega^2}{\mathbf{k}^2} \times \cdots$, so that the above singularity around $\omega \sim 0$ may disappear. However if the Ward identity is satisfied for some truncation or classification of self-energy, we can not prove the H-theorem by use of the gradient expansion.

6.7 Nonthermal fixed point in the non-Abelian gauge theory

In this subsection we derive the scaling solution of the Green's functions which will induce the nonthermal fixed point in non-Abelian gauge theory.

We shall start the derivation. As shown in Sec. 4.4, to seek the nonthermal fixed point corresponds to the trial to seek the solution which satisfies the relation

$$\begin{aligned} (d-1)\left(\Pi_{T,F}(X,k)\rho_T(X,k) - \Pi_{T,\rho}(X,k)F_T(X,k)\right) \\ + \left(\Pi_{L,F}(X,k)\rho_L(X,k) - \Pi_{L,\rho}(X,k)F_L(X,k)\right) &= 0. \end{aligned} \tag{439}$$

We only consider k^0 in which the collision term of longitudinal part has no singularity. First we assume the scaling relations for the statistical and spectral functions

$$F_{T,L}(k) = s^{2+\kappa} F_{T,L}(sk), \tag{440}$$

for $f_{T,L} \gg 1$ where we assume $\kappa > 0$ and

$$\rho_{T,L}(k) = s^2 \rho_{T,L}(sk). \tag{441}$$

This does not mean $F_T = F_L$ and $\rho_T = \rho_L$.

Next we can derive the scaling solutions of the self-energy under the assumptions (440) and (441) and take the dominant contribution with respect to the power law as

$$\begin{aligned}
\Pi_{L,F}(-k) &= \frac{1}{2}g^2 \int \frac{d^{d+1}p}{(2\pi)^{d+1}} \left[g_1(\mathbf{k}+\mathbf{p},\mathbf{p}) \left(F_T(p)F_T(-(k+p)) - \frac{1}{4}\rho_T(p)\rho_T(-(k+p)) \right) + \cdots \right] \\
&= \frac{1}{2}g^2 s^{-(d+1)} \int \frac{d^{d+1}(sp)}{(2\pi)^{d+1}} \left[s^{-2} g_1(s(\mathbf{k}+\mathbf{p}), s(\mathbf{p})) \right. \\
&\quad \left. \left(s^{2(2+\kappa)} F_T(sp)F_T(-s(k+p)) - \frac{1}{4}s^4 \rho_T(sp)\rho_T(-s(k+p)) \right) + \cdots \right] \\
&\simeq \frac{1}{2}g^2 s^{-(d+1)-2+2(2+\kappa)} \int \frac{d^{d+1}(sp)}{(2\pi)^{d+1}} \Big[g_1(s(\mathbf{k}+\mathbf{p}), s\mathbf{p}) F_T(sp)F_T(-s(k+p)) \\
&\quad + \cdots \Big] \\
&= s^{-(d+1)-2+2(2+\kappa)} \Pi_{L,F}(-sk),
\end{aligned} \tag{442}$$

$$\begin{aligned}
\Pi_{L,\rho}(-k) &= \frac{1}{2}g^2 \int \frac{d^{d+1}p}{(2\pi)^{d+1}} \left[g_1(\mathbf{k}+\mathbf{p},\mathbf{p}) \left(F_T(p)\rho_T(-(k+p)) + \rho_T(p)F_T(-(k+p)) \right) + \cdots \right] \\
&= \frac{1}{2}g^2 s^{-(d+1)} \int \frac{d^{d+1}(sp)}{(2\pi)^{d+1}} \left[s^{-2} g_1(s(\mathbf{k}+\mathbf{p}), s(\mathbf{p})) \right. \\
&\quad \left. \left(s^{(2+\kappa)+2} F_T(sp)\rho_T(-s(k+p)) + s^{(2+\kappa)+2} \rho_T(sp)F_T(-s(k+p)) \right) + \cdots \right] \\
&= \frac{1}{2}g^2 s^{-(d+1)-2+(2+\kappa)+2} \int \frac{d^{d+1}(sp)}{(2\pi)^{d+1}} \left[g_1(s(\mathbf{k}+\mathbf{p}), s(\mathbf{p})) \right. \\
&\quad \left. \left(F_T(sp)\rho_T(-s(k+p)) + \rho_T(sp)F_T(-s(k+p)) \right) + \cdots \right] \\
&= s^{-(d+1)-2+(2+\kappa)+2} \Pi_{L,\rho}(-sk).
\end{aligned} \tag{443}$$

In the similar way

$$\begin{aligned}
(d-1)\Pi_{T,F}(-k) &\simeq \frac{1}{2}g^2 s^{-(d+1)-2+2(2+\kappa)} \int \frac{d^{d+1}(sp)}{(2\pi)^{d+1}} \Big[\left(f_1(s(\mathbf{k}+\mathbf{p}), s\mathbf{p}) - g_1(s(\mathbf{k}+\mathbf{p}), s\mathbf{p}) \right) \\
&\quad \times F_T(sp)F_T(-s(k+p)) + \cdots \Big] \\
&= s^{-(d+1)-2+2(2+\kappa)} \Pi_{T,F}(-sk),
\end{aligned} \tag{444}$$

$$
\begin{aligned}
(d-1)\Pi_{T,\rho}(-k) &= \frac{1}{2}g^2 s^{-(d+1)-2+(2+\kappa)+2}\int\frac{d^{d+1}(sp)}{(2\pi)^{d+1}}\Big[\,(f_1(s(\mathbf{k}+\mathbf{p}),s(\mathbf{p}))-g_1(s(\mathbf{k}+\mathbf{p}),s(\mathbf{p})))\\
&\quad\times(F_T(sp)\rho_T(-s(k+p))+\rho_T(sp)F_T(-s(k+p)))+\cdots\Big]\\
&= s^{-(d+1)-2+(2+\kappa)+2}\Pi_{T,\rho}(-sk). \qquad (445)
\end{aligned}
$$

Here we can notice that we have no approximation for $\Pi_{T,L,\rho}$.

By seeking the leading part in the power scaling of the self-energy we have the following relation for the dominant contribution

$$
\begin{aligned}
&(d-1)\left(\Pi_{T,F}(-k)\rho_T(-k)-\Pi_{T,\rho}(-k)F_T(-k)\right)\\
&+\left(\Pi_{L,F}(X,-k)\rho_L(X,-k)-\Pi_{L,\rho}(X,-k)F_L(X,-k)\right)\\
=\;&(\text{TTT term})+(\text{TTL term})+(\text{TLL term}). \qquad (446)
\end{aligned}
$$

First (TTT) term is given by

$$
\begin{aligned}
(\text{TTT term}) &= -\frac{g^2}{2}\int_{p,r}\delta^{d+1}(r+k+p)(f_1(-\mathbf{r},\mathbf{p})-g_1(-\mathbf{r},\mathbf{p}))\\
&\quad\times(F_T(p)F_T(r)\rho_T(k)+F_T(p)\rho_T(r)F_T(k)+\rho_T(p)F_T(r)F_T(k)) \qquad (447)
\end{aligned}
$$

where we have used (442), (443), (444) and (445) and the relation of momentum symmetry $F(-k)=F(k)$ and $\rho(-k)=-\rho(k)$. It is very difficult to give the solution which satisfies (TTT term) = 0. Hence as we have done in Sec. 4.4 we shall take the looser equation of (439), which is integrated equation with respect to momentum $\mathbf{k}$ (not k^0).

Then by changing the variables:

$$
k\to\frac{k^0}{r^0}r,\;\; r\to\frac{k^0}{r^0}k,\;\; p\to\frac{k^0}{r^0}p, \qquad (448)
$$

which has a Jacobian (by differentiating $(\frac{(k^0)^2}{r^0},\frac{k^0p^0}{r^0})$ with (r^0,p^0)) in the energy part

$$
\begin{vmatrix} -\frac{(k^0)^2}{(r^0)^2} & -\frac{k^0p^0}{(r^0)^2}\\ 0 & \frac{k^0}{r^0}\end{vmatrix}=\left(\frac{k^0}{r^0}\right)^3, \qquad (449)
$$

using that f_1-g_1 is symmetric in the interchange of r,k and p, and adopting the scaling law in (440) and (441), the second term in the bracket of (447) is transformed as

$$
\begin{aligned}
&\int_{\mathbf{k},p,r}\delta^{d+1}(p+r+k)(f_1-g_1)\,(-\mathbf{r},\mathbf{p})\,F(p)\rho(r)F(k)\\
=\;&\left(\frac{k^0}{r^0}\right)^{3(d+1)}\int_{\mathbf{k},p,r}\delta^{d+1}\left(\frac{k^0}{r^0}(r+k+p)\right)(f_1-g_1)\left(-\frac{k^0}{r^0}\mathbf{r},\frac{k^0}{r^0}\mathbf{p}\right)\\
&\times F\left(\frac{k^0}{r^0}p\right)\rho\left(\frac{k^0}{r^0}k\right)F\left(\frac{k^0}{r^0}r\right)\\
=\;&\left(\frac{k^0}{r^0}\right)^{3(d+1)}\left(\frac{k^0}{r^0}\right)^{-(d+1)}\left(\frac{k^0}{r^0}\right)^{-2}\left(\frac{k^0}{r^0}\right)^{-2(\kappa+2)}\left(\frac{k^0}{r^0}\right)^{2}\operatorname{sgn}\left(\frac{k^0}{r^0}\right)\\
&\times\int_{\mathbf{k},p,r}\delta^{d+1}\,(r+k+p)\,(f_1-g_1)\,(\mathbf{r},\mathbf{p})\,F\,(p)\,\rho\,(k)\,F\,(r)\\
=\;&\left(\frac{k^0}{r^0}\right)^{2(d+1)-2(\kappa+2)}\operatorname{sgn}\left(\frac{k^0}{r^0}\right)\\
&\times\int_{\mathbf{k},p,r}\delta^{d+1}\,(r+k+p)\,(f_1-g_1)\,(-\mathbf{r},\mathbf{p})\,F\,(p)\,\rho\,(k)\,F\,(r) \qquad (450)
\end{aligned}
$$

Here we notice that $\left(\frac{k^0}{r^0}\right)^2$ appears because of the scaling of $f_1 - g_1$ in the second equality. This factor is peculiar for non-Abelian gauge theory and different from the case in ϕ^3 theory where 1-to-2 scattering processes are included in both KB eq. and Boltzmann eq. in its quasiparticle limit. This factor causes the difference in the scaling solution κ between KB eq. in gauge theory and simple Boltzmann model which contain 1-to-2 in Sec. 4.4.1.

Similarly under the change of variables:

$$k \to \frac{k^0}{p^0}p,\ p \to \frac{k^0}{p^0}k,\ r \to \frac{k^0}{p^0}r, \tag{451}$$

the third term in the bracket of (447) is rewritten as,

$$\begin{aligned} & \int_{\mathbf{k},p,r} \delta^{d+1}(p+r+k)(f_1-g_1)\,(-\mathbf{r},\mathbf{p})\,\rho(p)F(r)F(k) \\ = & \left(\frac{k^0}{p^0}\right)^{2(d+1)-2(\kappa+2)} \mathrm{sgn}\left(\frac{k^0}{p^0}\right) \\ & \times \int_{\mathbf{k},p,r} \delta^{d+1}\,(r+k+p)\,(f_1-g_1)\,(-\mathbf{r},\mathbf{p})\,F\,(p)\,F\,(r)\,\rho\,(k)\,. \end{aligned} \tag{452}$$

As a result the integrated (TTT term) (447) is given by

$$\int_{\mathbf{k}}(\mathrm{TTT}) = \int_{\mathbf{k},p,r} \delta^{d+1}(p+k+r)F(p)F(r)\rho(k)\left[1+\left|\frac{k^0}{r^0}\right|^{\tilde{\Delta}}\mathrm{sgn}\left(\frac{k^0}{r^0}\right)+\left|\frac{k^0}{p^0}\right|^{\tilde{\Delta}}\mathrm{sgn}\left(\frac{k^0}{p^0}\right)\right] \tag{453}$$

where

$$\tilde{\Delta} \equiv 2(d+1) - 2(2+\kappa) \tag{454}$$

In the next step let us investigate whether (453) becomes zero in the case of $\tilde{\Delta} = -1, 0$ in the similar way as in Sec. 4.4. For $\tilde{\Delta} = -1$, we have $\delta(k^0+p^0+r^0)\left[1+\frac{r^0}{k^0}+\frac{p^0}{k^0}\right] = 0$ in (453). Thus we have a solution

$$\begin{aligned} 2(d+1) - 2(2+\kappa) &= -1 \\ \kappa = d - \frac{1}{2} &= \frac{5}{2} \text{ for } d = 3. \end{aligned} \tag{455}$$

For $\tilde{\Delta} = 0$ Eq. (453) is found to have a factor

$$\begin{aligned} & \int_{\mathbf{k},r,p} \delta^{d+1}(p+k+r)F(p)F(r)\rho(k)\left[1+\mathrm{sgn}\left(\frac{k^0}{r^0}\right)+\mathrm{sgn}\left(\frac{k^0}{p^0}\right)\right] \\ \sim & \int_{\mathrm{k,r,p}}\int_0^\infty \frac{dr^0}{(2\pi)}\int_0^\infty \frac{dp^0}{(2\pi)}F(p)F(r)\rho(k)\delta^d(p+k+r) \\ \times & \left[3\cdot\delta(k^0+p^0+r^0)+1\cdot\delta(k^0-p^0+r^0)+1\cdot\delta(k^0+p^0-r^0)-1\cdot\delta(k^0-p^0-r^0)\right] \end{aligned} \tag{456}$$

for $k^0 \geq 0$. We have 0-to-3 and 1-to-2 scattering processes in the brackets. In the case of ϕ^4 theory the coefficient of the delta function in 2-to-2 processes becomes zero, so that $\tilde{\Delta} = 0$ beomes the scaling solution. In the case of gauge theory the coefficient of 1-to-2 scattering processes does not vanish. Therefore

$$\begin{aligned} 2(d+1) - 2(2+\kappa) &= 0 \text{ (not the scaling solution)} \\ \kappa = d - 1 &= 2 \text{ for } d = 3 \end{aligned} \tag{457}$$

is not the scaling solution for the non-thermal fixed point.

Next let us consider the (TTL) components

$$
\begin{aligned}
(\text{TTL term}) &= -\frac{g^2}{2}\int_{p,r}\delta^{d+1}(r+k+p) \\
&\times \Big[(f_2-g_2)\,(F_L(p)F_T(r)\rho_T(k)+\rho_L(p)F_T(r)F_T(k)+F_L(p)\rho_T(r)F_T(k)) \\
&+ (f_3-g_3)\,(F_T(p)F_L(r)\rho_T(k)+\rho_T(p)F_L(r)F_T(k)+F_T(p)\rho_L(r)F_T(k)) \\
&+ g_1\,(F_T(p)F_T(r)\rho_L(k)+\rho_T(p)F_T(r)F_L(k)+F_T(p)\rho_T(r)F_L(k))\Big]. \qquad (458)
\end{aligned}
$$

By integrating with $\mathbf{k}$ and using the symmetry $f_2-g_2 \leftrightarrow g_1$ for $p \leftrightarrow k$ and $f_3-g_3 \leftrightarrow g_1$ for $r \leftrightarrow k$, under the change of variables (448) for the $(f_3-g_3)(\cdots)$ term and (451) for $(f_2-g_2)(\cdots)$ term in the bracket, we obtain

$$
\begin{aligned}
\int_{\mathbf{k}}(\text{TTL term}) &= -\frac{g^2}{2}\int_{\mathbf{k},p,r}\delta^{d+1}(r+k+p) \\
&\quad g_1(-\mathbf{r},\mathbf{p})\left[1+\left(\frac{k^0}{r^0}\right)^{\bar\Delta}\mathrm{sgn}\left(\frac{k^0}{r^0}\right)+\left(\frac{k^0}{p^0}\right)^{\bar\Delta}\mathrm{sgn}\left(\frac{k^0}{p^0}\right)\right] \\
&\times (F_T(p)F_T(r)\rho_L(k)+\rho_T(p)F_T(r)F_L(k)+F_T(p)\rho_T(r)F_L(k)) \qquad (459)
\end{aligned}
$$

since for example the first term $\int(f_2-g_2)F_L(p)F_T(r)\rho_T(k)$ of $(f_2-g_2)(\cdots)$ in (458) is transformed to $\int|k^0/p^0|^{\bar\Delta}\mathrm{sgn}(k^0/p^0)g_1F_L(k)F_T(r)\rho_T(p)$ which is the second components of $g_1(\cdots)$ in (458) times the factor $|k^0/p^0|^{\bar\Delta}\mathrm{sgn}(k^0/p^0)$. Hence the scaling solution is the same as that for (TTT) term and given by $\kappa = d-\frac{1}{2}=\frac{5}{2}$.

In the similar way the (TLL) term can be transformed after the integration with $\mathbf{k}$ (by use of the symmetry $f_4-g_4 \leftrightarrow g_2$ for $r \leftrightarrow k$ and $f_4-g_4 \leftrightarrow g_3$ for $p \leftrightarrow k$) as

$$
\begin{aligned}
\int_{\mathbf{k}}(\text{TTL term}) &= -\frac{g^2}{2}\int_{\mathbf{k},p,r}\delta^{d+1}(r+k+p) \\
&\times (f_4-g_4)(-\mathbf{r},\mathbf{p})\left[1+\left(\frac{k^0}{r^0}\right)^{\bar\Delta}\mathrm{sgn}\left(\frac{k^0}{r^0}\right)+\left(\frac{k^0}{p^0}\right)^{\bar\Delta}\mathrm{sgn}\left(\frac{k^0}{p^0}\right)\right] \\
&\times (F_L(p)F_L(r)\rho_T(k)+F_L(p)\rho_L(r)F_T(k)+F_L(r)\rho_L(p)F_T(k))\,. \qquad (460)
\end{aligned}
$$

As a result the same scaling solution $\kappa = d-\frac{1}{2}=\frac{5}{2}$ for $d=3$ is derived.

In the end we shall compare the scaling relations for the KB equation for the gauge theory and those for the simple Boltzmann equation in Sec. 4.4. In Sec. 4.4. for the simple Boltzmann approach with 1-to-2 scattering processes, the scaling solution $\kappa_{\mathrm{Bol}} = d-\frac{3}{2}$, $\kappa \neq d-2$ is given. They are different from the scaling $\kappa = d-\frac{1}{2}$, $(\kappa \neq d-1)$ by the factor 1. This difference comes from the scaling dependence of momentum for f_i and g_i $i=1,2,3,4$, and it is peculiar for the gauge theory.

6.8 Discussion

In this section we have considered 2-Particle-Irreducible effective action in non-Abelian gauge theory. We have reviewed that 2PI effective action with truncation has controlled gauge invariance, which means that the truncated action has gauge dependent terms in higher order of the coupling and that it is gauge invariant within the truncated order. It is possible to derive thermodynamic variables with controlled gauge invariance from the action at thermal equilibrium.

Next we have written the Kadanoff-Baym equation and (Yang-Mills equation) by taking the stationary point of 2PI effective action for the gauge theory in Background (BG) and temporal axial gauge (TAG). The gauge invariance of the classical fields remains in the BG gauge. KB equation in this gauge is prepared to analyze the dynamics with nonzero classical fields in the future study. In

addition we have given KB equation with LO self-energy of the coupling in TAG in order to prove H-theorem and perform numerical analyses in the future. This self-energy contains the tadpole part that contributes to mass shift and the nonlocal part that contributes to 0-to-3, 1-to-2 and 2-to-1 processes in the particle picture.

We might guess that LO self-energy contribute to 1-to-2 and 2-to-1 particle number changing processes in the Boltzmann simulation without memory effects and spectral width and that these processes are allowed for in-coming and out-going gluons with collinear momenta in the massless limit. However the coefficient $f_1 - g_1$ in the LO self-energy vanishes for gluons with collinear momenta. Hence 1-to-2 and 2-to-1 processes in the Boltzmann approach are completely prohibited for the dynamics with only transverse fluctuations.

In the end we have tried to prove H-theorem for the self-energy in the KB approach with $\bar{A} = 0$. We have divided Green's functions and self-energy to transverse and longitudinal part with respect to spatial momentum. Transverse and longitudinal part in self-energy have coefficients $f_i - g_i$ $\{i = 1, 2, 3, 4\}$ and g_i, respectively. Symmetry of these coefficients in its interchange of momentum is convenient to prove the H-theorem. As a result the divergence of the derived entropy current appears to be positive definite in $d + 1$ dimensions with $d \geq 2$. The particle number changing processes, such as 0-to-3, 1-to-2 and 2-to-1, have a possibility of contributing to entropy production and thermalization at late times in the KB approach.

However two problems remain in the complete proof. First there may appear a problem in longitudinal Green's functions. If the Ward identity is satisfied for some truncation of self-energy, the approximation which has been the basis of the proof (gradient expansion) will be poorly reliable due to the singularity of the Green's function. Fortunately such a problem may not occur in the leading order of the coupling expansion since its self-energy does not satisfy the Ward identity in this order. In addition at thermal equilibrium our kinetic entropy is different from entropy derived from differentiating with its temperature ($\mathcal{S} = -\frac{\partial \Omega/V}{\partial T}$) by temperature (and time) independent factor $\mathcal{S}_L^{(0)}$ in the longitudinal part. We can not derive time independent factor such as $\mathcal{S}_L^{(0)}$ in the proof of H-theorem, while redefinition of our entropy by subtracting this factor does not affect the proof of H-theorem. So it might be necessary and significant to subtract this factor from our kinetic entropy in far from equilibrium case in order to compare with $\mathcal{S}$ near thermal equilibrium. Secondly the problem of gauge dependence of kinetic entropy remains. The gauge dependence of our entropy with factor $\mathcal{S}_L^{(0)}$ is controlled at thermal equilibrium due to controlled gauge invariance of 2PI effective action. However we must confirm gauge invariance or controlled gauge dependence of our entropy current in far-from equilibrium.

7 Summary and outlook

We have reviewed the derivation of the KB equation with NLO self-energy of the coupling expansion in ϕ^4 theory and with NLO self-energy of $1/N$ expansion in $O(N)$ theory. We have also prepared the KB equation with LO self-energy of the coupling expansion in the gauge theory with TAG in order to perform simulations in the future analyses. This LO self-energy reproduces the simple mass shift in Ref. [167] in the HTL approximation, while it might contribute to thermalization in TAG without the approximation.

We have introduced the relativistic kinetic entropy current on the basis of the KB equation in scalar ϕ^4 and $O(N)$ theory. We have derived it by use of 1st order gradient expansion in the similar way to non-relativistic case in Refs. [108, 109]. The derived kinetic entropy satisfies the H-theorem for the NLO of the skeleton expansion of the coupling in ϕ^4 theory and the NLO of the $1/N$ expansion of $\Gamma_2[G]$ in $O(N)$ theory in the symmetric phase $\langle\hat{\phi}\rangle = 0$. Furthermore at thermal equilibrium our kinetic entropy in the scalar theory is found to be the entropy derived by differentiating the thermodynamic potential by its temperature within the NLO of the coupling expansion. The proof of H-theorem is considered as one of the criteria to determine whether the system thermalizes or not for each microscopic process contained in its self-energy before trying numerical simulation (Table 4).

	$\lambda\phi^4$	$O(N)$	$SU(N)$
Exact 2PI (no Truncation)	$\times$	$\times$	$\times$
Numerically (Truncation)	$\triangle$ (NLO of λ)	$\triangle$ (NLO of $1/N$)	? (LO of g)
Gradient Expansion	$\bigcirc$	$\bigcirc$	$\triangle$ (TAG)

Table 4: Time Irreversibility (in $\langle\hat{\phi}\rangle = 0$)

The numerical simulations of the KB equation in the symmetric phase have been performed for $1+1$ and $2+1$ dimensions in scalar ϕ^4 theory and for $1+1$ dimensions in scalar $O(N)$ theory. We have prepared the "tsunami" and Woods-Saxon initial conditions in $1+1$ dimensions for the scalar theories. We have confirmed that the particle number distribution approaches the Bose-Einstein distribution at sufficiently later times, which reconfirms the results of Refs. [92, 93, 99]. We should note that no thermalization occurs in the Boltzmann equation with 2-to-2 scatterings in $1+1$ dimensions, so that off-shell effects in KB equation play a very significant role in scalar theories.

We have evaluated the kinetic entropy (91) numerically for scalar theories in 1+1 dimensions. In the numerical analyses of the entropy we have to estimate the spectral function $\rho(X,p)$ and the occupation number function $f(X,p)$ with the Fourier transformation. However the Fourier transformation within the limited time interval for $mX^0 \sim 1$ makes them oscillating in p^0 since the narrower width than $1/(mX^0)$ can not be resolved, so that numerical artifacts appear in the estimation of kinetic entropy. On the other hand the kinetic entropy is useful when the shape of $\rho(X,p)$ and $f(X,p)$ are well resolved and the gradient expansion is also valid. At later times $mX^0 \gg 1$ when they are well resolved, the kinetic entropy increases monotonically as time proceeds, which is consistent with the H-theorem.

As an alternative approach, we have also estimated the time evolution of the entropy in the Quasi-Particle (QP) approximation (95) for ϕ^4 theory in 1+1 and 2+1 dimensions and for $O(N)$ theory in 1+1 dimensions. We found that it increases almost monotonically and saturates at the equilibrium value. We also found that the late time behavior is similar to that of the kinetic entropy. This entropy (95) might be also useful in monitoring thermalization of the system although we should note that it is not based on H-theorem in KB approach.

The KB equations involve the off-shell effects of the finite memory time as well as the nontrivial spectral function $\rho(X,p)$ and occupation number function $f(X,p)$. In 1+1 dimensions the effects have a significant role for entropy production in the evolution and thermalization at late times. We examined effects of the finite memory time within the quasiparticle approximation, and showed that the 2-to-2 process as well as the number changing processes are operative for producing the entropy of the evolution in ϕ^4 theory.

Furthermore we have studied the dependence of the evolution on the coupling constant, the number of particle components N and the initial conditions for scalar theories in $1+1$ dimensions. When particle number changing processes are suppressed by its narrow spectral width, initial condition dependence for total number density remains at later times. Then both entropy becomes dependent on initial conditions even at later times. As initial condition dependence of the total number density disappears, that of both entropy does. In particular we can observe that the asymptotic behavior with exponential function tends to be less dependent on initial conditions as the total number density loses its initial condition dependence.

In 2+1 dimensions we have studied the time evolution of the QP entropy (95) for both anisotropic and isotropic initial conditions in momentum space with the same QP entropy in order to investigate whether the isotropization helps the thermalization. We should apply this analysis to gauge theory in the future study and carefully determine the initial conditions of the distribution functions before and after isotropization caused by the Weibel type instability.

For gauge theory we have prepared the KB equation with LO self-energy and tried to prove H-theorem in TAG by introducing the kinetic entropy in the similar way to the scalar theories. For $d \geq 2$ entropy production appears to occur by particle number changing processes. The H-theorem might be satisfied for the LO of the skeleton expansion of the coupling although the problems of infrared singularity and gauge dependence still remain.

The KB equation with the 2PI effective action is one of the most promising approaches to describe both thermal equilibrium systems and non-equilibrium processes in the quantum field theories. As off-shell effects naturally included in KB equation play a important role in the dynamics of 1+1 dimensions in scalar theories, they are expected to be important in higher dimensions. Especially for gauge theories, off-shell effects are also expected to play a significant role for entropy production in $d+1$ ($d \geq 2$) dimensions although it should be confirmed by simulations. In the study of ultrarelativistic heavy-ion collisions, how to explain fast thermalization of partons is one of the most important issues under debate. The KB dynamics may provide a suitable framework in investigating the early time behavior in the collisions. The kinetic entropy introduced in this paper may also be one of the most useful quantities to estimate thermalization processes of the system. Toward this end, practical numerical simulations in gluodynamics are desired in the future study.

Acknowledgement

The author is grateful to Profs. T. Matsui and H. Fujii for suggesting him topics on the nonequilibrium field theories and his useful comments and continuous encouragements. He also acknowledge the helpful comments provided by Profs. T. Kunihiro, J. Berges, T. Biro, K. Itakura, Y. Nara, S. Muroya, K. Fukushima and Dr. Y. Saito. The research described in this thesis has been supported by JSPS research fellowships for Young Scientists.

Appendix

A 2 Particle Irreducible Effective Action

In this paper we adopt Schwinger-Dyson equation which is equivalent to Kadanoff-Baym equation to investigate nonequilibrium quantum dynamics. This equation can be derived by differentiating 2 particle irreducible (2PI) effective action. The action is given by resummation of any two particle reducible diagrams and was used by Cornwall, Jackiw and Tomboulis to search the effective vacuum with the variational approach which uses mean field and Gaussian width [74]. In this appendix we show the derivation of the 2PI effective action on the basis of Ref. [172].

To simplify the explanation, we use only one field ϕ and the representation $(1) = (x_1^\mu), \phi(1)\phi(1) = \int d^{d+1}x\phi(x_1^\mu)\phi(x_1^\mu)$ for the omission. First let us introduce the action as

$$S[\phi] = -\frac{1}{2}G_0^{-1}(12)\phi(1)\phi(2) + \sum_{n=3}^{\infty}\frac{1}{n!}V^{(n)}(12\cdots n)\phi(1)\phi(2)\cdots\phi(n) \tag{461}$$

where $V^{(n)}(12\cdots n)$ are the fully symmetrized vertices. The expectation value $\langle A[\phi]\rangle$ is given by

$$\langle A[\phi]\rangle = \frac{\int D\phi A[\phi]\exp[S[\phi]]}{\int D\phi\exp[S[\phi]]}. \tag{462}$$

Hence it is convenient to introduce a generating functional $W[\lambda, J, K]$ defined as

$$W[\lambda, J, K] = \lambda\ln\left[c\int D\phi\exp\left[\frac{1}{\lambda}\left\{S[\phi] + J(1)\phi(1) + \frac{1}{2}\phi(1)K(12)\phi(2)\right\}\right]\right] \tag{463}$$

where c represents the normalization factor. In the non-equilibrium case J, K comes from both initial density matrix and local external sources. Then the expectation value of 1-point and 2-point Green's functions are derived by differentiating the generating functional as

$$\begin{aligned}
\bar{\phi}(1) &\equiv \langle\phi(1)\rangle = \frac{\delta W[\lambda, J, K]}{\delta J(1)} \\
G(12) &\equiv \frac{1}{\lambda}\left(\langle\phi(1)\phi(2)\rangle - \bar{\phi}(1)\bar{\phi}(2)\right) = \frac{\delta^2 W[\lambda, J, K]}{\delta J(1)\delta J(2)} \\
\frac{\delta W[\lambda, J, K]}{\delta K(12)} &= \frac{1}{2}\langle\phi(1)\phi(2)\rangle = \frac{1}{2}\left(\lambda G(12) + \bar{\phi}(1)\bar{\phi}(2)\right).
\end{aligned} \tag{464}$$

Furthermore we shall consider the Legendre transformation of the generating functional $W[\lambda, J, K]$ as

$$\Gamma[\bar{\phi}, G] = W[\lambda, J, K] - J(1)\bar{\phi}(1) - \frac{1}{2}K(12)\left(\lambda G(12) + \bar{\phi}(1)\bar{\phi}(2)\right) \tag{465}$$

where Γ is called effective action. We notice that Under the Legendre transformation variables are changed from $\{J, K\}$ to $\{\bar{\phi},\ G\}$. Then by differentiating the action we can derive the following

relations,

$$\begin{aligned}
\frac{\delta\Gamma[\bar{\phi},G]}{\delta\bar{\phi}(1)} &= \frac{\delta W[\lambda,J,K]}{\delta J(2)}\frac{\delta J(2)}{\delta\bar{\phi}(1)} + \frac{\delta W[\lambda,J,K]}{\delta K(23)}\frac{\delta K(23)}{\delta\bar{\phi}(1)} - \frac{\delta J(2)}{\delta\bar{\phi}(1)}\bar{\phi}(2) - J(1) \\
&\quad -\frac{1}{2}\frac{\delta K(23)}{\delta\bar{\phi}(1)}\left(\lambda G(23) + \bar{\phi}(2)\bar{\phi}(3)\right) - K(12)\bar{\phi}(2) \\
&= -J(1) - K(12)\bar{\phi}(2), \\
\frac{\delta\Gamma[\bar{\phi},G]}{\delta G(12)} &= \frac{\delta W[\lambda,J,K]}{\delta J(3)}\frac{\delta J(3)}{\delta G(12)} + \frac{\delta W[\lambda,J,K]}{\delta K(34)}\frac{\delta K(34)}{\delta G(12)} - \frac{\delta J(3)}{\delta G(12)}\phi(3) \\
&\quad -\frac{1}{2}\frac{\delta K(34)}{\delta G(12)}\left(\lambda G(34) + \bar{\phi}(3)\bar{\phi}(4)\right) - \frac{1}{2}\lambda K(12) \\
&= -\frac{1}{2}\lambda K(12)
\end{aligned} \tag{466}$$

where we have used the relations (464).

Next let us expand $W[\lambda,J,K]$ by λ around $\lambda=0$ in order to derive the explicit expression of $\Gamma[\phi,G]$ and leave only up to $O(\lambda^2)$, then we will later see that 1-loop 2PI diagrams are left and notice that higher order diagrams of the coupling $V^{(n)}$ are obtained by expanding higher order of λ. We write $W[\lambda,J,K]$ as

$$W[\lambda,J,K] = W_0[J,K] + W_1[J,K] + W_2[J,K] + O(\lambda^3) \tag{467}$$

where W_0, W_1 and W_2 represents terms of $O(\lambda^0), O(\lambda^1)$ and $O(\lambda^2)$ respectively.

First let us expand $S(\phi)+J(1)\phi(1)+\frac{1}{2}\phi(1)K(12)\phi(2)$ in the exponential function of $W[\lambda,J,K]$ around ϕ_c, where ϕ_c is the solution of $\frac{\delta S[\phi_c]}{\delta\phi_c(1)} + J(1) + K(12)\phi_c(2) = 0$ ($S(\phi)+J(1)\phi(1)+\frac{1}{2}\phi(1)K(12)\phi(2)$ has extremum at $\phi=\phi_c$), and write $\phi(1)=\phi_c(1)+\sqrt{\lambda}\chi(1)$, then we obtain

$$\begin{aligned}
S(\phi)+J(1)\phi(1)+\frac{1}{2}\phi(1)K(12)\phi(2) = \quad & (S(\phi_c)+J(1)\phi_c(1)+\tfrac{1}{2}\phi_c(1)K(12)\phi_c(2)) \\
& +\tfrac{\lambda}{2}\left(S_c^{(2)}(12,\phi_c)+K(12)\right)\chi(1)\chi(2) \\
& +\textstyle\sum_{n=3}^{\infty}\frac{\lambda^{n/2}}{n!}S_c^{(n)}(12\cdots n)\chi(1)\chi(2)\cdots\chi(n)
\end{aligned} \tag{468}$$

where $S^{(n)}(12\cdots) \equiv \frac{\delta^n S(\phi)}{\delta\phi(1)\delta(2)\cdots\delta\phi(n)}$. The $O(\lambda^{1/2})$ term vanishes since $S(\phi)+J(1)\phi(1)+\frac{1}{2}\phi(1)K(12)\phi(2)$ has extremum at $\phi=\phi_c$.

We can expand $W[\lambda,J,K]$ by λ with Eq. (468). The lowest component W_0 can be written in the limit $\lambda\to 0$ as,

$$W_0[J,K] = S[\phi_c] + J(1)\phi_c(1) + \frac{1}{2}\phi_c(1)K(12)\phi_c(2). \tag{469}$$

The second component W_1 can be written as

$$\begin{aligned}
W_1 &= \lambda\ln\left[\int D\chi\exp\left[\frac{1}{2}\left(S_c^{(2)}(12,\phi_c)+K(12)\right)\chi(1)\chi(2)\right]\right] \\
&\quad -\lambda\ln\left[\int D\chi\exp\left[\frac{1}{2}\left(S_c^{(2)}(12,\phi_c)+K(12)\right)\right]\right]_{J,K=0}
\end{aligned} \tag{470}$$

where the second term of the R.H.S. stems from the normalization factor c. Then we obtain

$$W_1 = -\frac{\lambda}{2}(\mathrm{Tr}\ln g^{-1} - \mathrm{Tr}\ln g^{-1}|_{J,K=0}) \tag{471}$$

where

$$g^{-1}(12;\phi_c) \equiv -S_c^{(2)}(12,\phi_c) - K(12) \tag{472}$$

and we have used the Gaussian integral $\int D\chi \exp\left[-\frac{1}{2}g^{-1}(12)\chi(1)\chi(2)\right] = \exp\left(-\frac{1}{2}\mathrm{Tr}\ln g^{-1}\right)$. Since $S_c^{(2)}(12,\phi_c)$ can be expanded as

$$S_c^{(2)}(12,\phi_c) = -G_0^{-1}(12) + V_3(123)\phi_c(3) + \frac{1}{2!}V_4(1234)\phi_c(3)\phi_c(4) + \cdots \tag{473}$$

and $\frac{\delta S[\phi_c]}{\delta\phi_c(1)} = -J(1) - K(12)\phi_c(2)$, any terms except first term of (473) vanish, so that

$$g^{-1}|_{J,K=0}(12) = G_0^{-1}(12). \tag{474}$$

As a result we obtain

$$W_1 = -\frac{\lambda}{2}\mathrm{Tr}\ln\left(g^{-1}\cdot G_0\right) \tag{475}$$

Next W_2 can be expanded in the following

$$\begin{aligned} W_2 &= \frac{\lambda^2}{4!}S_c^{(4)}\langle\chi(1)\chi(2)\chi(3)\chi(4)\rangle_0 \\ &\quad + \frac{\lambda^2}{2}\left(\frac{1}{3!}\right)^2 S_c^{(3)}(123)S_c^{(3)}(456)\langle\chi(1)\chi(2)\chi(3)\chi(4)\chi(5)\chi(6)\rangle_0 \end{aligned} \tag{476}$$

where $\langle\cdots\rangle_0$ is defined as

$$\langle\cdots\rangle_0 = \frac{\int D\chi(\cdots)\exp\left[\frac{1}{2}\left(S_c^{(2)}(12,\phi_c)+K(12)\right)\chi(1)\chi(2)\right]}{\int D\chi\exp\left[\frac{1}{2}\left(S_c^{(2)}(12,\phi_c)+K(12)\right)\chi(1)\chi(2)\right]}. \tag{477}$$

Here we have extracted the $O(\lambda^2)$ terms of

$$\begin{aligned} \ln\Bigg[c\int D\chi\exp\Bigg[&\left(S_c^{(2)}(12,\phi_c)+K(12)\right)\chi(1)\chi(2) + \frac{1}{3!}\lambda^{1/2}S_c^{(3)}(123)\chi(1)\chi(2)\chi(3) \\ &+\frac{1}{4!}\lambda S_c^{(4)}(1234)\chi(1)\chi(2)\chi(3)\chi(4)\Bigg]\Bigg]. \end{aligned} \tag{478}$$

This expansion correspond to a perturbative approach with respect to expansion parameter λ. By use of the Gaussian integral of (477) with respect to χ and symmetry of $S_c^{(3)}(123)$ and $S_c^{(4)}(1234)$, we obtain

$$\begin{aligned} W_2[J,K] &= \frac{\lambda^2}{8}S_c^{(4)}(1234)g(12)g(34) + \frac{\lambda^2}{12}S_c^{(3)}(123)S_c^{(3)}(456)g(14)g(25)g(36) \\ &\quad + \frac{\lambda^2}{8}S_c^{(3)}(123)S_c^{(3)}(456)g(12)g(34)g(56). \end{aligned} \tag{479}$$

Here expand Γ with $\phi_c - \bar{\phi}$. First with the relation

$$\bar{\phi}(1) = \frac{\delta W}{\delta J(1)} = \phi_c(1) + \lambda\frac{\delta W_1[J]}{\delta J(1)} + O(\lambda^2), \tag{480}$$

we obtain

$$\begin{aligned} \phi_c(1) - \bar{\phi}(1) &= -\lambda\frac{\delta W_1}{\delta J(1)} = -\lambda\frac{\delta\phi_c(2)}{\delta J(1)}\frac{\delta W_1}{\delta\phi_c(2)} \\ &= \lambda\frac{1}{K+S_c^{(2)}}(12;\phi_c)\frac{\delta W_1}{\delta\phi_c(2)} \\ &= -\lambda g(12;\bar{\phi})\frac{\delta W_1}{\delta\bar{\phi}(2)} + O(\lambda^2), \end{aligned} \tag{481}$$

where we have used (472). From Eq. (475) the factor $\frac{\delta W_1}{\delta\bar{\phi}(2)}$ is written as

$$\begin{aligned}
\frac{\delta W_1}{\delta\bar{\phi}(2)} &= -\frac{1}{2}\frac{\delta}{\delta\phi(2)}\left[\mathrm{Tr}\ln\left(g^{-1}(\bar{\phi})\cdot G_0\right)\right] \\
&= -\frac{1}{2}G_0^{-1}(11')g(1'3;\bar{\phi})\frac{\delta g^{-1}(33';\bar{\phi})}{\delta\bar{\phi}(2)}G_0(3'1) \\
&= -\frac{1}{2}\delta(1'3')g(1'3;\bar{\phi})\frac{\delta g^{-1}(33';\bar{\phi})}{\delta\bar{\phi}(2)} = -\frac{1}{2}g(33';\bar{\phi})\frac{\delta g^{-1}(33';\bar{\phi})}{\delta\bar{\phi}(2)} \\
&= \frac{1}{2}g(3'3;\bar{\phi})\frac{\delta(S^{(2)}(33';\bar{\phi})+K(33'))}{\delta\bar{\phi}(2)} = \frac{1}{2}S^{(3)}(233';\bar{\phi})g(33';\bar{\phi}). \qquad (482)
\end{aligned}$$

By use of the above relations we obtain

$$\phi_c(1)-\bar{\phi}(1) = -\frac{\lambda}{2}g(12;\bar{\phi})S^{(3)}(234;\bar{\phi})g(34;\bar{\phi})+O(\lambda^2). \qquad (483)$$

Then we notice that $\phi_c(1)-\bar{\phi}(1)=O(\lambda)$. Next we shall differentiate (483) with J, then we obtain

$$\begin{aligned}
G(12) &= \frac{\delta\bar{\phi}(1)}{\delta J(2)} = \frac{\delta\phi_c(1)}{\delta J(2)} + \frac{\lambda}{2}\frac{\delta\bar{\phi}(1')}{\delta J(2)}\frac{\delta\left[g(12';\bar{\phi})S^{(3)}(2'34;\bar{\phi})g(34;\bar{\phi})\right]}{\delta\bar{\phi}(1')}+O(\lambda^2) \\
&= g(12;\phi_c)+\frac{\lambda}{2}F(11';\bar{\phi})G(1'2)+O(\lambda^2), \qquad (484)
\end{aligned}$$

where $F(11';\bar{\phi})$ is defined as

$$F(11';\bar{\phi}) \equiv \frac{\delta}{\delta\bar{\phi}(1')}\left[g(12';\bar{\phi})S^{(3)}(2'34;\bar{\phi})g(34;\bar{\phi})\right]. \qquad (485)$$

Then $g^{-1}(\phi_c)$ is expressed as

$$g^{-1}(12;\phi_c) = G^{-1}(12)+\frac{\lambda}{2}G^{-1}(11')F(1'2;\bar{\phi})+O(\lambda^2). \qquad (486)$$

As a result we can expand the Legendre transformed $\Gamma[\bar{\phi},G]$ with $\phi_c(1)-\bar{\phi}(1)$ as

$$\begin{aligned}
\Gamma[\bar{\phi},G] &= -J(1)\bar{\phi}(1)-\frac{1}{2}K(12)\left(\lambda G(12)+\bar{\phi}(1)\bar{\phi}(2)\right) \\
&\quad +W_0[J,K]+W_1[J,K]+W_2[J,K]+\cdots \\
&= -J(1)\bar{\phi}(1)-\frac{1}{2}K(12)\left(\lambda G(12)+\bar{\phi}(1)\bar{\phi}(2)\right) \\
&\quad +S[\phi_c]+J(1)\phi_c(1)+\frac{1}{2}K(12)\phi_c(1)\phi_c(2)+W_1[J,K]+W_2[J,K]+\cdots \\
&= S[\phi_c]+(J(1)+K(12)\phi_c(2))(\phi_c(1)-\bar{\phi}(1))-\frac{1}{2}K(12)(\phi_c(1)-\bar{\phi}(1))(\phi_c(2)-\bar{\phi}(2)) \\
&\quad -\frac{\lambda}{2}K(12)G(12)+W_1[J,K]+W_2[J,K]+\cdots. \qquad (487)
\end{aligned}$$

Here the first term of three ones in the last line can be expanded by $\phi_c - \bar{\phi}$ as

$$\begin{aligned}
& S[\phi_c] + (J(1) + K(12)\phi_c(2))(\phi_c(1) - \bar{\phi}(1)) - \frac{1}{2}K(12)(\phi_c(1) - \bar{\phi}(1))(\phi_c(2) - \bar{\phi}(2)) \\
= \; & S[\phi_c] - \frac{\delta S[\phi_c]}{\delta \phi_c}(\phi_c(1) - \bar{\phi}(1)) - \frac{1}{2}K(12)(\phi_c(1) - \bar{\phi}(1))(\phi_c(2) - \bar{\phi}(2)) \\
= \; & S[\phi] + S^{(1)}(1;\phi)(\phi_c(1) - \phi(1)) + \frac{1}{2}S^{(2)}(12;\phi)(\phi_c(1) - \phi(1))(\phi_c(1) - \phi(2)) \\
& - \left(S^{(1)}(1;\bar{\phi}) + S^{(2)}(12;\bar{\phi})(12;\bar{\phi})(\phi_c(2) - \bar{\phi}(2)) + \cdots\right)(\phi_c(1) - \bar{\phi}(1)) \\
& - \frac{1}{2}K(12)(\phi_c(1) - \bar{\phi}(1))(\phi_c(2) - \bar{\phi}(2)) \\
= \; & S[\bar{\phi}] - \frac{1}{2}\left(S^{(2)}(12;\bar{\phi}) + K(12)\right)(\phi_c(1) - \bar{\phi}(1))(\phi_c(2) - \bar{\phi}(2)) + O(\lambda^3). \qquad (488)
\end{aligned}$$

Substituting (488) into (487), we obtain

$$\begin{aligned}
\Gamma[\bar{\phi}, G] \;=\; & S[\bar{\phi}] - \frac{1}{2}\left(S^{(2)}(12;\bar{\phi}) + K(12)\right)(\phi_c(1) - \bar{\phi}(1))(\phi_c(2) - \bar{\phi}(2)) \\
& - \frac{\lambda}{2}K(12)G(12) + W_1[J,K] + W_2[J,K] + \cdots. \qquad (489)
\end{aligned}$$

Next we shall reexpress $\Gamma[\bar{\phi}, G]$ in (489) with respect to $\bar{\phi}$ and G by use of Eqs. (472), (483) and (484) or (486). Here $K(12)G(12)$ is expanded by λ as

$$\begin{aligned}
& K(12)G(12) \\
= \; & -G(12)(S_c^{(2)}(12;\phi_c) + g^{-1}(12;\phi_c)) \\
= \; & -G(12)\left[S^{(2)}(12;\bar{\phi}) + S^{(3)}(123;\bar{\phi})(\phi_c(3) - \phi(3)) + G^{-1}(12) + \frac{\lambda}{2}G^{-1}(11')F(1'2;\bar{\phi})\right] \\
& + O(\lambda^2) \\
= \; & -G(12)\left(S^{(2)}(12;\bar{\phi}) + G^{-1}(12)\right) - G(12)S^{(3)}(123;\bar{\phi})(\phi_c(3) - \bar{\phi}(3)) \\
& - \frac{\lambda}{2}F(22;\bar{\phi}) + O(\lambda^2) \qquad (490)
\end{aligned}$$

where we have used Eq. (472) and (486) with (485). Next W_1 in (475) is expanded by λ as

$$\begin{aligned}
W_1[J,K] \;=\; & -\frac{\lambda}{2}\mathrm{Tr}\ln\left(g^{-1}(\phi_c)\cdot G_0\right) \\
=\; & -\frac{\lambda}{2}\mathrm{Tr}\left[\ln\left(G^{-1}\cdot G_0\right) + \ln\left(1 + \frac{\lambda}{2}F\right)\right] + O(\lambda^3) \\
=\; & -\frac{\lambda}{2}\mathrm{Tr}\ln\left(G^{-1}\cdot G_0\right) - \frac{\lambda^2}{4}\mathrm{Tr}F + O(\lambda^3) \qquad (491)
\end{aligned}$$

where we have used (486). We find that $\frac{\lambda^2}{4}F$ term cancels when $-\frac{\lambda}{2}KG$ and W_1 are added in (489).

Now $\Gamma[\bar{\phi}, G]$ can be written by

$$\begin{aligned}
\Gamma[\phi, G] \;=\; & S[\bar{\phi}] - \frac{\lambda}{2}\mathrm{Tr}\ln\left(G^{-1}\cdot G_0\right) + \frac{\lambda}{2}\mathrm{Tr}\left(G\cdot S^{(2)}(\bar{\phi}) + 1\right) \\
& - \frac{1}{2}\left(S^{(2)}(12;\bar{\phi}) + K(12)\right)(\phi_c(1) - \bar{\phi}(1))(\phi_c(2) - \bar{\phi}(2)) \\
& - \frac{\lambda}{2}G(12)S^{(3)}(123;\bar{\phi})(\phi_c(3) - \bar{\phi}(3)) + W_2[J,K] + O(\lambda^3). \qquad (492)
\end{aligned}$$

The remaining part is the fourth, fifth term and W_2. The fourth term of (492) is written as

$$\begin{aligned}
& \frac{1}{2}\left(S^{(2)}(12;\bar{\phi})+K(12)\right)(\phi_c(1)-\bar{\phi}(1))(\phi_c(2)-\bar{\phi}(2)) \\
= \quad & \frac{\lambda^2}{8}\left(S^2(12;\bar{\phi})+K(12)\right)g(12';\bar{\pi})S^{(3)}(2'3'4';\bar{\phi})g(3'4';\bar{\phi})g(23;\bar{\phi})S^{(3)}(345;\bar{\phi})g(45;\bar{\phi}) \\
& +O(\lambda^2) \\
= \quad & -\frac{\lambda^2}{8}S^{(3)}(23'4';\bar{\phi})g(3'4';\bar{\phi})g(23;\bar{\phi})S^{(3)}(345;\bar{\phi})g(45;\bar{\phi})+O(\lambda^2) \qquad (493)
\end{aligned}$$

where we have used Eqs. (483) and (472). Similarly the fifth term of (492) is written with Eqs. (483) and (484) as

$$\begin{aligned}
& \frac{\lambda}{2}G(12)S^{(3)}(123;\bar{\phi})(\phi_c(3)-\bar{\phi}(3)) \\
= \quad & \frac{\lambda^2}{4}S^{(3)}(123;\bar{\phi})S^{(3)}(456;\bar{\phi})g(12;\bar{\phi})g(34;\bar{\phi})g(56;\bar{\phi})+O(\lambda^3). \qquad (494)
\end{aligned}$$

Thus we obtain the sum of fourth, fifth and sixth term in the following,

$$\begin{aligned}
& -\frac{1}{2}\left(S^{(2)}(12;\bar{\phi})K(12)\right)(\phi_c(1)-\bar{\phi}(1))(\phi_c(2)-\bar{\phi}(2)) \\
& -\frac{1}{2}G(12)S^3(123;\bar{\phi})(\phi_c(3)-\bar{\phi}(3))+W_2[J,K] \\
= \quad & \frac{\lambda^2}{8}S^{(4)}(1234;\bar{\phi})G(12)G(34) \\
& +\frac{\lambda^2}{12}S^{(3)}(123;\bar{\phi})S^{(3)}(456;\bar{\phi})G(14)G(25)G(36)+O(\lambda^3). \qquad (495)
\end{aligned}$$

Here we notice that 2 particle reducible diagram cancels to vanish and only 2 particle irreducible diagrams are left.

Finally by setting $\lambda=1$, $\Gamma[\bar{\phi},G]$ can be expressed up to $O(\lambda^2)$ as

$$\begin{aligned}
\Gamma[\bar{\phi},G] \quad &= \quad S[\bar{\phi}]-\frac{1}{2}\mathrm{Tr}\ln\left(G^{-1}\cdot G_0\right)+\frac{1}{2}\mathrm{Tr}\left(G\cdot S^{(2)}(\bar{\phi})+1\right)+\Gamma_{2\mathrm{PI}}[\bar{\phi},G] \\
\Gamma_{2\mathrm{PI}} \quad &\equiv \quad \frac{1}{8}S^{(4)}(1234;\bar{\phi})G(12)G(34) \\
& \quad +\frac{1}{12}S^{(3)}(123;\bar{\phi})S^{(3)}(456;\bar{\phi})G(14)G(25)G(36). \qquad (496)
\end{aligned}$$

We can also derive 2PI diagrams with higher order loop by extracting $O(\lambda^3)$ terms [74].

B The soft gluon polarization tensor

In this appendix we derive the gluon polarization tensor (self-energy) $\Pi^{ab}_{\mu\nu}$ up to one-loop order. Figure 83 shows four diagrams which contribute to one-loop polarization tensor. Let us take the hard thermal loop (HTL) approximation where the internal lines carry the hard loop momenta $k \sim T$ while the external lines carry the soft momenta $p \sim gT$ that is negligible compared to k ($p \ll k$). We can omit color indices since all internal lines are thermalized and the color structure of this tensor is trivial, $\Pi^{ab}_{\mu\nu} = \delta^{ab}\Pi_{\mu\nu}$. In this appendix we analyze the thermal loop in the Feynman gauge (i.e. , $G[A] = \partial A$ with $\lambda = 1$). The final result for the HTL will be gauge-independent.

B.1 The quark loop

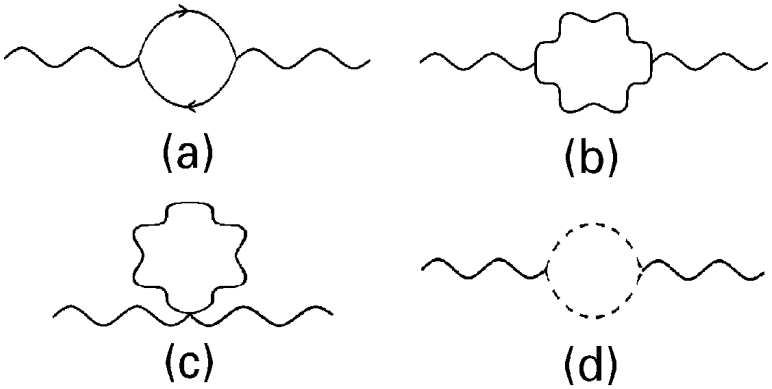

Figure 83: 1-loop polarization tensor for gluons [68].

First let us calculate the contribution for the quark loop in Fig.83a, which we express $\Pi^{(a)}_{\mu\nu}$. Feynman rules for the Lagrangian in the imaginary time formalism give for N_f quark flavors,

$$\Pi^{(a)}_{\mu\nu}(i\omega_n, \mathbf{p}) = \frac{g^2 N_f}{2}\int\frac{d^dk}{(2\pi)^d}T\sum_r \mathrm{tr}\,\{\gamma_\mu S_0(i\omega_r, \mathbf{k})\gamma_\nu S_0(i\omega_r - i\omega_n, \mathbf{k}-\mathbf{p})\} \tag{497}$$

where $p_0 = i\omega_n = i2n\pi T$ and $k_0 = i\omega_r = i(2r+1)\pi T$ with integers n and r. The trace in (497) refers to spin variables only. By use of the identity

$$T\sum_n e^{i\omega_n\tau} = \sum_l (\pm 1)^l \delta(\tau - l\beta) \tag{498}$$

we can expand $\Pi^{(a)}_{\mu\nu}$ as follows,

$$\begin{aligned}
\Pi^{(a)}_{\mu\nu} &= \frac{g^2N_f}{2}\int\frac{d^dk}{(2\pi)^d}T\sum_r\int_0^\beta d\tau e^{-i\omega_r\tau}\int_0^\beta d\tau' e^{-i(\omega_r-\omega_n)\tau'}\mathrm{tr}\,\{\gamma_\mu S_0(\tau,\mathbf{k})\gamma_\nu S_0(\tau',\mathbf{k}-\mathbf{p})\} \\
&= \frac{g^2N_f}{2}\int\frac{d^dk}{(2\pi)^d}\int_0^\beta d\tau\int_0^\beta d\tau'\sum_l\delta(\tau+\tau'-l\beta)e^{i\omega_n\tau'}\mathrm{tr}\,\{\gamma_\mu S_0(\tau,\mathbf{k})\gamma_\nu S_0(\tau',\mathbf{k}-\mathbf{p})\} \\
&= \frac{g^2N_f}{2}\int\frac{d^dk}{(2\pi)^d}\int_0^\beta d\tau e^{i\omega_n(\beta-\tau)}\mathrm{tr}\,\{\gamma_\mu S_0(\tau,\mathbf{k})\gamma_\nu S_0(\beta-\tau,\mathbf{k}-\mathbf{p})\} \\
&= \frac{g^2N_f}{2}\int\frac{d^dk}{(2\pi)^d}\int_0^\beta d\tau e^{i\omega_n\tau}\mathrm{tr}\,\{\gamma_\mu S_0(\beta-\tau,\mathbf{k})\gamma_\nu S_0(\tau,\mathbf{k}-\mathbf{p})\}\,.
\end{aligned} \tag{499}$$

Then let us use the following relation of the quark Green's function,

$$S_0(\tau,\mathbf{k})\int_{-\infty}^{\infty}\frac{dk_0}{2\pi}e^{-k_0\tau}\rho_0(k)(k^\mu\gamma_\mu+m)(\theta(\tau)-f_q(k_0)) \tag{500}$$

where $\rho_0(k)$ represents the spectral function of the quarks and $f_q(k_0)=\frac{1}{e^{\beta k_0}+1}$. By using the Eq. (500) we encounter the integral

$$\begin{aligned}\int_0^\beta d\tau e^{i\omega_n\tau}e^{-k_0(\beta-\tau)}e^{-q_0\tau} &= \int_0^\beta e^{-\beta k_0+\tau(i\omega_n+k_0-q_0)}\\ &= \frac{e^{-\beta q_0}-e^{-\beta k_0}}{k_0-q_0+i\omega_n}\end{aligned} \tag{501}$$

and the relation

$$(1-f_q(k_0))(1-f_q(q_0))(e^{-\beta q_0}-e^{-\beta k_0})=f_q(q_0)-f_q(k_0) \tag{502}$$

By using the above relations (500), (501) and (502), we can expand $\Pi^{(a)}_{\mu\nu}$ in the following way,

$$\begin{aligned}\Pi^{(a)}_{\mu\nu}(i\omega_n,\mathbf{p}) &= -\frac{g^2N_f}{2}\int\frac{d^dk}{(2\pi)^d}\int_0^\beta d\tau e^{i\omega_n\tau}\int_{-\infty}^{\infty}\frac{dk_0}{2\pi}e^{-k_0(\beta-\tau)}\rho_0(k)(1-f_q(k_0))\\ &\quad\int_{-\infty}^{\infty}\frac{dq_0}{2\pi}e^{-q_0\tau}\rho(q_0)(1-f_q(q_0))k^\rho q^\sigma\mathrm{tr}\left\{\gamma_\mu\gamma_\rho\gamma_\nu\gamma_\sigma\right\}\\ &= -\frac{g^2N_f}{2}\int\frac{d^dk}{(2\pi)^d}\int_{-\infty}^{\infty}\frac{dk_0}{2\pi}\int_{-\infty}^{\infty}\frac{dq_0}{2\pi}\frac{e^{\beta q_0}-e^{\beta k_0}}{k_0-q_0+i\omega_n}\rho_0(k)(1-f_q(k_0))\\ &\quad\rho(q_0)(1-f_q(q_0))k^\rho q^\sigma\mathrm{tr}\left\{\gamma_\mu\gamma_\rho\gamma_\nu\gamma_\sigma\right\}\\ &= -\frac{g^2N_f}{2}\int\frac{d^dk}{(2\pi)^d}\int_{-\infty}^{\infty}\frac{dk_0}{2\pi}\int_{-\infty}^{\infty}\frac{dq_0}{2\pi}\frac{1}{k_0-q_0+i\omega_n}\rho_0(k)\rho(q_0)(f_q(q_0)-f_q(k_0))\\ &\quad k^\rho q^\sigma\mathrm{tr}\left\{\gamma_\mu\gamma_\rho\gamma_\nu\gamma_\sigma\right\}\end{aligned} \tag{503}$$

where $\mathbf{q}=\mathbf{k}-\mathbf{p}$. Equation (503) can be continued in the complex energy plane by replacing $\imath\omega_n\to p_0$ with p_0 being the complex:

$$\begin{aligned}\Pi^{(a)}_{\mu\nu}(p_0,\mathbf{p}) &= \frac{g^2N_f}{2}\int\frac{d^dk}{(2\pi)^d}\int_{-\infty}^{\infty}\frac{dk_0}{2\pi}\int_{-\infty}^{\infty}\frac{dq_0}{2\pi}\rho_0(k)\rho(q)\\ &\quad k^\rho q^\sigma\mathrm{tr}(\gamma_\mu\gamma_\rho\gamma_\nu\gamma_\sigma)\frac{f_q(k_0)-f_q(q_0)}{k_0-q_0+p_0}.\end{aligned} \tag{504}$$

By using the relation

$$\mathrm{tr}(\gamma_\mu\gamma_\rho\gamma_\nu\gamma_\sigma)=4(g_{\mu\rho}g_{\nu\sigma}-g_{\mu\nu}g_{\rho\sigma}+g_{\mu\sigma}g_{\rho\nu}), \tag{505}$$

we obtain the relation;

$$\begin{aligned}\Pi^{(a)}_{\mu\nu}(p_0,\mathbf{p}) &= 2g^2N_f\int\frac{d^dk}{(2\pi)^d}\int_{-\infty}^{\infty}\frac{dk_0}{2\pi}\int_{-\infty}^{\infty}\frac{dq_0}{2\pi}\rho_0(k)\rho(q)\\ &\quad(k_\mu q_\nu+q_\mu k_\nu-g_{\mu\nu}k\cdot q)\frac{f_q(k_0)-f_q(q_0)}{k_0-q_0+p_0}.\end{aligned} \tag{506}$$

Then let us consider $\{ij\}$ components of the polarization tensor;

$$\begin{aligned}
\Pi_{ij}^{(a)}(p_0,\mathbf{p}) &= 2g^2N_f\int\frac{d^dk}{(2\pi)^d}\int\frac{dk_0}{2\pi}\int\frac{dq_0}{2\pi}2\pi\varepsilon(k_0)\delta(k_0^2-\epsilon_k^2)2\pi\varepsilon(q_0)\delta(q_0^2-\epsilon_q^2)\\
&\quad [k_iq_j+q_ik_j-\delta_{ij}\mathbf{k}\cdot\mathbf{q}+\delta_{ij}k_0q_0]\,\frac{f_q(k_0)-f_q(q_0)}{k_0-q_0-p_0}\\
&= 2g^2N_f\int\frac{d^dk}{(2\pi)^d}\int\frac{dk_0}{2\pi}\int\frac{dq_0}{2\pi}(2\pi)^2\frac{1}{2\epsilon_k^2 2\epsilon_q^2}(\delta(k_0-\epsilon_k)-\delta(k_0+\epsilon_k))\\
&\quad (\delta(q_0-\epsilon_q)-\delta(q_0+\epsilon))\,[k_iq_j+q_ik_j-\delta_{ij}\mathbf{k}\cdot\mathbf{q}+\delta_{ij}k_0q_0]\,\frac{f_q(k_0)-f_q(q_0)}{k_0-q_0-p_0}\\
&= \frac{g^2N_f}{2}\int\frac{d^dk}{(2\pi)^d}\frac{1}{\epsilon_k\epsilon_q}\Bigg\{(k_iq_j+q_ik_j-\delta_{ij}\mathbf{k}\cdot\mathbf{q}+\delta\epsilon_k\epsilon_q)\frac{f_q(\epsilon_k)-f_q(\epsilon_q)}{\epsilon_k-\epsilon_q+p_0}\\
&\quad -(k_iq_j+q_ik_j-\delta_{ij}\mathbf{k}\cdot\mathbf{q}-\delta_{ij}\epsilon_k\epsilon_q)\frac{f_q(\epsilon_k)-1+f_q(\epsilon_q)}{\epsilon_k+\epsilon_q+p_0}\\
&\quad -(k_iq_j+q_ik_j-\delta_{ij}\mathbf{k}\cdot\mathbf{q}-\delta_{ij}\epsilon_k\epsilon_q)\frac{1-f_q(\epsilon_k)-f_q(\epsilon_q)}{-\epsilon_k-\epsilon_q+p_0}\\
&\quad +(k_iq_j+q_ik_j-\delta_{ij}\mathbf{k}\cdot\mathbf{q}+\delta_{ij}\epsilon_k\epsilon_q)\frac{(1-f_q(\epsilon_k))-(1-f_q(\epsilon_q))}{-\epsilon_k+\epsilon_q+p_0}\Bigg\}
\end{aligned}\tag{507}$$

where we have used the relation

$$n(\epsilon_k)=\frac{1}{e^{-\beta\epsilon_k}+1}=\frac{e^{\beta\epsilon_k}+1-1}{e^{\beta\epsilon_k}+1}=1-f_q(\epsilon_k).\tag{508}$$

Finally Eq. (507) can be rewritten as

$$\begin{aligned}
\Pi_{ij}^{(a)}(p_0,\mathbf{p}) = \frac{g^2N_f}{2}\int\frac{d^dk}{(2\pi)^d}\frac{1}{\epsilon_k\epsilon_q}\Bigg\{&[k_iq_j+q_ik_j+\delta_{ij}(\epsilon_k\epsilon_q-\mathbf{k}\cdot\mathbf{q})]\\
&\left(\frac{f_q(\epsilon_k)-f_q(\epsilon_q)}{\epsilon_k-\epsilon_q+p_0}+\frac{f_q(\epsilon_k)-f_q(\epsilon_q)}{\epsilon_k-\epsilon_q-p_0}\right)\\
&+[k_iq_j+q_ik_j-\delta_{ij}(\epsilon_k\epsilon_q+\mathbf{k}\cdot\mathbf{q})]\\
&\left(\frac{1-f_q(\epsilon_k)-f_q(\epsilon_q)}{\epsilon_k-\epsilon_q+p_0}+\frac{1-f_q(\epsilon_k)-f_q(\epsilon_q)}{\epsilon_k+\epsilon_q-p_0}\right)
\end{aligned}\tag{509}$$

where we should remove the $T\to 0$ part ${\Pi_{ij}^{(a)}}_{T\to 0}(p)$ since it is UV divergent for $d\geq 1$.

$${\Pi_{ij}^{(a)}}_{T\to 0}(p)=\frac{g^2N_f}{2}\int\frac{d^dk}{(2\pi)^d}\frac{k_iq_j+q_ik_j-\delta_{ij}(\epsilon_k\epsilon_q+\mathbf{k}\cdot\mathbf{q})}{\epsilon_k\epsilon_q}\left(\frac{1}{\epsilon_k+\epsilon_q-p_0}+\frac{1}{\epsilon_k+\epsilon_q+p_0}\right)\tag{510}$$

We discuss only the thermal part $\Pi_T(p)$:

$$\Pi_T(p)\equiv\Pi(p)-\Pi_{T\to 0}(p).\tag{511}$$

When we remove the divergent part and apply the following separation of hard $k\sim T$ and soft mode $p\sim gT$:

$$\epsilon_q=|\mathbf{k}-\mathbf{p}|=\sqrt{\mathbf{k}^2-2\mathbf{k}\cdot\mathbf{p}+\mathbf{p}^2}\simeq|\mathbf{k}|-\frac{\mathbf{k}\cdot\mathbf{p}}{|\mathbf{k}|}=|\mathbf{k}|-\mathbf{v}\cdot\mathbf{p},\tag{512}$$

where $\mathbf{v} = \frac{\mathbf{k}}{|\mathbf{k}|}$, and then we obtain

$$\begin{aligned}
\epsilon_k + \epsilon_q \pm p_0 &= |\mathbf{k}| + |\mathbf{k}| - \mathbf{v}\cdot\mathbf{p} \pm p_0 \simeq 2|\mathbf{k}|, \\
\epsilon_k - \epsilon_q \pm p_0 &= |\mathbf{k}| - (|\mathbf{k}| - \mathbf{v}\cdot\mathbf{p}) \pm p_0 \simeq \mathbf{v}\cdot\mathbf{p} \pm p_0, \qquad (513) \\
f_q(\epsilon_k) - f_q(\epsilon_q) &\simeq -(\epsilon_q - \epsilon_k)\frac{df_q(|\mathbf{k}|)}{d|\mathbf{k}|} \simeq \mathbf{v}\cdot\mathbf{q}\frac{df_q(|\mathbf{k}|)}{d|\mathbf{k}|}, \\
1 - f_q(\epsilon_k) - f_q(\epsilon_q) &\simeq 1 - 2f_q(\epsilon_k), \qquad (514) \\
k_iq_j + q_ik_j + \delta_{ij}(\epsilon_k\epsilon_q - \mathbf{k}\cdot\mathbf{q}) &\simeq 2k_ik_j \\
k_iq_j + q_ik_j - \delta_{ij}(\epsilon_k\epsilon_q - \mathbf{k}\cdot\mathbf{q}) &\simeq 2(k_ik_j - \delta_{ij}|\mathbf{k}|^2). \qquad (515)
\end{aligned}$$

By use of the above approximation the $\Pi^{(a)}_{ij}(p)$ can be rewritten as

$$\begin{aligned}
\Pi^{(a)}_{ij}(p_0,\mathbf{p}) &= \frac{g^2N_f}{2}\int\frac{d^dk}{(2\pi)^d}\frac{1}{|\mathbf{k}|^2}\left[2k_ik_j\left(\frac{1}{\mathbf{v}\cdot\mathbf{p}+p_0} + \frac{1}{\mathbf{v}\cdot\mathbf{p}-p_0}\right)\mathbf{v}\cdot\mathbf{p}\frac{df_q(|\mathbf{k}|)}{d|\mathbf{k}|}\right. \\
&\quad \left. +2(k_ik_j - \delta_{ij}|\mathbf{k}|^2)\frac{1}{|\mathbf{k}|}(-2f_q(\mathbf{k}))\right] \\
&= -\frac{g^2N_f}{2}\int\frac{d^dk}{(2\pi)^d}\left[2v_iv_j\frac{\mathbf{v}\cdot\mathbf{p}}{\mathbf{v}\cdot\mathbf{p}-p_0}\frac{df_q(|\mathbf{k}|)}{d|\mathbf{k}|} + 4(v_iv_j - \delta_{ij})\frac{f_q(\mathbf{k})}{|\mathbf{k}|}\right]. \qquad (516)
\end{aligned}$$

In the end we use the integration of the distribution function in terms of $|\mathbf{k}|$:

$$\int_0^\infty d|\mathbf{k}|\,(|\mathbf{k}|f_q(|\mathbf{k}|)) = -\int_0^\infty\frac{|\mathbf{k}|^2}{2}\frac{df_q(|\mathbf{k}|)}{d|\mathbf{k}|} = \frac{\pi^2T^2}{12}. \qquad (517)$$

Then in the 3+1 dimension case we obtain

$$\Pi^{(a)}_{ij}(p_0,\mathbf{p}) = \frac{g^2N_fT^2}{6}\int\frac{d\Omega}{4\pi}\frac{p_0v_iv_j}{p_0 - \mathbf{v}\cdot\mathbf{p}}. \qquad (518)$$

By repeating the above calculations for Π_{00} and Π_{0i}, we obtain

$$\begin{aligned}
\Pi^{(a)}_{00}(p_0,\mathbf{p}) &= \frac{g^2N_fT^2}{6}\left[-1 + \int\frac{d\Omega}{4\pi}\frac{p_0}{p_0 - \mathbf{v}\cdot\mathbf{p}}\right]. \qquad (519) \\
\Pi^{(a)}_{0i}(p_0,\mathbf{p}) &= \Pi^{(a)}_{i0}(p_0,\mathbf{p}) = \frac{g^2N_fT^2}{6}\int\frac{d\Omega}{4\pi}\frac{p_0v_i}{p_0 - \mathbf{v}\cdot\mathbf{p}}. \qquad (520)
\end{aligned}$$

As a result by putting together (518), (519) and (520), the above relations are rewritten as

$$\Pi^{(a)}_{\mu\nu}(p_0,\mathbf{p}) = \frac{g^2N_fT^2}{6}\left[-\delta_{\mu0}\delta_{\nu0} + \int\frac{d\Omega}{4\pi}\frac{p_0v_\mu v_\nu}{p_0 - \mathbf{v}\cdot\mathbf{p}}\right], \qquad (521)$$

and we can confirm $p^\mu\Pi^{(a)}_{\mu\nu}(p_0,\mathbf{p}) = 0$.

B.2 The ghost and gluon loops

We shall evaluate the other parts of the one-loop polarization tensor which are given with one gluon or ghost loop in Figs. 83b-d. The tadpole diagram (Fig. 83c) is calculated as the local self energy in space-time:

$$\Pi^{(c)}_{\mu\nu} = -g_{\mu\nu}g^2dN\int[dk]\Delta(k) \qquad (522)$$

where $[dk] = \frac{d^dk}{(2\pi)}T\sum_n$. The factor N comes from colour trace.

The piece of the gluon loop in Fig. 83b is

$$\Pi^{(b)}_{\mu\nu}(p) = \frac{g^2 N}{2}\int [dk]\Gamma_{\sigma\mu\lambda}(-p+k,p,-k)D_0^{\lambda\rho}\Gamma^0_{\rho\nu\eta}(-k,p,-p+k)D_0^{\eta\sigma}(p-k) \tag{523}$$

where $\Gamma^0_{\mu\nu\rho}$ is the bare three-gluon vertex,

$$\Gamma^0_{\mu\nu\rho}(p,q,k) = g_{\mu\nu}(p-q)_\rho + g_{\nu\rho}(q-k)_\mu + g_{\mu\rho}(k-p)_\nu. \tag{524}$$

Before integrating in the momentum space let us reform the complicated momentum dependence of the three-point vertices[68, 141]. Since we are interested in the hard thermal loop $k \sim T$, we can use the approximation $p \sim gT \ll k \sim T$. The linear term in p in the three-gluon vertex can be ignored as

$$\begin{aligned}\Gamma^0_{\sigma\mu\lambda}(-p+k,p,-k) \simeq \Gamma^0_{\sigma\mu\lambda}(k,0,-k) &= g_{\sigma\mu}k_\lambda + g_{\mu\lambda}k_\sigma + g_{\sigma\lambda}(-2k_\mu)\\ &= -(2g_{\sigma\lambda}g_{\mu\alpha} - g_{\sigma\mu}g_{\lambda\alpha} - g_{\sigma\alpha}g_{\mu\lambda})k^\alpha\\ &= -\Gamma_{\alpha\mu\sigma\lambda}k^\alpha\end{aligned} \tag{525}$$

where we use the notation

$$\Gamma_{\mu\nu\rho\lambda} \equiv 2g_{\mu\nu}g_{\rho\lambda} - g_{\mu\rho}g_{\nu\lambda} - g_{\mu\lambda}g_{\nu\rho}. \tag{526}$$

(With respect to $p_0 = i2n\pi T$ we consider only the analytic continuation to $p_0 = \omega \sim gT$, so that $p_0 \ll k_0$ is valid in this case.) Similarly we obtain

$$\Gamma^0_{\rho\nu\eta}(-k,p,-p+k) \simeq \Gamma^0_{\rho\nu\eta}(-k,0,k) = \Gamma_{\beta\nu\rho\eta}k^\beta. \tag{527}$$

Due to the relations (525),(527) and

$$\begin{aligned}\Gamma_{\alpha\mu\sigma\lambda}\Gamma_{\beta\nu\rho\eta}g^{\lambda\rho}g^{\eta\sigma} &= (2g_{\sigma\lambda}g_{\mu\alpha} - g_{\sigma\mu}g_{\lambda\alpha} - g_{\sigma\alpha}g_{\mu\lambda})g^{\lambda\rho}g^{\eta\sigma}(2g_{\beta\nu}g_{\rho\eta} - g_{\beta\eta}g_{\rho\nu} - g_{\beta\rho}g_{\eta\nu})\\ &= (2\delta^\eta_\lambda g_{\mu\alpha} - \delta^\eta_\mu g_{\lambda\alpha} - \delta^\eta_\alpha g_{\mu\lambda})(2g_{\beta\nu}\delta^\lambda_\eta - g_{\beta\eta}\delta^\lambda_\nu - \delta^\lambda_\beta g_{\eta\nu})\\ &= 4Dg_{\mu\alpha}g_{\beta\nu} - 2g_{\mu\alpha}g_{\beta\eta}\delta^\eta_\nu - 2\delta^\eta_\beta g_{\mu\alpha}g_{\eta\nu} - 2g_{\lambda\alpha}g_{\beta\nu}\delta^\lambda_\mu + g_{\lambda\alpha}g_{\beta\mu}\delta^\lambda_\nu\\ &\quad +\delta^\eta_\mu g_{\lambda\alpha}\delta^\lambda_\beta g_{\eta\nu} - 2g_{\beta\nu}g_{\mu\lambda}\delta^\eta_\alpha\delta^\lambda_\eta + \delta^\eta_\alpha\delta^\lambda_\nu g_{\mu\lambda}g_{\beta\eta} + \delta^\eta_\alpha\delta^\lambda_\beta g_{\mu\lambda}g_{\eta\nu}\\ &= 4Dg_{\mu\alpha}g_\beta - 2g_{\mu\alpha}g_{\beta\nu} - 2g_{\mu\alpha}g_{\beta\nu} - 2g_{\mu\alpha}g_{\beta\nu} + g_{\nu\alpha}g_{\beta\mu}\\ &\quad +g_{\alpha\beta}g_{\mu\nu} - 2g_{\beta\nu}g_{\mu\alpha} + g_{\mu\nu}g_{\alpha\beta} + g_{\mu\beta}g_{\alpha\nu}\\ &= 4(D-2)g_{\mu\alpha}g_{\beta\nu} + 2g_{\alpha\beta}g_{\mu\nu} + 2g_{\mu\beta}g_{\alpha\nu}\end{aligned} \tag{528}$$

where $D = d+1$ and $D^0_{\mu\nu}(k) = -g_{\mu\nu}\Delta(k)$ in Feynman's gauge, we obtain

$$\begin{aligned}\Pi^{(b)}_{\mu\nu}(p) &\approx -\frac{g^2N}{2}\int [dk]k^\alpha k^\beta\Delta(k)\Delta(p-k)\\ &\quad [4(D-2)g_{\mu\alpha}g_{\beta\nu} + 2g_{\alpha\beta}g_{\mu\nu} + g_{\mu\beta}g_{\alpha\nu}]\\ &= -\frac{g^2N}{2}\int [dk]\Delta(k)\Delta(p-k)\left[4(D-2)k_\mu k_\nu + 2g_{\mu\nu}k^2 + 2k_\mu k_\nu\right]\\ &= -\frac{g^2N}{2}\int [dk]\Delta(k)\Delta(p-k)\left[(4D-6)k_\mu k_\nu + 2g_{\mu\nu}k^2\right].\end{aligned} \tag{529}$$

Similar analysis gives us the ghost loop in Fig. 83d where the ghost propagator is $\Delta(k)$:

$$\Pi^{(d)}_{\mu\nu} \approx g^2N\int [dk]k_\mu k_\nu\Delta(k)\Delta(p-k). \tag{530}$$

When we add together Eqs. (522), (529) and (530), we the following relation for the one-loop gluon polarization tensor $\Pi^{(g)}_{\mu\nu}$:

$$\begin{aligned}
\Pi^{(g)}_{\mu\nu}(p) &= \Pi^{(b)}_{\mu\nu} + \Pi^{(c)}_{\mu\nu} + \Pi^{(d)}_{\mu\nu} \\
&= g^2 N \int [dk] \Big\{ -\Delta(k)\Delta(p-k) \left[(2D-3) k_\mu k_\nu + g_{\mu\nu} k^2 \right] \\
&\quad -g_{\mu\nu}(D-1)\Delta(k) + k_\mu k_\nu \Delta(k)\Delta(p-k) \Big\} \\
&= g^2 N \int [dk] \left[-(2D-4)\Delta(k)\Delta(p-k) k_\mu k_\nu - g_{\mu\nu}(D-1)\Delta(k) + g_{\mu\nu}\Delta(k) \right] \\
&= -(D-2) g^2 N \int [dk] \left[2 k_\mu k_\nu \Delta(k)\Delta(p-k) + g_{\mu\nu}\Delta(k) \right]. \qquad (531)
\end{aligned}$$

We have derived the above relation in Feynamnn' gauge, but the result (531) is actually gauge-fixing independent [141]. The factor $D-2=2$ for $d=3$ case means that only the two physical transverse degrees of freedom of the hard gluons are involved in the hard thermal loop. Longitudinal gluons and ghosts cancel mutually in the calculation of (531).

let us estimate the $\{ij\}$ components of $\Pi^{(g)}_{\mu\nu}$ with the similar manner for quark loop, then

$$\begin{aligned}
\Pi^{(g)}_{ij} &= -(D-2) g^2 N \int [dk] \left[2 k_i k_j \Delta(k)\Delta(p-k) - \delta_{ij}\Delta(k) \right] \\
&= -(D-2) g^2 N \int [dk] \int \frac{dk_0}{2\pi} \int \frac{dq_0}{2\pi} \frac{e^{-\beta q_0} - e^{-\beta k_0}}{k_0 - q_0 - i\omega_n} (2 k_i k_j + k^2 \delta_{ij}) \\
&\quad \rho_0(k)\rho_0(q)(1+f_g(k_0))(1+f_g(q_0)). \qquad (532)
\end{aligned}$$

Due to the relation

$$\begin{aligned}
(1+f_g(k_0))(1+f_g(q_0))(e^{-\beta q_0} - e^{-\beta k_0}) &= \frac{e^{\beta k_0}}{e^{\beta k_0}-1} \frac{e^{\beta q_0}}{e^{\beta q_0 - 1}-1} (e^{-\beta q_0} - e^{-\beta k_0}) \\
&= (1+f_g(k_0)) f_g(q_0) - f_g(k_0)(1+f_g(q_0)) \\
&= f_g(q_0) - f_g(k_0), \qquad (533)
\end{aligned}$$

we obtain

$$\Pi^{(g)}_{\mu\nu}(p) = -(D-2) g^2 N \int \frac{d^d k}{(2\pi)^d} \int \frac{dk_0}{2\pi} \int \frac{dq_0}{2\pi} \rho_0(k)\rho_0(q) \left[2 k_i k_j + k^2 \delta_{ij} \right]. \qquad (534)$$

We can notice that the above relation resembles the first line of (507), so that we can expand similar way by changing the factor $2g^2 N_f \to (D-2) g^2 N$ as

$$\Pi^{(g)}_{ij}(p) = -(D-2) g^2 N \int \frac{d^d k}{(2\pi)^d} \left(\frac{k_i k_j}{\mathbf{k}^2} \frac{df_g}{d|\mathbf{k}|} \frac{\mathbf{v}\cdot\mathbf{p}}{\omega - \mathbf{v}\cdot\mathbf{p}} + \frac{k_i k_j - \delta_{ij}\mathbf{k}^2}{\mathbf{k^2}} \frac{f_g(k)}{|\mathbf{k}|} \right) \qquad (535)$$

Then in the case of 3+1 dimensions we can expand the relation

$$\begin{aligned}
\Pi^{(g)}_{ij}(p_0, \mathbf{p}) &= -(D-2) g^2 N \frac{\pi^2 T^2}{6} \int \frac{d\Omega}{(2\pi)^3} \left[-2 v_i v_j \frac{\mathbf{v}\cdot\mathbf{p}}{p_0 - \mathbf{v}\cdot\mathbf{p}} + (v_i v_j - \delta_{ij}) \right] \\
&= \frac{g^2 N T^2}{3} \int \frac{d\Omega}{4\pi} \frac{p_0 v_i v_j}{p_0 - \mathbf{v}\cdot\mathbf{p}}, \qquad (536)
\end{aligned}$$

where we have used the relation

$$\int_0^\infty d|\mathbf{k}| \; |\mathbf{k}| f_g(|\mathbf{k}|) = -\int_0^\infty d|\mathbf{k}| \frac{|\mathbf{k}|^2}{2} \frac{df_g(|\mathbf{k}|)}{d|\mathbf{k}|} = \frac{\pi^2 T^2}{6}. \qquad (537)$$

Similar calculations in terms of $\Pi_{00}^{(g)}$ and $\Pi_{0i}^{(g)} = \Pi_{i0}^{(g)}$ give the following self-energy with respect to the gluon propagator,

$$\Pi_{\mu\nu}^{(g)}(p_0, \mathbf{p}) \quad = \quad \frac{g^2 N T^2}{3} \left[-\delta_{0\mu}\delta_{0\nu} + \int \frac{d\Omega}{4\pi} \frac{p_0 v_\mu v_\nu}{p_0 - \mathbf{v}\cdot\mathbf{p}} \right]. \tag{538}$$

In terms of equation (538) $p^\mu \Pi_{\mu\nu}^{(g)} = 0$ is satisfied.

In the end by combining (521) and (538) we obtain the following 1-loop self energy

$$\Pi_{\mu\nu}^{1-\text{loop}}(p_0, \mathbf{p}) \quad = \quad m_D^2 \left[-\delta_{0\mu}\delta_{0\nu} + \int \frac{d\Omega}{4\pi} \frac{p_0 v_\mu v_\nu}{p_0 - \mathbf{v}\cdot\mathbf{p}} \right]. \tag{539}$$

where m_D is the Debye screening mass defined by

$$m_D^2 \equiv (2N + N_f)\frac{g^2 T^2}{6}. \tag{540}$$

C Effects of two-point source term at initial time

In this appendix we discuss the role of the two point source term $K(x,y)$ at initial time. When we consider the generating functional Z and the effective action $\Gamma_{\rm 2PI}$, we have to take into account the source term $K(x,y)$. The function $K(x,y)$ contains both external source term and initial Gaussian width for a certain initial density matrix. We can neglect the part of the external sources in the end of calculations, but must consider the part which stems from initial conditions in $K(x,y)$. To show the role of the remaining K or initial sources, we consider non-interacting massive scalar field as a simple example. The Lagrangian density is represented as $\mathcal{L} = \frac{1}{2}\partial^\mu\phi\partial_\mu\phi - \frac{1}{2}m^2\phi^2$. In this case the Schwinger-Dyson equation can be expanded as

$$\int_C dz \left[-(\partial_x^2 + m^2)\delta_C^{d+1}(x-z) + K(x,z)\right] G(z,y) = i\delta^{d+1}(x-y) \tag{541}$$

where $G(x,y)$ is a 2-point Green's function which is a 2×2 matrix and $K(x,y)$ is a 2-point sources which are also expressed by 2×2 matrix. When we define $G_0(x,y)$ from the equation

$$-(\partial_x^2 + m^2)G_0(x,y) = i\delta_C^{d+1}(x-y), \tag{542}$$

we obtain the relation from (541) expressed as

$$\begin{aligned} G(x,y) &= G_0(x,y) - \int_C du_1 du_2\; G_0(x,u_1)\frac{K(u_1,u_2)}{i}G(u_2,y) \\ &= G_0(x,y) - \int_C du_1 du_2\; G_0(x,u_1)\frac{K(u_1,u_2)}{i}G_0(u_2,y) \\ &+ \int_C du_1 du_2 du_3 du_4\; G_0(x,u_1)\frac{K(u_1,u_2)}{i}G_0(u_2,u_3)\frac{K(u_3,u_4)}{i}G_0(u_4,y) - \cdots, \end{aligned} \tag{543}$$

which is called a full 2-point Green's function. Here Green's function $G_0(x,y)$ can be written as the sum of the homogeneous solution and an inhomogeneous one

$$G_0(x,y) = G_0^{\rm in}(x,y) + G_0^{\rm hom}(x,y) \tag{544}$$

where each term should satisfy the relations

$$\begin{aligned} -(\partial_x^2 + m^2)G_0^{\rm in}(x,y) &= i\delta_C(x-y) \\ -(-\partial_x^2 + m^2)G_0^{\rm hom}(x,y) &= 0. \end{aligned} \tag{545}$$

The solutions can be written in the Fourier space as

$$G_0(p,q) = G_0(p)\delta^{d+1}(p-q), \quad G_0(p) = G_0^{\rm in}(p) + G_0^{\rm hom}(p), \tag{546}$$

where $G_0^{\rm in}(p)$ and $G_0^{\rm hom}(p)$ are expressed in the following;

$$\begin{aligned} G_0^{\rm in}(p) &= \begin{pmatrix} \frac{i}{p^2-m^2+i\epsilon} & 0 \\ 0 & \frac{-i}{p^2-m^2-i\epsilon} \end{pmatrix}, \\ G_0^{\rm hom}(p) &= 2\pi\delta(p^2-m^2)\begin{pmatrix} f_0(\mathbf{p}) & \theta(-p^0)+f_0(\mathbf{p}) \\ \theta(p^0)+f_0(\mathbf{p}) & f_0(\mathbf{p}) \end{pmatrix} \\ &= 2\pi\delta(p^2-m^2)\left[\Lambda_1 + f_0(\mathbf{p})\Lambda_2\right], \end{aligned} \tag{547}$$

with

$$\Lambda_1 = \begin{pmatrix} 0 & \theta(-p^0) \\ \theta(p^0) & 0 \end{pmatrix}, \quad \Lambda_2 = \begin{pmatrix} 1 & 1 \\ 1 & 1 \end{pmatrix}. \tag{548}$$

Since we now consider $K(x_1, x_2)$ which stems only from initial conditions of the density matrix, we can put $K^{ij}(x_1, x_2)$ in the following way:

$$K^{ij}(x_1, x_2) = K^{ij}(\mathbf{x_1} - \mathbf{x_2})\delta(x_1^0 - t_0^i)\delta(x_2^0 - t_0^j), \tag{549}$$

where $i, j = 1, 2$ and t_0^1 and t_0^2 are the starting and ending points of the Closed Time Path. When we assume the source term $K^{ij}(\mathbf{x_1} - \mathbf{x_2})$ is translationally invariant in space, we can give its Fourier transform of the source terms as

$$\begin{aligned} K^{ij}(k_1, k_2) &= \int d^{d+1}x_1 d^{d+1}x_2 K^{ij}(x_1, x_2) = K^{ij}(\mathbf{k_1})\delta^d(\mathbf{k_1} - \mathbf{k_2}), \\ K^{ij}(\mathbf{k_1}) &\equiv \int d^d y K^{ij}(\mathbf{y}) e^{-i\mathbf{k_1}\cdot\mathbf{y}}. \end{aligned} \tag{550}$$

We can now deal with the integration with respect to $u_1, u_2, \cdots, u_n$ in (543). First we pay attention to $G_0(x, u_1)$ and $G_0(u_n, x)$ which is in the leading and the end of each term. When we remember that u_1^0 and u_2^0 are t_0^1 or t_0^2, we notice that since $x^0 > t_0^1, t_0^2$ we rewrite down $G_0^{ij}(x, u_1)$ and $G_0^{ij}(u_n, y)$ as

$$G_0^{ij}(x, u_1) = \begin{pmatrix} G_0^{11}(x, u_1) & G_0^{12}(x, u_1) \\ G_0^{21}(x, u_1) & G_0^{22}(x, u_1) \end{pmatrix} \to \begin{pmatrix} G_0^{21}(x, u_1) & G_0^{12}(x, u_1) \\ G_0^{21}(x, u_1) & G_0^{12}(x, u_1) \end{pmatrix}, \tag{551}$$

and

$$G_0^{ij}(u_n, x) = \begin{pmatrix} G_0^{11}(u_n, x) & G_0^{12}(u_n, x) \\ G_0^{21}(u_n, x) & G_0^{22}(u_n, x) \end{pmatrix} \to \begin{pmatrix} G_0^{12}(u_n, x) & G_0^{12}(u_n, x) \\ G_0^{21}(u_n, x) & G_0^{21}(u_n, x) \end{pmatrix}. \tag{552}$$

Therefore by substituting $\{12\}$ and $\{21\}$ components of $G_0(p)$ in (547) the leading part $G_0^l(p)$ and the ending part $G_0^e(p)$ expressed in the Fourier space can be written in the following

$$\begin{aligned} G_0^l(p) &= 2\pi\delta(p^2 - m^2)\left[\Lambda_3 + f_0(\mathbf{p})\Lambda_2\right], \\ G_0^e(q) &= 2\pi\delta(q^2 - m^2)\left[\Lambda_4 + f_0(\mathbf{q})\Lambda_2\right], \end{aligned} \tag{553}$$

where $G_0^l(p)$ and $G_0^e(p)$ are Fourier transform of $G_0(x, u_1)$ and $G_0(u_n, y)$, respectively, and we define Λ_3 and Λ_4 as

$$\Lambda_3 = \begin{pmatrix} \theta(p^0) & \theta(-p^0) \\ \theta(p^0) & \theta(-p^0) \end{pmatrix}, \quad \Lambda_4 = \begin{pmatrix} \theta(-q^0) & \theta(-q^0) \\ \theta(q^0) & \theta(q^0) \end{pmatrix}. \tag{554}$$

Next let us consider the inner Green's functions $G_0(u_i, u_{i+1})$ in (543). Since the coordinates u_i are localized only on $t_0 = -\infty$, all 2×2 components of $G_0(u_i, u_{i+1})$ are the same one ($G_0(u_i, u_{i+1}) = \tilde{G}_0(u_i, u_{i+1})\Lambda_2$ where $\tilde{G}_0$ is not a matrix), so that (543) are expanded in the Fourier space as

$$\begin{aligned} G(p, q) &= G_0(p)\delta^{d+1}(p - q) - G_0^l(p)\sigma_z \frac{K(\mathbf{p})}{i} G_0^e(q)\delta^d(\mathbf{p} - \mathbf{q}) \\ &\quad + G_0^l(p)\sigma_z \frac{K(\mathbf{p})}{i}\sigma_z \Lambda_2 \tilde{G}_0(\mathbf{p})\sigma_z \frac{K(\mathbf{p})}{i}\sigma_z G_0^e(q)\delta^d(\mathbf{p} - \mathbf{q}) \\ &= G_0(p)\delta^{d+1}(p - q) - G_0^l(p)\mathcal{K}(\mathbf{p})G_0^e(q)\delta^d(\mathbf{p} - \mathbf{q}), \end{aligned} \tag{555}$$

where $\sigma_z = \mathrm{diag}(1, -1)$, $\tilde{G}_0(\mathbf{p}) = \int dp^0 G_0(p)$ and $\mathcal{K}(p)$ are expressed by

$$\begin{aligned} \mathcal{K}(\mathbf{p}) &= \sigma_z \frac{K(\mathbf{p})}{i}\sigma_z - \sigma_z \frac{K(\mathbf{p})}{i}\sigma_z \tilde{G}_0(\mathbf{p})\Lambda_2\sigma_z \frac{K(\mathbf{p})}{i}\sigma_z \\ &\quad + \sigma_z \frac{K(\mathbf{p})}{i}\sigma_z \tilde{G}_0(\mathbf{p})\Lambda_2\sigma_z \frac{K(\mathbf{p})}{i}\sigma_z \tilde{G}_0(\mathbf{p})\Lambda_2\sigma_z \frac{K(\mathbf{p})}{i}\sigma_z - \cdots. \\ &= \frac{\sigma_z K(\mathbf{p})\sigma_z}{i} \cdot \frac{1}{1 + \tilde{G}_0(\mathbf{p})\Lambda_2\sigma_z K(\mathbf{p})\sigma_z}. \end{aligned} \tag{556}$$

The denominator can be written as

$$\begin{aligned}
\sigma_z K(\mathbf{p})\sigma_z &= \begin{pmatrix} K^{11} & -K^{12} \\ -K^{21} & K^{22} \end{pmatrix}, \\
\Lambda_2\sigma_z K(\mathbf{p})\sigma_z &= \begin{pmatrix} K^{11}-K^{21} & -K^{12}+K^{22} \\ K^{11}-K^{21} & -K^{12}+K^{22} \end{pmatrix}, \\
1+\tilde{G}_0(\mathbf{p})\Lambda_2\sigma_z K(\mathbf{p})\sigma_z &= \begin{pmatrix} 1+\tilde{G}_0(\mathbf{p})\left(K^{11}-K^{21}\right) & \tilde{G}_0(\mathbf{p})\left(-K^{12}+K^{22}\right) \\ \tilde{G}_0(\mathbf{p})\left(K^{11}-K^{21}\right) & 1+\tilde{G}_0(\mathbf{p})\left(-K^{12}+K^{22}\right) \end{pmatrix} \\
&= \begin{pmatrix} 1+AB_2 & AB_2 \\ AB_1 & 1+AB_2 \end{pmatrix}. \qquad (557)
\end{aligned}$$

Here we define

$$\begin{aligned}
&A \equiv \tilde{G}_0(\mathbf{p}), \quad B_1 \equiv K^{11}(\mathbf{p}) - K^{21}(\mathbf{p}), \quad B_2 \equiv K^{22}(\mathbf{p}) - K^{12}(\mathbf{p}) \\
&C^{-1} \equiv (1+AB_2)(1+AB_2) - AB_1 \cdot AB_2 = 1 + A(B_1+B_2). \qquad (558)
\end{aligned}$$

Then we obtain

$$\left(1+\tilde{G}_0(\mathbf{p})\Lambda_2\sigma_z K(\mathbf{p})\sigma_z\right)^{-1} = C\begin{pmatrix} 1+AB_2 & -AB_2 \\ -AB_1 & 1+AB_1 \end{pmatrix}, \qquad (559)$$

and

$$\begin{aligned}
\mathcal{K}(\mathbf{p}) &= \frac{\sigma_z K(\mathbf{p})\sigma_z}{i}\cdot\frac{1}{1+\tilde{G}_0(\mathbf{p})\Lambda_2\sigma_z K(\mathbf{p})\sigma_z} \\
&= \frac{1}{i}\begin{pmatrix} K^{11} & -K^{12} \\ -K^{21} & K^{22} \end{pmatrix} C \begin{pmatrix} 1+AB_2 & -AB_2 \\ -AB_1 & 1+AB_1 \end{pmatrix} \\
&= \frac{C}{i}\begin{pmatrix} (1+AB_2)K^{11}+AB_1K^{12} & -AB_2K^{11}-(1+AB_1)K^{12} \\ -(1+AB_2)K^{21}-AB_1K^{22} & AB_2K^{21}+(1+AB_1)K^{22} \end{pmatrix}. \qquad (560)
\end{aligned}$$

Now we need to calculate $-G_0^l(p)\mathcal{K}(\mathbf{p})G_0^e(q)\delta^d(\mathbf{p}-\mathbf{q}) = I_1+I_2+I_3$ in (555) which has the components $I_1 \equiv -(2\pi i)^2\delta(p^2-m^2)\delta(q^2-m^2)\Lambda_3\mathcal{K}(\mathbf{p})\ \Lambda_4\delta^d(\mathbf{p}-\mathbf{q})$, $I_2 \equiv -(2\pi i)^2\delta(p^2-m^2)\delta(q^2-m^2)f_0(\mathbf{p})(\Lambda_3\mathcal{K}(\mathbf{p})\Lambda_2+\Lambda_2\mathbf{K}(\mathbf{p})\Lambda_4)\delta^d(\mathbf{p}-\mathbf{q})$ and $I_3 \equiv -(2\pi i)^2\delta(p^2-m^2)\delta(q^2-m^2)\ \left(f_0(\mathbf{p})\right)^2\ \Lambda_2\ \mathcal{K}(\mathbf{p})\ \Lambda_2\ \delta^d(\mathbf{p}-\mathbf{q})$. By use of

$$\delta(p^2-m^2)\delta(q^2-m^2)\delta^d(\mathbf{p}-\mathbf{q}) = \delta(p^2-m^2)\frac{1}{2E_\mathbf{p}}\left[\delta(p^0-q^0)+\delta(p^0+q^0)\right] \qquad (561)$$

and the properties of the initial conditions of the density matrix, $K^{11}=K^{22}$ and $K^{12}=K^{21}$ which implies $\mathcal{K}^{11}=\mathcal{K}^{22}$ and $\mathcal{K}^{21}=\mathcal{K}^{12}$, we can calculate I_1 as

$$\begin{aligned}
I_1 &\equiv -(2\pi i)^2\delta(p^2-m^2)\delta(q^2-m^2)\Lambda_3\mathcal{K}(\mathbf{p})\Lambda_4\delta^d(\mathbf{p}-\mathbf{q}) \\
&= (2\pi)^2\delta(p^2-m^2)\delta(q^2-m^2)\delta^d(\mathbf{p}-\mathbf{q})\Big[(\theta(p^0)\theta(-q^0)+\theta(-p^0)\theta(q^0))\mathcal{K}^{11} \\
&\quad +(\theta(-p^0)\theta(-q^0)+\theta(p^0)\theta(q^0))\mathcal{K}^{12}\Big]\Lambda_2 \\
&= 8\pi^2\delta^d(\mathbf{p}-\mathbf{q})\delta(p^2-m^2)\frac{1}{2E_\mathbf{p}}\left(\mathcal{K}^{11}\delta(p^0+q^0)+\mathcal{K}^{12}\delta(p^0-q^0)\right)\Lambda_2 \\
&= I_0\left(\mathcal{K}^{11}\delta(p^0+q^0)+\mathcal{K}^{12}\delta(p^0-q^0)\right)\Lambda_2 \qquad (562)
\end{aligned}$$

where we define

$$I_0 \equiv 8\pi^2\delta^d(\mathbf{p}-\mathbf{q})\delta(p^2-m^2)\frac{1}{2E_\mathbf{p}}. \qquad (563)$$

In the similar way I_2 and I_3 can be calculated as

$$I_2 = I_0 f_0(\mathbf{p}) \left(\mathcal{K}^{11} + \mathcal{K}^{12}\right) \left[\delta(p^0 - q^0) + \delta(p^0 + q^0)\right] \Lambda_2, \tag{564}$$

$$I_3 = I_0 \left[f_0(\mathbf{p})\right]^2 \left(\mathcal{K}^{11} + \mathcal{K}^{12}\right) \left[\delta(p^0 - q^0) + \delta(p^0 + q^0)\right] \Lambda_2. \tag{565}$$

As a result $G(p,q)$ in (555) becomes

$$\begin{aligned} G(p,q) &= G_0(p)\delta^{d+1}(p-q) + I_1 + I_2 + I_3 \\ &= \left[G_0^{\rm in}(p) + 2\pi\delta(p^2 - m^2)\left(\Lambda_1 + f(\mathbf{p})\Lambda_2\right)\right]\delta^{d+1}(p-q) \\ &\quad + 2\pi\delta(p^2 - m^2) f'(\mathbf{p})\Lambda_2 \delta(p^0 + q^0)\delta^d(\mathbf{p} - \mathbf{q}), \end{aligned} \tag{566}$$

where $f(\mathbf{p})$ and $f'(\mathbf{p})$ are expressed as

$$\begin{aligned} f(\mathbf{p}) &= f_0(\mathbf{p}) + i\frac{2\pi i}{E_{\mathbf{p}}}\left[\mathcal{K}^{12}(\mathbf{p}) + \left(f_0(\mathbf{p}) + (f_0(\mathbf{p}))^2\right)\left(\mathcal{K}^{11}(\mathbf{p} + \mathcal{K}^{12}(\mathbf{p}))\right)\right], \\ f'(\mathbf{p}) &= \frac{2\pi i}{E_{\mathbf{p}}}\left[\mathcal{K}^{11}(\mathbf{p}) + \left(f_0(\mathbf{p}) + (f_0(\mathbf{p}))^2\right)\left(\mathcal{K}^{11}(\mathbf{p}) + \mathcal{K}^{12}(\mathbf{p})\right)\right]. \end{aligned} \tag{567}$$

The second term proportional to $\delta(p^0+q^0)$ which produces time dependence in $G(x,y) \propto e^{-ip^0(x^0+y^0-2t_0)}$ vanishes for finite x^0, y^0 and $t_0 = -\infty$, so that in the end we obtain

$$G(p,q)\left[G_0^{\rm in}(p) + 2\pi\delta(p^2 - m^2)\left(\Lambda_1 + f(\mathbf{p})\Lambda_2\right)\right]\delta^{d+1}(p-q). \tag{568}$$

We see that the information of $K(\mathbf{p})$ which is singular only at $x^0 = y^0 = t_0$ is included in the definition of $f(\mathbf{p})$. Therefore in substituting proper initial conditions for $f(p)$, the initial condition of the density matrix never affect the time evolution of the Kadanoff-Baym equation.

D Microscopic processes in the Kadanoff-Baym equation

The evolution of the particle number distribution can be understood in terms of the microscopic processes in the quasi-particle approximation. See [89, 173] for a similar discussion.

First, we differentiate the distribution $n_{\mathbf{p}}$ defined in Eq. (72) with respect to the time t to find

$$\begin{aligned}\left(\frac{1}{2}+n_{\mathbf{p}}\right)\partial_t n_{\mathbf{p}} &= \int_{t_0}^{t} dz^0 \Big\{ \left[\Sigma_\rho(t,z^0;\mathbf{p})F(z^0,t;\mathbf{p}) - \Sigma_F(t,z^0;\mathbf{p})\rho(z^0,t;\mathbf{p})\right]\partial_t F(t,t';\mathbf{p})|_{t=t'} \\ &\quad - \left[\Sigma_\rho(t,z^0;\mathbf{p})\partial_t F(z^0,t;\mathbf{p}) - \Sigma_F(t,z^0;\mathbf{p})\partial_t\rho(z^0,t;\mathbf{p})\right]F(t,t;\mathbf{p})\Big\}. \qquad (569)\end{aligned}$$

Meaning of the memory integrals on the RHS of Eq. (569) becomes clear if we take the quasi-particle limit for ρ and F as given in Eqs. (58) and (59). We find $\rho(t,t';\mathbf{p}) = \tilde{\omega}(\mathbf{p})^{-1}\sin[(\tilde{\omega}(\mathbf{p})(t-t')]$ and $F(t,t';\mathbf{p}) = \tilde{\omega}(\mathbf{p})^{-1}\cos[\tilde{\omega}(\mathbf{p})(t-t')](n_{\mathbf{p}}+\frac{1}{2})$. We substitute these to the self-energy Σ_ρ and Σ_F at the NLO in Eq. (569) and obtain the following expression:

$$\begin{aligned}\partial_t n_{\mathbf{p}}(t) &= \frac{\lambda^2}{3}\int\frac{d^d\mathbf{q}}{(2\pi)^d}\frac{d^d\mathbf{k}}{(2\pi)^d}\int_{t_0}^{t}dt'\frac{1}{2\tilde{\omega}(\mathbf{p})2\tilde{\omega}(\mathbf{q})2\tilde{\omega}(\mathbf{k})2\tilde{\omega}(\mathbf{p}-\mathbf{k}-\mathbf{q})} \\ &\quad \Big\{ \left[(1+n_{\mathbf{p}})(1+n_{\mathbf{q}})(1+n_{\mathbf{k}})(1+n_{\mathbf{p}-\mathbf{k}-\mathbf{q}}) - n_{\mathbf{p}}n_{\mathbf{q}}n_{\mathbf{k}}n_{\mathbf{p}-\mathbf{k}-\mathbf{q}}(t')\right] \\ &\quad\times \cos\left[(\tilde{\omega}(\mathbf{p})+\tilde{\omega}(\mathbf{q})+\tilde{\omega}(\mathbf{k})+\tilde{\omega}(\mathbf{p}-\mathbf{k}-\mathbf{q}))(t-t')\right] \\ &\quad +3\left[(1+n_{\mathbf{p}})(1+n_{\mathbf{q}})(1+n_{\mathbf{k}})n_{\mathbf{p}-\mathbf{k}-\mathbf{q}} - n_{\mathbf{p}}n_{\mathbf{q}}n_{\mathbf{k}}(1+n_{\mathbf{p}-\mathbf{k}-\mathbf{q}})(t')\right] \\ &\quad\times \cos\left[(\tilde{\omega}(\mathbf{p})+\tilde{\omega}(\mathbf{q})+\tilde{\omega}(\mathbf{k})-\tilde{\omega}(\mathbf{p}-\mathbf{k}-\mathbf{q}))(t-t')\right] \\ &\quad +3\left[(1+n_{\mathbf{p}})(1+n_{\mathbf{q}})n_{\mathbf{k}}n_{\mathbf{p}-\mathbf{k}-\mathbf{q}} - n_{\mathbf{p}}n_{\mathbf{q}}(1+n_{\mathbf{k}})(1+n_{\mathbf{p}-\mathbf{k}-\mathbf{q}})(t')\right] \\ &\quad\times \cos\left[(\tilde{\omega}(\mathbf{p})+\tilde{\omega}(\mathbf{q})-\tilde{\omega}(\mathbf{k})-\tilde{\omega}(\mathbf{p}-\mathbf{k}-\mathbf{q}))(t-t')\right] \\ &\quad +\left[(1+n_{\mathbf{p}})n_{\mathbf{q}}n_{\mathbf{k}}n_{\mathbf{p}-\mathbf{k}-\mathbf{q}} - n_{\mathbf{p}}(1+n_{\mathbf{q}})(1+n_{\mathbf{k}})(1+n_{\mathbf{p}-\mathbf{k}-\mathbf{q}})(t')\right] \\ &\quad\times \cos\left[(\tilde{\omega}(\mathbf{p})-\tilde{\omega}(\mathbf{q})-\tilde{\omega}(\mathbf{k})-\tilde{\omega}(\mathbf{p}-\mathbf{k}-\mathbf{q}))(t-t')\right]\Big\}. \qquad (570)\end{aligned}$$

We can interpret physically each microscopic process in the bracket $\{\cdots\}$ of Eq. (570). The first term represents creation and annihilation processes of four particles $0 \leftrightarrow 4$. The second term describes the process $1 \to 3$ where $n_{\mathbf{p}}$ is involved as one of the three particles and its reverse. The third term corresponds to $2 \leftrightarrow 2$ scattering process. The last term describes the decay of $n_{\mathbf{p}}$ to 3 particles and its reverse.

The number changing processes are allowed because of the finite memory time $t-t'$; the energy conservation in each microscopic process can be violated [173]. We evaluated these contributions and showed then in Figs. 19, 20, 21 and 22 in Sec. 3.4. Oscillatory behaviors seen in these figures obviously come from cos functions. Removing the memory time effect by taking the infinite time limit $t - t_0 \to \infty$, we recover the strict energy conservation in the microscopic process, $\lim_{t-t_0\to\infty}\int_{t_0}^{t}dt'\cos(\omega(t-t')) = \pi\delta(\omega)$. In this limit only the $2 \leftrightarrow 2$ scatterings are allowed and then we obtain the Boltzmann equation (74).

E Entropy from 2PI effective action at thermal equilibrium

In this appendix we derive the entropy density at thermal equilibrium from the thermodynamic potential. The derivation is based on Refs. [170, 171]. The entropy is given by differentiating 2PI effective action or thermodynamic potential with respect to temperature T. We will find that the derived entropy in ϕ^4 theory corresponds to the kinetic entropy (91) at thermal equilibrium in the range of three loop order skeleton expansion.

First we start with scalar field theories with interactions $\mathcal{L}_{\rm int} = -\frac{g}{3!}\hat{\phi}^3 - \frac{\lambda}{4!}\hat{\phi}^4$ as a toy model and present the general framework in systems with cubic and quadratic interactions. This discussion can be extended to the case of non-Abelian gauge theories by changing $\frac{g}{3!} \to \Gamma^{(0)}_{mnp}(a^3)$ and $\frac{\lambda}{4!} \to \Gamma^{(0)}_{mnpq}(a^4)$ in Sec. 6.1. We adopt the imaginary time formalism in the following discussions.

The thermodynamic potential $\Omega = -PV$, which corresponds to the 2PI effective action, of the scalar field can be written as the following functional of the full Green's function D [70, 74]:

$$\beta\Omega[D] = -\log Z = \frac{1}{2}{\rm Tr}\log D^{-1} - \frac{1}{2}{\rm Tr}\Pi D + \frac{1}{2}\Phi[D], \tag{571}$$

where Z represents the generating function, Tr denotes the trace in configuration space, $\beta = \frac{1}{T}$, $\frac{1}{2}\Phi[D]$ is the infinite series of two-particle-irreducible skeletons depicted in Fig.84 and the self-energy Π is defined by

$$\Pi \equiv \frac{\delta\Phi[D]}{\delta D}. \tag{572}$$

The self-energy Π is related to Green's function D by the Schwinger-Dyson equation $D^{-1} =$

Figure 84: 2PI skeleton expansions with cubic and quadratic interactions [170].

$D_0^{-1} + \Pi$, where D_0^{-1} is the bare Green's function, and this relation is derived by imposing the stationary condition for the thermodynamic potential Ω:

$$\delta\Omega[D]/\delta D = 0. \tag{573}$$

We only consider thermodynamic potential at the stationary point in the following analyses.

The thermodynamic potential $\Omega[D]$ can be expanded in the momentum space as

$$\Omega/V = \int \frac{d^{d+1}k}{(2\pi)^{d+1}} f(k^0)\left[{\rm Im}\,\log(D^{-1}) - {\rm Im}\Pi D\right] + \frac{T\Phi[D]}{2V}, \tag{574}$$

where $d+1$ is the number of space-time dimensions, $f(k^0) = 1/(e^{\beta k^0} - 1)$, the summation with Matsubara frequencies can be converted to the integration with k^0 times $f(k^0)$ by using standard contour integration techniques.

The analytic Green's function $D(k)$ can be expressed in terms of the spectral function;

$$D(k^0, \mathbf{k}) = \int_{-\infty}^{\infty} \frac{dq^0}{(2\pi)} \frac{\rho(q^0, \mathbf{k})}{q^0 - k^0} \tag{575}$$

and we define, for real k^0,

$${\rm Im}D(k^0, \mathbf{k}) \equiv {\rm Im}D(k^0 + i\epsilon, \mathbf{k}) = \frac{\rho(k^0, \mathbf{k})}{2}, \tag{576}$$

and

$$\mathrm{Re}D(k^0,\mathbf{k}) \equiv \mathrm{Re}D(k^0+i\epsilon,\mathbf{k}) = \mathrm{Re}D_R(k^0,\mathbf{k}). \tag{577}$$

The real and imaginary parts for Π are defined in the similar way.

Next we shall derive entropy density $\mathcal{S}$ by differentiating Ω by T:

$$\mathcal{S} = -\frac{\partial \Omega/V}{\partial T}. \tag{578}$$

The thermodynamic potential, as given by Eq. (574), depends on the temperature through the distribution function $f(k^0)$ and the spectral function ρ (or analytic Green's function D). Due to the relation (573), the temperature derivative of the analytic Green's function or spectral function ρ cancels out in the entropy density and we obtain [168, 169, 170, 171]

$$\mathcal{S} = -\int \frac{d^{d+1}k}{(2\pi)^{d+1}} \frac{\partial f(k^0)}{\partial T} \mathrm{Im}\ \log D^{-1}(k) + \int \frac{d^{d+1}k}{(2\pi)^{d+1}} \frac{\partial f(k^0)}{\partial T} \mathrm{Im}\Pi(k) \mathrm{Re}D(k) + \mathcal{S}' \tag{579}$$

with

$$\mathcal{S}' = -\frac{\partial (T\Phi/V)}{\partial T} + \int \frac{d^{d+1}k}{(2\pi)^{d+1}} \frac{\partial f(k^0)}{\partial T} \mathrm{Re}\Pi(k) \mathrm{Im}D(k). \tag{580}$$

Since

$$\frac{\partial f(k^0)}{\partial T} = -\frac{\partial f(k^0)}{\partial k^0} \log \frac{1+f}{f} = -\frac{\partial \sigma(k^0)}{\partial k^0}, \tag{581}$$

where $\sigma(k^0) = -f\log f + (1+f)\log(1+f)$, we can partially integrate with respect to k^0 and obtain

$$\begin{aligned}
\mathcal{S} &= \int \frac{d^{d+1}k}{(2\pi)^{d+1}} \left[-\mathrm{Im}\left(D \frac{\partial D^{-1}}{\partial k^0} \right) + \frac{\partial}{\partial k^0} (\mathrm{Im}\Pi\ \mathrm{Re}D) \right] \sigma + \mathcal{S}' \\
&= \int \frac{d^{d+1}k}{(2\pi)^{d+1}} \left[\left(2k^0 - \frac{\partial \mathrm{Re}\Pi}{\partial k^0} \right) \mathrm{Im}D + \mathrm{Im}\Pi \frac{\partial \mathrm{Re}D}{\partial k^0} \right] \sigma + \mathcal{S}' \\
&= \int \frac{d^{d+1}k}{(2\pi)^{d+1}} \left[\left(k^0 - \frac{1}{2} \frac{\partial \mathrm{Re}\Pi_R}{\partial k^0} \right) \rho + \frac{1}{2} \frac{\partial \mathrm{Re}D_R}{\partial k^0} \Pi_\rho \right] \sigma + \mathcal{S}'
\end{aligned} \tag{582}$$

where we have used $D^{-1} = D_0^{-1} + \Pi = -k^2 + m^2 + \Pi$ and the definitions (576) and (577).

The remaining part is $\mathcal{S}'$ in the above expression. In the end we shall verify that

$$\mathcal{S}' = 0 \tag{583}$$

is satisfied for two-loop skeletons ($O(g^2)$ and $O(\lambda)$) and three-loop skeletons ($O(\lambda^2)$) with $g = 0$. Two skeletons denoted in the left and the center of Fig.84 are left in the two-loop approximation. (They correspond to the leading order skeletons in non-Abelian gauge theory.) The contribution which stems from two 3-vertices can be written as

$$\begin{aligned}
-\frac{T}{2V}\Phi^{(g^2)} &= \frac{g^2}{12} T^2 \sum_{\omega_1,\omega_2} \int \frac{d^d k_1}{(2\pi)^d} \int \frac{d^d k_2}{(2\pi)^d} D(\omega_1,\mathbf{k}_1) D(\omega_2,\mathbf{k}_2) D(-\omega_1-\omega_2, -\mathbf{k_1}-\mathbf{k_2}) \\
&= \frac{g^2}{12} \int \frac{d^{d+1}k_1}{(2\pi)^{d+1}} \int \frac{d^{d+1}k_2}{(2\pi)^{d+1}} \int \frac{d^{d+1}k_3}{(2\pi)^{d+1}} (2\pi)^d \delta^3(\mathbf{k_1}+\mathbf{k_2}+\mathbf{k_3}) \rho(k_1)\rho(k_2)\rho(k_3) \\
&\quad \times \mathbf{P} \frac{1}{k_1^0+k_2^0+k_3^0} \left[(f(k_1^0)+1)(f(k_2^0)+f(k_3^0)+1) + f(k_2^0)f(k_3^0) \right],
\end{aligned} \tag{584}$$

where $\mathbf{P}$ denotes the principal value prescription. Here we have used Eq. (575) and the following transformation with the standard contour integration in the change $\sum_{\omega_1,\omega_2,\omega_3} \to \int \frac{dk_1^0}{2\pi}\frac{dk_2^0}{2\pi}\frac{dk_3^0}{2\pi}$

$$\begin{aligned}
\frac{1}{(k_1^0-\omega_1)(k_2^0-\omega_2)(k_3+\omega_1+\omega_2)} &= \frac{1}{k_2^0-\omega_2}\frac{1}{k_1^0+k_3+\omega_2}\left[\frac{1}{k_3^0+\omega_1+\omega_2}+\frac{1}{k_1^0-\omega_1}\right] \\
&\to \frac{1}{k_2^0-\omega_2}\frac{1}{k_1^0+k_3+\omega_2}\left(f(k_1^0)-f(-k_3^0)\right) \\
&= \frac{1}{k_1^0+k_2^0+k_3^0}\left[\frac{1}{k_1^0+k_3^0+\omega_2}+\frac{1}{k_2^0-\omega_2}\right] \\
&\quad \times\left(f(k_1^0)+f(k_3^0)+1\right) \\
&\to \frac{1}{k_1^0+k_2^0+k_3^0}\left(f(k_2^0)-f(-k_1^0-k_3^0)\right)\left(f(k_1^0)+f(k_3^0)+1\right) \\
&= \frac{1}{k_1^0+k_2^0+k_3^0}\big[\left(f(k_2^0)+1\right)\left(f(k_1^0)+f(k_3^0)+1\right) \\
&\quad +f(k_1^0)f(k_3^0)\big], \qquad (585)
\end{aligned}$$

where we have used the relation

$$f(x+y)(f(x)+f(y)+1)=f(x)f(y) \qquad (586)$$

for $f(x)=\frac{1}{e^x-1}$. Similarly the two-loop skeleton involving the 4-vertex is given by the expression

$$\begin{aligned}
-\frac{T}{2V}\Phi^{(\lambda)} &= -\frac{\lambda}{8}\left(\sum_\omega\int\frac{d^dk}{(2\pi)^d}D(\omega,\mathbf{k})\right)^2 \\
&= -\frac{\lambda}{8}\int\frac{d^{d+1}k_1}{(2\pi)^{d+1}}\int\frac{d^{d+1}k_2}{(2\pi)^{d+1}}\rho(k_1)\rho(k_2)f(k_1^0)f(k_2^0) \qquad (587)
\end{aligned}$$

where the sum of the Matsubara frequency is transformed to the integration of k_1^0 and k_2^0. (Then note that temperature dependence remains only in occupation number function f.)

By differentiating by T we obtain the first component in $\mathcal{S}'$ (580) as

$$\begin{aligned}
-\frac{\partial}{\partial T}\left(\frac{T}{2V}\Phi^{(g^2)}\right) &= \frac{g^2}{4}\int\frac{d^{d+1}k_1}{(2\pi)^{d+1}}\int\frac{d^{d+1}k_2}{(2\pi)^{d+1}}\int\frac{d^{d+1}k_3}{(2\pi)^{d+1}} \\
&\quad \times\delta^d(\mathbf{k_1}+\mathbf{k_2}+\mathbf{k_3})\mathbf{P}\frac{1}{k_1^0+k_2^0+k_3^0}\frac{\partial f(k_1^0)}{\partial T} \\
&\quad \times(1+f(k_2^0)+f(k_3^0))\rho(k_1)\rho(k_2)\rho(k_3), \qquad (588)
\end{aligned}$$

and

$$-\frac{\partial}{\partial T}\left(\frac{T}{2V}\Phi^{(\lambda)}\right) = -\frac{\lambda}{4}\int\frac{d^{d+1}k_1}{(2\pi)^{d+1}}\int\frac{d^{d+1}k_2}{(2\pi)^{d+1}}f(k_1^0)\frac{\partial f(k_2^0)}{\partial T}\rho(k_1)\rho(k_2). \qquad (589)$$

The second component of $\mathcal{S}'$ (580) has the real part of the self-energy which is given by opening one line in the left two diagrams in Fig.84. The self-energy from two-loop order skeletons $O(g^2)$ and $O(\lambda)$ and its real part can be written as

$$\begin{aligned}
\Pi^{(g^2)}(\omega_n,\mathbf{q}) &= -\frac{g^2}{2}T\sum_{\omega_1}\int\frac{d^dk_1}{(2\pi)^d}D(\omega_1,\mathbf{k_1})D(-\omega_1-\omega_n,-\mathbf{k_1}-\mathbf{q}), \\
\mathrm{Re}\Pi^{(g^2)}(\omega,\mathbf{q}) &= -\frac{g^2}{2}\int\frac{d^dk_1}{(2\pi)^d}\int\frac{dk_1^0}{2\pi}\frac{dk_2^0}{2\pi}\mathbf{P}\frac{1}{k_1^0+k_2^0+\omega} \\
&\quad \times\left(f(k_1^0)+f(k_2^0)+1\right)\rho(k_1^0,\mathbf{k_1})\rho(k_2^0,-\mathbf{k_1}-\mathbf{q}), \qquad (590)
\end{aligned}$$

where we have used transformation of the sum of Matsubara frequency to integration of energy components, and

$$\mathrm{Re}\,\Pi^{(\lambda)} = \Pi^{(\lambda)} = \frac{\lambda}{2}\int \frac{d^{d+1}k}{(2\pi)^{d+1}} f(k^0)\rho(k). \tag{591}$$

These relations (590) and (591) give the following second component of $\mathcal{S}'$ (580) for two-loop order skeletons:

$$\begin{aligned}\int \frac{d^{d+1}q}{(2\pi)^{d+1}} \frac{\partial f(q^0)}{\partial T} \mathrm{Re}\Pi^{(g^2)}(q)\mathrm{Im}D(q) &= -\frac{g^2}{4}\int \frac{d^{d+1}k_1}{(2\pi)^{d+1}}\int \frac{d^{d+1}k_2}{(2\pi)^{d+1}}\int \frac{d^{d+1}q}{(2\pi)^{d+1}} \\ &\times \delta^d(\mathbf{k_1}+\mathbf{k_2}+\mathbf{q})\mathbf{P}\frac{1}{k_1^0+k_2^0+q^0}\frac{\partial f(q^0)}{\partial T} \\ &\times (1+f(k_1^0)+f(k_2^0))\rho(k_1)\rho(k_2)\rho(q), \end{aligned}\tag{592}$$

and

$$\int \frac{d^{d+1}q}{(2\pi)^{d+1}} \frac{\partial f(q^0)}{\partial T} \mathrm{Re}\Pi^{(\lambda)}(q)\mathrm{Im}D(q) = \frac{\lambda}{4}\int \frac{d^{d+1}k}{(2\pi)^{d+1}}\int \frac{d^{d+1}q}{(2\pi)^{d+1}} f(k^0)\frac{\partial f(q^0)}{\partial T}\rho(k)\rho(q), \tag{593}$$

where we have used Im $D = \rho/2$. We can confirm that the components (592), (593) (588) and (589) cancel precisely and that $\mathcal{S}' = 0$ is satisfied for the two-loop order.

Furthermore we shall derive the expression of $\mathcal{S}'$ with three-loop order (next-to-leading order) skeletons in $\lambda\phi^4$ theory (only in the case of $g = 0$ in the above model) by writing down $\mathcal{S}'$ explicitly and confirm $\mathcal{S}' = 0$ for this order. The expression of $\mathcal{S}$ for this order is necessary to compare s^0 (91) derived from SD equation with three-loop order (NLO) skeletons in our work and $\mathcal{S} - \frac{\partial \Omega/V}{\partial T}$ for three-loop order in the end. The right skeleton ($O(\lambda^2)$) in Fig.84 can be expressed as

$$\begin{aligned} -\frac{T}{2V}\Phi^{(\lambda^2)} &= \frac{\lambda^2}{48}T^3\sum_{\omega_1,\omega_2,\omega_3}\int \frac{d^dk_1}{(2\pi)^d}\int \frac{d^dk_2}{(2\pi)^d}\int \frac{d^dk_3}{(2\pi)^d} D(\omega_1,\mathbf{k}_1)D(\omega_2,\mathbf{k}_2) \\ &\times D(\omega_3,\mathbf{k}_3)D(-\omega_1-\omega_2-\omega_3,-\mathbf{k_1}-\mathbf{k_2}-\mathbf{k_3}) \\ &= \frac{\lambda^2}{48}\int \frac{d^{d+1}k_1}{(2\pi)^{d+1}}\int \frac{d^{d+1}k_2}{(2\pi)^{d+1}}\int \frac{d^{d+1}k_3}{(2\pi)^{d+1}}\int \frac{d^{d+1}k_4}{(2\pi)^{d+1}} \\ &\times (2\pi)^d\delta^3(\mathbf{k_1}+\mathbf{k_2}+\mathbf{k_3}+\mathbf{k_4})\rho(k_1)\rho(k_2)\rho(k_3)\rho(k_4)\mathbf{P}\frac{1}{k_1^0+k_2^0+k_3^0+k_4^0} \\ &\times \left[(2f(k_2^0)f(k_3^0)+f(k_2^0)+f(k_3^0)+1)(f(k_1^0)+f(k_4^0)+1)\right] \end{aligned}\tag{594}$$

where we have used the transformation of the Matsubara frequency to integration of energy components in the similar way to (585) with (586) for the later convenience. We can derive the first and the second component in $\mathcal{S}'$ (580) from (594).

The first component can be written as

$$\begin{aligned} -\frac{\partial}{\partial T}\left(\frac{T}{2V}\Phi^{(\lambda^2)}\right) &= \frac{\lambda^2}{12}\int \frac{d^{d+1}k_1}{(2\pi)^{d+1}}\int \frac{d^{d+1}k_2}{(2\pi)^{d+1}}\int \frac{d^{d+1}k_3}{(2\pi)^{d+1}}\int \frac{d^{d+1}k_4}{(2\pi)^{d+1}} \\ &\times \delta^d(\mathbf{k_1}+\mathbf{k_2}+\mathbf{k_3}+\mathbf{k_4})\mathbf{P}\frac{1}{k_1^0+k_2^0+k_3^0+k_4^0}\frac{\partial f(k_1^0)}{\partial T} \\ &\times \left[(1+f(k_2^0))(1+f(k_3^0)+f(k_4^0))+f(k_3^0)f(k_4^0)\right] \\ &\times \rho(k_1)\rho(k_2)\rho(k_3)\rho(k_4) \end{aligned}\tag{595}$$

where we have used the symmetry for the interchange of four momentum $\{k_1, k_2, k_3, k_4\}$ in the

integration. The second component in $\mathcal{S}'$ involves the real part of the self-energy expressed as

$$\begin{aligned}\Pi^{(\lambda^2)}(\omega_n,\mathbf{q}) &= -\frac{\lambda^2}{6}T^2\sum_{\omega_1,\omega_2}\int\frac{d^dk_1}{(2\pi)^d}\int\frac{d^dk_2}{(2\pi)^d}\\ &\times D(\omega_1,\mathbf{k_1})D(\omega_2,\mathbf{k_2})D(-\omega_1-\omega_2-\omega_n,-\mathbf{k_1}-\mathbf{k_2}-\mathbf{q})\end{aligned} \tag{596}$$

$$\begin{aligned}\text{Re }\Pi^{(\lambda^2)}(\omega,\mathbf{q}) &= -\frac{\lambda^2}{6}\int\frac{d^dk_1}{(2\pi)^d}\int\frac{d^dk_2}{(2\pi)^d}\int\frac{dk_1^0}{2\pi}\frac{dk_2^0}{2\pi}\frac{dk_3^0}{2\pi}\mathbf{P}\frac{1}{k_1^0+k_2^0+k_3^0+\omega}\\ &\times\left[(f(k_1^0)+1)(f(k_2^0)+f(k_3^0)+1)+f(k_2^0)+f(k_3^0)\right]\\ &\times\rho(k_1^0,\mathbf{k_1})\rho(k_2^0,\mathbf{k_2})\rho(k_3^0,-\mathbf{k_1}-\mathbf{k_2}-\mathbf{q}).\end{aligned} \tag{597}$$

Then the second contribution to $\mathcal{S}'$ in this order can be written as

$$\begin{aligned}\int\frac{d^{d+1}q}{(2\pi)^{d+1}}\frac{\partial f(q^0)}{\partial T}\text{Re }\Pi^{(\lambda^2)}(q)\text{Im }D(q) &= -\frac{\lambda^2}{12}\int\frac{d^{d+1}k_1}{(2\pi)^{d+1}}\int\frac{d^{d+1}k_2}{(2\pi)^{d+1}}\int\frac{d^{d+1}k_3}{(2\pi)^{d+1}}\int\frac{d^{d+1}q}{(2\pi)^{d+1}}\\ &\times\delta^d(\mathbf{k_1}+\mathbf{k_2}+\mathbf{k_3}+\mathbf{q})\mathbf{P}\frac{1}{k_1^0+k_2^0+k_3^0+q^0}\frac{\partial f(q^0)}{\partial T}\\ &\times\left[(1+f(k_1^0))(1+f(k_2^0)+f(k_3^0))+f(k_2^0)f(k_3^0)\right]\\ &\times\rho(k_1)\rho(k_2)\rho(k_3)\rho(q).\end{aligned} \tag{598}$$

We find that the sum of the first (595) and second component (598) vanishes and $\mathcal{S}'=0$ is satisfied for NLO of $\lambda\phi^4$ theory.

Hence we can prove that the kinetic entropy s^0 in (91) is equivalent to $\mathcal{S}=-\frac{\partial\Omega/V}{\partial T}$ at thermal equilibrium for three-loop order $O(\lambda^2)$ in $\lambda\phi^4$ theory. Furthermore the kinetic entropy s^0 in (91) corresponds to $\mathcal{S}=-\frac{\partial\Omega/V}{\partial T}$ in the two-loop (leading) order skeletons for the interaction $\mathcal{L}_{\rm int}=-\frac{g}{3!}\hat{\phi}^3-\frac{g^2}{4!}\hat{\phi}^4$. The extension of this property to the non-Abelian gauge theory is trivial, so that $\mathcal{S}'=0$ is also satisfied in the gauge theory [170, 171].

References

[1] H.D. Politzer, Phys. Rev. Lett. **30** (1973) 1346.

[2] D.J. Gross and F. Wilczek, Phys. Rev. Lett. **30** (1973) 1343.

[3] J. Collins and M. Perry, Phys. Rev. Lett. 34 (1975) 135.

[4] J.D. Bjorken, Lect. Notes Phys. **56**, ed. K. Korner et al. (Springer, New York, 1976).

[5] L.N. Lipatov, Sov. J. Nucl. Phys. 23 (1976) 338.

[6] E.A. Kuraev, L.N. Lipatov and V.S. Fadin, Sov. Phys. JETP 45 (1977) 199.

[7] I.I. Balitsky and L.N. Lipatov, Sov. J. Nucl. Phys. 28 (1978) 822.

[8] A. Linde, Particle Physics and Inflationary Cosmology, Harwood, Philadelphia, (1990)

[9] J.D. Bjorken, Phys. Rev. D **27** (1983) 140.

[10] E. V. Shuryak, Phys. Rep. **61** (1980) 71.

[11] J. Adams et al. (STAR Collaboration), Nucl. Phys. **A 757** (2005) 102.

[12] K.H. Ackermann et al. (STAR Collaboration), Nucl. Instrum. Meth. A **449** (2003) 624.

[13] B.I. Abelev et al. (STAR Collaboration), nucl-ex/08082041.

[14] I. Arsene et al. (BRAHMS Collaboration), Nucl. Phys. **A 757** (2005) 1.

[15] K. Adcox et al. (PHENIX Collaboration), Nucl. Phys. **A 757** (2005) 184.

[16] B. B. Back et al. (PHOBOS Collaboration), Nucl. Phys. **A 757** (2005) 28.

[17] T. Matsui, Nucl. Phys. **A 461** (1987) 27.

[18] U. Heinz, Expanded Version of Lecture Notes given at the 2002 European School of High-Energy Physics in Pylos (Greece), [hep-ph/0407360].

[19] R. Sorensen, [nucl-ex/09050174].

[20] For review, see F. Gelis, T. Lappi and R. Venugopalan, Int. J. Mod. Phys. E 16 (2007) 2595, [hep-ph/07080047]; E. Iancu and R. Venugopalan, The color glass condensate and high energy scattering in QCD, in R.C. Hwa. X.N. Wang (Eds.), QGP3, World Scientific, 2004, [hep-ph/0303204].

[21] A. Kovner, L. McLerran and H. Weigert, Phys. Rev. D52 (1995) 6231; A. Kovner, L. McLerran and H. Weigert, Phys. Rev. D52 (1995) 3809.

[22] T. Lappi and L. McLerran, Nucl. Phys. **A772** (2006) 200.

[23] P.F. Kolb and U. Heinz, in Quark-Gluon Plasma 3 edited by R.C. Hwa and X.-N. Wang (World Scientific, Singapore, 2004), p. 634, [nucl-th/0305084].

[24] Y. Hama, et al., Nucl. Phys. **A774** (2006) 169.

[25] T. Hirano, Phys. Rev. C **65** (2001) 011901.

[26] T. Hirano and K. Tsuda, Phys. Rev. C **66** (2002) 054905.

[27] C. Nonaka, S. A. Bass, Phys. Rev. **C75** (2007) 014902.

[28] T. Hirano, U. Heinz, D. Kharzeev, R. Lacey and Y. Nara, J. Phys. **G34** (2007) S879.

[29] L.D. Landau, Izv. Akad. Nauk SSSR, Ser. Fiz. **17** (1953) 51.

[30] U. Heinz, J. Phys. G: Nucl. Part. Phys. **31** (2005). S717

[31] T. Hirano, Nucl. Phys. **A 774** (2006) 531.

[32] S.A. Bass and A. Dumitru, Phys. Rev. **C61** (2000) 064909.

[33] S.V. Akkelin, Y. Hama, I.A. Karpenko and Y.M. Sinyukov, Phys. Rev. **C78** (2008) 034906

[34] K. H. Ackermann et al. (STAR Collaboration), Phys. Rev. Lett. **86** (2001) 402.

[35] P.F. Kolb, P. Huovinen, U. Heinz and H. Heiselberg, Phys. Lett. B **500** (2001) 232.

[36] R. Baier, A. H. Mueller, D. Schiff and D. T. Son, Phys. Lett. **B502**, 51 (2001).

[37] P.F. Kolb, J. Sollfrank and U. Heinz, Phys. Lett. B **439** (1999) 667; Phys. Rev. C **62** (2000) 054909.

[38] D. Teaney and E.V. Shuryak, Phys. Rev. Lett **83** (1999) 4951; D. Teaney, J. Lauret and E.V. Shuryak, Phys. Rev. Lett. **86** (2001) 4783; D. Teaney, J. Lauret and E.V. Shuryak, [nucl-th/0110037]; D. Teaney, J. Lauret and E.V. Shuryak, Nucl. Phys. A **698** (2002) 479.

[39] P. Huovinen, P.F. Kolb, U. Heinz, P.V. Ruuskanen and S.A. Voloshin, Phys. Lett. B **503** (2001) 58; P.F. Kolb, P. Huovinen, U. Heinz, K. Eskola and K. Tuominen, Nucl. Phys. A **696** (2001) 175.

[40] U. Heinz and P.F. Kolb, Nucl. Phys. A **702** (2002) 269; Phys. Lett. B **542** (2002) 216; P.F. Kolb and U. Heinz, Nucl. Phys. A **715** (2003) 653; P.F. Kolb and U. Heinz, in Quark Gluon Plasma 3, R.C. Hwa and X.N. Wang (eds.) (World Scientific, Singapore, 2004), p. 634, [nucl-th/0305084];

[41] P.F. Kolb and R. Rapp, Phys. Rev. C **67** (2003) 044903; P.F. Kolb, Heavy Ion Phys. **21** (2004) 243.

[42] M. Chojnacki and W. Florkowski, Phys. Rev. C **74** (2006) 034905; W. Broniowski, M. Chojnacki, W. Florkowski and A. Kisiel, Phys. Rev. Lett. **101** (2008) 022301; A. Kisiel, W. Broniowski, M. Chojnacki and W. Florkowski, Phys. Rev. C **79** (2009) 014902.

[43] K. Morita, S. Muroya, H. Nakamura and C. Nonaka, Phys. Rev. C **61** (2000) 034904.

[44] C. Nonaka, E. Honda and S. Muroya, Eur. Phys. J. C **17** (2000) 663.

[45] T. Hirano, K. Morita, S. Muroya and C. Nonaka, Phys. Rev. C **65** (2002) 061902.

[46] K. Morita, S. Muroya, C. Nonaka and T. Hirano, Phys. Rev. C **66** (2002) 054904.

[47] C. Nonaka and M. Asakawa, Phys. Rev. C **71** (2005) 044904.

[48] H. Song and U. Heinz, Phys. Rev. C **77** (2008) 064901; Phys. Rev. C **78** (2008) 024902; Phys. Lett. B **658** (2008) 279; Plenary talk at International Conference on Strangeness in Quark Matter (SQM 2008), Beijing, China, 6-10 Oct 2008, [nucl-th/08124274]; U. Heinz, H. Song and A.K. Chaudhuri, Phys. Rev. C **73** (2006) 034904; A.K. Chaudhuri and U. Heinz, J. Phys. Conf. Ser. **50** (2006) 251; A.K. Chaudhuri, Phys. Rev. C **74** (2006) 044904; A.K. Chaudhuri, [nucl-th/07040134]; [nucl-th/08013180]; U. Heinz and H. Song, J. Phys. G **35** (2008) 104126.

[49] R. Baier, P. Romatschke and U.A. Wiedemann, Phys. Rev. C **73** (2006) 064903; R. Baier and P. Romatschke, Eur. Phys. J. C **51** (2007) 677; P. Romatschke, Eur. Phys. C **52** (2007) 203; P. Romatschke and U. Romatschke, Phys. Rev. Lett. **99** (2007) 172301; M. Luzum and P. Romatschke, Phys. Rev. C **78** (2008) 034915.

[50] G.S. Denicol, T. Kodama, T. Koide and Ph. Mota, [hep-ph/08083170]; J. Phys. G **35** (2008) 115102; Phys. Rev. C **78** (2008) 034901.

[51] R.J. Glauber, in "Lectures on Theoretical Physics", Vol. 1, W.E. Brittin, L.G. Dunham (eds.), (Interscience, NY, 1959).

[52] A. Bialas, M. Bleszynski, and W. Czyz, Nucl. Phys. B **111** (1976) 461.

[53] D. Kharzeev and E. Levin, Phys. Lett. B **523** (2001) 79.

[54] D. Kharzeev, E. Levin and M. Nardi, Phys. Rev. C **71** (2005) 054903.

[55] T. Hirano and Y. Nara, Nucl. Phys. A **743** (2004) 305.

[56] D. Kharzeev, E. Levin and M. Nardi, Nucl. Phys. A **747** (2005) 609.

[57] H.J. Drescher, A. Dumitru, A. Hayashigaki and Y. Nara, Phys. Rev. C **74** (2006) 044905.

[58] T. Lappi and R. Venugopalan, Phys. Rev. C **74** (2006) 054905.

[59] H.J. Drescher and Y. Nara, Phys. Rev. C **75** (2007) 034905

[60] For review, S. Mrowczynski, PoS CPOD2006: 042 (2006) [hep-ph/0611067].

[61] S. Mrowczynski, Phys. Lett. B **214** (1988) 587.

[62] S. Mrowczynski, Phys. Lett. **B314**, 118 (1993); Phys. Rev. C **49**, 2191 (1994); Phys. Lett. B **393**, 26 (1997).

[63] P. Arnold, J. Lenaghan and G. D. Moore, JHEP **0308**, 002 (2003).

[64] A. Rebhan, P. Romatschke and M. Strickland, Phys. Rev. Lett. **94**, 102303 (2005).

[65] J.I. Kapusta, Finite-Temperature Field Theory, Cambridge University Press, Cambridge, 1989.

[66] M. Le Bellac, Thermal Field Theory, Cambridge University Press, Cambridge, 1996.

[67] V.P. Silin, Sov. Phys. JETP 11 (1960) 1136.

[68] J.P. Blaizot and E. Iancu, Phys. Rep. 359 (2002) 355.

[69] J.P. Blaizot and E. Iancu, Nucl. Phys. B 390 (1993) 589.

[70] J. Luttinger and J. Ward, Phys. Rev. **118**, 1417 (1960).

[71] G. Baym and L. Kadanoff, Phys. Rev. **124**, 287 (1961).

[72] G. Baym, Phys. Rev. **127**, 1391 (1962).

[73] L.P. Kadanoff, G. Baym, *Quantum Statistical Mechanics* (Benjamin, New York, 1962).

[74] J. M. Cornwall, R. Jackiw and E. Tomboulis, Phys. Rev. D **10**, 2428 (1974)

[75] J. Schwinger, J. Math. Phys. **2** (1961) 407.

[76] L.V. Keldysh, ZHETF **47** 1515 (1964); Sov. Phys. JETP **20**, 235 (1965).

[77] A.J. Niemi and G.W. Semenoff, Ann. Phys. 152 (1984) 105; Nucl. Phys. B **230** (1984) 181.

[78] J.H. Traschen and R.H. Brandenberger, Phys. Rev. D **42** (1990) 2491.

[79] L. Kofman, A.D. Linde, A.A. Starobinsky, Phys. Rev. Lett. **73** (1994) 3195.

[80] J. Berges and J. Serreau, Phys. Rev. Lett. **91** (2003) 111601.

[81] G. Aarts and A. Tranberg, Phys. Rev. D **77** (2008) 123521; Phys. Rev. D **77** (2008) 123521.

[82] A. Tranberg, JHEP 0811037 (2008); A. Tranberg, Nucl. Phys A 820 (2009) 195C-198C, [hep-ph/08102887].

[83] A. Arrizabalaga, J. Smit and A. Tranberg, JHEP **0410** (2004) 017.

[84] A. Einstein, Sitzungsberichte der Preussichen Akademie der Wissenschaften Physikalisch-Mathematische Klasse, (1924) 261.

[85] A. Einstein, Sitzungsberichte der Preussichen Akademie der Wissenschaften Physikalisch-Mathematische Klasse, (1925) 3.

[86] E.A. Cornell and C.E. Wieman, Rev. Mod. Phys. **74** (2002) 875.

[87] W. Ketterle, Rev. Mod. Phys. **74** (2002) 1131.

[88] N.M. Hugenholtz and D. Pines, Phys. Rev. **116** (1959) 489.

[89] J. Berges, AIP Conf. Proc. **739**, 3 (2005) [hep-ph/0409233].

[90] A. Griffin, Phys. Rev. B **53** (1996) 9341.

[91] P. Danielewicz, Ann. Phys. (N.Y.) **152**, 305 (1984).

[92] G. Aarts and J. Berges, Phys. Rev. D **64**, 105010 (2001).

[93] J. Berges and J. Cox, Phys .Lett. B **517**, 369 (2001).

[94] S. Juchem, W. Cassing and C. Greiner, Phys. Rev. D **69**, 025006 (2004).

[95] M. Lindner and M. M. Müller; Phys. Rev. D **73** 125002 (2006).

[96] F. Cooper, J.F. Dawson and B. Mihaila, Phys. Rev. D **67** (2003) 056003.

[97] A. Arrizabalaga, J. Smit and A. Tranberg, Phys. Rev. D **72**, 025014 (2005).

[98] G. Aarts, D. Ahrensmeier, R. Baier, J. Berges and J. Serreau, Phys. Rev. **D 66** (2002) 045008.

[99] J. Berges, Nucl. Phys. **A 699** (2002) 847.

[100] G. Aarts and A. Tranberg, Phys. Rev. D **74** (2006) 025004.

[101] G. Aarts, N. Laurie and A. Tranberg, Phys. Rev. D **78** (2008) 125028.

[102] J. Berges. S. Borsanyi and J. Serreau, Nucl. Phys. **B660** (2003) 51.

[103] M. Lindner and M.M. Muller, Phys. Rev. D **77** (2008) 025027.

[104] J. Berges, J. Pruschke and A. Rothkopf, Phys. Rev. D **80** (2009) 023522.

[105] J. Berges, S. Borsányi and C. Wetterich, Phys. Rev. Lett. **93** (2004) 142002.

[106] G. Aarts and J. M. Martínez Resco, Phys. Rev. D **68** (2003) 085009; JHEP 0402:061, (2004).

[107] G. Aarts and J. M. Martínez Resco, JHEP. 0503:074, (2005).

[108] Y.B. Ivanov, J. Knoll, and D.N. Voskresensky, Nucl. Phys. **A672**, 313 (2000).

[109] T. Kita, J. Phys. Soc. Jpn. **75**, 114005 (2006).

[110] A. Nishiyama, Nucl. Phys. A832 (2010) 289, [nucl-th/08105003].

[111] J. Rau and B. Müller, Phys. Rep. 272 (1996) 1.

[112] For example, see "*Progress in Nonequilibrium Green's Functions III*," M. Bonitz and A. Filinov (eds.), J. Phys. Conf. **35**, 1 (2006).

[113] J. Berges and J. Serreau, 6th Conference on Strong and Electroweak Matter 2004 (SEWM04), Helsinki, Finland, 16-19 Jun 2004, [hep-ph 0410330].

[114] E. Calzetta, B.L. Hu, Phys. Rev. D **37** (1988) 2878.

[115] U. W. Heinz, AIP Conf. Proc. **739**, 163 (2005).

[116] W. Botermans and R. Malfliet, Phys. Rep. 198 (1990) 115.

[117] W. Cassing, Eur. Phys. J. ST 168 (2009) 3 [nucl-th 08080715].

[118] Y.B. Ivanov, J. Knoll, and D.N. Voskresensky, Nucl. Phys. **A657**, 413 (1999).

[119] I. Montvay and G. Münster; Quantum Fields on a Lattice, Cambridge University Press (1994).

[120] F. Cooper, Y. Kluger, E. Mottola and J.P. Paz, Phys. Rev. **D 51** (1995) 2377.

[121] M.A. Lampert, J.F. Dawson and F. Cooper, Phys. Rev. **D 54** (1996) 2213.

[122] H.E. Stanley, Phys. Rev. **176** (1968) 718.

[123] K. Wilson, Phys. Rev. **D 7**, (1973) 2911.

[124] S. Coleman, R. Jackiw and H. D. Politzer, Phys Rev. **D 10** (1974) 2491.

[125] B. Mihaila, J. F. Dawson and F. Cooper, Phys. Rev. **D 56** (1997) 5400.

[126] B. Mihaila, T. Athan, F. Cooper, J. Dawson and S. Habib, Phys. Rev. **D 62** (2000) 125015.

[127] J. Berges, Lectures in the Yukawa International Program for Quark-Hadron Sciences international molecule workshop on "Non-equilibrium quantum field theories and dynamic critical phenomena", March 2009.

[128] A.K. Kolmogorov, Dokl. Akad. Nauk SSSR **30**, 301 (1941).

[129] A.K. Kolmogorov, Dokl. Akad. Nauk SSSR **31**, 538 (1941).

[130] R. Micha and I.I. Tkachev, Phys. Rev. **D 70** (2004) 043538.

[131] J. Berges, A. Rothkopf and J. Schmidt, Phys. Rev. Lett. **101** (2008) 041603.

[132] J. Berges and G. Hoffmeister, Nucl. Phys. B **813** (2009) 383.

[133] S. Chiku and T. Hatsuda, Phys. Rev. **D 58** (1998) 076001.

[134] F. Karsch, A. PPatkos and P. Petreczky, Phys. Lett. **B401** (1997) 69.

[135] J.O. Andersen, E. Braaten and M. Strickland, Phys. Rev. **D63** (2001) 105008.

[136] J.O. Andersen, E. Braaten and M. Strickland, Phys. Rev. Lett. **83** (1999) 2139.
[137] J.O. Andersen, E. Braaten and M. Strickland, Phys. Rev. **D61** (2000) 014017.
[138] J.O. Andersen, E. Braaten and M. Strickland, Phys. Rev. **D61** (2000) 074016.
[139] J.O. Andersen, E. Braaten and M. Strickland, Phys. Rev. **D66** (2002) 085016.
[140] J. Frenkel and J.C. Taylor, Nucl. Phys. B 334 (1990) 199.
[141] E. Braaten and R.D. Pisarski, Nucl. Phys. B 337 (1990) 569.
[142] O.K. Kalashnikov and V.V. Klimov, Sov. J. Nucl. Phys. 31 (1980) 699.
[143] V.V. Klimov, Sov. J. Nucl. Phys. 33 (1981) 934; Sov. Phys. JETP 55 (1982) 199.
[144] H.A. Weldon, Phys. Rev. D 26 (1982) 1394.
[145] H.A. Weldon, Phys. Rev. D 26 (1982) 2789.
[146] R.D. Pisarski, Phys. Rev. Lett. 63 (1989) 1129.
[147] J. P. Blaizot, Lect. Notes Phys. 583 (2002) 117, [hep-ph/0107131].
[148] J. P. Blaizot, E. Iancu and A. Rebhan, : in Quark gluon plasma edited by R.C. Hwa, et al, (World Scientific, 2003) 60-122, [hep-ph/0303185].
[149] H. van Hees and J. Knoll, Phys. Rev. D **65**, 025010 (2002);Phys. Rev. D **65**, 105005 (2002); Phys. Rev. D **66**, 025028 (2002).
[150] A. Dumitru, Y. Nara and M. Strickland, Phys. Rev. D **75**, 025016 (2007).
[151] P. Romatschke and R. Venugopalan, Phys. Rev. Lett. **96** (2006) 062302; P. Romatschke and R. Venugopalan, Phys. Rev. D **74**, 045011 (2006).
[152] A. Iwazaki, Phys. Rev. C **77**, 034907 (2008).
H. Fujii and K. Itakura, Nucl. Phys. A **809**, 88 (2008).
[153] Z. Xu and C. Greiner, Phys. Rev. C **71**, 064901 (2005); Phys. Rev. C **76**, 024911 (2007); J. Phys. G34 (2007) S855; Nucl. Phys. A **806** (2008) 287; J.Phys. G35 (2008) 104072; Acta Phys. Polon. B40 (2009) 925.
[154] B.S. De Witt, Phys. Rev. 162 (1967) 1195, 1239; Phys. Rep. 19C (1975) 295.
[155] L.F. Abbott, Nucl. Phys. B **185** (1981) 189.
[156] R.B. Sohn, Nucl. Phys. B **273** (1986) 468.
[157] H. Kluberg-Stern, J.B. Zuber, Phys. Rev. **D 12** (1975) 482.
[158] T.H. Hansson and I. Zahed, Phys. Rev. Lett. 58 (1987) 2397; Nucl. Phys. B 292 (1987) 725.
[159] B.S. DeWitt, in: C.J. Isham, et al. (Eds.), Quantum Gravity, Oxford Univ. Press, New York, 1981.
[160] Q. Wang, K. Redlich, H. Stöcker and W. Greiner, Nucl. Phys. A 714 (2003) 293.
[161] P. Arnold, J. Lenaghan, G. D. Moore and L. G. Yaffe, Phys. Rev. Lett. **94** (2005) 072302.
[162] N.K. Nielsen, Nucl. Phys. **B 101** (1975) 173.
[163] R. Fukuda and T. Kugo, Phys. Rev. **D 13** (1976) 3469.
[164] A. Arrizabalaga and J. Smit, Phys. Rev. **D 66** (2002) 065014.
[165] M.E. Carrington, G. Kunstatter and H. Zaraket, Eur. Phys. J C 42, 253 (2005).
[166] E. Mottola, Proceedings of SEWM 2002 (World Scientific 2003), hep-ph/0304279.
[167] K. Kajantie and J. Kapusta, Ann. Phys. **160** (1985) 477.
[168] E. Riedel, Z. Phys. **210** (1968) 403.
[169] B. Vanderheyden and G. Baym, J. Stat. Phys. **93** (1998) 843.
[170] J. P. Blaizot, E. Iancu and A. Rebhan, Phys. Rev. Lett. **83** (1999) 2906; Phys. Lett. B470 (1999) 181.
[171] J. P. Blaizot, E. Iancu and A. Rebhan, Phys. Rev. **D 63** (2001) 065003.
[172] B. Kim and K. Kawasaki, J. Stat. Mech, P02004, (2008).
[173] T. Ikeda, Phys. Rev. D **69**, 105018 (2004).